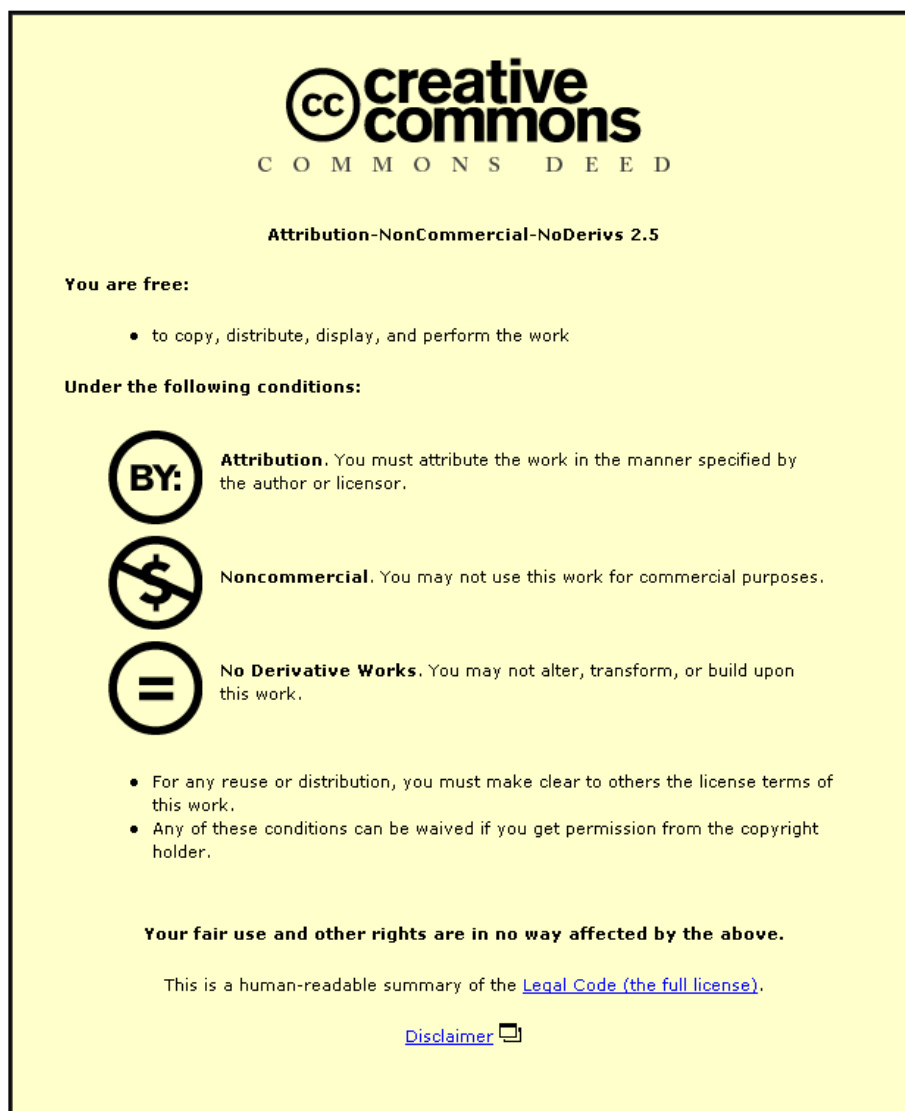


This item was submitted to Loughborough University as a PhD thesis by the author and is made available in the Institutional Repository (<https://dspace.lboro.ac.uk/>) under the following Creative Commons Licence conditions.



For the full text of this licence, please go to:  
<http://creativecommons.org/licenses/by-nc-nd/2.5/>

BLDSC no:- DX 174569

LOUGHBOROUGH  
UNIVERSITY OF TECHNOLOGY  
LIBRARY

AUTHOR/FILING TITLE

BEGG, J

ACCESSION/COPY NO

040060494

VOL NO

CLASS MARK

LOAN COPY

26 JUN 1999

25 JUN 1999

14 JAN 2000

08 JAN 2001

24 NOV 2000

FOR REFERENCE ONLY

0400604949



BADMINTON PRESS  
98 THE HALEGROFT  
SYSTON  
LEICESTER LE17 8LD

BLDSC no :- DX 174569

LOUGHBOROUGH  
UNIVERSITY OF TECHNOLOGY  
LIBRARY

AUTHOR/FILING TITLE

BEGG, J

ACCESSION/COPY NO

040060494

~~1 JUL 1994~~

~~13 MAR 1995~~

~~14 MAY 1996~~

2 30 JUN 1995

13 MAR 1995

16 APR 1996

28 JUN 1996

14 MAY 1996

29 JUN 1996

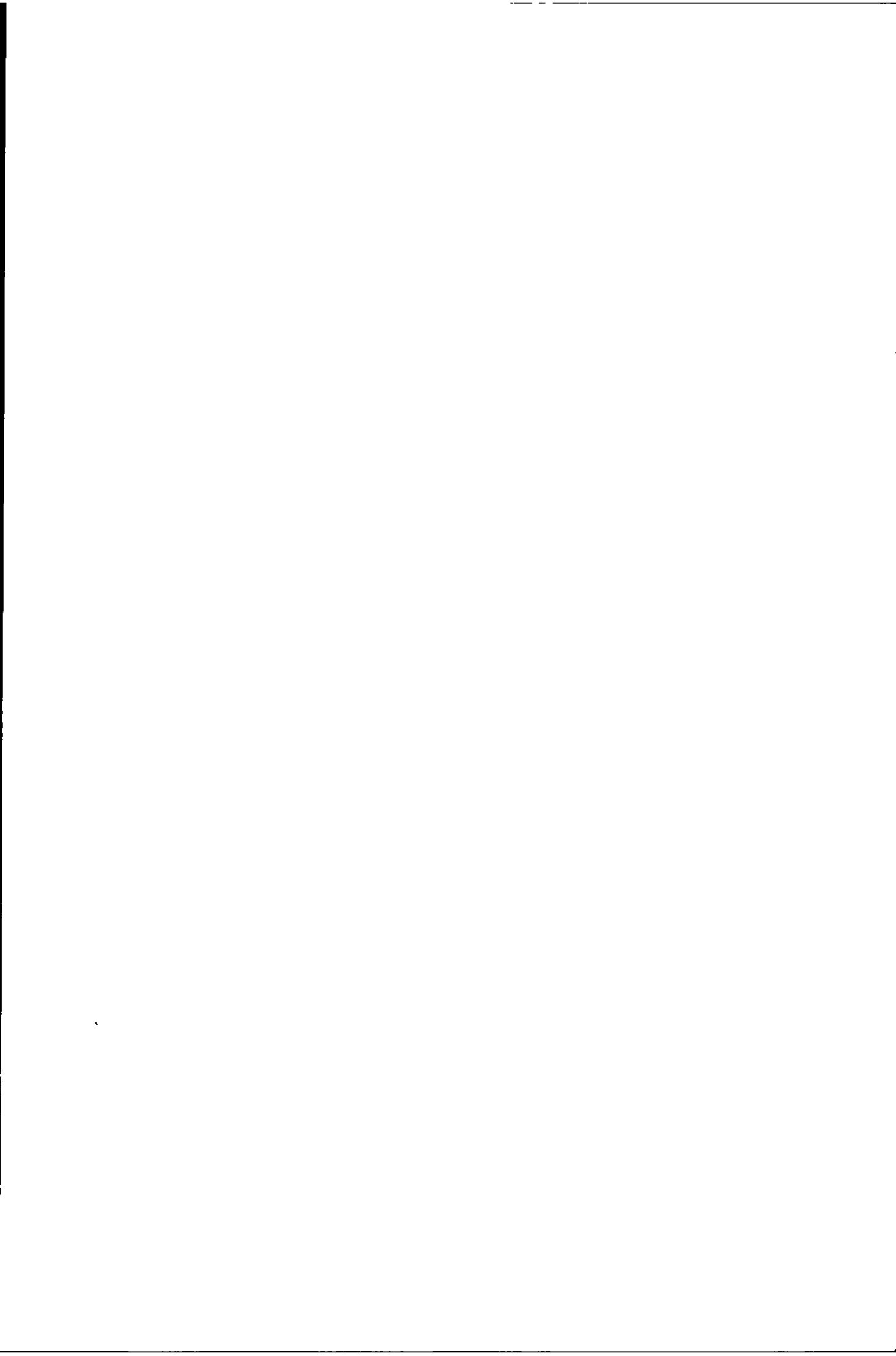
~~27 JUN 1997~~

27 JUN 1997

0400604949



BADMINTON PRESS  
48 THE HALEGROFT  
SYSTON  
LEICESTER LE7 8LD



**Process Optimisation in the Squeeze Casting  
of Zinc-Aluminium Alloys and Composites**

by

**John Begg**

A Doctoral Thesis  
Submitted in Partial Fulfilment of the Requirements  
for the Award of  
Ph.D. of the Loughborough University of Technology

August 1992

© by John Begg 1992



## CONTENTS

	Page
Contents	i
Summary	vi
Statement of Originality	vii
Acknowledgements	viii
<b>Chapter 1: Introduction</b>	<b>1</b>
<b>Chapter 2: Metallurgy of Zinc-Base Alloys</b>	<b>4</b>
2.1 Introduction	4
2.2 Zinc	5
2.2.1 General Properties of Zinc	5
2.2.2 Physical Metallurgy of Zinc	5
2.3 Zinc-Base Casting Alloys	6
2.3.1 Die Casting Alloys	6
2.3.2 Characteristics of Alloying Elements in Die Casting Alloys	6
2.3.2.1 Aluminium	6
2.3.2.2 Copper	9
2.3.2.3 Magnesium	9
2.3.2.4 Iron	9
2.3.2.5 Lead, Tin and Cadmium	9
2.3.3 Creep Resistant Die Casting Alloy	9
2.3.4 Zinc-Base Foundry Alloys (ZA Alloys)	10
2.3.4.1 ZA8 and ZA12	14
2.3.4.2 ZA27	14
2.3.4.3 Solid State Transformations	15
2.3.4.4 Dimensional Changes in ZA Alloys	16
2.4 Processing Effects in ZA Alloys	19
2.5 Creep in ZA Alloys	25
2.5.1 General Comments on Creep	25
2.5.2 Secondary Creep	28
2.5.3 Formula for Creep in Zn Alloys	31
2.5.4 Rules for the Development of Creep Resistance	31
2.6 Summary	32

<b>Chapter 3: Squeeze-Casting</b>	<b>33</b>
<b>3.1 Near-Net Shape Processing</b>	<b>33</b>
<b>3.2 Process Fundamentals</b>	<b>34</b>
<b>3.3 Theory</b>	<b>38</b>
3.3.1 Effect of Pressure on Solidifying Metals & Alloys	38
<b>3.4 Effect of Processing Variables</b>	<b>41</b>
3.4.1 Design	41
3.4.2 Melt Quality	41
3.4.3 Melt Temperature	41
3.4.4 Pouring Temperature	43
3.4.5 Die Temperature	43
3.4.6 Die Lubrication	43
3.4.7 Casting Temperature	43
3.4.8 Time Before Application of Pressure	43
3.4.9 Time to Build up to Full Pressure	43
3.4.10 Pressure Level	43
3.4.11 Pressure Duration	44
3.4.12 Delay Before Ejection	44
<b>3.5 Specific Examples</b>	<b>44</b>
3.5.1 Aluminium Casting Alloys	44
3.5.1.1 Aluminium-Silicon Alloys	44
3.5.1.2 Alloyed Aluminium-Silicon Alloys	46
3.5.1.3 Aluminium-Magnesium Alloys	47
3.5.1.4 Wrought Aluminium Alloys	47
3.5.1.5 Aluminium-Copper Binary Alloys	47
3.5.1.6 Aluminium-Copper-Magnesium Alloys	48
3.5.2 Aluminium Forging Alloys	48
3.5.3 Other Alloy Systems	49
3.5.3.1 Non-Ferrous Alloys	49
3.5.3.2 Ferrous Materials	51
3.5.4 Zinc Base Alloys	51
<b>3.6 Applications</b>	<b>53</b>
<b>3.7 Summary</b>	<b>54</b>
<b>Chapter 4: Metal Matrix Composites Utilising ZA Alloy as a Matrix</b>	<b>55</b>
<b>4.1 Introduction</b>	<b>55</b>
<b>4.2 Synthesis of Materials</b>	<b>56</b>
<b>4.3 Review of MMC Manufacturing Routes</b>	<b>58</b>
<b>4.4 Cast Metal Matrix Composites</b>	<b>59</b>
4.4.1 Interfaces in Metal Matrix Composites	61
4.4.2 Bonding in Metal Matrix Composites	61
4.4.2.1 Mechanical Bonding	61
4.4.2.2 Dissolution and Wetting Bonds	61
4.4.2.3 Oxide Bonds	61
4.4.2.4 Reaction Bonds	62

4.4.2.5	Exchange Reaction Bonds	62
4.4.2.6	Mixed Bonds	62
4.4.2.7	Summary	62
4.4.3	Interfacial Physics	63
4.4.3.1	Surface Energy and Surface Tension	63
4.4.3.2	Three Phase Interfaces	63
4.4.4	Cause of Wetting	66
4.4.5	Wettability	66
4.4.5.1	Wettability of High Melting Point Oxide Fibres	66
4.4.5.2	Wettability of Covalent Solids	69
4.4.5.3	Concluding Remarks	74
4.4.6	Manufacturing Methods	74
4.4.6.1	Infiltration Methods	74
4.4.6.2	Casting a Pre-Mixed Melt	75
4.5	Zinc-Base Alloy Metal Matrix Composites	76
4.6	Summary	80
 <b>Chapter 5: Experimentation</b>		 81
5.1	Introduction	81
5.2	Manufacturing Equipment	82
5.2.1	Squeeze Casting Press	82
5.2.1.1	Main Piston	82
5.2.1.2	Ejector Piston	82
5.2.1.3	Squeeze Casting Dies	84
5.2.1.4	Ingot Die	84
5.2.1.5	Shaped Die	84
5.2.1.6	Die with Varying Section Thickness	86
5.2.1.7	Die Coatings	89
5.2.1.8	Die Temperature Ranges	89
5.2.2	Melting Equipment	89
5.2.2.1	Melting Furnace	89
5.2.2.2	Melting Crucibles	92
5.2.2.3	Ancillary Equipment	92
5.2.2.4	Equipment for Composite Manufacture	92
5.2.2.5	Stirring Equipment	92
5.2.2.6	Vibratory Feed System	92
5.2.2.7	Inert Gas Covers	94
5.3	Manufacturing Programme	94
5.3.1	Plain Alloys in the Ingot Die	94
5.3.1.1	ZA27	94
5.3.1.2	ZA8	96
5.3.1.3	ZA12	96
5.3.1.4	Zn-37Al	98
5.3.2	Plain Alloys in Backward Extrusion Die	98
5.3.2.1	ZA27	98
5.3.2.2	ZA8	98
5.3.2.3	ZA12	100
5.3.2.4	Zn-37Al	100
5.3.3	Composite Manufacture	100
5.3.3.1	Initial Experimentation	100

5.3.3.2	Production Run	100
5.3.3.3	Further Trials	100
5.4	Testing	102
5.4.1	Mechanical Properties	102
5.4.1.1	Tensile Mechanical Properties	102
5.4.1.2	Compressive Mechanical Properties	102
5.4.2	Metallography	105
5.4.2.1	Light Microscopy	105
5.4.2.2	Electron Microscopy	105
5.4.3	Chemical Analysis	106
5.4.3.1	Bulk Chemical Analysis	106
5.4.3.2	Microstructural Analysis	106
5.4.4	Dilatometry	106
Chapter 6: Results		108
6.1	Processing Comments	108
6.2	Mechanical Properties of Squeeze-Cast Alloys	108
6.2.1	ZA27	108
6.2.2	ZA8	122
6.2.3	ZA12	129
6.2.4	Zn-37Al	129
6.3	Microstructures of Squeeze-Cast Alloys	133
6.3.1	ZA27	133
6.3.2	ZA8	137
6.3.3	ZA12	145
6.3.4	Zn-37Al	145
6.4	Chemical Analysis	159
6.5	Dilatometry	159
6.6	Composites	159
6.7	Properties of Squeeze-Cast Composites	164
6.7.1	Room Temperature Tensile Tests	164
6.7.2	High Temperature Tensile Tests	164
6.7.3	Compression Testing	167
6.7.4	Creep Testing	167
6.8	Microstructures of Squeeze-Cast Composites	171
6.9	Chemical Analysis of Squeeze-Cast Composites	180
Chapter 7: Discussion of Results		
7.1	Introduction	182
7.2	ZA27	186
7.2.1	Thick Sections	186
7.2.2	Thin Sections	193
7.2.3	Processing Map for ZA27	195

7.2.4	Comparison of Squeeze Casting with Other Processes	195
7.3	<b>ZA8</b>	198
7.3.1	Thick Sections	198
7.3.2	Thin Sections	200
7.3.3	Processing Map for Squeeze-Cast ZA8	200
7.3.4	Comparison of Squeeze Casting with Other Processes	200
7.4	<b>ZA12</b>	202
7.4.1	Thick Sections	202
7.4.2	Thin Sections	202
7.4.3	Processing Map for Squeeze-Cast ZA12	204
7.4.4	Comparison of Squeeze Casting with Other Processes	204
7.5	<b>Zn-37Al</b>	204
7.5.1	Thick Sections	204
7.5.2	Thin Sections	207
7.5.3	Processing Map for Squeeze-Cast Zn-37Al	207
7.6	<b>Composite Materials</b>	209
7.6.1	Composite Manufacture	209
7.6.2	Distribution	210
7.6.3	Mechanical Properties	210
	7.6.3.1 Tensile Testing	210
	7.6.3.2 Composite Compression Testing	211
	7.6.3.3 Modelling Properties	212
7.6.4	Creep of ZA Alloys and Composites	217
7.7	<b>Exploitation and Applications</b>	218
	<b>Chapter 8: Conclusions and Recommendations</b>	221
8.1	<b>Conclusions</b>	221
8.2	<b>Recommendations</b>	224
	<b>References</b>	225
	<b>Appendix 1</b>	232
	<b>Appendix 2</b>	246

## Process Optimisation in the Squeeze Casting of Zinc-Aluminium Alloys and Composites

### Summary

Squeeze casting is a process which has the potential to produce castings with exceptional mechanical properties. It also appears to be the most suitable route to produce sound cast metal matrix composites.

An investigation was carried out into the squeeze casting of four zinc-aluminium alloys:

- commercial ZA8 (simple eutectic alloy)
- commercial ZA12 (simple eutectic alloy)
- commercial ZA27 (peritectic alloy)
- binary Zn-37Al (solid solution alloy).

Although the three commercial alloys can be cast by a variety of conventional gravity and pressure processes it was considered that squeeze casting would produce castings with more homogeneous microstructures and enhanced room temperature properties. The binary Zn-37Al was considered to be a suitable alloy for squeeze casting.

The effects of die temperature, pouring temperature, pressure application time and level and section thickness were investigated. Provided that there was sufficient pressure to produce sound castings the significant parameters affecting properties were die temperature, pouring temperature and section thickness.

The strengths of squeeze-cast ZA8 and ZA12 were optimised at the lowest die temperature (150°C) and thinnest section (8mm) but elongation values were generally low. In ZA27 the highest strengths were obtained at the highest die temperature (>200°C) but elongation values were optimised at a die temperature of around 150°C. High elongation was promoted by high temperature gradients. Thinner section castings had higher strengths and lower elongations. The strength of Zn-37Al decreased with increasing die temperature accompanied by an increase in elongation. All properties were related to microstructures and processing maps proposed.

In order to try to improve the elevated temperature performance of ZA27, squeeze-cast composites containing up to 20 v/o silicon carbide particulate reinforcement were produced. They were manufactured by squeeze casting a melt of ZA27 and particulate, the latter having been introduced by the vortex method. Testing of the composites showed that those with high volume fractions of particulate produced the better material, in terms of stiffness and strength, at all testing temperatures. Results compared to the base alloy were disappointing because of lower strengths and elongations. Creep resistance of the composites at high temperatures and high stresses were improved relative to the base alloy but the results were largely inconclusive.

DECLARATION

This thesis is the own work of J Begg. No part of this thesis has been submitted for an award of this or any other institute of learning or the C.N.A.A..

### Acknowledgements

The author is grateful to both the SERC and the Brock Metal Company of Cannock for providing the funds for this project and to Professor R Bell of the Department of Manufacturing Engineering for the facilities to carry out this work.

The author also acknowledges the technical assistance received from the technicians at Loughborough University, particularly J Mistry, J T W Smith, R Temple, J Jones, and F Page.

Many thanks also are given to Mr M J D Frier of Cast Metals Development Limited who stayed behind after work to help the author finish off printing of the photographs in this thesis.

Special thanks are reserved for the author's wife, Dorothy, without whose continuous encouragement this thesis would probably not have been completed.

Finally the author would like to thank Dr A J Clegg for his support and comprehensive proof reading of the thesis.

## 1. Introduction

The traditional market for zinc as a casting material is in the area of small intricate components produced at high speed and in very large quantities by both hot and cold chamber pressure die-casting machines [1].

The material performs very well in these applications but newer materials, for example polymers, began to compete with zinc in terms of performance and, more importantly, cost. Large producers of zinc naturally became worried about this situation and began looking for new markets for zinc castings [2]. Research, initially at the International Lead and Zinc Research Organisation (ILRZO) and subsequently, under contract, by Noranda in Canada resulted in the development of a range of zinc-base/aluminium gravity casting alloys designated ZA alloys. The range comprises three alloys ZA8, ZA12 and ZA27 with the number corresponding to the approximate aluminium content in the alloy [3].

ZA8 was developed as a gravity die casting alloy, ZA12 as a general purpose foundry alloy and ZA27 as a high strength sand casting alloy (strength increases with increase in aluminium content). This range of alloys competes well with conventional casting alloys, for example, cast iron, bronze, aluminium etc., in terms of castability and mechanical properties. Major advantages claimed are: low energy, pollution-free melting; non-sparking characteristics; good corrosion resistance and good bearing properties (eg wear resistance) [4]. Disadvantages quoted are segregation, especially in higher aluminium alloys at slower cooling rates; possible underside shrinkage in ZA27; dimensional instability in as-cast structures [5] and poor elevated temperature properties at moderate temperatures (80°C). The latter is most evident as poor creep resistance.

The objectives of this investigation were to produce near-net shape castings in ZA alloys which possess improved mechanical properties both at room and elevated temperature (up to

150°C) compared with conventionally cast materials. Possible applications appear to be in under-bonnet components in the motor industry and wear resistant bearing parts [6].

Previous work at Loughborough [7-10] has shown that the properties of aluminium base alloys were improved by squeeze casting both the alloy and a composite melt of alloy plus reinforcement of randomly orientated short fibres or whiskers. Improvements in the alloy were increases in tensile strength and ductility, while the reinforced alloys showed improved stiffness and strength compared to the base alloy, particularly at higher temperatures. No evidence of macro-segregation was reported.

It was considered that squeeze casting could also improve some of the properties of ZA alloys. Reinforcement of these alloys should also help develop the higher temperature performance. The use of short fibres or whiskers as a reinforcement is expensive and the resulting material is difficult to process. It has been reported [11] that, theoretically, similar strengthening could be achieved by using a particulate material as the reinforcing phase. This is much cheaper than other forms of reinforcement and the resulting melt mixture is easier to process.

Much interest in this area has been generated in the United States and at least two firms are selling cast silicon carbide particulate reinforced aluminium alloy ingot [12,13]. However, it appears that the material has to be mechanically worked and heat treated to achieve optimum properties. Working appears necessary, both to 'weld-up' porosity and to achieve a uniform distribution of particles. It will be shown in this thesis that correct melt processing followed by controlled squeeze casting produces a pore-free structure with good particulate distribution in ZA27.

## Aims of Research

- to study the effect of squeeze casting parameters (pressure, temperature etc.) on the structure and properties of ZA alloys and Zn-37%Al alloy.
- to study the effect of section thickness on the structure and properties of these alloys.
- to optimise squeeze casting conditions with respect to room temperature properties.
- to develop an inexpensive composite system based on ZA alloys.
- to make near-net shape composite components in ZA alloys.
- to evaluate the high temperature properties of the composite.

## 2. Metallurgy of Zinc-Base Alloys

### 2.1 Introduction [14]

Zinc is not a glamorous material. In its pure state its mechanical properties are mediocre. It has no quoted modulus of elasticity for long term loading because of its tendency to creep. The density of zinc ( $7140\text{kg/m}^3$ ) is more than 2.5 times that of aluminium ( $2700\text{kg/m}^3$ ) and approaches that of iron ( $7870\text{kg/m}^3$ ).

Alloying opportunities with zinc are limited and wrought alloys generally only contain small additions of elements such as copper and titanium, to improve creep resistance. Alloyed with 60-70wt% copper, zinc forms the industrially important brass alloys. Zinc forms a useful series of alloys when combined with 4wt% aluminium, creating a range of alloys which have high fluidity and a relatively low melting point, that are widely used in die casting. A new series of alloys has recently been developed for general foundry applications [3]. Designated as ZA alloys they have many attractive properties but their use is restricted by relatively poor mechanical properties above about  $80^\circ\text{C}$ . They also suffer from dimensional instability on ageing, caused by solid state transformations. Poor creep resistance at elevated temperature is seen to be the major drawback against wider acceptance and use of these alloys [5].

It was considered that the room temperature properties of ZA alloys could be enhanced by squeeze casting and that higher temperature performance could be enhanced by squeeze-cast composite production. In order to explain any benefits it is necessary to understand the metallurgy of the alloys.

This chapter describes the metallurgy of zinc and its casting alloys, alloy development, microstructures, ageing, creep and processing effects.

## 2.2 Zinc

### 2.2.1 General Properties of Zinc [14]

Zinc is a silvery white metal with a relatively low melting point ( $419.5^{\circ}\text{C}$ ) and boiling point ( $970^{\circ}\text{C}$ ). Unalloyed, zinc is stronger than lead or tin, but appreciably weaker than aluminium and copper. It cannot be used in high stress applications, due to its low creep resistance. Zinc is brittle at ordinary temperatures but malleable and workable above  $100^{\circ}\text{C}$ . Copper and titanium improve creep resistance of rolled sheet. When alloyed with 4wt% aluminium, strength and hardness are dramatically increased.

Zinc has many attractive properties, ie low corrosion rate, low melting point, ease of precision casting, ease of finish and low energy/clean melting characteristics. Its main uses are in protecting steel (galvanising) and casting production. Other uses are as an alloying element, eg in brasses, high strength magnesium and aluminium alloys and in coinage and construction.

### 2.2.2 Physical Metallurgy of Zinc

Pure zinc crystallises into hexagonal structures with  $a=0.2664\text{nm}$  and a  $c/a$  ratio of 1.656 compared with the theoretical of 1.633. The coordination number is 12, but the six atoms on the basal plane are at  $0.2664\text{nm}$  and the six others are at  $0.2907\text{nm}$ . Bonds on the basal plane are stronger and consequently slip occurs between basal planes (0001). At higher temperatures other slip planes become active eg  $(10\bar{1}0)$ . Twinning can occur on the  $(10\bar{1}2)$  pyramidal plane, leading to further slip due to reorientation. Atomic mobility is high and recrystallisation readily takes place. Pure zinc readily crystallises after deformation at room temperature. However, with certain alloying additions such as copper and cadmium, which form solid solutions, somewhat higher temperatures are required.

### 2.3 Zinc-Base Casting Alloys [14]

The main characteristic of zinc as an alloying element is that its solid solubility in other metals is limited and additionally, few metals have any appreciable solid solubility in zinc. Zinc does not form a continuous series of solid solutions with any other metal, but solubility can reach 80% in aluminium, 39% in copper and 20% in iron. It is soluble, to a lesser degree, in magnesium, manganese, nickel, cobalt and gold. With most other metals the solubility is less than 3%. The solubility of other metals is low, eg silver and gold are soluble to about 10% and cadmium and copper to 3%.

#### 2.3.1 Die Casting Alloys

Zinc die casting alloys are based on near eutectic compositions of binary zinc-aluminium alloys. Attempts were made to die-cast zinc in the early part of this century. However, tests showed that components tended to fail prematurely and with disastrous effects because of intercrystalline corrosion caused by lead or tin from ore refining operations [1]. These problems were overcome by using high purity zinc. As a result of the investigation, a range of Mazak alloys (Zamak in the U.S.) were introduced. These original alloys are still in use today. In 1942 the British Standards Institute produced BS1004, covering two alloys which had good all round performance and a wide range of applications, which are summarised in Tables 2.1 to 2.3.

#### 2.3.2 Characteristics of Alloying Elements in Die Casting Alloys [15]

##### 2.3.2.1 Aluminium

This is the main alloying constituent. Its major effects are increasing strength and grain size reduction. Impact strength reduces at compositions greater than 4.3% and at 5% the alloy becomes brittle. If the percentage drops below 3.7% then ease of casting and mechanical properties deteriorate. Aluminium reduces the attack of zinc on iron,

**Table 2.1**  
**Composition of Zinc Pressure Die Casting Alloys**  
**Casting Limits - wt%**

Element	Alloy Designation	
	3	5
Aluminium	3.5 - 4.3	3.5 - 4.3
Magnesium	0.02 - 0.05	0.03 - 0.08
Copper	0.25	0.75-1.25
Iron	0.10	0.10
Lead	0.005	0.005
Cadmium	0.004	0.004
Tin	0.003	0.003
Zinc	balance	balance

NB: Single Figures are Maxima

**Table 2.2**  
**Physical Characteristics of Zinc Die Casting Alloys**

Physical Property	Alloy Designation	
	3	5
Density (kg/m <sup>3</sup> )	6600	6700
Shrinkage (%)	1.17	1.17
Solidification Range (°C)	387-381	386-380
Thermal Expansion (µm/mm/K at 20-100°C)	27.4	27.4
Specific Heat Capacity (J/kg/K at 20-100°C)	418.7	418.7
Thermal Conductivity (W/m/hr/m <sup>2</sup> /K at 20°C)	113.0	108.9
Electrical Conductivity (%IACS)	27	26
Electrical Resistivity (µ ohm-cm at 20°C)	6.3694	6.5359

**Table 2.3**  
**Mechanical Properties of Zinc Die Casting Alloys**

Mechanical Properties		Alloy Designation	
		3	5
UTS	MPa	282.7	328
Elongation	%	10	7
Hardness	Brinell (500kg)	82	91
Shear Strength	MPa	213	262
Compressive Yield Strength (0.1% offset)	MPa	413.7	413.7
Impact Energy (unnotched bar)	J	58.3	65.1
Fatigue Strength (500 million cycles)	MPa	47.6	56.5

**Table 2.4: Composition of ZA Alloys**

Element	Alloy		
	ZA8	ZA12	ZA27
Aluminium	8.0 - 8.8	10.5 - 11.5	25.0 - 28.0
Magnesium	0.015 - 0.030	0.015 - 0.030	0.010 - 0.020
Copper	0.8 - 1.3	0.5 - 1.2	2.0 - 2.5
Iron	0.075	0.075	0.075
Lead	0.006	0.006	0.006
Cadmium	0.006	0.006	0.006
Tin	0.003	0.003	0.003
Zinc	Balance	Balance	Balance

permitting the use of hot chamber pressure die casting machines.

#### 2.3.2.2 Copper

Copper increases the tensile strength and hardness at the expense of impact strength. It causes dimensional instability on ageing. Copper tends to retard the eutectoid transformation.

#### 2.3.2.3 Magnesium

At low concentrations (less than 0.6%) magnesium reduces the susceptibility of the alloys to intercrystalline corrosion. At higher concentrations impact strength and ductility are adversely affected and the alloys become hot short.

#### 2.3.2.4 Iron

Iron is soluble in zinc, to the extent of 0.02%. At higher percentages a hard phase forms, which is detrimental to properties and can cause machining problems.

#### 2.3.2.5 Lead, Tin and Cadmium

These are present in trace quantities from refining operations. Lead and tin cause intercrystalline corrosion. Cadmium affects casting and mechanical properties detrimentally.

#### 2.3.3 Creep Resistant Die Casting Alloy [1].

The only alloy marketed specifically as a creep resistant alloy is not based on the Zn-Al system. The alloy, ILZRO 16, is based on zinc, with additions of chromium and titanium. the nominal composition is:

0.5 - 1.5%	Cu
0.01 - 0.04%	Al
0.15 - 0.25%	Ti
0.1 - 0.2%	Cr
balance	Zn

This is a cold chamber pressure die casting alloy. The chromium and titanium provide creep improvements by solution hardening and precipitation methods.

#### 2.3.4 Zinc-Base Foundry Alloys (ZA alloys)

Due to design improvements and new material developments, the volume of zinc used in die casting has declined [2]. In 1950 35% of zinc consumption was in die casting but currently this figure is less than 15%. The industry is worried about its declining share of an increasingly competitive market, due to competition from newer materials. Much money has been spent on research and development, to protect zinc's market position in the casting field and increase its market potential. Since the early sixties ILZRO has been sponsoring a programme to develop a new range of zinc-base alloys, containing aluminium, for general foundry application (ZA alloys) [3]. These have been widely accepted and can compete with cast aluminium alloys, bronzes and cast iron in general engineering situations and are suitable as bearing materials.

ZA12 (formerly ILZRO 12) was the first to become available, followed by ZA8 and finally the higher strength ZA27. The numbers corresponding to the approximate aluminium contents in the alloys, as defined in Table 2.4. Gervais, Levert and Bess [3] give guidelines on casting conditions for the three alloys. One of the major problems is macro-segregation, which can cause underside shrinkage. Stirring during melting must be adopted to overcome this problem. Table 2.5 gives physical properties of ZA alloys.

The alloys are based on the Zn-Al binary system with additions of copper and magnesium. These additions, particularly the copper, produce a fairly complex ternary alloy, but the basic microstructures can be explained with reference to the binary Zn-Al diagram.

**Table 2.5: Physical Properties of ZA Alloys**

Physical Property	Alloy Designation		
	ZA8	ZA12	ZA27
Density (kg/m <sup>3</sup> )	6300	6030	5010
Shrinkage (%)	1.1	1.25	1.25
Solidification Range (°C)	404-375	432-377	484-376
Thermal Expansion at 20-100°C (µm/mm/K)	23.3	24.1	26.0
Specific Heat Capacity at 20-100°C (J/kg/K)	435	450	525
Thermal Conductivity at 20°C (W/m/hr/m <sup>2</sup> /K)	66.3	67.1	72.5
Electrical Conductivity (%IACS)	27.7	28.3	29.7
Electrical Resistivity at 20°C (µ ohm-cm)	6.2	6.1	5.8
Latent Heat of Fusion (kJ/kg)	112	118	128

Knowledge of the Zn-Al phase diagram has increased over the years and one version is shown in Figure 2.1 [16]. The system shows a eutectic at 380°C, 96% Zn and a peritectic at 443°C, 71.6% Zn. A eutectoid transformation occurs at 275°C, 78% Zn. (Alloys of eutectoid composition are used for superplastic forming operations.)

The phases most often encountered in ZA alloy metallography are as follows:

$\alpha$	FCC	aluminium rich Zn/Al solid solution
$\beta$	FCC	zinc rich Zn/Al solid solution (intermediate eutectoid phase)
$\eta$	HCP	zinc rich solid solution
$\alpha'$	FCC	similar to $\alpha$ but less rich in aluminium
$\epsilon$		zinc-copper compound, $\text{CuZn}_4$
$T'$		Al-Cu-Zn equilibrium ternary phase ( $\text{Al}_4\text{Cu}_3\text{Zn}$ )

Copper is used as an alloying element in all ZA alloys, as a strengthener and a hardener. Additions of up to 2% copper increase alloy tensile strength and reduce elongation. The addition of copper also increases alloy creep and corrosion resistance. The eutectoid reaction, which occurs at 275°C, is retarded by the presence of copper. For example, a Zn-20wt%Al alloy, on quenching from above the eutectoid temperature, is completely decomposed to the equilibrium phase in 90 seconds. The same alloy, containing 1wt%Cu or 3wt%Cu takes 3500s or 4320s respectively for complete transformation [15]. Though beneficial in small amounts, a high copper content is detrimental because it causes a decrease in mechanical properties and a loss of dimensional stability with time, due to the ageing response.

Magnesium is used to strengthen and harden ZA alloys and, like copper, it retards the eutectoid transformation. The addition of 0.1wt% magnesium increases the time for decomposition of a quenched 20wt%Al alloy from 90 seconds at

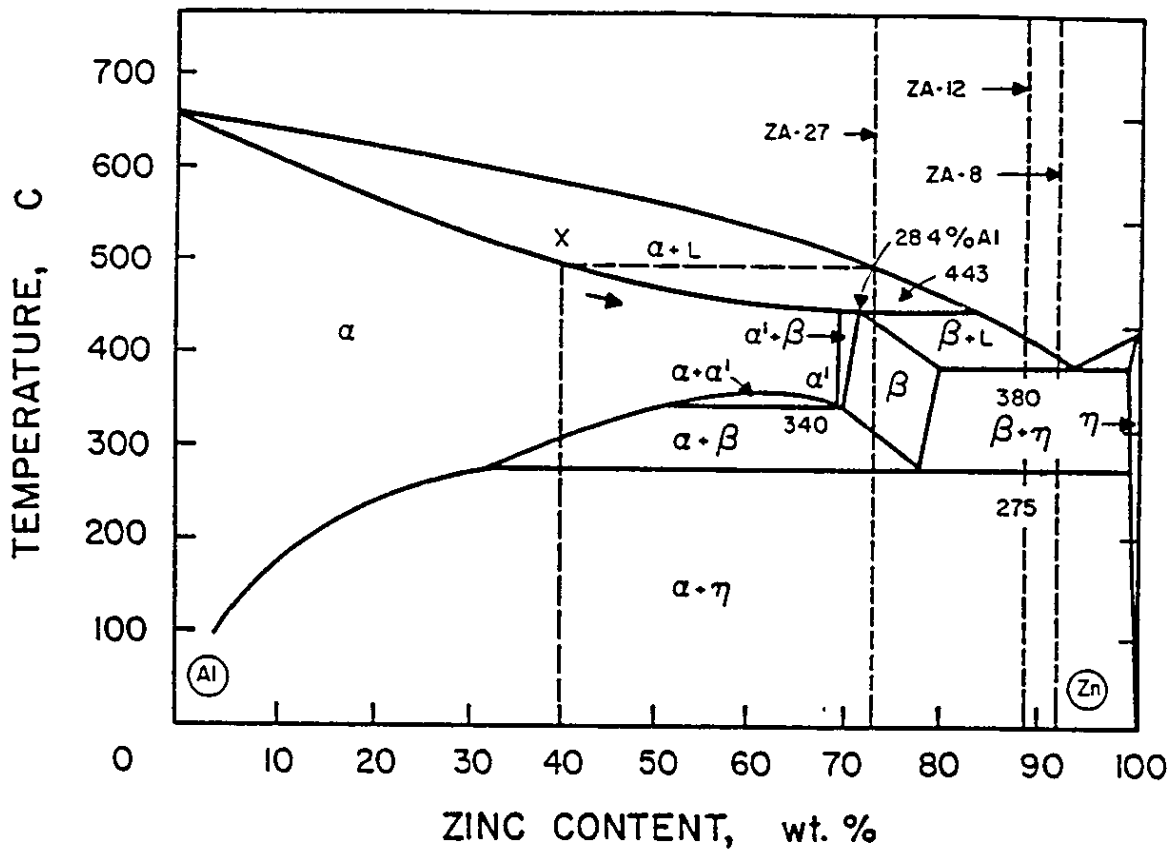


Figure 2.1 Zinc-Aluminium Phase Diagram

room temperature, to 7 weeks. Even at 100°C the reaction still takes 7200 seconds [15]. Magnesium is reported to be evenly distributed throughout the structure [17].

Solidification of ZA alloys can be explained with reference to the Zn-Al binary phase diagram .

#### 2.3.4.1 ZA8 and ZA12

ZA8 has the lowest liquidus and smallest freezing range of the three alloys. Solidification begins at about 404°C, with the formation of  $\beta$  phase dendrites. Coring will be slight. The eutectic solidifies at 380°C. The as-solidified structure will be  $\beta$  in a  $\beta + \eta$  eutectic.

ZA12 solidifies in a similar manner, except that solidification starts at a higher temperature, approximately 430°C. Coring of beta will probably be more evident and the amount of eutectic will be less. The low copper contents of the alloys result in this element being held in solid solution.

#### 2.3.4.2 ZA27

Solidification begins at about 490°C with the formation of  $\alpha$ . This continues to 443°C, where the cored  $\alpha$  undergoes a peritectic reaction with the remaining liquid, L



resulting in a rim of  $\beta$  around the original  $\alpha$ . Further precipitation of  $\beta$  will occur and at the eutectic temperature the remaining zinc enriched liquid will solidify as  $\beta$  and  $\eta$ . The as-solidified structure will be cored  $\alpha$  with a rim of  $\beta$  in a mixture of  $\beta$  and eutectic  $\beta + \eta$ .

The high copper content of ZA27 means that  $\epsilon$  phase may also appear in the interdendritic channels.

### 2.3.4.3 Solid State Transformations

Reference to the binary Al-Zn phase diagram shows that solid state transformations to the microstructure are possible.

Decomposition reactions involving binary zinc-aluminium alloys and ternary zinc-aluminium-copper alloys have been studied by several investigators [18-21]. The favoured study technique is quench ageing. Quenching has been employed following solidification [21], but more usually after a solution treatment [18-20]. The reactions have been studied by SEM, TEM and XRD methods and by hardness testing and conventional metallography.

Decomposition reactions will ultimately result in equilibrium phases  $\alpha$  and  $\eta$ , and in copper containing alloys  $T'$ . However, actual mechanisms depend on time, temperature and composition. It has been established that the following equilibrium solid state reactions occur in the Zn-Al-Cu system in the composition range of ZA alloys [20].



All ZA alloys will contain  $\beta$  on solidification. In binary zinc-aluminium alloys the eutectoid transformation will occur below  $275^{\circ}\text{C}$ , to form  $\alpha + \eta$ . Vijayalakshmi et al [18] discuss the morphological features of the decomposition reaction.

Three types of decomposition are observed:

- conventional cellular reaction (occurring at grain boundaries)
- autocatalytic cellular reaction (occurring within the grains)
- granular reaction

Lecomte-Beckers et al [19] have investigated quench ageing in

binary Zn-11%Al and Zn-27%Al and conclude that decomposition of supersaturated  $\beta$  occurs in the stages outlined in Figure 2.2.

Savaskan and Murphy [20] have described the metallographic features of gravity-cast Zn-25%Al binary alloy and Zn-25%Al-3%Cu alloy in both the as-cast and the aged (150°C for 240 hours) conditions. They report that the as-cast binary alloy  $\alpha$  ( $\alpha'$ ) and  $\beta$  phases decompose in a number of ways. In the binary alloy three changes are noted:

- coarse reaction at edges of zinc/prior  $\beta$  boundary
- fine lamellar decomposition within the prior  $\beta$
- fine zinc precipitation within the prior  $\alpha$  cores.

A study on the effects of ageing on chill cast ZA27 has been carried out by Zhu et al. [21]. Chilling will cause supersaturation of the phases. Zhu's main conclusions on the decomposition are summarised in Figure 2.3. The final structure being a mixture of  $T'$ ,  $\eta$  and  $\alpha$  phases.

#### 2.3.4.4 Dimensional Changes in ZA Alloys [22].

All three ZA alloys can undergo dimensional changes with time, as a result of ageing processes, which are related to structure reorganisation.

Ageing processes have been studied at room temperature and elevated temperatures. The first stage of dimensional change, a contraction, is ascribed to precipitation of solutes in supersaturation. For instance, decomposition of  $\beta$  to form  $\alpha$  and  $\eta$  typically causes 0.05-0.15% contraction. This is slowed by the presence of copper and magnesium but is completed within one day.

The second stage observed during artificial ageing concerns precipitation of  $\alpha$  from the supersaturated zinc rich interdendritic phase,  $\eta$ . The loss of aluminium, through  $\alpha$ ,

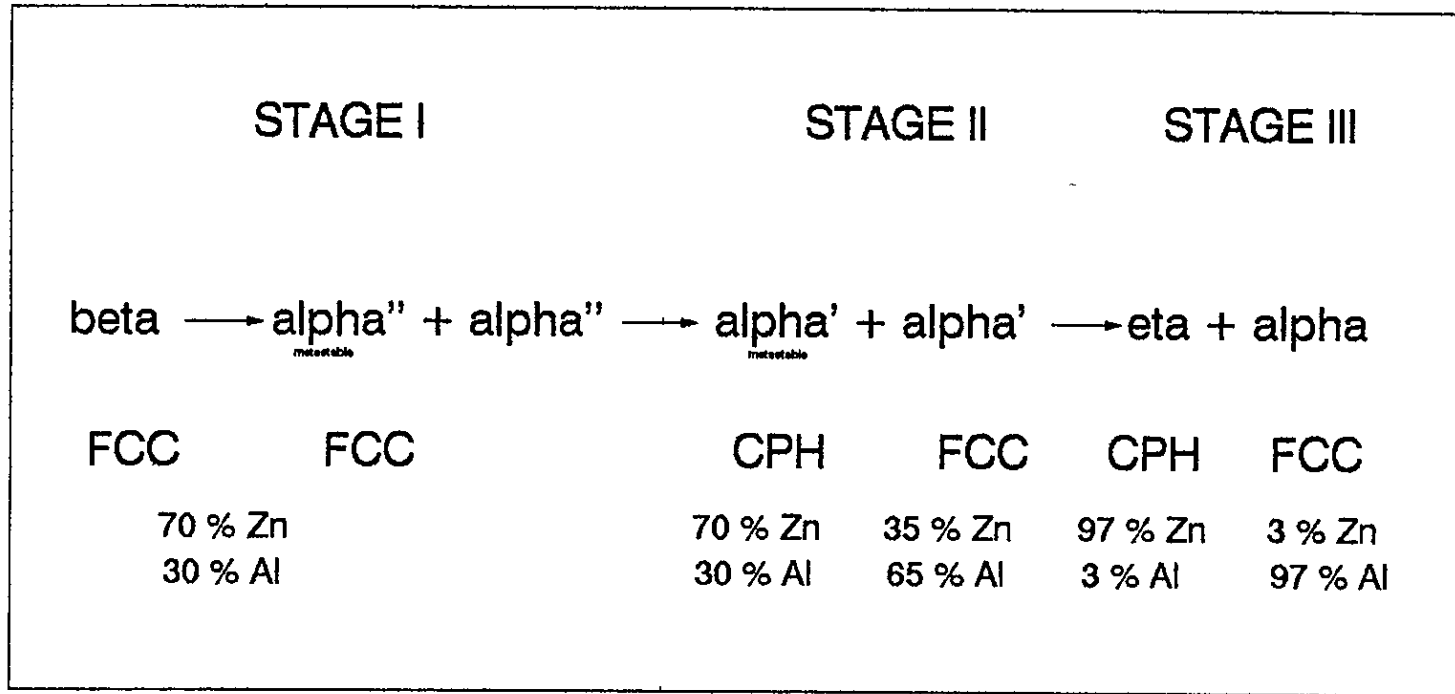


Figure 2 2 Decomposition seequence in Zn - Al alloys

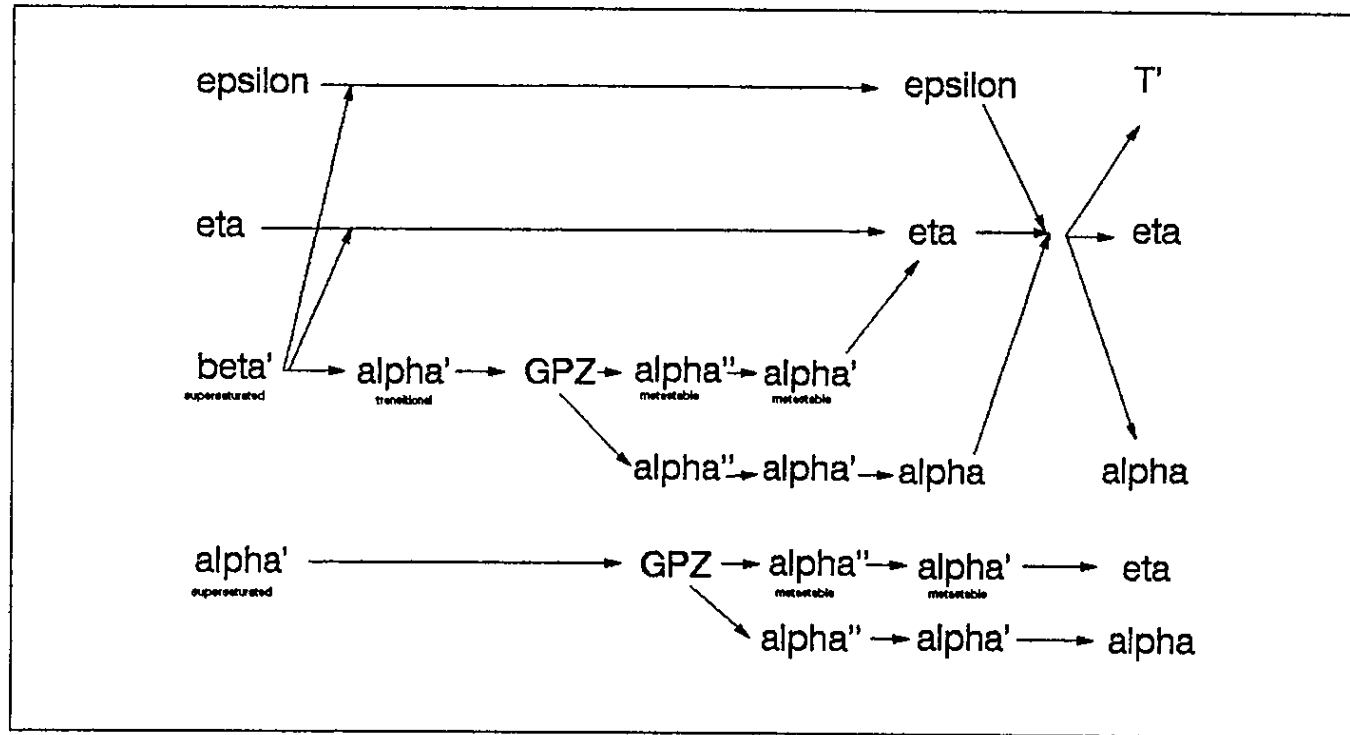


Figure 2 3 Decomposition sequence in chill-cast ZA27

produces a net contraction of the zinc unit cell. This is because the atomic diameter of aluminium is 2.86Å, which is greater than that for zinc at 2.664Å. Copper slows this transformation and exaggerates the volume change, by increasing the solubility of aluminium in  $\eta$  at the eutectic by 1%.

The third stage involves the formation of T' phase through the reaction:



leading to a volume increase of 1.2%. This reportedly takes a long time for complete transformation. Also rejection of copper from inter-dendritic zinc increases the volume of the zinc cell, since the atomic diameter of copper is 2.556Å.

As the amount of  $\epsilon$  phase increases the expansion caused by T' formation is increased. There is more copper in ZA27 and hence this tends to show greater volume increases compared to ZA8 and ZA12. Figure 2.4 [1] shows a typical growth on ageing, for sand-cast ZA27.

#### 2.4 Processing Effects in ZA Alloys

Although ZA alloys were designed for gravity casting purposes - ZA8 as a permanent mould alloy, ZA12 as a general purpose alloy and ZA27 as a high strength sand casting alloy - all alloys have been cast by a variety of methods, including pressure die casting and continuous casting.

In the handbook Engineering Properties of Zinc Alloy [1] ZA8 is described as being processed by:

- pressure die casting
- sand casting
- permanent mould casting.

The mechanical properties for ZA8, cast by these methods, are

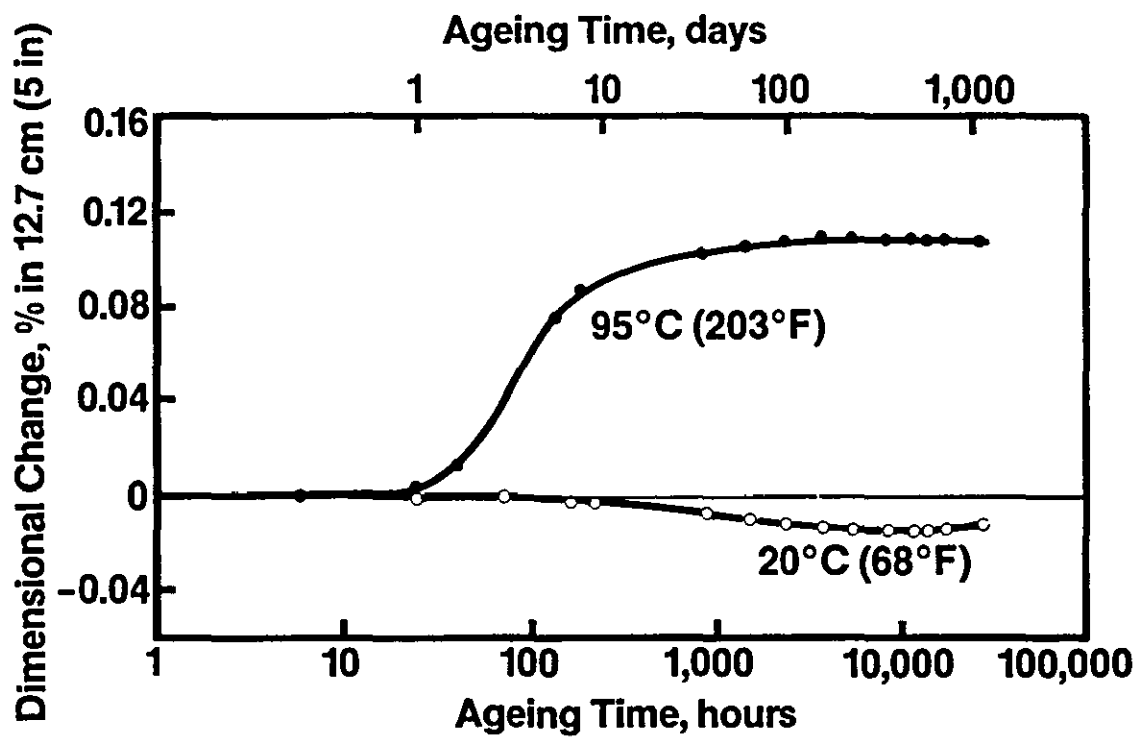


Figure 2 4 Growth on ageing - ZA27 sand-cast [1]

quoted in Table 2.6. These properties appear to improve with high cooling rates, i.e. in pressure die casting.

Similarly, ZA12 has been processed by:

- pressure die casting
- sand casting
- permanent mould casting
- graphite mould casting.

The properties for all these methods are included in Table 2.7. As with ZA8, the properties of ZA12 appear to improve with higher cooling rates, when the processes are compared.

ZA27 has been processed by:

- pressure die casting
- sand casting
- continuous casting.

Properties are shown in Table 2.8. Less variations in strength properties are evident for this alloy. In contrast to ZA8 and ZA12 high mechanical properties are developed in the sand-cast material. The poor impact strength of pressure die cast ZA27 is evident from the table.

This information on its own is not sufficient to compare processes, as section thicknesses no doubt differ and the use of chills and/or feeding is not quoted. The results are probably on the optimistic side. However, they do show that by different processing methods, different properties can be obtained. These properties are thus influenced by cooling rates and heat treatment. The case for using a high cooling rate process, for example squeeze casting, is thus of much interest.

Other references to processing ZA alloys are by rheocasting and stir casting [17]. These processes produce a

**Table 2.6**  
**Mechanical Properties of ZA8 Cast by Different Methods**  
**(As - Cast)**

Property		Pressure Die-Cast	Sand Cast	Permanent Mould
UTS	MPa	374	240 - 276	221 - 255
0.2% Proof Stress	MPa	290	200	207
Elongation	%	6 - 10	1 - 2	1 - 2
Hardness	Brinell (500kg)	100 - 106	80 - 90	85 - 95
Shear Strength	MPa	275	-	241
Compressive Yield Strength (0.1% offset)	MPa	252	200	210
Impact Energy (Unnotched Bar)	J	42	20	
Fatigue Strength (500 Million Cycles)	MPa	103		
Young's Modulus	GPa		85.5	
Poisson's Ratio	-			0.296

**Table 2.7**  
**Mechanical Properties of ZA12 Cast by Different Methods**  
**(As - Cast)**

Property		Pressure Die-Cast	Sand Cast	Perm. Mould	Graphite Mould
UTS	MPa	404	276 - 317	310 - 345	345
0.2% Proof Stress	MPa	320	207	268	214
Elongation	%	4 - 7	1 - 2	1.5 - 2.5	2 - 3
Hardness	Brinell (500kg)	100 - 106	92 - 96	85 - 95	110 - 125
Shear Strength	MPa	275	255		
Compressive Yield Strength (0.1% offset)	MPa	252	228	234	
Impact Energy (Unnotched Bar)	J	42	25		
Fatigue Strength (500 Million Cycles)	MPa	103	103		103
Young's Modulus	GPa		82.7		
Poisson's Ratio	-		0.302		

**Table 2.8**  
**Mechanical Properties of ZA27 Cast by Different Methods**

Property		Pressure Die-Cast	Sand Cast	Sand Cast (Heat Treated)	Contin. Cast
UTS	MPa	426	400 - 441	310 - 324	414 - 441
0.2% Proof Stress	MPa	371	372	255	379 - 393
Elongation	%	2.5	3 - 6	8 - 11	8 - 11
Hardness	Brinell (500kg)	116 - 122	110 - 120	90 - 100	115 - 130
Shear Strength	MPa	325	290	228	269
Compressive Yield Strength (0.1% offset)	MPa	385	331	255	441 *
Impact Energy (Unnotched Bar)	J	5	47	58	73
Fatigue Strength (500 Million Cycles)	MPa	145	172	103	
Young's Modulus	GPa		77.9		
Poisson's Ratio	-		0.23	0.23	

Note: \* 0.2% Offset

microstructure consisting of large rounded primary phase particles of different composition to conventionally cast material. Reported work appears to show that rheocast materials may be weaker at room temperature than conventionally cast materials, but at higher temperature they may be slightly stronger. There are no references to the processes being used for any commercial applications.

## 2.5 Creep in ZA Alloys

Creep deformation in ZA alloys (especially ZA27) is complicated by the fact that the as-cast alloys are unstable metallurgically. This is because of an incomplete eutectoid reaction. Various other reactions can contribute to growth on ageing, so accentuating the amount of creep, especially primary. The presence of copper is particularly significant. It is added to increase strength and secondary creep resistance but it slows down the eutectoid transformation and contributes to growth on ageing (as described in 2.3.4.4).

As has already been stated in the introduction, creep is a major problem hindering the wider use of zinc base alloys. It is instructive to look at the theories and mechanisms behind creep phenomena.

### 2.5.1 General Comments on Creep [23-24]

A generalised creep curve is shown in figure 2.5. The curve has three stages, some of which may be absent, depending on the stress, temperature or type of test, eg constant load or constant stress.

Creep can be treated from a mechanical engineering or a macro viewpoint, where equations can be used to describe the shape of the curve at different temperatures. The metallurgical approach uses the microstructure in an attempt to explain events in terms of the three main creep mechanisms, ie slip, subgrain formation and grain boundary sliding. A combination of these two approaches will be used in an attempt to describe creep in zinc base alloys and how it may be reduced.

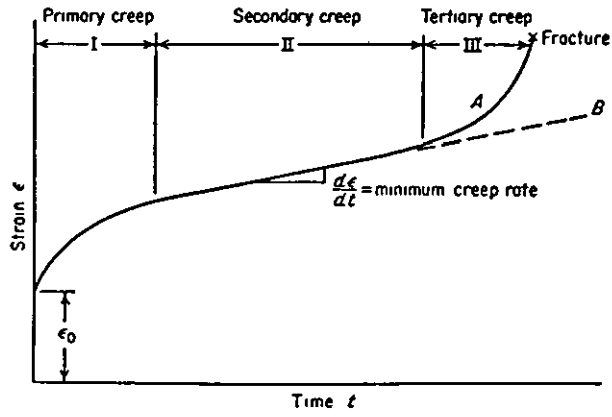


Figure 2.5 Typical Creep Curve

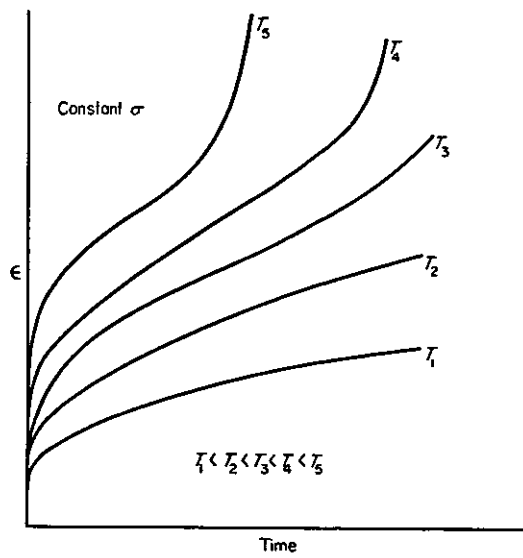


Figure 2.6 Effect of Temperature on Creep

The first stage of creep, called variously primary, logarithmic or transient creep, occurs in the absence of thermal activation (eg at 4K). It is most obvious below  $\frac{1}{2}T_m$ , where  $T_m$  is the melting point of the metal on the absolute scale. The rate determining step is the activation energy required to move a dislocation. The strain rate decreases with time. The behaviour can be modelled by a mechanical equation of state.

The second stage, steady state or power law creep, is a balance between work hardening and recovery which occurs only if the temperature is high enough ( $>\frac{1}{2}T_m$ ). It depends on thermally activated processes, eg vacancy formation.

The third stage, tertiary or linear creep, is a region of rapidly increasing strain rate which finally ends in creep fracture. The accelerated rate only occurs in constant load tests. Void growth occurs at grain boundaries. These voids extend and open up as grain boundary sliding takes place, leading to intergranular creep fracture.

Changing the temperature changes the shape of creep curves, as shown in Figure 2.6. Note at  $T_1$  only primary creep has occurred.

Many authors have tried to characterise creep curves. For example Andrade [reported in 23] defines the creep as:

$$\epsilon = \epsilon_0 \cdot (1 + \beta t^{1/3}) \cdot e^{kt} \quad (2.3)$$

where  $\epsilon$  is the extension of the specimen at time  $t$  and  $\epsilon_0$ ,  $\beta$  and  $k$  are constants. Here the  $\beta$  component describes primary creep arising from slip processes within the grains. When  $k=0$ , the equation can be expressed as

$$\epsilon = \epsilon_0 \cdot (1 + \beta t^{1/3}) \quad (2.4)$$

This contribution diminishes with time and describes the

shape of primary creep curves. When  $B=0$ , the equation:

$$\epsilon = \epsilon_0 \cdot e^{kt} \quad (2.5)$$

describes the steady state or secondary creep. The  $k$  component is caused by both grain boundary sliding and dislocation movements within grains.

Equations like Andrade's are not applicable over a whole range of conditions. Wyatt [reported in 23] conducted tests with polycrystalline copper and discovered that at low temperatures the curve was logarithmic, but at higher temperatures the strain was greater than that predicted. He thus proposed:

$$\epsilon = a \log t + bt^n + ct \quad (2.6)$$

where  $a$ ,  $b$ , and  $c$  are constants and  $n=1/3$ .

In general all equations tend to be empirical and whereas they may be applicable at low temperatures are not so at higher ones.

### 2.5.2 Secondary Creep

The second stage, or steady state creep, occurs as a linear function of time and is related to both temperature and stress. Several attempts have been made to model secondary creep rate. For example,

$$d\epsilon/dt = A \cdot \exp(-(Q-\alpha \cdot \sigma)/RT) \quad (2.7)$$

where  $A$  and  $\alpha$  are constants and  $R$  is the gas constant.  $T$  is the temperature and  $Q$  is the activation energy, when the applied stress  $\sigma=0$ .

Where self diffusion (eg vacancy movement) is important:

$$\frac{d\epsilon}{dt} = \frac{B \cdot \sigma^n}{G} \cdot \exp(-Q_{SD}/RT) \quad (2.8)$$

where B is a constant, G the shear modulus and  $Q_{SD}$  is the activation energy for self diffusion.

Much attention has been given to determining Q which provides a way of distinguishing deformation mechanisms. A significant variation in Q leads to the idea that a substantially different mechanism is occurring, (at low temperatures dislocation climb is the rate controlling process).

Structural changes during secondary (and tertiary) creep are caused by slip, grain boundary sliding and sub-grain formation. There is evidence that grain boundary migration is an important mechanism in the creep deformation of zinc and its alloys [25]. Increasing the temperature leads to an increase in the coarseness of slip bands, however, much finer slip bands can be observed between larger ones. In metals with a high stacking fault energy (eg Zn) where dislocations are wide, sub-structures are found within grains. In aluminium, sub-grain orientation is related to strain. At higher temperatures sub-grain size increases. All of these changes depend on thermally activated processes and occur at temperatures greater than  $\frac{1}{2}T_m$ .

A general equation can be used to describe secondary creep rate:

$$d\epsilon/dt = A \cdot \exp(-\delta H/RT) \quad (2.9)$$

where  $\delta H$  is the activation energy for the rate controlling process.

Note that if the creep mechanisms operate independently of

each other then the lowest activation energy is the rate controlling mechanism. However, if the mechanisms are dependent on each other then the rate controlling mechanism is the one with the highest activation energy.

If dislocation sub-structure remains constant then the activation energy for secondary creep is equal to the activation energy for self diffusion.

The activation energy for self diffusion,  $Q_{SD}$ , is equal to the sum of energies for the formation and movement of vacancies:

$$Q_{SD} = Q_F + Q_M \quad (2.10)$$

Vacancy formation and movement allows dislocations to move by climb and intersect (jog formation) leading to the view that vacancy movement is the rate controlling process. This is backed up by evidence of sub-structure formation. Metals with large self diffusion coefficients show less creep resistance than metals with smaller ones.

Other mechanisms operate at different temperatures and stress conditions. With cross slip, activation energy decreases with increasing stress. Grain boundary sliding is a problem with decreasing strain rate and higher temperature. Cavities can easily form.

It is also useful to consider the equi-cohesive temperature. This is the temperature at which fracture changes from transgranular to intergranular. A material with a large grain size will have a higher strength above the equi-cohesive temperature. Below this temperature the reverse is true. Dislocation climb is also slower in a coarse grained material, since it becomes more difficult for vacancies to nucleate.

### 2.5.3 Formula For Creep in Zn Alloys

A detailed investigation of creep behaviour in die-cast alloys No.3, ZA8 and ZA27 was carried out by Murphy [reported in 1]. He derived a formula, relating maximum design stress ( $\sigma$ ), in MPa, to temperature (T), in Kelvin, and service life (t) in seconds:

$$\ln \sigma = \frac{c' + Q/RT - \ln t}{n} \quad (2.11)$$

where:  $n = 3.5$  (stress exponent)  
 $Q = 106$  kJ/mol (activation energy)  
 $R =$  gas constant  
 $c' =$  constant relating to structure

This equation is valid for stresses up to 50MPa.

The equation can be rearranged to the form:

$$1/t = \sigma^n \cdot e^{-(Q/RT+c')} \quad (2.12)$$

This is the same form as the generalised equation for secondary creep stated earlier (equation 2.9).

### 2.5.4 Rules for the Development of Creep Resistance [24]

Several guidelines for the promotion of good creep behaviour are listed below.

- use below  $\frac{1}{2}T_m$  (- for pure zinc  $\frac{1}{2}T_m=73^\circ\text{C}$ )
- use of solute additions to lower stacking fault energy
- solid solution hardening
- long range order
- use of fine precipitates to prevent dislocation movements
- use of precipitates in association with crystal defects
- composite material

The basic reason for the poor creep resistance in zinc above  $100^\circ\text{C}$  is because this is above  $0.5T_m$ . The use of a composite material may be a viable solution to the creep problem.

## 2.6 Summary

The economic necessity to retain the market position of zinc as an engineering material was the driving force behind the development of ZA alloys. As a result, zinc base alloys, traditionally pressure die-cast alloys, now compete with other alloys of aluminium, copper and iron, in general foundry applications, particularly where wear resistance or bearing properties are required.

Advantages claimed for ZA alloys are ease of casting, cheaper, pollution free melting and good finishing characteristics. Disadvantages of the alloys arise because of structural re-organisation, due to the incompleting solid state reactions. These reactions have been studied in detail and can cause dimensional changes and loss of strength as they proceed towards equilibrium. Important factors affecting solid state transformations are solidification rate, which controls the scale of the as-cast structure, and cooling rate to room temperature, which affects their extent. The mechanical properties of ZA alloys are process dependent.

The effect of processing by squeeze casting is an interesting avenue for research. Squeeze casting is a method for producing near-net shape metal matrix composites. Its use in producing composites in ZA alloys is attractive from the view point of better higher temperature properties, ie those above 100°C. This work is intended to be a process based approach. It is not the intention to try to study the progress of solid state transformations, rather to be aware of their existence and perhaps to cite them as reasons for property differences. For instance, rapid solidification and solid state cooling may produce different properties to those produced by slower solidification and moderate solid state cooling.

### 3. Squeeze Casting

#### 3.1 Near-Net Shape Processes

Near-net shape processes are attractive from the point of view of materials utilisation and reduction in machining and finishing costs. The easiest way to transform an ingot of metal into a shaped component is to melt it and cast it into a mould. Many processes are available, each with different capabilities, but the range is such that components with weights from a few grammes to 300 tonnes can be commercially produced [26]. (Casting processes do suffer from some problems. Mechanical properties of cast structures tend to be weaker than say forge processed structures, due to gas and shrinkage porosity in the casting, variations in grain size, type and segregation. Mechanical properties in castings are, however, isotropic in a section, whereas forged structures can be anisotropic. Surface finishes of castings depend on mould material and can vary from CLA 3-25 $\mu$ m for castings produced in a green sand mould, to CLA 1-12 $\mu$ m for those produced by investment, or pressure die casting [26].

Techniques for improving the soundness of cast components include feeding, the use of chills, directional solidification and melt treatments. Generally, the easiest type of alloy to cast sound is one with a short solidification range, for example a pure metal or eutectic. Long freezing range alloys, ie those whose liquidus-solidus is greater than 50 $^{\circ}$ C, are more difficult to cast sound when cooled slowly. The extended freezing range provides more opportunity for micro-shrinkage, segregation effects and gross changes in microstructure to occur, which will result in poor mechanical and physical properties. The inherent heterogeneous structure of a large ingot can to some extent be homogenised in specific directions, by secondary thermo-mechanical working processes, which weld-up defects. These processes give a texture to the structure and improve properties. However, this is not an option in near-net shape casting production. Many steps are required to produce an

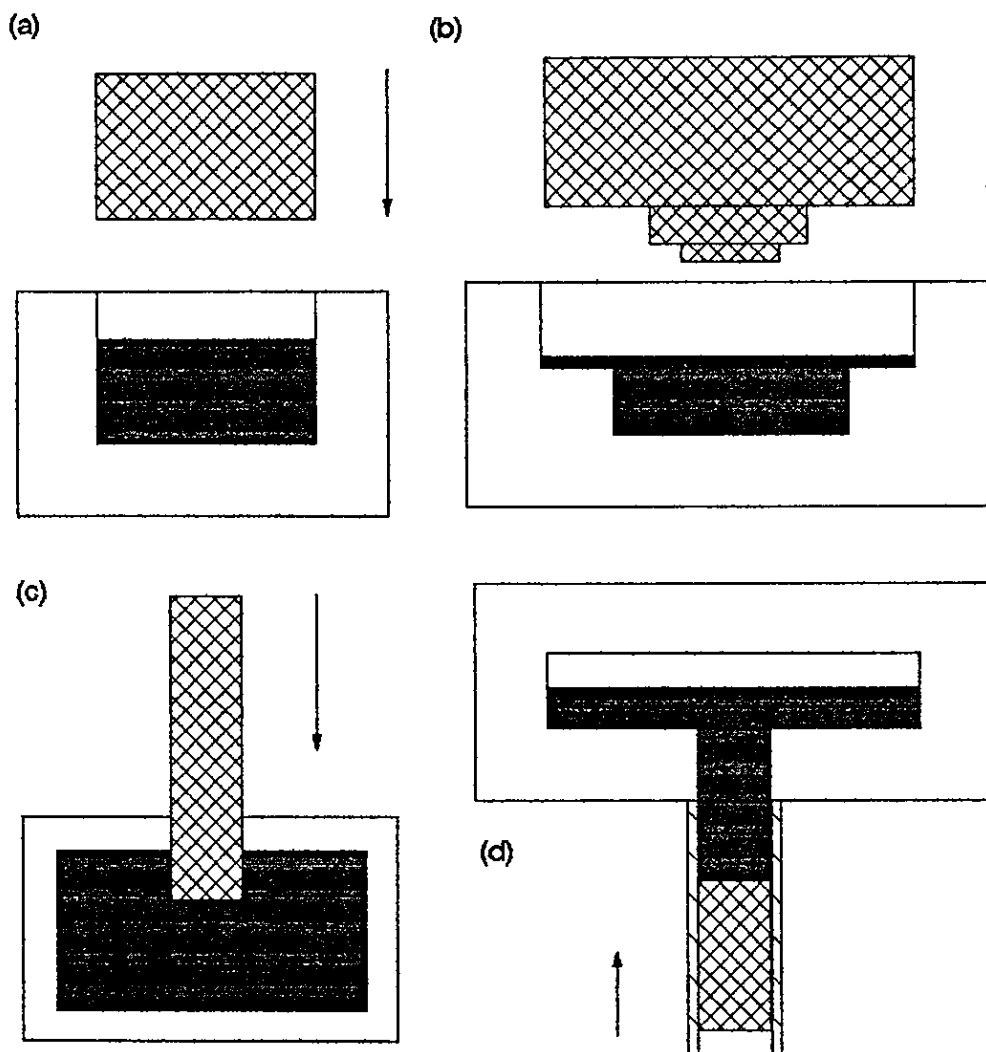
article, such as a connecting rod, by forging.

A process which was able to transform an ingot into a near-net shape component, with uniform microstructure, no porosity and a good surface finish would be, in theory, most useful. Squeeze casting is such a near-net shape manufacturing process, which is used for the production of high integrity components in both non-ferrous and ferrous alloys. However, most interest appears to be with lower melting point alloys, for example aluminium [27]. Recently, the process has been used for the production of near-net shape metal matrix composites.

*Squeeze Casting*  
The process is often considered to be a hybrid of die casting and closed die forging. It offers the designer the opportunity to specify components with the complexity of gravity or pressure die casting, but with the mechanical properties of hot forging. The process described in the following sections, has never attained widespread acceptance. This may be because of relatively high equipment and set-up costs and perhaps design limitations. Its ability to produce sound metal matrix composites may see its popularity increase.

### 3.2 Process Fundamentals

Four variants of squeeze casting exist, as shown in Figure 3.1, but each utilises pressure on the metal throughout the whole of the solidification process. This differs from other processes. In gravity die casting only atmospheric and metallostatic pressures are used and there is a need for runners and risers, to ensure soundness in the finished product. In pressure die casting, pressure is used to force the metal into the die, through small ingates. These ingates solidify soon after injection and pressure is not exerted on the solidifying metal. Porosity can be a problem in pressure die casting. However, good design can ensure that it is limited to non-critical areas. The Acurad process [28] utilises an inner plunger and wider ingates, in an attempt to



(a) direct pressure, no metal movement

(b) direct pressure, metal movement

(c) indirect pressure, no metal movement

(d) indirect pressure, metal movement



die



punch



metal

Figure 3.1 Forms of squeeze casting

consolidate metal in the die. As mentioned previously, forging processes use pressure on solid metal to impart a change of shape and to improve mechanical properties. These are improved as a result of structure modification and 'welding-up' of voids, although there is often anisotropy in properties. The basic aim in squeeze casting is to apply a hydrostatic pressure over the whole surface area and to achieve solidification across the whole section concurrently. This results in elimination of any directionality and production of a fine equiaxed grain structure throughout the cross section.

System 1 is a direct pressure system, which does not involve metal movement. It can generally be used for components with a section thickness upwards of 7mm [29]. System 2 involves backward extrusion of liquid metal, which results in reduced solidification time [29]. It is most useful for hollow shaped components with wall thicknesses from 2 - 100mm. Systems 3 and 4 are indirect pressure systems, useful for shaped components. System 4 is utilised commercially in the UBE design of squeeze casting machines [30].

Whichever variation is used, a measured amount of metal is poured into the female side of a heated die. When the metal is completely liquid or partially solidified pressure is applied via a heated male die and then maintained throughout solidification. After solidification the casting is ejected and the process can be repeated. Important parameters are pouring temperature, die temperature, squeeze time, squeeze pressure and holding time under pressure.

The cycle time for squeeze casting is less than for gravity die casting and the yield is higher. One effect of pressure is to force the molten/semi-molten metal against the mould wall, thereby increasing heat transfer and decreasing solidification time. Thus, the structure is refined and the casting detail is improved. Pressure aids feeding, by compaction and so called inter-granular burst feeding [29],

promoting soundness and obviating the need for feeders. Pressure helps to keep the gases in solution, preventing bubbles from nucleating. It also affects the metal thermodynamically and metallurgically (see later), resulting in refined structures and non-equilibrium phase precipitation (cf rapid solidification processed alloys). The pressure used is less than that required for forging, which results in an increased die life. However, the mechanical properties are comparable and non-directional. In fact, some alloys which are not castable, due to their long freezing range can be effectively squeeze cast, with isotropic properties [31].

Advantages claimed for the process are as follows [32]:

- an ability to produce parts with complex profile and thin sections beyond the capability of conventional casting and forging techniques.
- substantial improvement in material yield because of the elimination of gating and feeding systems.
- significant reduction in pressure requirements, in comparison with conventional forgings, while at the same time increasing the degree of complexity that can be achieved with the parts.
- ability to use both cast and wrought compositions.
- improvements in product quality with regard to surface finish, dimensional accuracy and mechanical properties.
- complete elimination of shrinkage and/or gas porosity.
- castings can be heat treated.
- potential for using cheaper, recycled material without the loss of properties that would occur with other processes.
- the potential for increased productivity in comparison with gravity die casting or low pressure die casting.
- suitable for the production of cast composite materials.

### 3.3 Theory

#### 3.3.1 Effect of Pressure on Solidifying Metals and Alloys

Pressure applied to a solidifying metal or alloy can affect its microstructure relative to the slow cooled alloy. A combination of accelerated cooling (because of good heat conduction) and a thermodynamic effect (modelled by the Clausius Clapyeron equation) which causes a change in the metal melting point and may affect nucleation [33-35], help to explain differences in microstructure.

The Clausius Clapyeron equation for a liquid/solid transformation in a pure substance can be written as:

$$\frac{\Delta T}{\Delta P} = \frac{T_f (V_L - V_S)}{L_f} \quad (3.1)$$

where:  $T_f$  = equilibrium freezing temperature  
 $V_L$  = specific volume of the liquid  
 $V_S$  = specific volume of the solid  
 $L_f$  = latent heat of freezing  
 $\Delta T$  = change in melting point  
 $\Delta P$  = change in pressure

When the specific volume of the solid is less than that of the liquid  $dT/dP$  is positive and an increase in pressure raises the melting point. This is the case for most metals which solidify with a close packed structure. When the reverse is true then an increase in pressure causes a decrease in melting point (eg silicon and bismuth). To quantify this effect, for a rise in pressure of 98.1MPa pure aluminium undergoes a change in melting point of +6.3K and pure zinc +3K, [35].

The effect for alloys is more difficult to quantify exactly but it is generally accepted that similar effects will occur across the whole range of compositions (Figure 3.2). Eutectic points tend to move upwards and towards the



component whose melting point is least affected. Thus it is possible for an alloy which is hypereutectic under equilibrium cooling to exhibit a hypoeutectic microstructure when solidified under pressure.

Nucleation may be induced by enforced supercooling, if pressure is applied to a melt held just a few degrees above its equilibrium melting point. Sudden application of pressure causes juxtaposition of the liquidus, to the extent that the liquid is supercooled, resulting in nucleation across the whole section. A similar nucleating effect may also occur if pressure is applied at the nil fluidity point, which is usually half way between the liquidus and solidus lines. This, according to some investigators [36] is the optimum time to apply the pressure, although higher levels need to be applied compared to the liquid state. Nucleation may be stimulated in the remaining liquid, due to undercooling, since the liquid has a lower liquidus than the initial melt. Fragmentation of the skeletal structure will no doubt ensue, providing kindred nuclei, which promote increased grain nucleation.

Pressure above a critical level [29] will tend to eliminate the usual air gap between the solidifying casting and the mould wall. In conventional gravity die casting of certain long freezing range alloys this air gap can cause problems. Inverse segregation, for example, can occur because the metallostatic pressure developed during solidification can be sufficient to cause the low melting point residual liquid to flow into this gap. This will result in voids being left in the casting and a poor surface finish.

Air gap elimination also results in high heat conduction away from the solidifying casting. Various estimates as to the effectiveness of pressure in increasing heat transfer coefficients give the maximum effects at between 50MPa and 100MPa [27]. High heat transfer coefficients coupled with fast solidification and steep temperature gradients, which

depend primarily on mould and pouring temperatures, can result in supersaturation of primary phases and alterations in amount and distribution of secondary phases. Lipchin and Tomsinskaya [35] have studied the effects of solidification under pressures of 0-400MPa, in steel and copper chill moulds, using Al-Mg, Al-Cu, Al-Si and Mg-Al alloys. They concluded that the eutectic point shift was a result of the pressure, as previously described, and that solid solution concentration varied primarily with crystallisation conditions (ie temperature gradients). Pressure tended to reduce the solid solution ranges to the extent that eutectic was visible in alloys of low solute concentration which would normally be single phase. These changes appeared to improve strength through a reduction in porosity, an increase in dislocation density and grain refinement.

### 3.4 Effect of Processing Variables [37]

#### ✓ 3.4.1 Design

The design of the casting and the way it is manufactured must be such that pressure can be applied to a liquid metal throughout the whole of the solidification process. In the example in Figure 3.3a the thin flange would solidify first and pressure could not be applied to the base of the casting. One solution may be to use a uniform section thickness combined with a shaped punch, as shown in figure 3.3b.

#### ✓ 3.4.2 Melt Quality

Good quality metal, which is skimmed free from oxide, is necessary, as no provision for dross traps can be made. Degassing is usually advised for aluminium alloys but pressure application should inhibit hydrogen bubble formation.

#### ✓ 3.4.3 Melt Temperature

Holding temperatures should be low, to minimise oxidation.

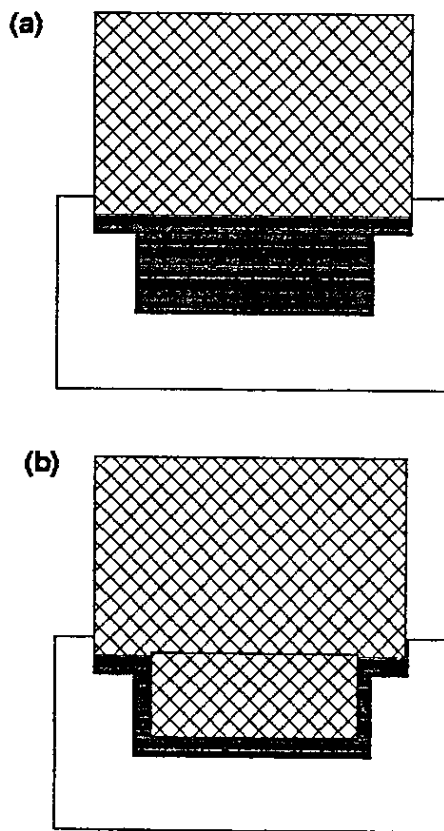


**Figure 3.3 Example of bad (a),  
and good (b) design.**

#### **3.4.4 Pouring Technique**

Transfer from ladle to crucible should be done in such a way as to reduce turbulence and to minimise oxidation.

#### **✓3.4.5 Die Temperature**

This factor needs to be optimised for particular alloy systems and casting designs. Temperatures of greater than 150°C are used, to reduce the incidence of thermal cycling cracks. However, too high a temperature may lead to die to casting welding.

#### **3.4.6 Die Lubrication**

An even coating of water based, graphite solution is usually used for aluminium alloys. The die usually needs to be re-coated for each casting because the coating is removed, by abrasion due to the intimate contact between the solidifying casting and the mould wall.

#### **✓3.4.7 Casting Temperature**

As with die temperature, this factor needs to be optimised for particular combinations of casting and alloy. Longer freezing range alloys should be poured only a few degrees above the liquidus, whereas short freezing range alloys can be poured at higher levels of superheat.

#### **3.4.8 Time Before Application of Pressure**

This delay can be compensated for by careful choice of die and pouring temperatures, to ensure that the metal is pressurised at the prerequisite temperature.

#### **3.4.9 Time to Build up to Full Pressure**

Some investigators [29] have reported that if pressure is applied to partially solidified metal, then a short build up to full pressure is required.

#### **✓3.4.10 Pressure Level**

The amount of pressure required depends on the complexity of the casting and the point in time at which it is applied.

Ingots appear to need about 100MPa. Thin sections, especially in extrusion type castings, may require much less.

#### ✓ 3.4.11 Pressure Duration

One second per mm of casting cross section is normally quoted as being sufficient to solidify castings [38]. Longer levels of pressure duration may affect solid state transformations, during cooling.

#### 3.4.12 Delay Before Ejection

Too long a delay may make the casting difficult to eject and may result in the casting becoming heat treated.

### 3.5 Specific Examples

Both casting and forging alloys of non-ferrous and ferrous metals have been studied. Most effort appears to have been directed towards the lower melting point alloys, eg aluminium.

#### 3.5.1 Aluminium Casting Alloys

Aluminium casting alloys usually contain silicon, with additions of copper, magnesium, manganese and other elements.

##### 3.5.1.1 Aluminium-Silicon Alloys

Aluminium-silicon alloys have been studied by several authors [8,27,39].

Chatterjee and Das [8] considered the squeeze casting of LM6, which is near eutectic Al-Si (actual composition not quoted). The alloy is widely used because of its good fluidity, but can be brittle due to angular  $\beta$ -silicon particles. Modification of the alloy is commonly carried out to alter the form of the eutectic  $\beta$ -silicon particles. Modification changes the growth form of the  $\beta$ -silicon phase from a faceted angular appearance to a fibrous, rod like form. This can be achieved by rapid solidification (quench modification) or by elemental additions. Chatterjee and Das found that a combination of both factors produced a casting with superior

strength and elongation properties. A critical level of pressure had to be applied to the solidifying ingots.

Chatterjee and Das found increased tensile strength and elongation in squeeze-cast unmodified LM6 with increases in pressure up to 300MPa at a fixed die temperature. Strength increases were attributed to both changes in eutectic amount and morphology (positive effect) and to increase in alpha phase (less significant negative effect) resulting in a non-linear increase in strength with pressure. Elongation increases were attributed to more primary alpha phase (positive effect) and less, but finer, eutectic (also positive). Increases in alpha phase were due to shift in the eutectic towards higher silicon contents. This also caused a decrease in the amount of eutectic.

Squeeze cast modified LM6 showed a peak UTS value of 207MPa. Elongation values were exceptionally high at up to 18%.

Williams [39] quotes a UTS value of 187MPa, a 0.2% proof stress value of 103MPa and 13% elongation in squeeze formed LM18 (Al-5Si). These results were from a number of test pieces extracted from actual castings. They compare with typical chill cast properties of UTS 140-150MPa, 0.2% proof stress (PS) of 60-80MPa and elongation of 4-6%.

Chadwick and Yue [27] report on the squeeze casting of Al-Si alloys with 7 and 14wt% Si. They measured an upward movement of the liquidus and eutectic of 9K and 2.25K respectively, but state that this has little, if any, effect on refinements in grain structure. Thus they repudiated claims made by Franklin and Das [40] on structural refinement by pressure related effects. They claim that the only effect pressure has on the microstructure is to increase heat transfer coefficients up to a maximum at 100MPa. Presumably any further increase in pressure would not affect grain size but may be necessary to promote feeding in alloys when the pressure was applied between the liquidus and solidus lines.

### 3.5.1.2 Alloyed Aluminium-Silicon Alloys

These alloys have been studied more extensively than the binary Al-Si alloys. In the United States, the IIT Research Institute [41] studied A356 and noted a refinement in the squeeze-cast alloy relative to the chill-cast alloy.

Das and Chatterjee [7] investigated two Al-Si-Cu alloys, LM4 and LM24. Pressure applied during solidification tended to suppress the formation of the  $\alpha(\text{Fe Al Si})$  phase, which would normally cause embrittlement. Both alloys showed increases in strength and hardness, with increasing squeeze pressures.

Various authors affiliated with GKN [31,39,42] have reported on the squeeze-forming of LM25 alloy. In all heat treatment conditions, M, TE, and TF, the squeeze-cast alloy was stronger and had better elongation than the chill-cast alloy. Significant increase in fatigue resistance of the squeeze-cast alloy is also reported. The main advantage of squeeze casting is claimed to be the use of an alloy with higher levels of iron (0.5% v 0.2%) than would be acceptable for gravity casting. The formation of brittle iron aluminide and Fe-Al-Si needles appears to be suppressed in squeeze-cast samples.

Chadwick and Yue [27] reviewed work on squeeze-cast LM24, LM25 and A357. They considered that the dynamic properties of squeeze-cast LM24 were superior to those of conventionally cast material. LM24, a lower cost, higher iron alloy, when squeeze-cast, can exhibit better fatigue behaviour than conventionally cast, higher purity alloys. This is due to the absence of large plates of embrittling Fe-Al-Si compounds, the refinement of the primary phase and eutectic constituents and the absence of porosity.

Kaneko et al. [43] describe the use of JIS AC4C (356) alloy, which, in the squeeze-cast condition, has mechanical properties intermediate between gravity cast and forge processed alloy.

### 3.5.1.3 Aluminium-Magnesium Alloys

Authors affiliated with GKN have also reported the results for squeeze-formed LM5 [31,39,42]. Mechanical properties of the squeeze formed alloy were UTS 250MPa, 0.2%PS 142MPa, and elongation of 14% relative to typical chill-cast properties of UTS 170-230MPa, 0.2%PS 90MPa, and elongation values of 5-10%.

Zantout [10] squeeze-cast LM5 and also found increases in strength and elongation with increases in squeeze pressure.

Weinberg [44] has carried out squeeze-casting on the binary alloy Al-10Mg. The material showed little change in 0.2%PS with applied squeeze pressure, but did show large increases in UTS. The explanation for this is probably due to the increased soundness relative to gravity-cast material. Elongation values were increased accordingly.

### 3.5.1.4 Wrought Aluminium Alloys

Wrought aluminium alloys have poor casting properties and are generally difficult to cast sound. The use of squeeze casting greatly aids casting capability and several high strength alloys have been produced by this route and their properties evaluated. A general observation is that squeeze-cast material is fully isotropic, whereas there may be differences in forged material properties in the longitudinal (L) and transverse (ST) properties.

### 3.5.1.5 Aluminium-Copper Binary Alloys

Asaeda [36] investigated the partial solidification under pressure of Al-Cu alloys where the pressure was applied when the alloy was in a mushy state. Previously cast billets were reheated to various temperatures and then squeezed at various pressures into dies held at different temperatures. Tensile strengths and elongations were seen to increase with pressure, to the extent of 3-4 times in strength and 6-10 times in elongation, compared to gravity-cast material. The gravity-cast material had a grain size of 50-70 $\mu$ m with CuAl<sub>2</sub>

present at the grain boundaries. The extent of this phase decreased and virtually disappeared at higher processing pressures. Asaeda suggested that grain size is not affected but sub-boundaries increase. The best property improvements occurred when pressure was applied when the metal was at a point mid-way between its liquidus and solidus. Asaeda's observations about grain size may be due to the fact that a skeletal structure from the solid ingot could still be present as the billet would not be completely remelted. [36]

Weinberg [44] noticed that elongation values in Al-Cu alloys were improved with increasing load but found no effect on UTS and 0.2%PS.

#### 3.5.1.6 Aluminium-Copper-Magnesium Alloys

Asaeda [36] also investigated Al-4.5Cu alloys with magnesium additions from 0.5 to 5% at one die temperature and one pressure. Again, maximum properties were obtained at the mid-point, between liquidus and solidus. Maximum tensile strengths were achieved in the 1% alloy. Asaeda's explanation is not translated clearly, but changes appear to be related to the distribution of copper/magnesium compounds and the extent of the dendritic structure in the ingot.

#### 3.5.2 Aluminium Forging Alloys

Benedyk [41] studied the squeeze-casting of 6061 alloy and found that it had a fine, equiaxed appearance, no gas porosity and no shrinkage voids. It compared favourably with wrought 6061 material. His work led the way for low pressure forming of wrought alloys.

Williams and Fisher [42] report on work done with 7075, 2014, 6061, 6066 and 6082 aluminium alloys, to either T6 or T73 condition and on a non-standard Al-4Zn-2Mg alloy in T73 condition. Poor ductility in these squeeze-cast alloys was attributable to the presence of appreciable amounts of copper, as  $\text{CuAl}_2$ , at the grain boundaries, which was difficult to disperse by heat treatment. Some reservations

about the materials were cited but their properties were deemed acceptable. The ability to cast 7000 series alloys was most significant.

Chadwick and Yue [27] suggest that the 2000 and 6000 series alloys respond in individual fashion to squeeze-casting and not all the alloys respond well. 6066 and 2014 were found to have lower strengths than type L forgings. The lower copper containing 6061 appeared to respond well. They expressed the opinion that Al-Mg-Si alloys should respond well to squeeze casting.

Yue [reported in 27] has looked at the influence of squeeze-casting on 7010 aerospace alloy and has shown grain size of squeeze-castings to be a significant factor in the control of mechanical properties. No improvements in properties were obtained after 50MPa, which was enough to eliminate porosity. The fatigue limit increased with decreasing grain size, whereas the fracture toughness increased with increasing grain size, in the range of 70-800 $\mu$ m, which can be controlled by the squeeze-casting parameters.

### **3.5.3 Other Alloy Systems**

Relatively little information is available about other squeeze-cast alloy systems. The following information is gathered from a number of review articles.

#### **3.5.3.1 Non-Ferrous Alloys**

**Magnesium Base** Chadwick and Yue [27] summarise work done on three magnesium alloys: AZ91, a casting alloy; and AZ31 and ZCM711, which are both wrought alloys.

Advantages of processing AZ91 by squeeze casting are grain size control and considerable reduction in porosity, when compared to conventional sand, gravity and pressure die casting processes. Strength and elongation values are superior in the squeeze-cast material, although the authors

state that these are only marginal, especially in the fully treated condition. Squeeze-cast AZ31 has inferior properties to longitudinal values from the wrought material. ZCM711, which contains 7% Zn, 1% Cu and 1% Mn, is a precipitation hardening alloy. In the wrought state it has stringers of  $Mg_2Cu$  in the microstructure, giving superior properties in the longitudinal direction, in comparison to those in the transverse direction. The squeeze-cast alloy produces a structure with dispersed  $Mg_2Cu$  but does not respond to heat treatment. The development of a new alloy, HTM1, which will be able to withstand loading of up to 50MPa and temperatures of up to 453K, is suggested. The need to tailor alloys for the process is highlighted.

**Copper Base** Outside Russian literature several authors have described squeeze casting of copper base alloys [reported in 38]. Two alloys, 85Cu, 5Sn, 5Pb 5Zn and 63Cu 1Sn 1Pb 35Zn were investigated. The alloys, although having long freezing ranges, showed an absence of micro-porosity and had a fine structure.

Lynch [45] reported on squeeze casting research into the following copper base alloys:

CDA377	forging brass
CDA865	cast Mn-bronze
CDA674	wrought Al-bronze
CDA925	leaded Sn-bronze.

Squeeze casting produced materials with superior mechanical properties, compared to conventional casting specifications. They met or slightly exceeded wrought specifications but produced slightly lower elongation.

Benedyk [41] described the squeeze casting of a long freezing range super-alloy, X-40. Excellent surface finish was noted. Microstructurally, the grain size was fine and this improved

the room temperature properties relative to conventional casting.

### 3.5.3.2 Ferrous Materials

**Steels** Bedyk also reported on squeeze-cast M2 tool steel and type 347 stainless steel [41]. Excellent surface finish was noted on the M2 sample, which was produced with a ceramic mould coating. Squeeze-cast 347 stainless steel showed a higher strength and elongation than the sand-cast equivalent.

**Cast Irons** A Russian paper [33] describes the squeeze casting of a grey cast iron, at pressures of up to 3GPa. Fast cooling resulted in white iron formation. SG iron has also been squeeze-cast [38], but castings had to be annealed to break-down the white structure.

### 3.5.4 Zinc Base Alloys

As part of a wider investigation into ZA alloys, ILZRO via Noranda carried out some work into the squeeze-casting of Zn-27Al alloy [46]. The squeeze-casting of 50 components was sub-contracted to the Nippon Light Metal Company Ltd, in Tokyo. They produced ingots of 43mm diameter by 78.5mm long, with the following processing conditions:

Pour	: 650°C
Pressure	: 79MPa
Pressure Duration	: 45s

A thick graphite mould release agent was reported to have been used. A homogeneous microstructure was observed and no porosity was present. Dendrite size in the squeeze-cast specimens was the same across the section.

Comparison of mechanical properties between the squeeze-cast and sand-cast results was probably not accurate because of the low copper content of 0.88% in the squeeze-cast samples compared to 2.2% in the sand cast samples.

Mould temperature was not recorded but was reported to be about 335°C.

It was concluded that the effect of pressure, temperature and time on the properties of squeeze-cast alloys should be studied further.

Yakoub [47] conducted a study into the squeeze casting of ZA alloys. His results were based on experimentation, using an ingot die, which produced castings of 75mm L and 52mm dia. He manufactured his samples under the following parameters:

Squeeze Pressures	:	92	139	185	MPa
Press Loads	:	20	30	40	Tons
Delay before pressure application	:	6s			
Pressure duration	:	60s			
Die coating	:	colloidal graphite			

ZA27 was squeeze cast at die temperatures of 20, 50, 90, 180 and 250°C with pouring temperatures of 514 and 535°C.

ZA8 and ZA12 were produced with die temperatures of 50, 90, 130, and 190°C. ZA12 was poured at 481°C and ZA8 at 464°C. They were compared to gravity cast material produced under the following conditions:

ZA27 Die Temps	20	50	90	180	250 °C
Pour Temps	535°C				
ZA8/ZA12 Die Temps	20	90	130	180	°C
Pour Temps ZA8	464 °C	ZA12	481 °C		

Ingots were examined both as-cast, as homogenised (320°C, 3hrs, slow 0.5°C per minute cool) and as aged (95°C various times).

His assessment was based on mechanical (tensile uni-axial) property evaluation and metallographic analysis.

Yakoub also investigated dimensional changes in squeeze-cast alloys at  $95^{\circ}\text{C} \pm 2^{\circ}\text{C}$ .

Yakoub reported pore-free ingots for all alloys. He stated that the die temperature had a considerable effect on the structure and mechanical properties of squeeze-cast ZA alloys and that 92MPa was sufficient pressure to form ingots. Further increase in pressure appeared to have little effect on properties. Higher mechanical properties with respect to gravity ingots of the same section thickness were apparent.

Squeeze casting appeared to have little effect on the ductility of ZA8 and ZA12 but improvements of up to 50% were noted for ZA27.

### 3.6 Applications

Commercial applications of squeeze casting have tended to be for high volume products. Squeeze-cast aluminium alloy pistons, especially for diesel engines, have been manufactured by AE [48] and Gould [49]. An increase in rotating bending fatigue strength of the squeeze-cast alloy relative to the gravity-cast alloy was reported.

Toyota have produced a squeeze-cast wheel [43]. A pilot plant, at Alures in Portoscuso, Sardinia, also produces squeeze-cast wheels, using the UBE process [50].

The most publicised example of a squeeze-cast product is GKN Squeezeform's MCV80 tank wheel [31]. This wheel, of 20kg mass, is approximately one third of the mass of a forged steel wheel. This greatly extends the range and speed of the tank. The wheel is produced on a 1500 tonne press, from a 7000 series aluminium alloy. It incorporates a wear resistant stud chain, which is cast in situ.

Kulkarni [51] has described the manufacture of hubs, turbine blades and gun barrel supports on a development basis.

### 3.7 Summary

Squeeze casting has never gained widespread commercial acceptance, although the products are of high integrity, as for example the GKN Squeezeform tank wheel shows. The process is more suited to chunky type castings, with a wall thickness upwards of 8mm.

In research and pilot plant development, several alloys have been cast and most show improvements in properties. It is clear that process parameters have to be optimised for a particular set of alloy/die combinations. However, no information is available as to how these parameters can be quantified. It would be useful to know the cooling rates, their associated temperature gradients and the rate of movement of solidification fronts to obtain the optimum properties. However, these may be difficult to obtain in a high solidification rate process.

The use of squeeze casting, to enhance the room temperature mechanical properties of zinc-base alloys, is attractive. In addition, the use of squeeze casting to produce near-net shape metal matrix composites and an investigation of their properties at elevated temperatures would be useful.

Yacoub's work on squeeze casting of ZA alloys was performed at squeeze pressures of up to 185MPa. Rajogopal [38] has suggested that higher pressures may be required, for consolidation, in some alloys, especially during the final stages of solidification.

The effect of section thickness of squeeze-cast alloys has not been widely reported. Such information would provide useful information for designers. The high fluidity of ZA alloys should enable them to fill thin sections relatively easily.

## 4. Metal Matrix Composites Utilising ZA Alloy as a Matrix

### 4.1 Introduction

ZA alloys have many potential applications, for instance, in transportation. However, the alloys have not gained widespread acceptance, because of their comparatively poor mechanical properties at temperatures upwards of 80°C.

In the keynote address paper to the 25th Annual Conference of the Canadian Institute of Metallurgists, Gervais [3] notes that ZA alloys have raised the limiting operating temperatures for zinc base alloy castings. However, further raising of the temperature would open up more markets. There is a need to double the present creep resistance above 75°C, but at the same time achieving ductility in the region of 15%.

One possible solution to the creep problem, as well as benefitting for instance, elastic moduli and perhaps weight saving, would be to manufacture metal matrix composite materials using suitable reinforcements. Previous work has shown that it is possible to use a number of materials as reinforcements in zinc base alloys, for example:

continuous fibres or wires	[52]
chopped fibres	[53,54]
particulates	[55]

It is seldom the case that castings are stressed uni-axially. Continuous reinforcements will tend to be unsuitable for off-axis loading. Continuously aligned composites tend to perform less well, when loaded perpendicular to the fibre direction. A random arrangement of chopped fibres, whiskers or particulates, whilst not attaining the maximum properties obtainable in unidirectional composites, should be most suitable for the majority of loading regimes.

Successful metal matrix composites have utilised ductile, pore-free matrices for effective transfer of load from the

matrix to the fibre [56]. Any porosity could result in stress raisers and lowering of mechanical properties.

The best way to produce a cast, ductile, pore-free matrix is by squeeze casting. It is also possible to produce composites by squeeze casting a suitably prepared melt of matrix and reinforcement [54], by squeeze infiltration of a preformed mat [53], or by squeezing a slurry (compcasting) [57].

This chapter discusses the manufacture of, and potential mechanical property improvements that could be expected by reinforcement of ZA alloys, using the forms previously mentioned. Analysis from both the microstructural and macrostructural points of view is attempted, in order to explain possible property improvements.

#### 4.2 Synthesised Materials

The concept of composite materials has been exploited for a number of years, with the most common example being glass reinforced plastic (GRP). This material has the characteristics of being lightweight, stiff and tough, although it is made up from a low modulus, fairly weak, brittle, thermosetting plastic and a brittle, stiff, strong (if defect-free) reinforcement, glass. The two materials combine synergistically, to give a tough material with crack stopping, or deflecting capability. Other properties, eg elastic modulus, tend to be a weighted average of those of the separate ingredients and can be modelled by a rule of mixtures type equation.

Composite materials have been manufactured with metal, polymer and ceramic matrices, reinforced with metal, polymer and ceramic reinforcements. Reinforcements are available in various forms: continuous fibre or wire; chopped, aligned or random fibre; aligned or random whiskers and particulate. Hybrid composites, with two or more types of reinforcement, have also been produced [58].

At present there is worldwide interest in the manufacture and application of metal matrix composites. Metal matrix composite materials considered here have microstructures which are synthesised from component phases, eg metal matrix and ceramic fibre. Conventional metal alloys, however, have microstructures which are achieved by the control of naturally occurring phase transformations during solidification or thermo-mechanical processing [59]. This is in contrast to in-situ composites, which are formed by controlled solidification of specific types of alloys, eg nickel-cobalt. The driving force behind the development of metal matrix composites is improved and/or tailored properties, particularly at higher temperature.

Metal matrix composite (MMC) production in the US has tended to be directed towards high technology aerospace applications [60], using continuous fibre reinforcements, although there is now more interest in other materials and applications. In Japan, more emphasis has been given to commercial products [61]. The potential benefits of metal matrix composites could be applicable to many other industries, for example the automotive industry, if lower cost materials and processes could be utilised.

Ways of achieving this are by near net shape production, which eliminates or drastically reduces machining and/or secondary processing operations), using low cost materials (metal ingot, rather than atomised metal powder and particulates, rather than continuous fibre) together with mass production capability. The projected costs of many reinforcements will fall with time, provided that there is sufficient demand for them, when economy of scale factors will become apparent.

The most promising route for widespread application of low cost metal matrix composites is particulate reinforced alloys, manufactured by a solidification processing route. Although not able to compete with continuous fibre reinforced

materials in terms of strength, particulate reinforced materials can show significant increases in elastic modulus and wear resistance at room temperature. They can also show improved creep performance at higher temperature, compared to the base alloy.

Such is the interest in these materials that Alcan have commissioned a plant to produce silicon carbide particulate ( $\text{SiC}_p$ ) reinforced aluminium alloy which will have a projected cost premium of 10% over the conventional alloy [62]. Sample ingots of this material have been produced by an Alcan subsidiary, Dural of San Diego. The material is called Duralcan. It is claimed that the ingots can be remelted and cast by conventional foundry techniques. One of the major problems that has to be overcome is when trying to remelt or degas foundry returns. Any attempts to do so result in separation of the reinforcement from the alloy. Squeeze casting could certainly benefit this situation because runners and risers are not required and any gas problems would be eliminated with pressure.

The main focus of this chapter is cast metal matrix composites.

#### 4.3 Review of MMC Manufacturing Routes

Several methods are available for fabricating metal matrix composites. Chou et al [63], in their extensive review of fibre reinforced metal matrix composites, classify the methods as follows:

- fibre surface coatings and preforming techniques
  - chemical coating
  - CVD
  - PVD
  - plasma spraying
  - electrochemical plating

- **solid phase fabrication methods**
  - diffusion bonding
  - hot rolling
  - extrusion and drawing
  - hot isostatic pressing
  - high speed pressing
  - explosive welding
- **liquid phase fabrication methods**
  - infiltration under atmospheric pressure
  - infiltration under inert gas pressure
  - vacuum infiltration
  - combination methods
  - squeeze casting
  - rheocasting and compocasting

The choice of fabrication method is governed by the type of matrix and reinforcement. Those listed in the first category above are applicable to long fibres, which are coated with the matrix and then formed into composites by either solid or liquid phase techniques. Coating of fibres is necessary, because of their reactivity towards the molten metal alloy, or to enhance wetting in the liquid phase. The reactivity problem is such that solid phase fabrication methods, for example roll bonding between metal foils (especially with carbon fibre reinforced aluminium), were the only practical solutions.

Harris [64] conveniently summarised process routes for continuous fibre (Figure 4.1) and discontinuous fibre or particulate composites (Figure 4.2) in his review of cast metal matrix composites.

#### **4.4 Cast Metal Matrix Composites**

Three extensive reviews [64-66] and several other papers [67] have recently been published on the subject of cast metal matrix composites. Rather than repeat verbatim their contents, it is useful here to delve more deeply into some of

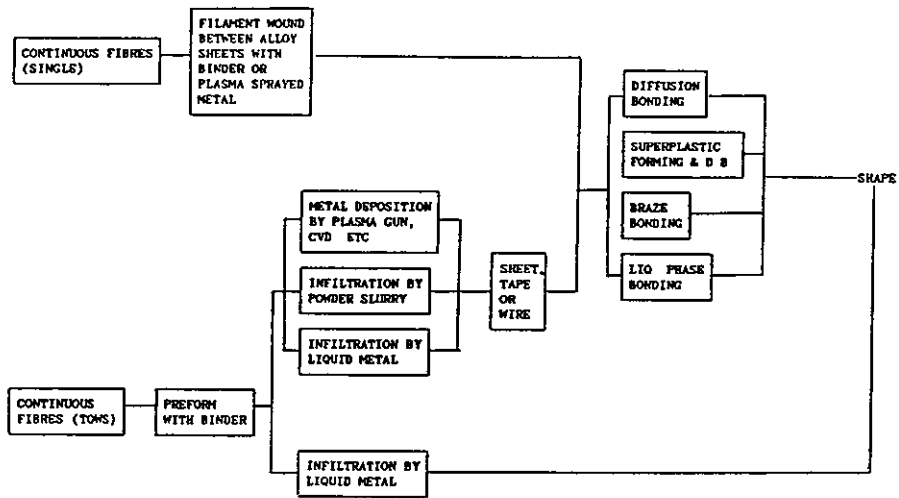


Figure 4 1 Process Routes for continuous fibre composites

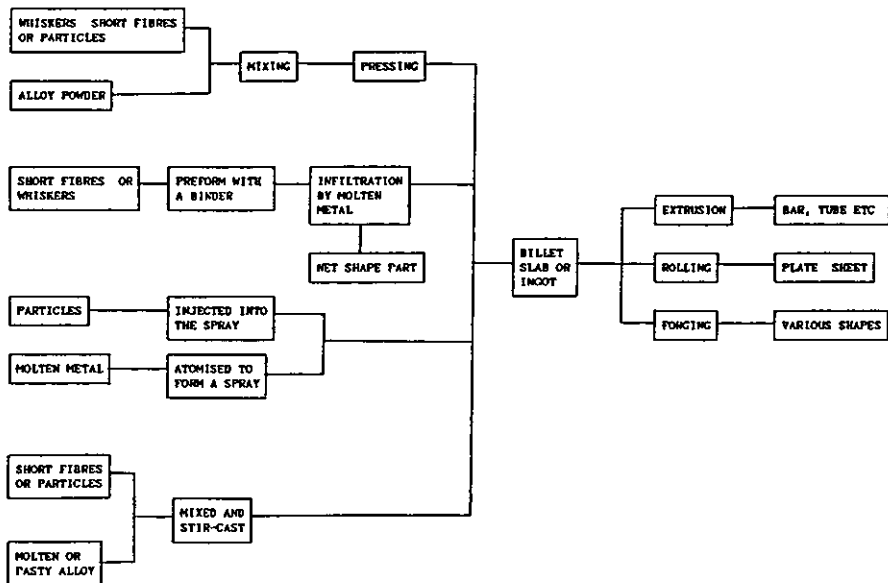


Figure 4 2 Process Routes for discontinuous fibre/particulate composites

the processing aspects of the subject, particularly the ideas on interfacial interactions and component manufacture.

#### 4.4.1 Interfaces in Metal Matrix Composites

The development of successful metal matrix composite systems, manufactured by liquid processing routes, requires an understanding of the interfacial interactions between the matrix and the reinforcing phase(s). There has to be a balance between the ability of the matrix to successfully wet a reinforcement, whilst at the same time ensuring that there are no adverse reactions, causing fibre degradation and low composite strength.

#### 4.4.2 Bonding in Metal Matrix Composites

Bonds can be a result of mechanical, physical or chemical interactions. Metcalfe [68] describes six bonds generally accepted to exist between the matrix and the reinforcement phase in metal matrix composites. These have been considered too provisional and simplistic [69], but do form a good starting point for discussion.

##### 4.4.2.1 Mechanical Bonding

Here there is no chemical bonding, the mechanism being one of interlocking formed by contraction of the matrix during solidification. The bonds are weak under transverse loads.

##### 4.4.2.2 Dissolution and Wetting Bonds

These are bonds caused by interactions of electrons on the atomic scale. The main requirements are clean surfaces and proximity. No chemical compounds are formed, but the matrix may dissolve the reinforcement.

##### 4.4.2.3 Oxide Bonds

These bonds may be generated by wetting but also include bonds where intermediate compounds form at the interface. In general, for example, metals having oxides with small free energies of formation do not form strong bonds with alumina. However, traces of oxygen or active elements will enhance the

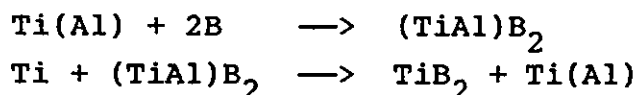
bond by forming intermediate zones. All of these are included in the oxide bond.

#### 4.4.2.4 Reaction Bonds

These are restricted to composites with other than oxide reinforcements. Titanium-boron provides a good illustration, where titanium diboride is formed at the interface.

#### 4.4.2.5 Exchange Reaction Bonds

Here, a second element in the matrix or reinforcement begins to exchange lattice sites with elements in the reaction product. For example, with aluminium in solid solution with titanium/boron:



#### 4.4.2.6 Mixed Bonds

These are combinations of the above bonds.

#### 4.4.2.7 Summary

The high temperatures involved in liquid metal processing require that some of the above reactions have to be controlled, as some of the products may be brittle. One route is to use coatings on the fibre, to suppress reactions. In aluminium-boron composites a coating of silicon carbide on the boron (trade name - Borsic) provides some protection [68]. Other methods include alloying the reinforcement to change the form of the reaction products.

In cases where wetting is a problem, the reinforcements can be coated, for example with copper or nickel on graphite fibres in aluminium, or surface active elements can be added to the melt, for example lithium additions.

At this point it is instructive to consider the theory behind wetting and interfacial phenomena.

### 4.4.3 Interfacial Physics

#### 4.4.3.1 Surface Energy and Surface Tension

These terms are not always clearly defined in the literature. If a simple model of a surface is considered (Figure 4.3), the atom in the middle is attracted equally on all sides. There is an imbalance of forces on the atom at the surface. Bond formation involves a lowering of energy, mainly through electron rearrangement in the atom, resulting in a higher free energy on the surface. Increasing the surface area increases the surface energy.

The surface energy,  $\gamma$ , is the energy required to create  $\text{lm}^2$  of new surface. It is measured in  $\text{Jm}^{-2}$ . For liquids, a reduction in surface area results in a reduction in free energy of the system. That is, surface area reduction is favourable in liquids. The surface tends to contract as small as possible, thus forming a sphere. The tendency to contract causes a tension force in the free surface. This force is known as the surface tension and is defined as the force in Newtons, acting at right angles to a line one metre long, at the surface. The work done in moving the line for one metre is the surface free energy. Solids have surface free energy but surface tension cannot be easily defined.

Surface tension measurements are made in air saturated with the vapour of the liquid [70]. Different values are obtained in different atmospheres, for example air or argon.

Liquid metal measurements require the control of oxides on the surface. Thus, they need to be made in inert gas atmospheres.

#### 4.4.3.2 Three Phase Interfaces [70]

Consider the case of a common boundary, for example between a liquid, a solid and a gas (Figure 4.4), where  $\theta$  is the contact angle:

$$\gamma_{SV} = \gamma_{LS} + \gamma_{LV} \cdot \cos\theta \quad (4.1)$$

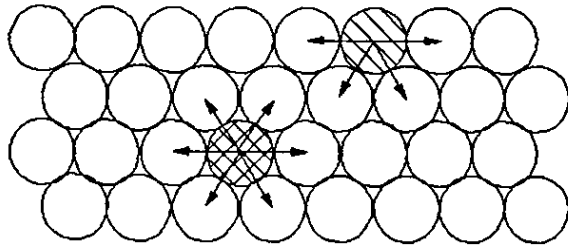


Figure 4 3 Simple model of a surface

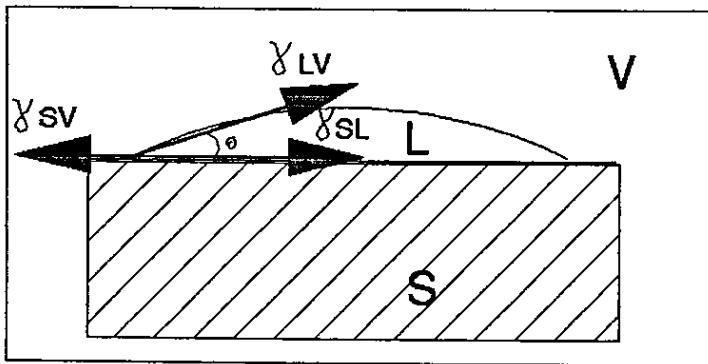


Figure 4 4 Three phase interface

If  $\theta > 90^\circ$  then  $\cos\theta$  is negative and  $\gamma_{LS} > \gamma_{SV}$  and this means that the attraction between L and S is not strong. That is, there is no wetting. Here, it should be noted that the criterion for wetting is defined as  $\theta < 90^\circ$ . If  $\theta < 90^\circ$  then  $\cos\theta$  is positive and there is strong attraction between L and S. If  $\theta = 0^\circ$  then there is complete spreading and if  $\theta = 180^\circ$  there is no appreciable attraction.

Dupré defined work of adhesion as:

$$W_a = \gamma_{LV} + \gamma_{SV} - \gamma_{LS} \quad (4.2)$$

where  $W_a$  is the work required to separate L from S in the presence of V. If LS is decreased by  $1\text{m}^2$ , areas of LV and SV both increase by  $1\text{m}^2$ . The higher the work of adhesion then the stronger the bonding. Combining equations 4.1 and 4.2 gives:

$$\begin{aligned} W_a &= \gamma_{LV} + (\gamma_{SV} - \gamma_{LS}) \\ &= \gamma_{LV} + \gamma_{LV} \cdot \cos\theta \\ &= \gamma_{LV} \cdot (1 + \cos\theta) \end{aligned} \quad (4.3)$$

This expression gives a means of calculating the work of adhesion.  $\gamma_{LV}$  is the surface energy of the liquid and  $\theta$  can be measured by the sessile drop method,  $\gamma_{LS}$  need not be known.

When  $\theta = 0^\circ$ ,

$$W_a = 2 \cdot \gamma_{LV} \quad (4.4)$$

this is known as the work of cohesion, ie the work necessary to pull the liquid apart, over an area of  $1\text{m}^2$  with no solid.

Fletcher et al. [71] have calculated the work of immersion of some zinc base metals by a pressure infiltration method. The work of immersion is defined below:

$$W_i = \gamma_{LS} - \gamma_{SV} \quad (4.5)$$

They quote values for Zn-11Al and Zn-27Al at 545°C as 0.380 Jm<sup>-2</sup>. Some re-arrangement of the equations gives the following relationship between  $W_a$  and  $W_i$ :

$$W_a = \gamma_{LV} - W_i \quad (4.6)$$

Surface roughness is important. Strong wetting liquids give a lower contact angle on rough surfaces, whilst weakly wetting liquids give a lower contact angle on smooth surfaces.

#### 4.4.4 Cause of Wetting

Attraction forces are of two types - physical and chemical. The relative contributions of each depends on whether or not the system is in equilibrium. In equilibrium systems, solid and liquid contacting phases are under conditions of thermodynamic equilibrium - the chemical potential of each component and the temperature and pressure in each of the phases are the same. Naidich [74] and Delannay et al [70] in their reviews on wettability discuss the importance of equilibrium. Work of adhesion,  $W_a$ , is considered to be made up of two components,  $W_a(eq)$ , covering equilibrium physical interactions, and  $W_a(non-eq)$ , caused by chemical interactions.

#### 4.4.5 Wettability

##### 4.4.5.1 Wettability of High Melting Point Oxide Fibres

Commercial reinforcements available for consideration are based on alumina, alumina-silica mixtures and zirconia. The fibres are ionic in nature and the oxides have high negative free energies of formation, indicating stability.

As a rule, high melting point oxides are poorly wetted ( $\theta > 90^\circ$ ) by pure liquid metals. For example, with mercury, tin, lead, silver, copper, nickel, cobalt, iron and platinum,

$\theta$  is of the order  $120-150^\circ$  [72]. However, some metals, eg titanium, zirconium, barium and aluminium intensively wet the surfaces.

Some authors [reported in 72] thought that metals which are able to form highly charged ions, for example Al and Sn would wet ceramic surfaces better, due to high electrostatic interaction. Tin, however, poorly wets oxides. Other authors [reported in 72] have suggested that metals in general, should wet oxides, because of the electrostatic nature of the ionic bond.

Weyl [reported in 70] probably best summarises the problem by proposing a model of the oxide surface as being composed of a layer of oxygen anions, which, because of their high polarisation, push the small cations away from the surface, see Figure 4.5.

There is thus no propensity for chemical interaction, as the negative sea of valence electrons in the liquid metal structure would tend to repel contact. However, there will be Van der Waal's interaction.

If there were chemical interaction, the liquid metal could 'reduce' the solid surface layer to metal and wetting would thus be improved.

Some authors [72] have shown that the wettability of oxide and adhesion in such a system increases with growing affinity of the liquid phase for oxygen. This is indicated by variations in the free energy of metal oxide formation.

With reference to Ellingham diagrams for the oxide formation, any element (in pure or in alloy form) below the Al/Al<sub>2</sub>O<sub>3</sub> line should 'wet' alumina by reduction of alumina to aluminium. Examples of suitable elements include barium, zirconium, magnesium [73], lithium and calcium. According to the diagram, titanium should not reduce alumina (ie  $+\delta G$ ), but

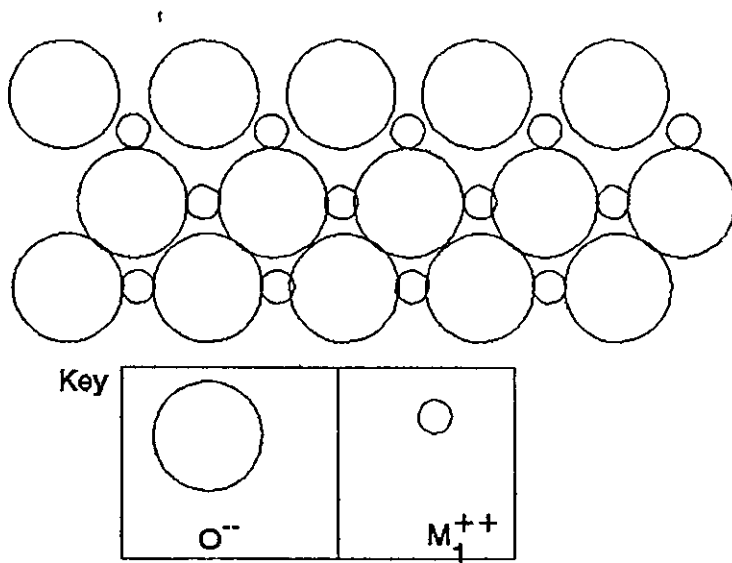


Figure 4.5 Weyl model of surface of ionic compound

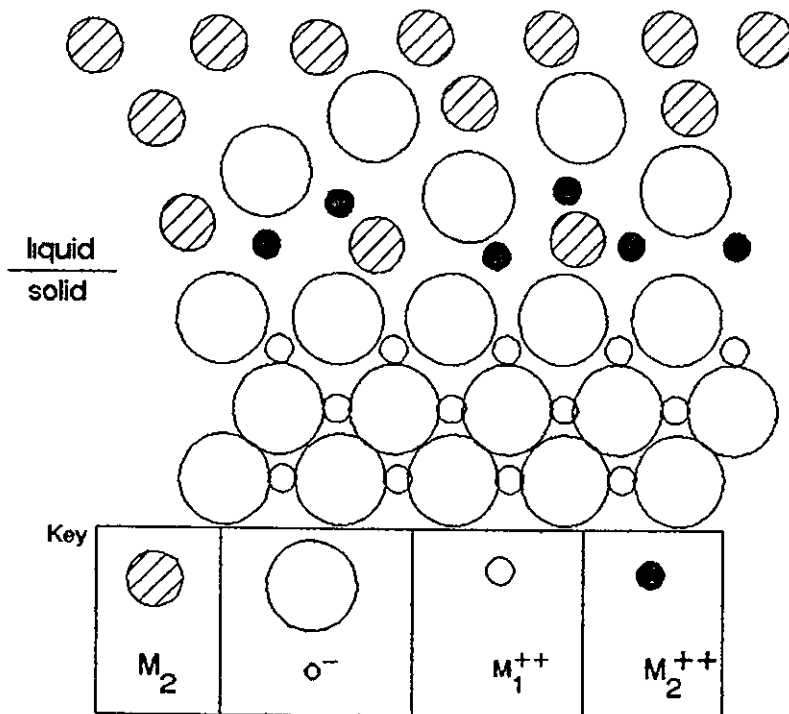


Figure 4.6 Naidich model of liquid metal-oxide interface.

in practice it does, due to the oxygen from the alumina being dissolved in the titanium (see later).

On the basis of general considerations, it can be expected that the interaction of any substance with a chemical compound will be less intensive, the stronger the atomic bonds are.

A second mechanism of wetting relies on oxygen being present in the melt. Oxygen is surface active and thus, even in small quantities can improve wetting, by the formation of (liquid metal)<sup>n+</sup>O<sup>2-</sup> complexes. The (liquid metal) ion is then attracted electrostatically to the surface layer of the oxide. The bond is thus ionic in nature. So, titanium and copper can both wet alumina, as shown in Figure 4.6 [70].

#### 4.4.5.2 Wettability of Covalent Solids [70]

Candidate materials for reinforcement are graphite, silicon carbide and possibly silicon nitride. However, the latter appears to be available in whisker form only. Materials are characterised by a closed stable electronic configuration and high strength inter-atomic bonds. The equilibrium work of adhesion,  $W_a(\text{eq})$ , which depends on polarisation, is negligible. The  $W_a(\text{non-eq})$  is important through reactions in general, since for wetting, the liquid metal should have a high chemical affinity to the solid.

#### Graphite

For effective graphite wetting, the elements in the liquid state should:

- react to form carbides, or
- dissolve carbon, or
- diffuse into the solid.

Groups Ib - VIb and periods 4 - 6 of the periodic table (including zinc and copper) are practically inert with graphite. Alkali metals form carbides with ionic bonding

with graphite, the metals assuming the spaces in between the basal layers and forming carbides of the type  $MC_3$ . Alkalines form compounds (mainly ionic in nature) of the type  $MC_2$ .

On interaction with transition metals (with unfilled shells) carbon displays its donor properties. Interaction increases with temperature and decreasing number of 'd' electrons.

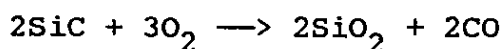
Ti > V > .... > Ni.

Covalent bonds are formed when elements have outer 2p or 3p electrons, eg Al, Si, B ( $W_a$  1000-1200mJ). The wetting of carbon by aluminium is not observed below 900°C. More electropositive elements are needed to break the oxide film. As regards a reinforcement phase for ZA27 it would appear that graphite is unsuitable, since temperatures around 900°C would vapourise the zinc.

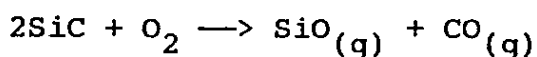
#### Silicon Carbide

As a rule, covalent carbides, eg SiC, follow the same dependence on wetting as the wettability of carbon. However, copper and silicon do react. This would explain the success of wetting of silicon carbide fibres by ZA27 [54].

One of the main problems with the use of SiC fibres is oxidation resistance in air, due to oxide formation:



The SiC behaves in the same way as a stainless steel. Provided that there is enough oxygen in the atmosphere, to maintain a 'passive film' of  $SiO_2$ , then oxidation is slow. It depends on the diffusion of  $O_2$ , or CO. However, at low partial pressures of oxygen (Figure 4.7), active oxidation can occur. One mechanism may be:



At low  $P_{O_2}$ , oxidation rate is low. At a critical value of

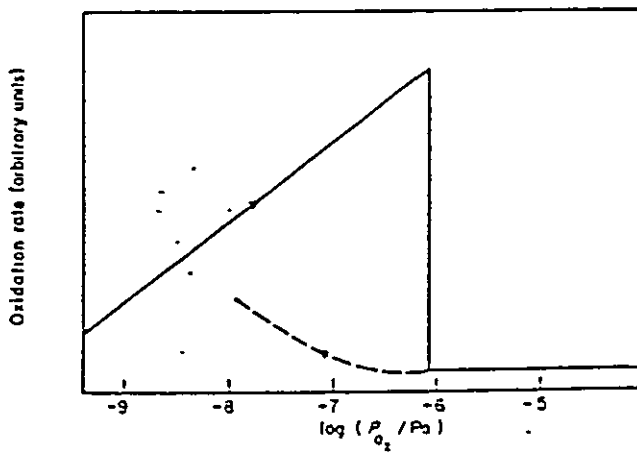


Figure 4 7 Schematic of the effect of oxygen partial pressure on the oxidation rate of SiC at a given temperature (1100°C in this case)

$PO_2$ , the oxidation rate drops. If the  $PO_2$  were then to be reduced, the curve may show a lag, until breakdown of the  $SiO_2$  film caused active oxidation.

One possible mechanism of breakdown is:



(This occurs at the oxide/carbide interface, leading to rupture).

From a practical viewpoint, this means that if melting a metal/SiC system in argon, if  $PO_2 < \text{critical}$ , this would lead to a weight loss. The situation is worse in impure hydrogen atmospheres, since hydrogen encourages the decomposition of silicon dioxide to silicon monoxide. Oxide film growth is more rapid in water than in oxygen, because of greater solubility of the smaller water molecule in the oxide.

Active oxidation causes weakening. In fibre testing or composite manufacture, use should be made of pure inert environments, or atmospheres with oxygen potentials sufficient to form passive films.

Warren and Andersson [74] classify metals in combination with silicon carbide as reactive or stable.

In reactive systems the silicon carbide does not exist in equilibrium with the metal form of the third constituent, because chemical reactions occur to form silicides and/or carbides or graphite (eg Ni or Ti). There is no two phase field of SiC + metal.

In stable systems a two phase metal + SiC region exists, for example aluminium, silver, gold, copper, magnesium, lead, tin and zinc. This does not mean that the metals are immune from attack. In aluminium - silicon carbide composites a fraction of silicon carbide, reinforced with molten aluminium can be

expected to dissolve and react, to form  $Al_4C_3$ . However, this can be avoided by prior alloying.

Wetting experiments of SiC, by pure metals can be complicated by the presence of the silicon dioxide film. In some cases, atmospheric impurities can depress the interfacial energy between L and S. Normally, the contact angle decreases slowly with increasing temperature, but a change in the interface can be expected to lead to a more marked change in angle. The loss of the passive oxide film is likely to cause an increase in the interfacial energy between L and S, and a consequent fall in  $\theta$ , since silicon dioxide has a much lower surface energy than silicon carbide.

Warren and Andersson [74] state that the wetting of silicon carbide, by pure, non-reactive metals is poor and not adequate for composite preparation. The main exception to this is aluminium at around  $1000^\circ C$ . However, this temperature is too high for ZA alloys. Other sources [reported in 70] state that liquid copper dissolves silicon and that copper in Al alloys is essential for wetting SiC fibres.

Wetting is improved by alloying additions. The most effective additions will be elements which react with the substrate sufficiently, to form a mono-layer. The addition should itself have a similar or higher surface energy than the parent metal, otherwise it may segregate to the free surface and lower the interfacial energy between L and S.

In summary, with particular reference to ZA alloys, it will be observed that the main constituents, Zn, Al, Cu form 'stable' systems with silicon carbide. The reaction can be enhanced by adding elements to form a mono-layer, for example, magnesium and titanium. The oxygen potential is important and it would probably be best to melt the alloy in air.

#### 4.4.5.3 Concluding Remarks

Wettability appears to be a subject that is not well understood. This review was a simplified account of the main factors and excluded the thermodynamics of the interface. However, it appears that ZA alloys can wet both alumina and silicon carbide reinforcements although the mechanisms in each case may be different.

#### 4.4.6 Manufacturing Methods

Two basic approaches are available for the production of cast metal matrix composites. The first is to infiltrate a pre-form or a bunch of fibres or particles with liquid metal. The second is to cast a pre-mixed melt (liquid or semi-solid) of metal and reinforcement by a suitable process, either squeeze casting or a conventional gravity process.

##### 4.4.6.1 Infiltration Methods

###### Squeeze Infiltration

Many authors refer to squeeze infiltration incorrectly as squeeze casting. Granted similar equipment is used and the composite solidifies under a pressure of 50-100 MPa, but close control over micro-structure cannot be exercised because the metal is poured with a high degree of superheat. For MMC production, a pre-heated fibre preform is inserted into the die. Liquid metal is metered into the die cavity and the punch pressure is then applied. This method is most suitable for selective reinforcement. High volume fractions of reinforcement phase are possible.

###### Pressure Infiltration

These methods involve the use of pressure casting to infiltrate a preform by the application of a hydrostatic pressure to the infiltrating liquid. Generally some pressure is required even for wetting systems because of velocity related flow rate limitations. Using pressures of about 15MPa, applied by a hydraulic ram on a die casting machine or

by pneumatic pressurisation, intricate shapes may be cast. Cray Materials [75] use a pressure assisted method involving a vacuum 'pull' and pressure 'push' approach.

#### **Vacuum Infiltration**

If fibre and matrix are wetted this method can be effective. Champion et al. [76] have used this method to reinforce Al-2%Li alloy with Du Pont FP (alumina) fibre.

#### **Gravity Infiltration**

Conventional gravity casting routes can be used to infiltrate large diameter, widely-spaced reinforcements where there is good wetting.

#### **4.4.6.2 Casting a Pre-Mixed Melt**

Melts can be pre-mixed with short fibres or particles by several methods which have been extensively reviewed by Rohatgi et al. [66]. The approach has been called semi-solid slurry casting. The metal can be completely liquid or partially solid. In the latter case processing a semi-solid melt with an addition of reinforcement is called compocasting. The methods represent the most cost effective of all the solidification processes for producing MMCs, provided that the many quality-related processing difficulties can be overcome.

Although many methods for introducing particles to a melt are available, including gas injection, re-dispersing infiltrated preforms, centrifugal techniques and ultrasonic mixing, only the vortex method seems widely accepted. Dural use an adaptation of the vortex method to introduce silicon carbide particulate material into aluminium alloy ingot for subsequent remelting [77].

Squeeze casting and conventional gravity processes have been used to shape pre-mixed melts.

#### 4.5 Zinc-Base Alloy Metal Matrix Composites

Table 4.1 summarises the constituents and manufacturing methods that have been used to make composites in zinc-base alloys. The favoured method is infiltration.

Dent and Murphy [53] described the manufacture and properties of inexpensive composites based on a zinc alloy infiltration of Saffil pads. The alloy had the composition 69Al-29Zn-1.8Cu. Details of the infiltration method were not given but it was reported that some porosity was present in the samples. Ambient temperature testing of the composites showed that they had superior hardness and flexural modulus compared to the unreinforced alloy, but inferior tensile strength, flexural strength and impact resistance. At 300°C the composite showed higher tensile strength and superior creep rupture properties compared to the unreinforced alloy.

Das et al. [54] outlined the possibility of using the vortex method to introduce Nicalon silicon carbide fibre into ZA27. The mixture could then be squeeze-cast. The need for the contact time between the fibre and the melt to be optimised was highlighted. There must be sufficient time to develop wetting but there must be no interaction leading to fibre degradation. Optimum contact time was 9 minutes. This did not allow enough time to add volume fractions greater than 0.03. Das and his co-workers later reported [56] that a two stage mixing method had to be developed to minimise contact times. In the first stage a high density Nicalon preform was squeeze infiltrated with ZA27. The high density slug was then remelted quickly in a high frequency induction furnace with an appropriate amount of diluting alloy. When melted this mixture could be gently stirred and then squeeze cast. Yakoub [47] describes the work in detail.

Yakoub only found strengthening in composites above 150°C when compared to the unreinforced squeeze-cast alloy.

GENERIC REINFORCEMENT	TYPE	ALLOY	METHOD	REF
LONG FIBRES	7 MICRON C	Zn	INFILTRATION	52
		Zn 4Al 1Cu	INFILTRATION	52
	E-GLASS	Zn	INFILTRATION	55
		Zn 27Al 3Cu	INFILTRATION	55
SHORT FIBRES	NICALON SiC	ZA27	SQUEEZE INFILTRATION + SQUEEZE-CAST	47
	SAFFIL PAD	Al 30Zn 2Cu	SQUEEZE	53
		Zn 32Al 2Cu	INFILTRATION	79 80
	SAFFIL	Zn	INFILTRATION	55
		Zn 27Al 3Cu	INFILTRATION	55
	SAFFIL + Cu	Zn	INFILTRATION	55
		Zn 27Al 3Cu	INFILTRATION	55
	10Ni-20Cr STEEL	Zn 27Al 3Cu	INFILTRATION	55
PARTICLES	SILICON CARBIDE	Zn	INFILTRATION	71
		Zn 27Al 3Cu	INFILTRATION	55
		ZA12	INFILTRATION / VORTEX	71
		ZA27	INFILTRATION / VORTEX	71

**Table 4.1: Composite Materials in Zinc Base Alloys**

Wang Chengfu [52] and his co-workers used nickel coated 7 $\mu$ m diameter carbon fibres (typical strength 2940 MPa) to reinforce pure zinc and zinc 4Al 1Cu 0.05Mg alloy by an infiltration method. Uniform distribution of the fibres was achieved. Strengthening of the composite was noted at room temperature.

Guerriero et al. [55] investigated the pressure infiltration at 2.5 bar of silicon carbide particles, short alumina fibres, E-glass, and 10Ni-20Cr short steel fibres by Zn and Zn-27Al-3Cu alloy. The aim of the work was to investigate wettability. Copper coating of the alumina fibres was used to enhance wetting. All samples contained macro-porosity which was due to the limitations of the infiltration equipment. The alumina and E-glass samples were not well infiltrated. Best results were obtained with silicon carbide particles. The steel fibres exhibited fibre pull-out during fracture, attributed to the formation of a thick brittle inter-metallic zone. The projected use of semi-solid slurry processing is also discussed as a suitable method of introducing pre-infiltrated briquettes containing a high volume fraction of reinforcement phase. The paper also describes a pressure infiltration apparatus which was being constructed.

Fletcher, Cornie and Russel [71] conducted experiments on the pressure infiltration of silicon carbide (8.37 $\mu$ m particulate) with pure Zn, Zn-4.5Al, Zn-11Al, and Zn-27Al. They derived works of immersion ( $W_i$ ) values for the systems at 545°C and 645°C.

Cornie et al. [78] report on the production of composites based on ZA12 and ZA27 reinforced with either short Saffil fibres or abrasive grade silicon carbide grit. Composites could be manufactured by a number of routes. Addition of the reinforcement to the alloy was made either by stirring or by pressure infiltration. In some cases high volume fraction materials with up to 50 volume percent of reinforcement were

manufactured. These could then be diluted and cast. Thixo-forging was used to produce tubes by a backward extrusion technique and samples for tensile testing. Diluted composites were also subject to further processing by hot rolling and hot extrusion. The authors report good bonding between the reinforcement and the matrix and a good distribution of particles. The distribution appeared improved in the plastically deformed samples. Typical mechanical properties in ZA27 reinforced with SiC 500 grade grit and tested as-cast, showed that ultimate tensile strength decreased with increased volume fraction of reinforcement. The unreinforced matrix showed a strength of 410 MPa and this decreased to 330 MPa for a 20 volume percent composite. No elongation was noted in the fracture of composites. Extruded composites showed improved strength. In all cases the addition of the reinforcement phase increased the Young's modulus of the material.

Lo et al. [79] have investigated the mechanical properties and fracture behaviour of Zn-32Al-2Cu alloy reinforced with Saffil fibres. Composites containing 12 and 24 volume percent Saffil were made by squeeze infiltration of a preform pad. At room temperature the unreinforced alloy was stronger than the composite. Only at 150°C did the 24 volume percent composite show higher tensile strength. Impact properties of the composites were poor at room temperature and they did not significantly increase at 150°C. In the unreinforced alloy a transgranular fracture was noted at room temperature. This changed to intergranular at 150°C. This observation was attributed to a weakening of the eta phase and eta/eutectoid interfaces at higher temperatures. At all temperatures failure in the composite occurred by fibre-matrix debonding. The fibre-matrix bond was thought to be higher than the eta/eutectoid bond at higher temperatures.

Dignard-Bailey, Dionne and Lo [80] reported further on the work in [79]. They reported increased compressive yield strength in the composites over the unreinforced matrix at

temperatures up to 150°C. They used Auger Electron Spectroscopy to show that failure in the composites was as a result of fracture through a SiO<sub>2</sub> binder phase used to bond the preformed Saffil pads. This resulted in general matrix-fibre de-cohesion before general yielding of the matrix could occur. It is suggested that an improved binder could increase the strength of the composite materials.

#### 4.6 Summary

This chapter has reviewed the main thinking behind metal matrix composites with particular emphasis on cast products. It is clear that to attain wide-spread applications the cost of these materials must be reduced. Low cost reinforcements and a castable material offer the best potential routes.

Considering Zn-base materials, the development of a composite material in ingot form which could be remelted and cast by a variety of process would be most useful, just as Dural have shown with Duralcan material. Silicon carbide has been shown to be a material that is wet by Zn-base alloys. It is widely available in particulate form.

The squeeze casting route would allow production of near-net shape products with no porosity, so allowing optimum mechanical properties to be attained. The material could then be evaluated in terms of its ambient and high temperature properties, particularly creep behaviour.

## 5. Experimentation

### 5.1 Introduction

Following the literature review and some preliminary experimentation, it was decided to carry out the following programme of work:

a). investigation into the effects of squeeze casting parameters on the mechanical properties and microstructures of the three commercial ZA alloys: ZA8, ZA12 and ZA27; and a binary Zn37wt%Al alloy. This work involved the use of an ingot die, producing castings of 50mm diameter by 110mm length at high pressure (>185MPa), to complement the work of Yacoub [47].

b). design and make a squeeze casting die, to produce castings with section thicknesses in the range 8-20mm.

c). investigation into the effects of squeeze casting parameters and section thickness on the mechanical properties of the alloys listed in a) above.

d). make an inexpensive composite system, based on ZA alloys and silicon carbide particulate material produced by squeeze casting.

e). evaluation of the mechanical properties of the composite at temperatures up to 150°C.

The main processing parameters in squeeze casting are:

- die temperature
- metal casting temperature
- delay before application of pressure
- time to build up to full pressure
- pressure level

There appears to be no published data on the effect of section thickness on the mechanical properties of squeeze-cast alloys. The following section describes the characteristics of the equipment employed and indicates how the parameters listed above could be controlled.

## 5.2 Manufacturing Equipment

### 5.2.1 Squeeze Casting Press

Squeeze casting experiments were carried out using a 100 tonne Norton press, as shown in Figure 5.1, which included a separate ejector piston. The hydraulic operating system could be operated manually or controlled pneumatically. The major components of the press are listed below.

#### 5.2.1.1 Main Piston (100 tonne)

It was possible to alter approach speed with a speed control and fast approach selector. Squeeze time was controlled by power pressure control. This governed the pressure build-up rate. Applied pressure was controlled by a sustain pressure circuit and dwell time under full pressure by a timer. A digital readout from a transducer, connected to the main cylinder, gave the pressure in the piston, thus the pressure exerted on the solidifying metal could be calculated. In this investigation, pressures of up to 380MPa were considered. For a 50mm diameter ingot, at 380MPa, the load required was 76 tonnes. This was well within the capability of the press. A stop limited the maximum pressure load to 80 tonnes.

#### 5.2.1.2 Ejector Piston (50 tonne)

The ejector could be altered by an ejector piston controller. On operation, the ejector would activate to a fixed, preset pressure and then drop to a low value, making its operation less versatile than the main piston and hence, excluding possible operation that mimicked the UBE design of squeeze casting machine (as described in section 3.2)

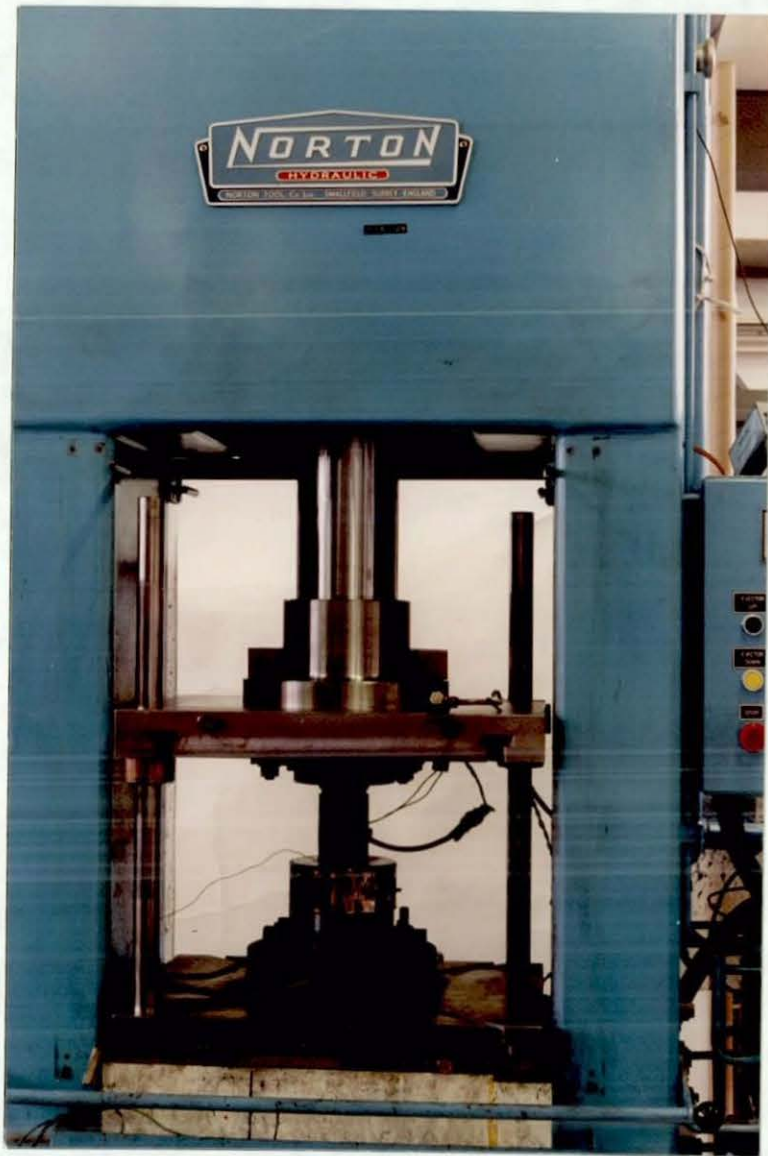


Figure 5.1 100 tonne Norton Press

### 5.2.1.3 Squeeze Casting Dies

Initial trials were carried out with an existing squeeze casting die, which produced an ingot of 50mm diameter by 110mm length. This die gave no indication of the effect of variable section thickness but a further existing die based on direct pressure was also utilised. This die produced castings of approximately 10mm thickness but specimens for mechanical testing could not easily be extracted from the casting. A relatively large amount of metal was required to fill the cavity. This was a drawback on the composites processing side. A new die, based on the principle of backward extrusion, was designed and manufactured. It was of relatively simple construction and allowed the production of a component with different section thicknesses in one operation.

### 5.2.1.4 Ingot Die

This die produced castings by the direct pressure / no metal movement system. A schematic of the die is shown in Figure 5.2. It was manufactured from H13 die steel. Die heating was carried out with seven 500W cartridge heaters controlled by a Eurotherm temperature controller and a chromel-alumel thermocouple placed in the top insert 5mm from the die wall.

Operation of the die was straight forward, on automatic press cycle. Approximately 600g of zinc alloy would be charged into the open, male die. On closing the press safety doors, the punch would drop at fast approach, change to slow approach at 10mm above the surface of the metal, squeeze, then build up to full pressure. After the required dwell time, the punch retracts and the casting could be ejected by the bottom piston.

### 5.2.1.5 Shaped Die

As was the case with the ingot die, this die produced castings by the direct pressure/no metal movement system. The die is more complex in design and was originally manufactured for operation on a single action press [81]. No

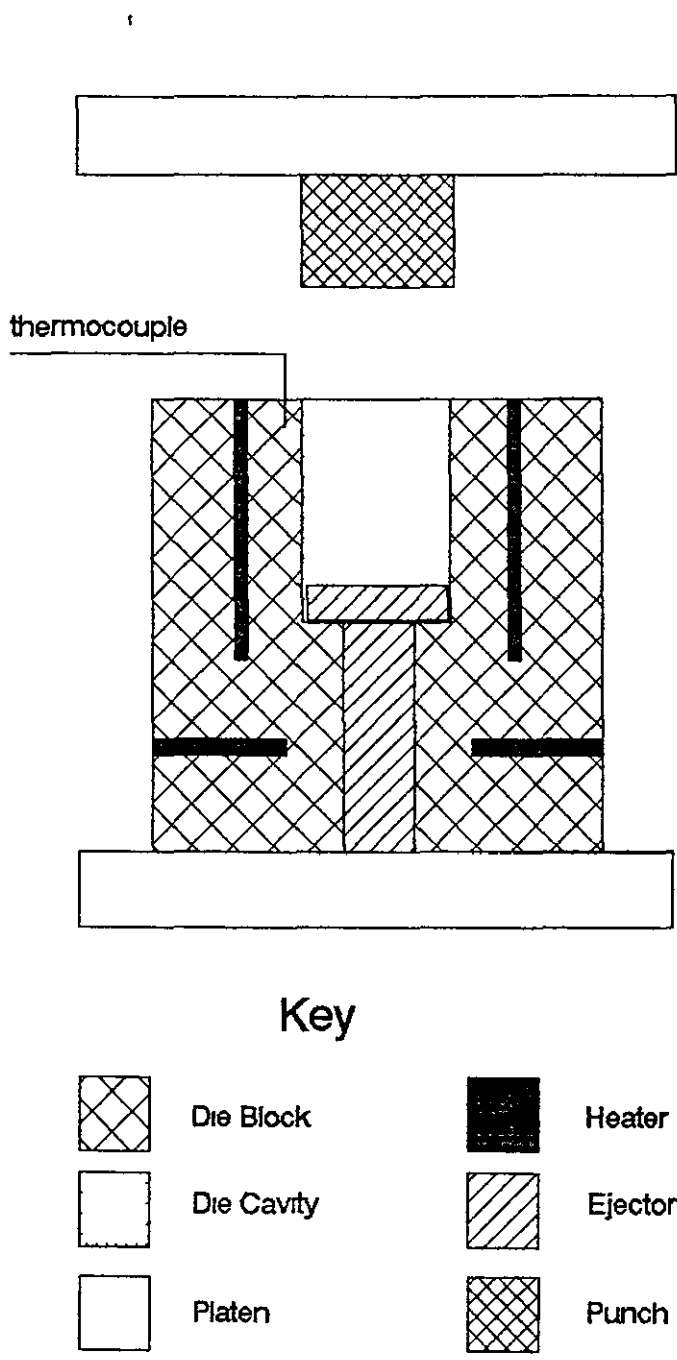


Figure 5.2 Schematic of Ingot Die

provision for the use of the ejector system is provided. Ejection is achieved by a dovetail built into the punch section. The die was constructed from H13 die steel, a photograph of the die is shown in Figure 5.3(a), with castings shown in Figure 5.3(b) on the right. (The casting on the left hand side of Figure 5.3(b), formed by backward extrusion around the punch, could also be produced in this die.) Sealing was provided by the top plate and pressure applied by a telescopic punch. The die was used mainly for distribution analysis for composite materials and gave design information for the die described in the following section.

#### 5.2.1.6 Die with Varying Section Thickness

This die was based on the principle of direct pressure with metal movement. By this method, shapes are formed by juxtaposition of the die and the punch. The design adopted was backward extrusion of metal, using a formed punch with an internal cavity. This appears to be a novel approach, requiring a die of simple construction. In backward extrusion around a punch, sealing faces have to be incorporated into the design. Here there was no such requirement, because a flat-bottomed punch covered the whole surface area of the lower die cavity. The main problem envisaged was ejection of the casting from the punch, because a top ejector system was not available. This problem was solved by incorporating a dovetail on the ejector, which would hold the casting in the base during retraction of the punch.

It was possible with this design to manufacture a number of shapes. It was decided, after experience with the shaped die mentioned in section 5.2.1.5, to design a die to facilitate the manufacture of tensile test pieces. The die was also designed to evaluate the effects of section thickness. A design enabling circular sections of 8, 12 and 16mm diameter to be formed in the punch was adopted. Additionally, the base thickness could be varied. A schematic of the die design is shown in Figure 5.4. It was constructed from P20



Figure 5.3(a) Die for Shaped Squeeze Casting



Figure 5.3(b) Squeeze Castings from Shaped Die

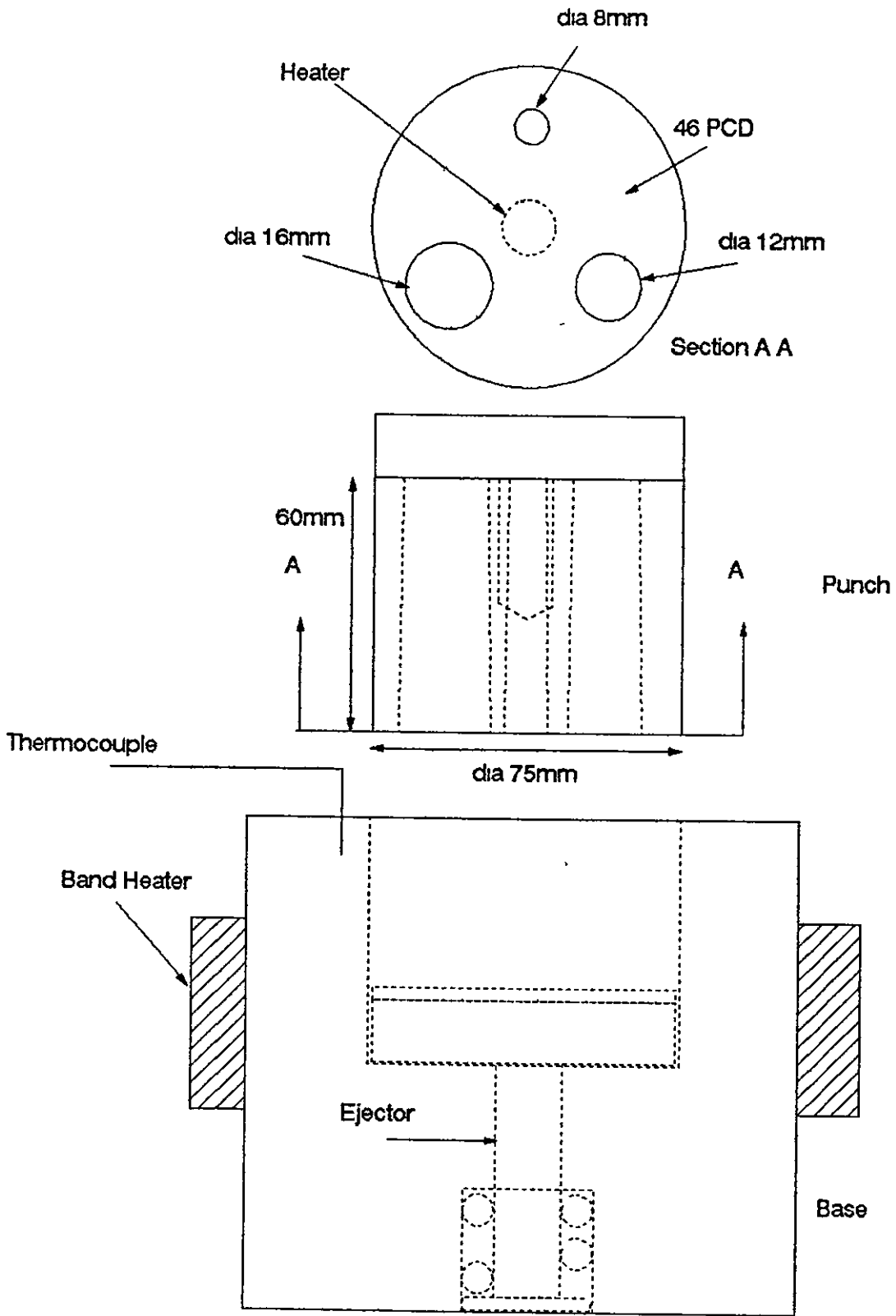


Figure 5 4 Schematic of Die to produce a casting of Varying Section

die steel. The internal diameters in the punch required a 1° ground taper to aid component extraction. The punch was split to allow an internal heater to be inserted. This split also facilitated venting from the punch cavities. The base acted as a pouring well with the punch being at the desired die temperature attained by a cartridge heater.

On operation, the punch would approach at fast speed, then change to slow speed during which time the metal would be backward extruded into the cavities, prior to the pressure being applied. The design produced sections with aspect ratios of 3.75, 5 and 7.5. The 7.5 aspect ratio was too great to produce consistently sound castings in all the alloys. However, the design was successful in producing the larger sections in all the alloys, regardless of whether the thin section was formed. A photograph of the die and a casting is included in Figure 5.5.

Heating of the base was provided by a band heater, controlled by a Eurotherm temperature controller. On ejection the casting, held in place by the dovetailed cast iron insert, would be raised above the base of the die when it could be removed. A photograph showing the casting in the ejected position is shown in Figure 5.6.

#### 5.2.1.7 Die Coatings

In all cases a water based graphite lubricant was used. It was applied either by hand or by spraying.

#### 5.2.1.8 Die Temperature Ranges

Die temperatures could be altered between ambient and 300°C in the ingot die. Operation in the thin section dies was kept below 250°C.

### 5.2.2 Melting Equipment

#### 5.2.2.1 Melting Furnace

Alloy melting and composite manufacture was carried out using an experimental laboratory electrical resistance furnace. A

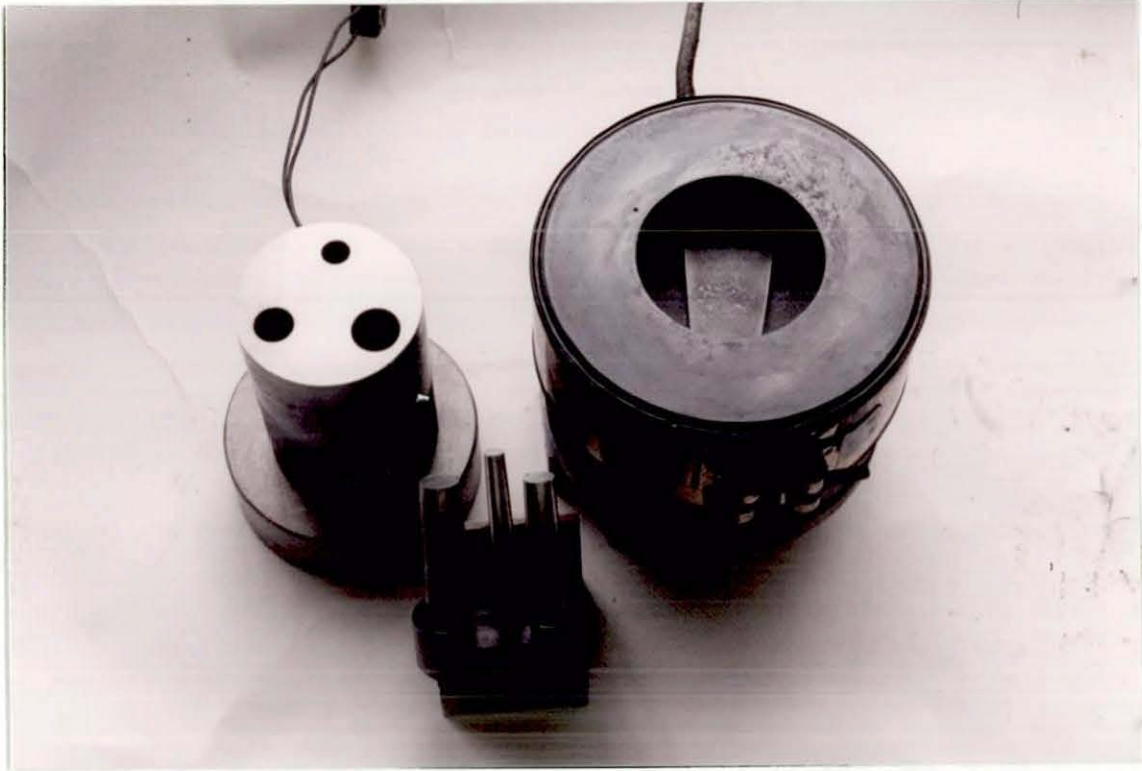


Figure 5.5 Punch, Casting and Die for variable section design

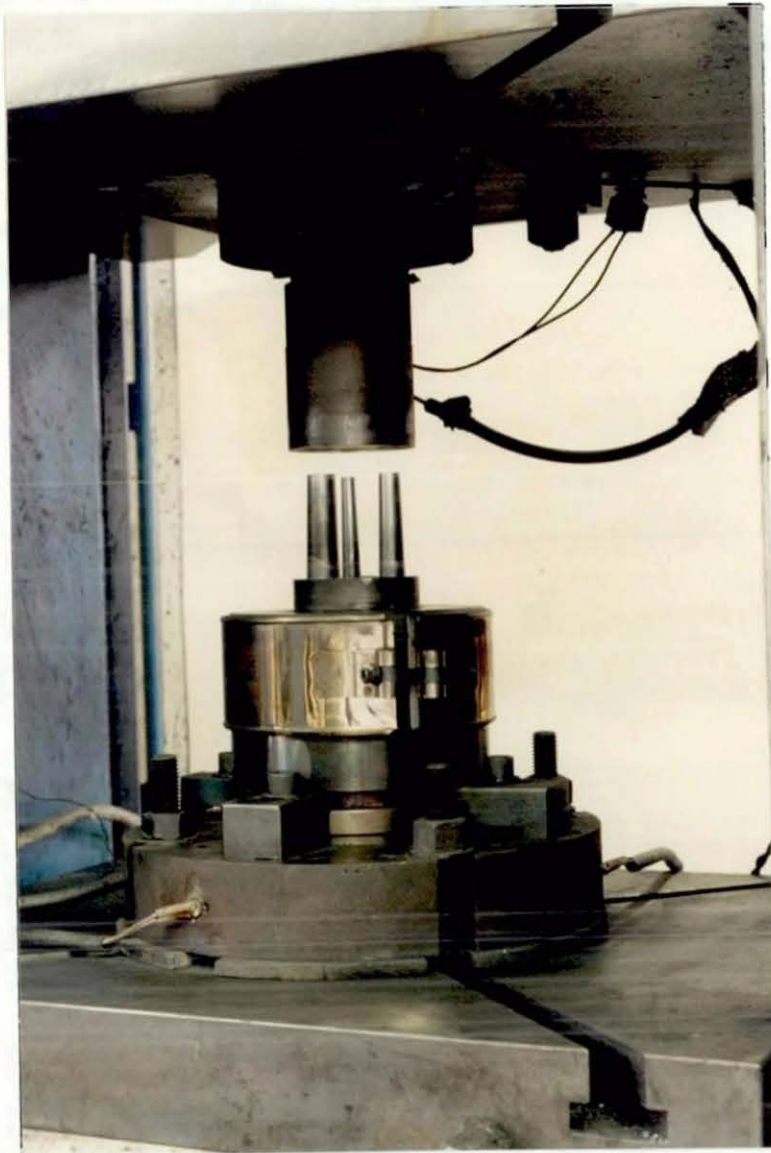


Figure 5.6 Casting in Eject Position  
(Note Band Heater)

superheat of 20°C in the melting furnace allowed time for metal preparation prior to casting.

#### 5.2.2.2 Melting Crucibles

The recommended melting and holding medium for ZA alloys is silicon carbide [3]. Silicon carbide crucibles, supplied by Magna Industrials, were employed.

Zinc alloys are not prone to gas absorption during melting and no degassing, fluxing or grain refinement treatment was used. Melts were, however, stirred and skimmed prior to pouring.

#### 5.2.2.3 Ancillary Equipment

General foundry tools, coated and preheated when in contact with the metal, were used as required during handling.

#### 5.2.2.4 Equipment for Composite Manufacture

It was decided to manufacture silicon carbide particulate reinforced composites by the vortex method, followed by squeeze casting. The vortex method has been described by many authors [e.g.82] and requires simple stirring equipment.

#### 5.2.2.5 Stirring Equipment

The stirring equipment used was similar to that used by Yacoub [47]. It comprised a silicon carbide propeller attached to a cast iron shaft, driven by an electric motor.

#### 5.2.2.6 Vibratory Feed System

It was found that controlled, slow addition of particulate to the melt was desirable and a vibratory feed system, as shown schematically in Figure 5.7, was employed. Up to 25 volume% of SiC<sub>p</sub> (F320 grit) could be added to ZA27 by the vortex method and subsequently squeeze cast. The only drawback with this method was the size of particulate which could be introduced. It appeared to be limited to 30 micron particles, whereas other producers can use smaller particles, for example Dural incorporate 10 micron particles in

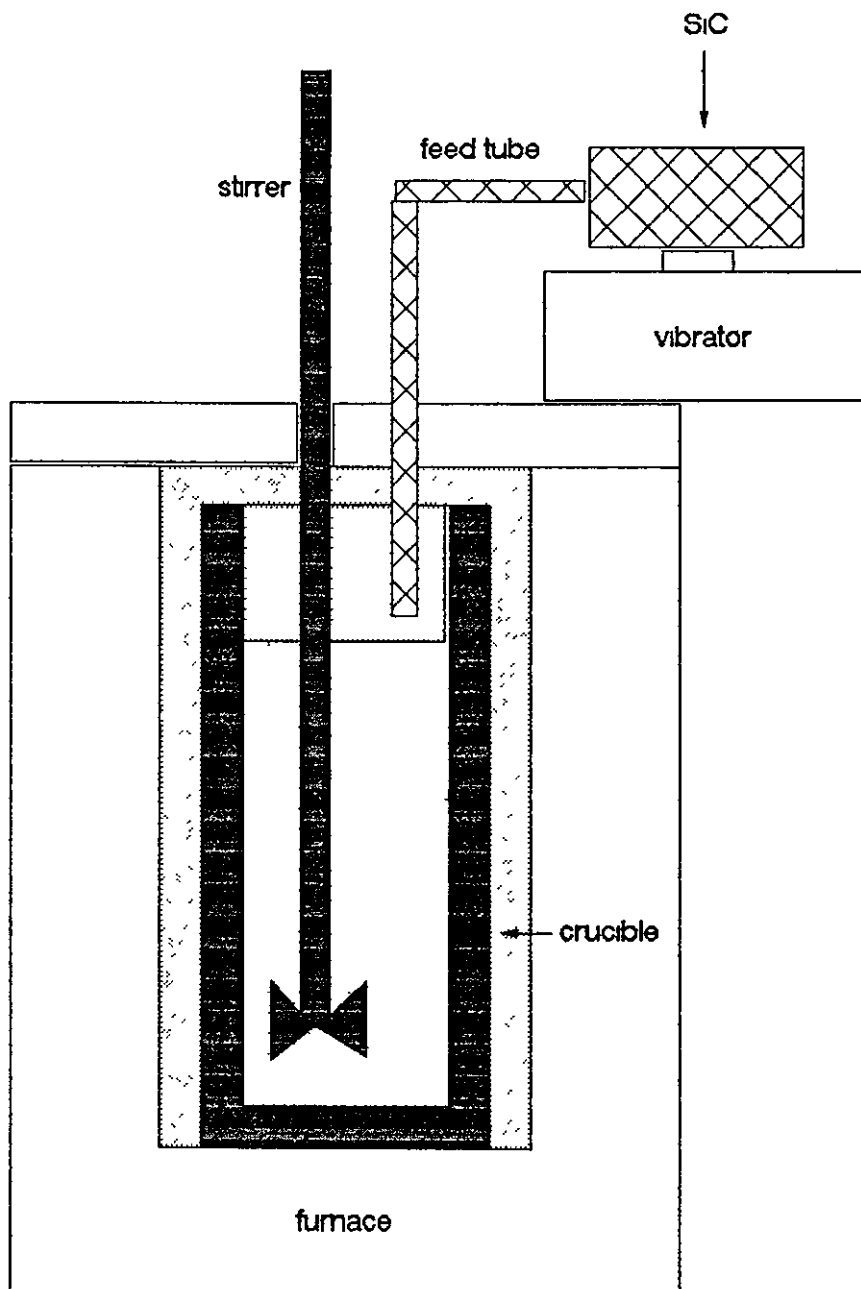


Figure 5 7 Schematic of Vortex Arrangement

A356 material. However, the principle of operation was established.

#### 5.2.2.7 Gas Covers

Turbulence cannot be avoided during the introduction of particles, so the equipment inside the enclosed furnace was shrouded in an gas cover of nitrogen.

### 5.3 Manufacturing Programme

#### 5.3.1 Plain Alloys in the Ingot Die

The initial programme of work was to investigate the effects of squeeze casting parameters on the mechanical properties and microstructures of ZA alloys, using the ingot die described in section 5.2.1. Alloys, all from the same batch, were melted in silicon carbide crucibles in the resistance furnace, as required.

##### 5.3.1.1 ZA27

An extensive programme of work was carried out on ZA27. Six groups of castings (56 ingots) were cast under the process parameters shown in Table 5.1. Press speeds were chosen from presets on the press control equipment. Two power settings (full and half) were employed. Press speed 2 involved a delay of 6 seconds before the load was applied and press speed 3 a delay of 4 seconds. At full power pressure the load build-up was 11.5 tonnes per second and at half power pressure the build-up was at 8.3 tonnes per second. Die temperatures were chosen as being typical values for both squeeze casting [27] and zinc alloy die casting production [3]. In line with industrial practice, a minimum die temperature of 150°C was chosen, to avoid the risk of die failure by thermal fatigue. Some difficulties were encountered on ejection at high die temperatures and high pressures. Squeeze pressures were limited at the top end of the range by the capacity of the press and at the lower end by the ability to produce a sound casting. Yacoub [47] reported that a pressure of 92MPa was required to produce

		GROUP1	GROUP2	GROUP3	GROUP4	GROUP5	GROUP6
DIE TEMP (°C)	SQUEEZE PRESSURE (MPa)	POUR 555°C Process 2F	POUR 555°C Process 2H	POUR 555°C Process 3F	POUR 555°C Process 3H	POUR 515°C Process 3F	POUR 595°C Process 3F
150	185	1	13	25	37	49	53
	270	2	14	26	38		
	380	3	15	27	39		
200	185	4	16	28	40	50	54
	270	5	17	29	41		
	380	6	18	30	42		
250	185	7	19	31	43	51	55
	270	8	20	32	44		
	380	9	21	33	45		
300	185	10	22	34	46	52	56
	270	11	23	35	47		
	380	12	24	36	48		

(2=delay of 6 secs, 3=delay of 4 secs F=11.5 t/s and H=8.3 t/s)

**TABLE 5.1 PROCESSING PARAMETERS FOR ZA27 IN INGOT DIE  
(56 CASTINGS PRODUCED)**

sound ZA alloy ingots by squeeze casting. The effect of higher squeeze casting pressures, in the range 185-370MPa was considered in this work.

A typical pouring temperature for ZA27 is 555°C. The first four groups, totalling 48 castings, were produced at this temperature. A shorter investigation, using both a lower (515°C) and a higher (595°C) pouring temperature, was conducted on groups 5 and 6. The medium and high pouring temperatures ensured that the alloy was still liquid when the load was applied. However, some solidification was likely at the lower pouring temperature prior to the load being applied.

Cooling rate measurements were undertaken by inserting a chromel-alumel thermocouple into the ingot die. One gravity casting and one squeeze casting were attempted using this method.

#### 5.3.1.2 ZA8

Twelve ingots of ZA8 were manufactured according to the conditions listed in table 5.2. Melting stock was supplied by the Brock Metal Company and conformed to their specification. Similar conditions to those used in the manufacture of ZA27 were employed, using a pouring temperature of 450°C. The press speed and power pressure values had the same values as those discussed in section 5.3.1.1.

#### 5.3.1.3 ZA12

A similar programme to that described for ZA8 was carried out for ZA12 (Table 5.3). Melting stock, complying to standard specification, was supplied by the Brock Metal Company. Pouring temperature for ZA12 was 480°C, reflecting its higher liquidus temperature compared to ZA8.

DIE TEMP (°C)	SQUEEZE PRESSURE MPa	PROCESS PARAMS	CASTING NUMBER
150	185	2F	1
	270	3F	2
	380	2H	3
200	185	3H	4
	270	2H	5
	380	3F	6
250	185	2H	7
	270	2F	8
	380	3H	9
300	185	3F	10
	270	3H	11
	380	2F	12

**TABLE 5.2 ZA8 IN INGOT DIE**

(2=delay of 6 secs, 3=delay of 4 secs)  
(F=11.5 t/sec, H=8.3 t/sec)

DIE TEMP (°C)	SQUEEZE PRESSURE MPa	PROCESS PARAMS	CASTING NUMBER
150	185	2F	1
	270	3F	2
	380	2H	3
200	185	3H	4
	270	2H	5
	380	3F	6
250	185	2H	7
	270	2F	8
	380	3H	9
300	185	3F	10
	270	3H	11
	380	2F	12

**TABLE 5.3 ZA12 IN INGOT DIE**

#### 5.3.1.4 Zn-37Al

Zn-37Al is not a standard alloy. It is difficult to process, due to its long freezing range. However, it was chosen as being an alloy that may be suitable for squeeze casting. The alloy was prepared on-site, using commercially pure aluminium and electrolytic zinc. Analysis was carried out at the Brock Metal Company, using a Quantovac. The manufacturing programme shown in Table 5.4 involved fixed press speed, approach speed and load build-up rate, at a squeeze pressure of 185MPa. It had become clear that die temperature and pouring temperature had most influence on the properties of long freezing range squeeze-cast ZA alloys.

#### 5.3.2 Plain Alloys in Backward Extrusion Die

The main aim of this section of work was to study the effects of section thickness on the mechanical properties and microstructure of squeeze-cast ZA alloys. The die has been described in section 5.2.2.3. This die, because of its inherently difficult design, was more sensitive to processing conditions. Too fast an approach speed or too fast a build-up of pressure did not allow air to be vented from the cavities and resulted in mis-runs. Optimum processing conditions were at press speed 2 and half power pressure. A pressure of 68MPa was found sufficient to produce sound castings. These conditions resulted in a delay of 8 seconds after pouring, before pressure was built-up. Die temperatures in thin sections were kept below 250°C.

##### 5.3.2.1 ZA27

High pouring temperatures relative to the ingot die were required, to fill the backward extrusion die with ZA27. Processing conditions to produce 27 castings in ZA27, are shown in Table 5.5. The alloy used was from the same batch of material as was used for processing by the ingot die.

##### 5.3.2.2 ZA8

ZA8, being a fluid alloy, presented no problems in filling the cavities at 450°C pouring temperature. This was similar

POURING TEMP (°C)	565	595
DIE TEMP (°C)		
150	1	5
200	2	6
250	3	7
300	4	8

**TABLE 5.4: CASTING PARAMETERS FOR Zn-37Al INGOT DIE (CASTINGS 1 - 8)**

POURING TEMP (°C)	595	620	650
DIE TEMP (°C)			
150	1-3	10-12	19-21
180	4-6	13-15	22-24
220	7-9	16-18	25-27

**TABLE 5.5: CASTING PARAMETERS FOR ZA27 THIN SECTIONS (CASTINGS 1 - 27)**

to the method using the ingot die. Nine castings were produced, using metal from the same batch of material as for the ingot die, according to the processing parameters shown in Table 5.6.

#### 5.3.2.3 ZA12

ZA12 was processed in the same manner as ZA8. However, a pouring temperature of 480°C was used. Material from the same batch as that used with the ingot die was used. Processing parameters are shown in Table 5.6.

#### 5.3.2.4 Zn-37Al

Attempts were made to process Zn-37Al material but the alloy proved difficult to handle. Only the 16mm and 12mm sections could be filled.

### 5.3.3 Composite Manufacture

#### 5.3.3.1 Initial Experimentation

Preliminary work was geared towards establishing a suitable alloy for reinforcement and the development of optimum processing conditions for the introduction of particulate material. Approximately 5 volume% of SiC<sub>p</sub> was added to the chosen alloy. To standardise conditions the particulate was heated for 2 hours at 900°C. This gave information on optimum mixing time for good distribution.

#### 5.3.3.2 Production Run

It was decided to produce composite materials on ZA27 with 10, 15 and 20 volume% fractions of SiC<sub>p</sub>, processed under optimum conditions of mixing time and squeeze casting conditions. Twelve ingots were produced according to the parameters shown in Table 5.7.

#### 5.3.3.3 Further Trials

Additional experimentation to assess the capability of the reinforced alloys to fill thin sections, was carried out

PROCESSING PARAMETERS		
	ZA8 POUR 450°C 68 MPa 2H	ZA12 POUR 480°C 68 MPa 2H
DIE TEMP (°C)	CASTING NO.	CASTING NO.
150	1-3	1-3
180	4-6	4-6
220	7-9	7-9

TABLE 5.6 ZA8/ZA12 IN THIN SECTIONS  
(CASTINGS 1-9)

PROCESSING PARAMETERS	
POUR 595°C DIE TEMP 180°C 3F	
VOLUME %	CASTING NO.
10	1-4
15	5-8
20	9-12

TABLE 5.7 COMPOSITES PRODUCTION  
(CASTINGS 1-12)

using the shaped die and the backward extrusion die, but extended runs were not attempted.

#### **5.4 Testing**

Assessment was based on uni-axial mechanical property evaluation, metallography, chemical analysis, and dilatometry.

##### **5.4.1 Mechanical Properties**

###### **5.4.1.1 Tensile Mechanical Properties**

Room temperature tests were conducted using standard Hounsfield Specimens machined from the castings. Size 16 specimens could be machined from the ingots and the 16mm section of the backward extrusion die. The 12mm and 8mm sections were tested with size 14 and size 12 specimens respectively. Details of the specimens and testing conditions are shown in Table 5.8. Tests were carried out, using a 50kN Mayes testing machine.

Elevated temperature tensile tests were conducted at 60, 100 and 150°C by enclosing the specimens and grips in a furnace. A thermocouple was attached next to the specimen and the temperature allowed to stabilise for two hours prior to the test. Strain gauges were used to measure strain and hence Young's Modulus values. Equipment details are given in Table 5.9 and Figure 5.8.

###### **5.4.1.2 Compressive Mechanical Properties**

The 50kN Mayes machine could be fitted with an in-house, purpose built compression testing rig, which could be enclosed in a furnace. Use was made of this equipment, to conduct compression tests at both room and elevated temperatures. It could also be used for compressive creep testing at constant load.

Compression testing was carried out under load control, using cylindrical samples of 9mm diameter by 13mm length. Creep

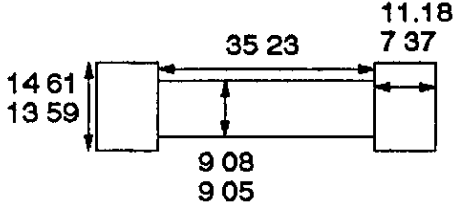
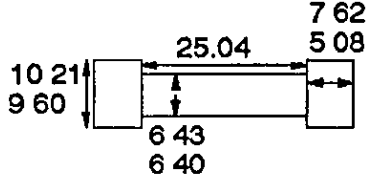
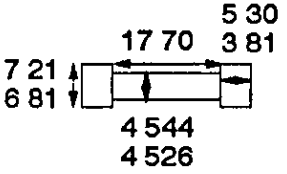
	SPECIMEN TYPE	TESTING CONDITIONS
	Hounsfield 16 used for testing ingot samples and 16mm diameter sections	10mm / minute
 <p data-bbox="659 1026 917 1055">(dimensions in mm)</p>	Hounsfield 14 used for testing 12mm diameter specimens	7mm / minute
	Hounsfield 12 used for testing 8mm diameter specimens	5mm / minute

Table 5.8 Details of Tensile Test Specimens

Machine	Mayes 50kN
Recorder	Advance HR2000
Strain Gauge Bridge	Tinsley Sovereign
Strain Gauge	Tokyo Sokki Kenkyujo Co., Ltd
length	3mm
type	QFLA-3
resistance	120+/-0.3 ohms
gauge factor	2.14

Table 5.9 High Temperature Tensile Test Equipment Details



Figure 5.8 Photograph Showing the High Temperature Tensile Test Equipment

testing, using the same sized samples, was carried out under constant load, with cross head movements being recorded against time., Pressures of 70MPa and 140MPa, and temperatures of 100 and 150°C were used to generate comparative data on the behaviour of squeeze-cast alloys and squeeze-cast composite materials.

#### **5.4.2 Metallography**

Samples for metallographic examination were prepared, according to the following sequence:

- section, using abrasive disc or saw
- finish
- mount in bakelite
- grind to 1200 grit, using SiC paper/water
- polish to 1 micron with diamond
- gamma alumina polish

(the last step was for electron microscope metallography)

##### **5.4.2.1 Light Microscopy**

Specimens were examined unetched then etched in 2% Nital, using white light. Photographs were taken where appropriate, using standard procedures.

##### **5.4.2.2 Electron Microscopy**

Electron Microscopy was used, both for fracture surface examination and microstructures. The two methods used were:

**SEM** A Stereoscan 360 electron microscope, equipped with a back scatter detector, was used to generate atomic number contrast images of the ZA alloy microstructures.

**TEM** Ion beam etching and TEM examination were carried out on selected samples using a Jeol 650 machine.

### 5.4.3 Chemical Analysis

#### 5.4.3.1 Bulk Chemical Analysis

This was carried out by a Quantovac machine, at the Brock Metal Company, in Cannock.

#### 5.4.3.2 Microstructural Analysis

An EDS Link system, attached to the electron microscopes, was used to gain information on the chemical nature of phases in the samples.

### 5.4.4 Dilatometry

Dilatometry work, to assess the stability of squeeze-cast ZA27 and to understand the differences in squeeze-cast ingots, was carried out using the equipment shown in Figure 5.9. Work involving both holding a specimen at constant temperature and heating selective specimens to the  $\beta$  solid solution range was carried out to try to explain differences in mechanical behaviour of ZA27.

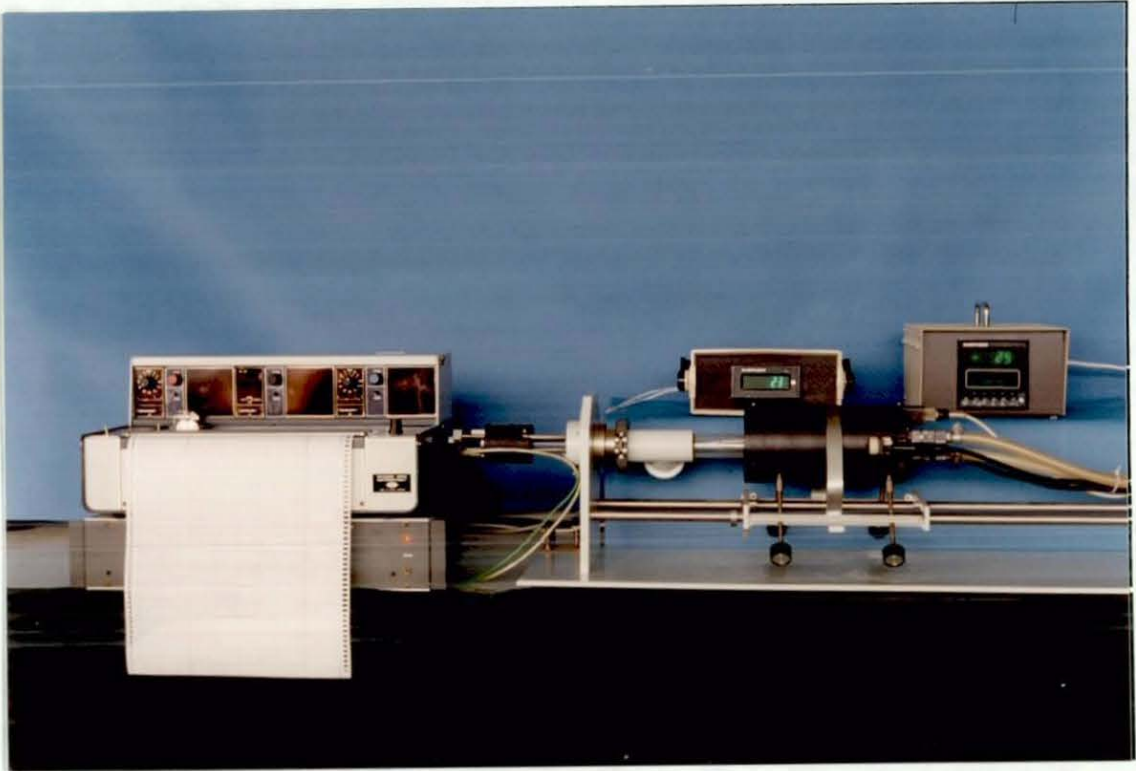


Figure 5.9 Dilatometry Equipment

## 6. Results

### 6.1 Processing Comments

Castings were produced from certified materials, having the compositions shown in Table 6.1.

Castings were generally produced sound, of excellent surface finish and with no visible indications of inverse segregation. Some of the thick section ingots of ZA8 and ZA12, although appearing sound on the outside, had large shrinkage holes in the centre section. The most likely explanation for this is that there was insufficient metal in the die prior to the application of pressure, combined with the mode of solidification of the alloys (skin freezing).

Ingots of metal matrix composites (ZA27 + SiC<sub>p</sub>), squeeze-cast after addition of SiC<sub>p</sub> by the vortex method, showed a large amount of compaction contraction. This was probably caused by air entrapments in the viscous mixture. The higher volume fraction composites (15 and 20vol%) were produced from remelted unsound composite ingots, stirred gently prior to casting. Less air was then entrapped in the melt and the amount of compaction contraction reduced.

Squeeze casting produced a very fine grain structure in all ingots. However, no macrostructures are shown because of the difficulty in obtaining a satisfactory contrast during etching.

Table 6.2 shows results of attempts to measure cooling rates during solidification in squeeze-cast ZA27. These are related, in section 7.2.1, to secondary dendrite arm spacing (SDAS).

### 6.2 Mechanical Properties of Squeeze-Cast Alloys

#### 6.2.1 ZA27

Tables A-E in Appendix 1 show the results of tensile testing

Table 6.1 Composition of Alloys

Alloy	Al	Mg	Cu	Fe	Sn	Pb	Cd
ZA27	26.66	0.019	2.11	0.039	0.0005	0.0017	0.0007
ZA8	8.53	0.022	1.07	0.012	0.0007	0.0016	0.0012
ZA12	11.21	0.026	1.11	0.033	0.0018	0.0019	0.001
Zn-37Al	37.03	0	0.06	0.204	0.0002	0.0012	0.0013

(All figures are weight %)

**Table 6.2: Cooling Rate Data for ZA27 in a 50mm Ingot Die**

Conditions	Die temperature (°C)	Pouring Temp (°C)	Cooling Rate (°C/s)
Method			
Gravity-Cast	150	555	1.67
Squeeze-Cast (185MPa)	150	555	78 26

of thick section ZA27, produced under various processing conditions. Tables A-D show the results at four die temperatures and three pressures, at a fixed pouring temperature. They vary in terms of press speed and pressure build-up level. Table E shows the effect of pouring temperature. The results are presented graphically in Figures 6.1 to 6.20, using average values.

Figures 6.1 to 6.4 show the effect of squeeze pressure, at four die temperatures, on the UTS. UTS results are consistently low at 200°C. Press speed, pressure build-up and pressure level do not appear to greatly influence properties.

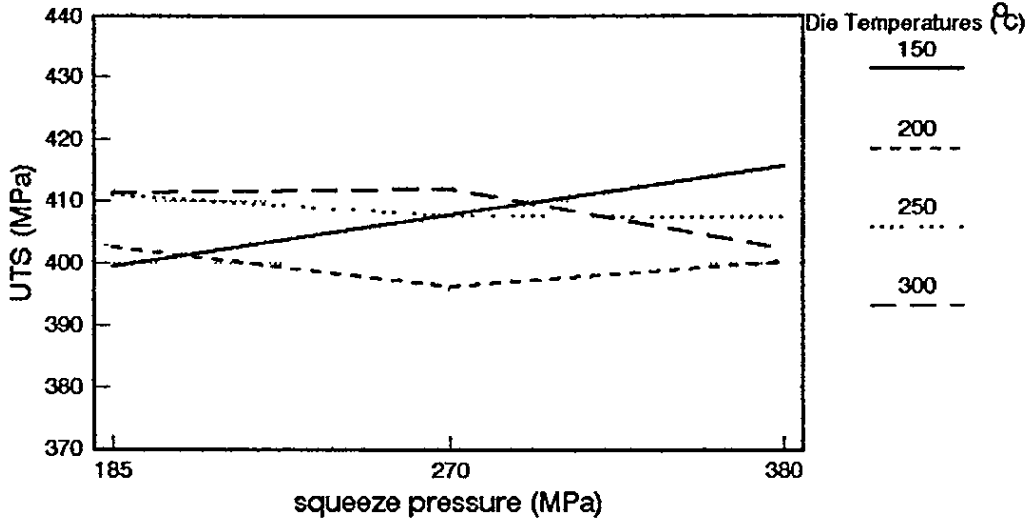
Figures 6.5 to 6.8 show the effect of squeeze pressure, at four die temperatures, on the 0.2%PS of ZA27. The 0.2%PS values are highest at high die temperatures and are increased at higher press speeds. The time for build-up of pressure does not appear significant. Lowest 0.2%PS values occur at a die temperature of 200°C.

Ductility values, from Tables A-D, are shown in Figures 6.9 - 6.16. In both cases, significant trends are not apparent.

The effect of pouring temperature is considered in Figures 6.17 - 6.20. Here, squeeze pressure and processing parameters are constant. As previously noted, tensile strength results are low at 200°C die temperature. A pouring temperature of 515°C produces low strengths, elongations and reduction in area. The highest elongation and reduction in area values were obtained with a 595°C pouring temperature and a 150°C die temperature.

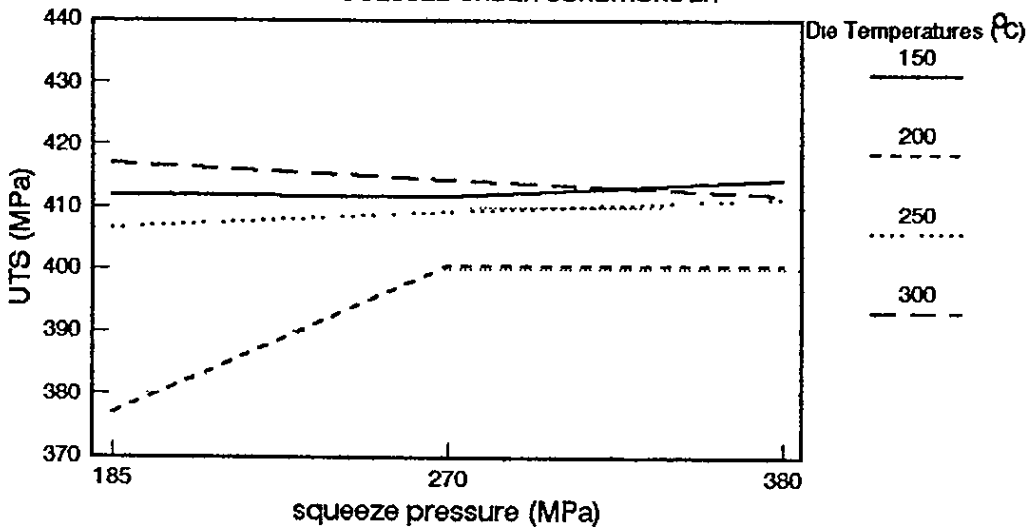
Tables F-H, in Appendix 1, show that the results of tensile tests on thin section squeeze-cast ZA27. These results were obtained at higher pouring temperatures, that is 595°C, 620°C and 650°C. Processing conditions were those which allowed filling of the die cavities, press speed 2 and half power

Figure 6.1 UTS OF SQUEEZE-CAST ZA27  
IN AN INGOT DIE  
PROCESSED UNDER CONDITIONS 2F



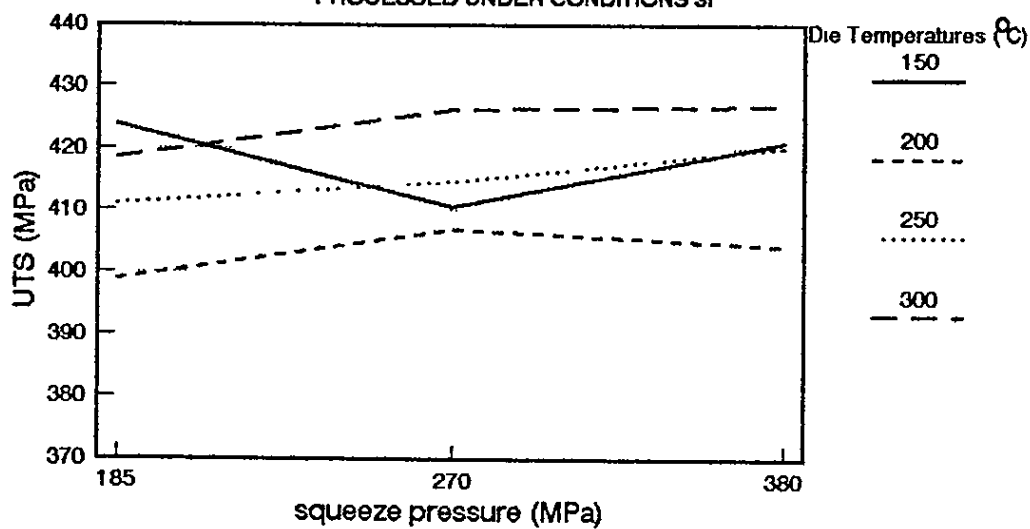
2F represents a delay of 6 seconds before the load is applied with a build-up of 11.5 tonnes per second.

Figure 6.2 UTS OF SQUEEZE-CAST ZA27  
IN AN INGOT DIE  
PROCESSED UNDER CONDITIONS 2H



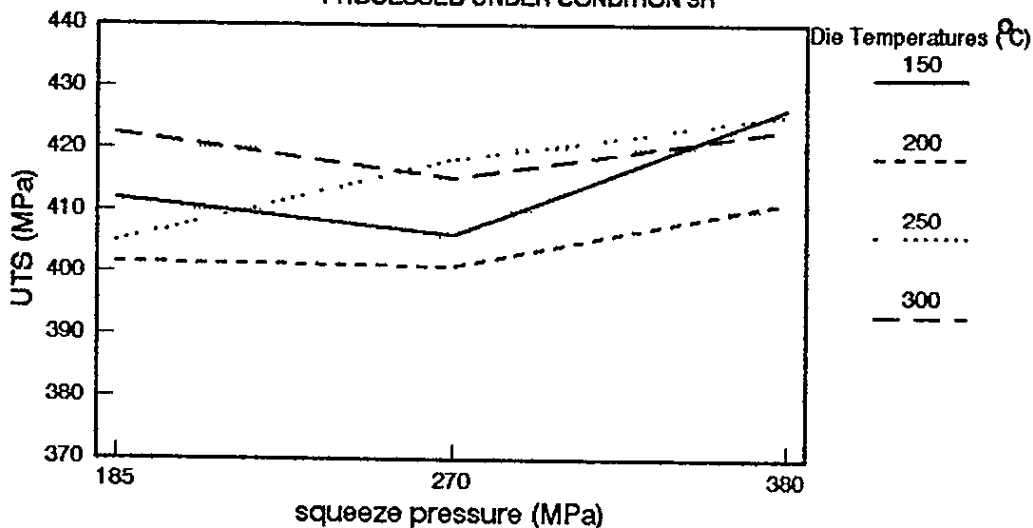
2H represents a delay of 6 seconds before the load is applied with a build-up of 8.3 tonnes per second.

Figure 6.3 UTS OF SQUEEZE-CAST ZA27  
IN AN INGOT DIE  
PROCESSED UNDER CONDITIONS 3F



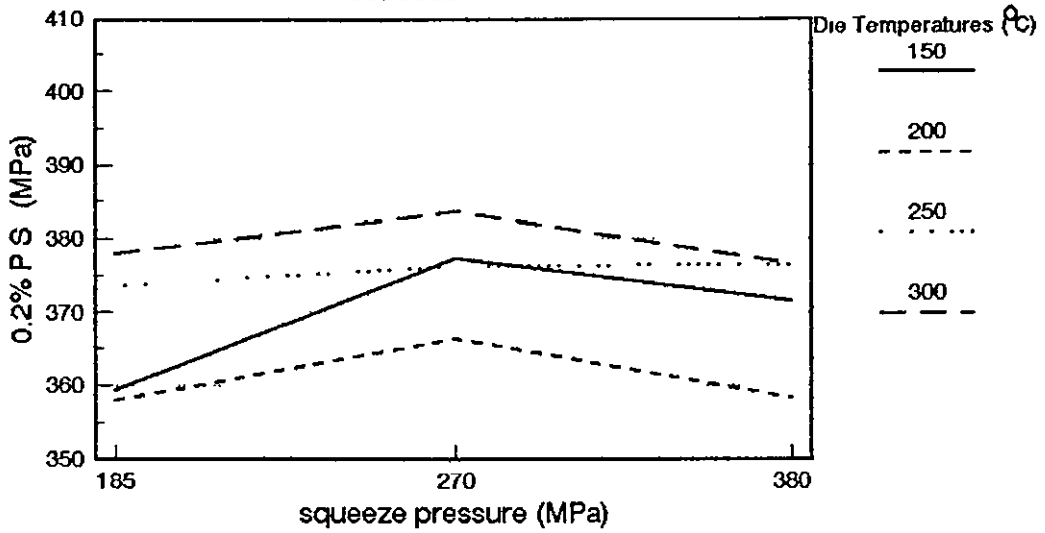
3F represents a delay of 4 seconds before the load is applied with a build-up of 11.5 tonnes per second.

Figure 6.4 UTS OF SQUEEZE-CAST ZA27  
IN AN INGOT DIE  
PROCESSED UNDER CONDITION 3H



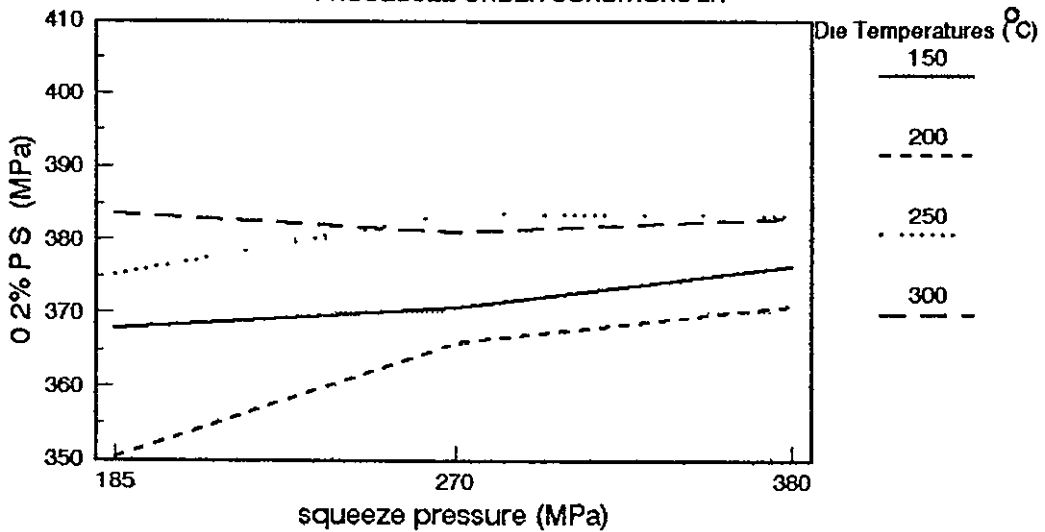
3H represents a delay of 4 seconds before the load is applied with a build-up of 8.3 tonnes per second.

Figure 6.5 0.2% P.S. OF SQUEEZE-CAST ZA27  
IN AN INGOT DIE  
PROCESSED UNDER CONDITIONS 2F



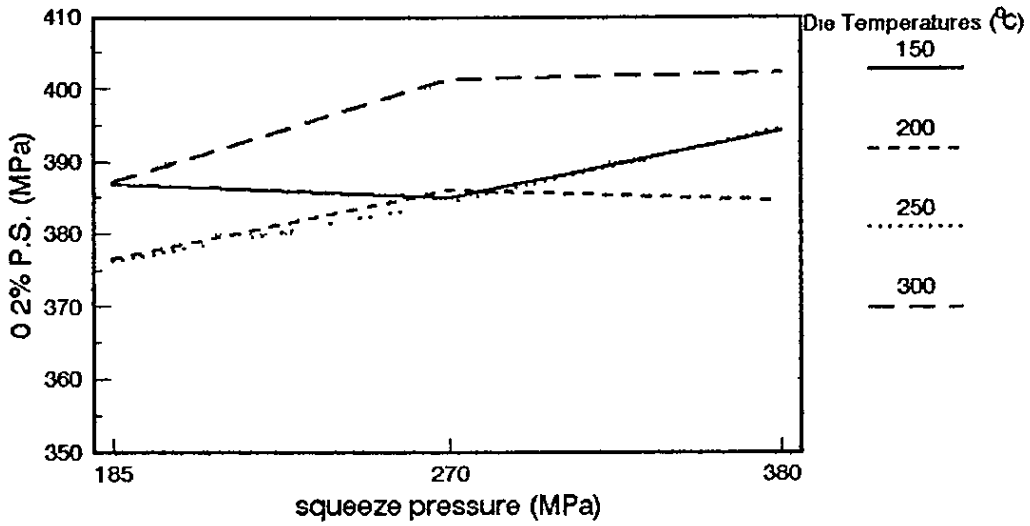
2F represents a delay of 6 seconds before the load is applied and with a build-up of 11.5 tonnes per second.

Figure 6.6 0.2% P.S. OF SQUEEZE-CAST ZA27  
IN AN INGOT DIE  
PROCESSED UNDER CONDITIONS 2H



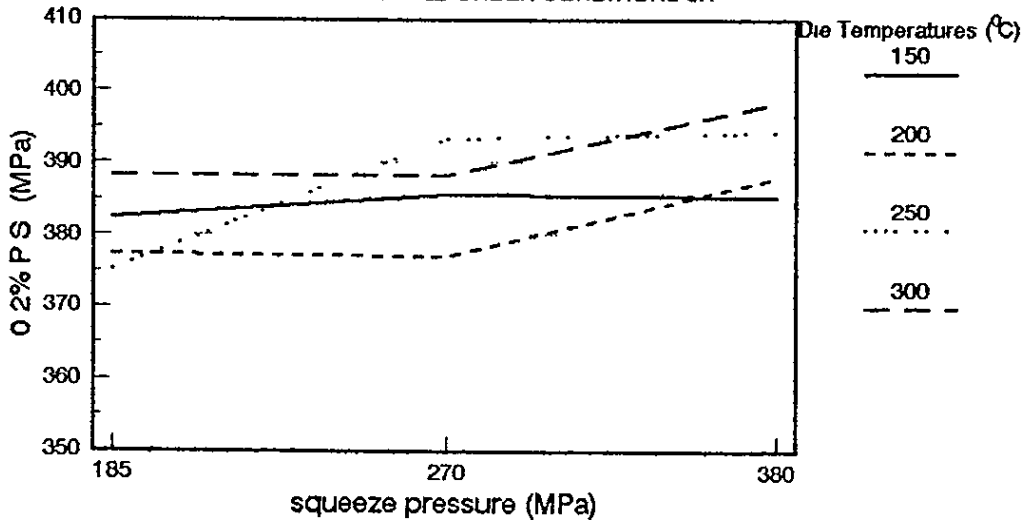
2H represents a delay of 6 seconds before the load is applied with a build-up of 8.3 tonnes per second.

Figure 6.7 0.2% P.S. OF SQUEEZE-CAST ZA27  
IN AN INGOT DIE  
PROCESSED UNDER CONDITIONS 3F



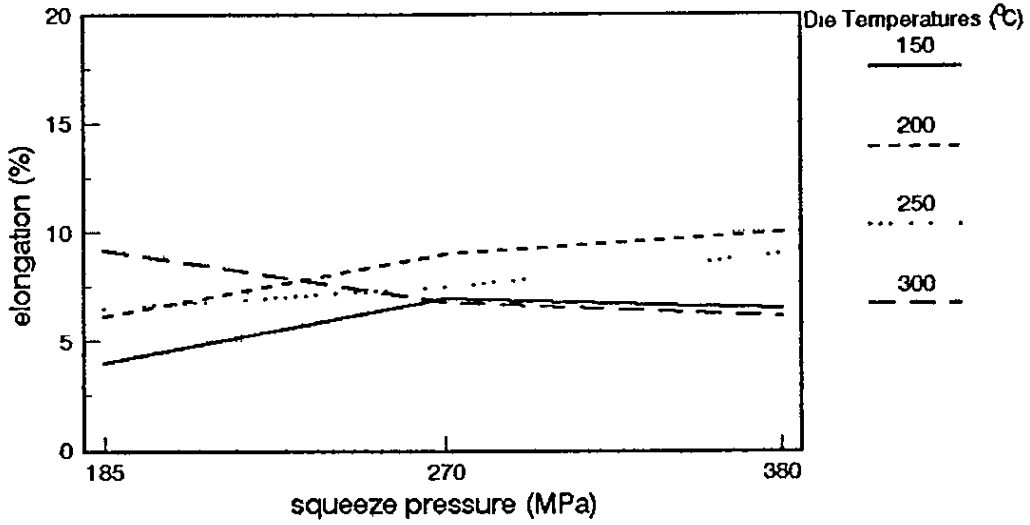
3F represents a delay of 4 seconds before the load is applied with a build-up of 11.5 tonnes per second.

Figure 6.8 0.2% P.S. OF SQUEEZE-CAST ZA27  
IN AN INGOT DIE  
PROCESSED UNDER CONDITIONS 3H



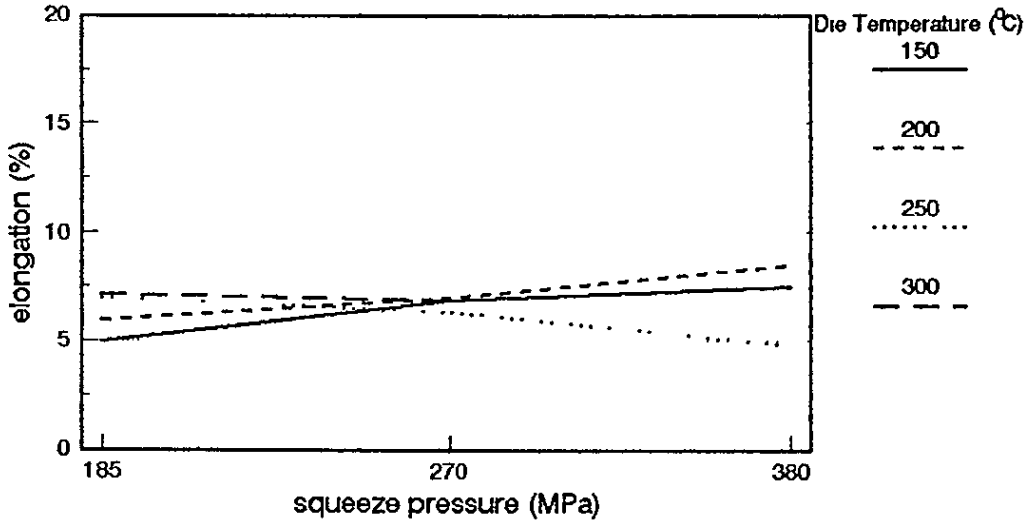
3H represents a delay of 4 seconds before the load is applied with a build-up of 8.3 tonnes per second.

Figure 6.9 % ELONGATION OF SQUEEZE-CAST ZA27  
IN AN INGOT DIE  
PROCESSED UNDER CONDITIONS 2F



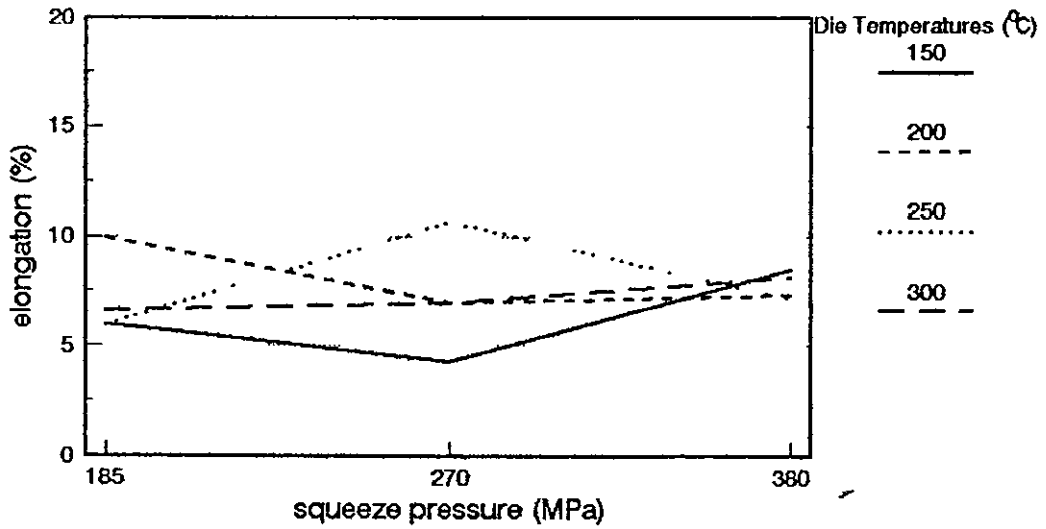
2F represents a delay of 6 seconds before the load is applied with a build-up of 11.5 tonnes per second.

Figure 6.10 % ELONGATION OF SQUEEZE-CAST ZA27  
IN AN INGOT DIE  
PROCESSED UNDER CONDITIONS 2H



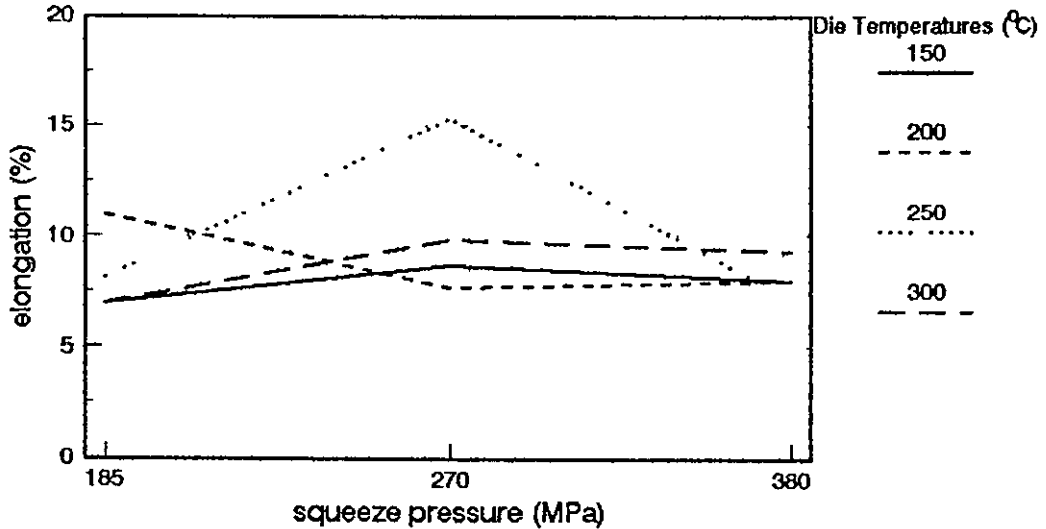
2H represents a delay of 6 seconds before the load is applied with a build-up of 8.3 tonnes per second.

Figure 6.11 % ELONGATION OF SQUEEZE-CAST ZA27  
IN AN INGOT DIE  
PROCESSED UNDER CONDITIONS 3F



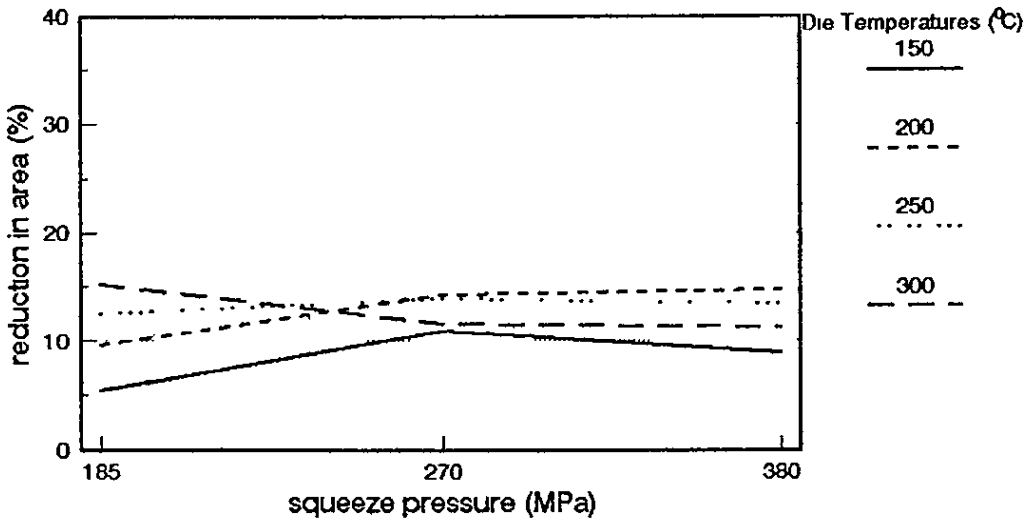
3F represents a delay of 4 seconds before the load is applied with a build-up of 11.5 tonnes per second.

Figure 6.12 % ELONGATION OF SQUEEZE-CAST ZA27  
IN AN INGOT DIE  
PROCESSED UNDER CONDITIONS 3H



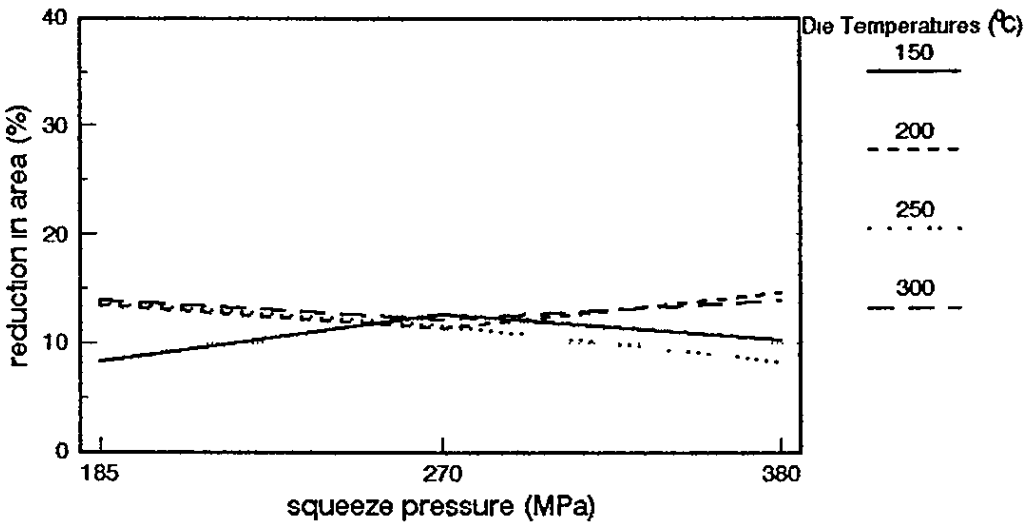
3H represents a delay of 4 seconds before the load is applied with a build-up of 8.3 tonnes per second.

Figure 6.13 % REDUCTION IN AREA OF SQUEEZE  
CAST ZA27 IN AN INGOT DIE  
PROCESSED UNDER CONDITIONS 2F



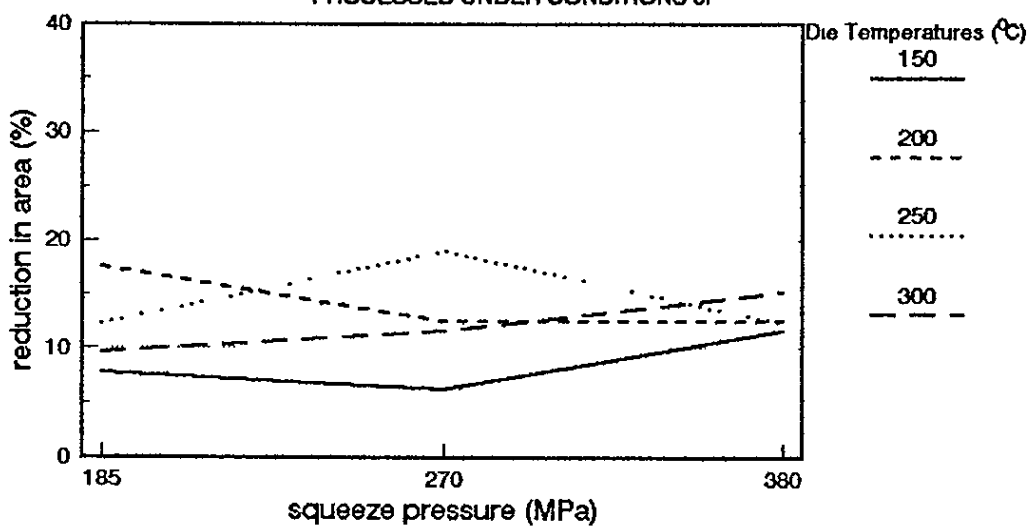
2F represents a delay of 6 seconds before the load is applied with a build-up of 11.5 tonnes per second.

Figure 6.14 % REDUCTION IN AREA OF SQUEEZE  
CAST ZA27 IN AN INGOT DIE  
PROCESSED UNDER CONDITIONS 2H



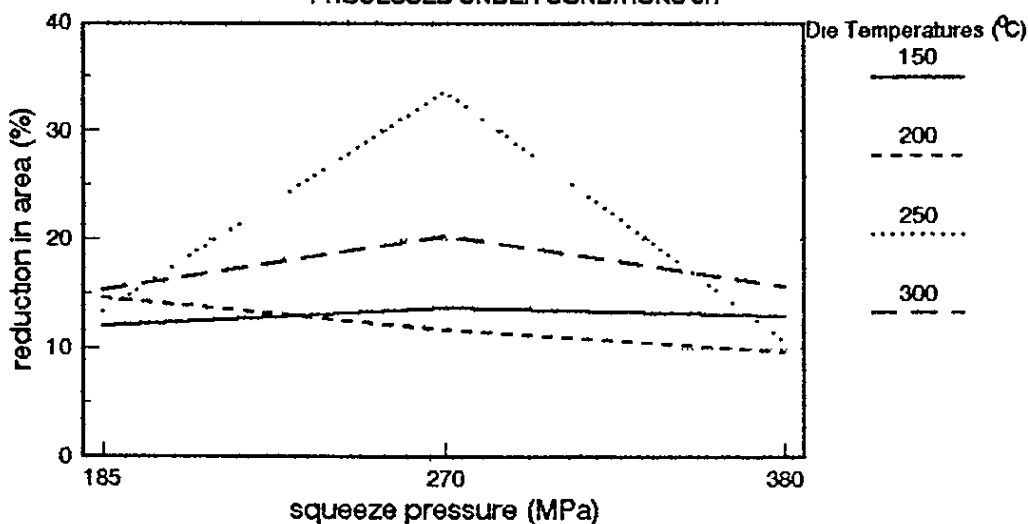
2H represents a delay of 6 seconds before the load is applied with a build-up of 8.3 tonnes per second.

Figure 6.15 % REDUCTION IN AREA OF SQUEEZE  
CAST ZA27 IN AN INGOT DIE  
PROCESSED UNDER CONDITIONS 3F



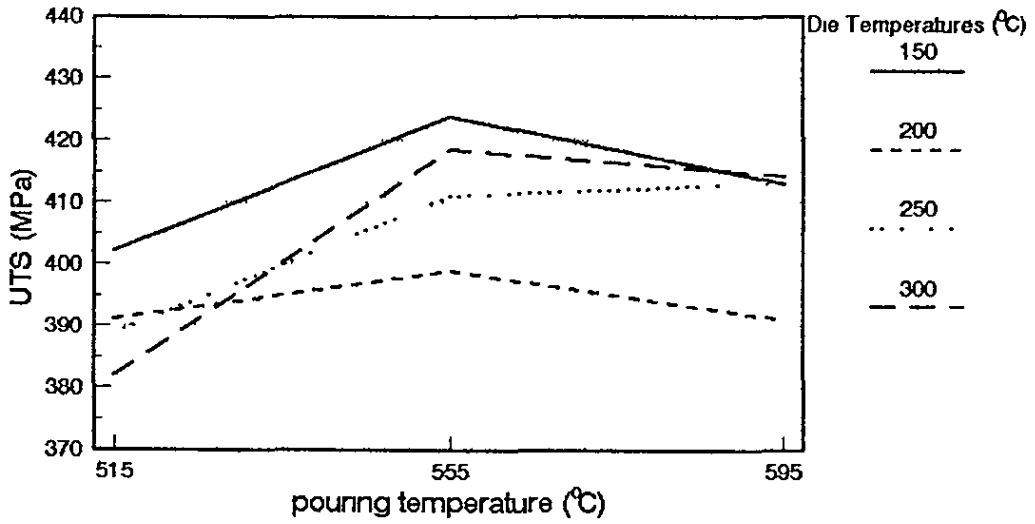
3F represents a delay of 4 seconds before the load is applied with a build-up of 11.5 tonnes per second.

Figure 6.16 % REDUCTION IN AREA OF SQUEEZE  
CAST ZA27 IN AN INGOT DIE  
PROCESSED UNDER CONDITIONS 3H



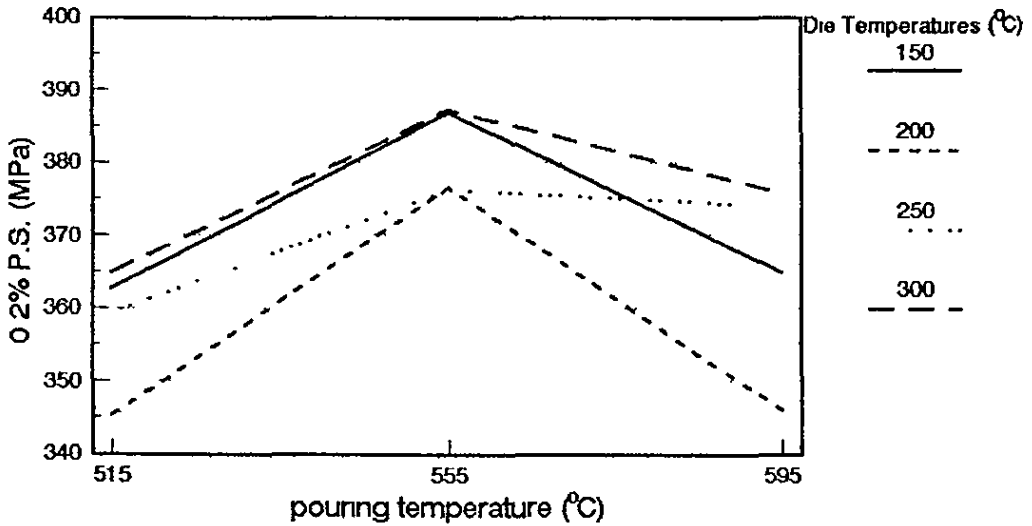
3H represents a delay of 4 seconds before the load is applied with a build-up of 8.3 tonnes per second.

Figure 6.17 UTS OF SQUEEZE CAST ZA27  
IN AN INGOT DIE  
PROCESSED UNDER CONDITIONS 3F



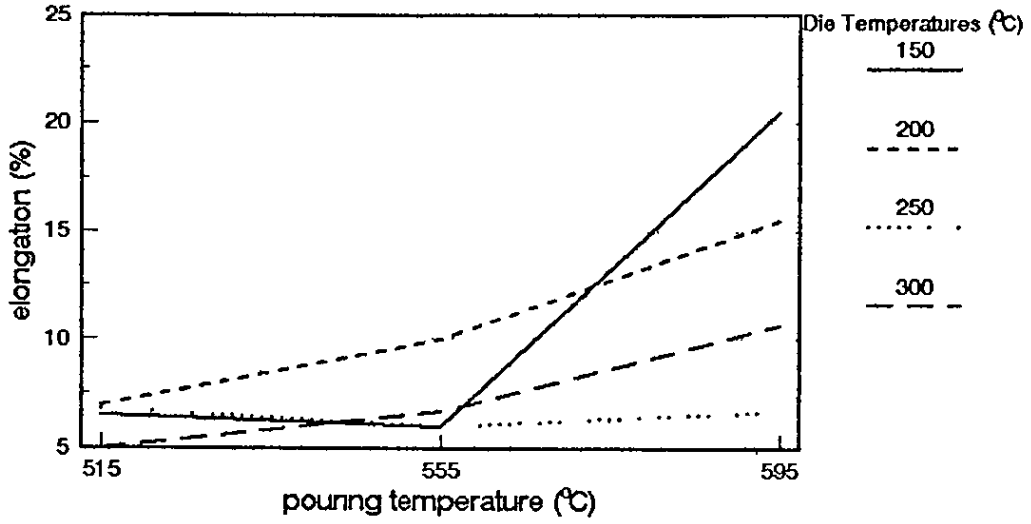
3F represents a delay of 4 seconds before the load is applied with a build-up of 11.5 tonnes per second.

Figure 6.18 0.2% P.S. OF SQUEEZE CAST ZA27  
IN AN INGOT DIE  
PROCESSED UNDER CONDITIONS 3F



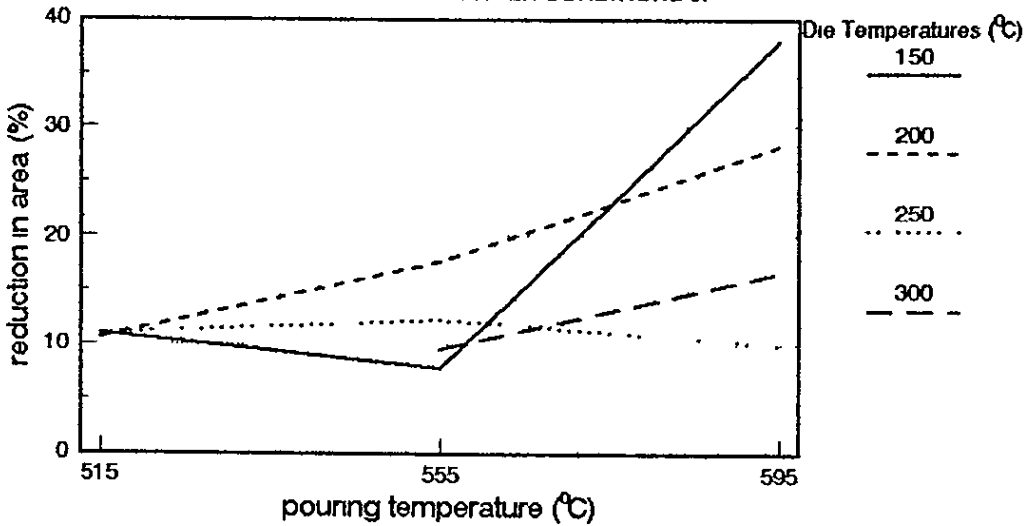
3F represents a delay of 4 seconds before the load is applied with a build-up of 11.5 tonnes per second.

Figure 6.19 % ELONGATION OF SQUEEZE CAST ZA27  
IN AN INGOT DIE  
PROCESSED UNDER CONDITIONS 3F



3F represents a delay of 4 seconds before the load is applied with a build-up of 11.5 tonnes per second.

Figure 6.20 % REDUCTION IN AREA OF SQUEEZE  
CAST ZA27 IN AN INGOT DIE  
PROCESSED UNDER CONDITIONS 3F



3F represents a delay of 4 seconds before the load is applied with a build-up of 11.5 tonnes per second.

pressure, corresponding to a delay of 8 seconds before the load was applied and a build up of 8.3 tonnes per second. Die temperatures of 150°C, 180°C and 220°C were employed. Figures 6.21 to 6.29 show the effects of section thickness, at different die temperatures, for the three pouring temperatures on mechanical properties.

Figures 6.21 to 6.23 show that ultimate strengths in thin section squeeze-cast ZA27 are highest at highest die temperature, in some cases in excess of 450MPa. This is improved over thicker section material where the highest strength noted was 429MPa. Figures 6.24 to 6.26 show that 0.2% Proof Stress values are also highest at highest die temperatures, in some cases greater than 420MPa.

Elongation values, shown in Figures 6.27-6.29 show variable behaviour. Maximum elongation values of around 10% were lower than those realised in thicker section material.

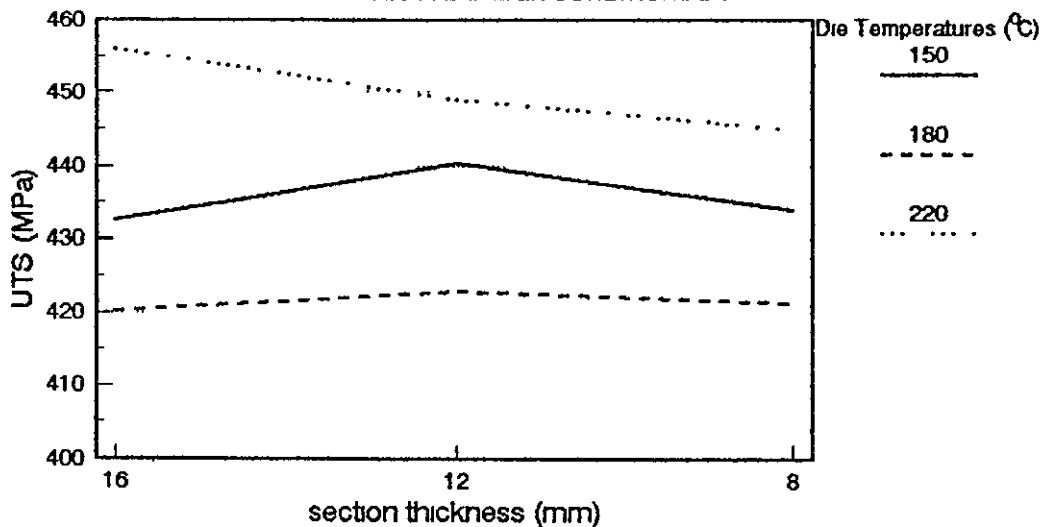
#### 6.2.2 ZA8

Table I, in Appendix 1, shows the effects of processing parameters on the mechanical properties of thick section squeeze-cast ZA8. The result at 200°C die temperature and 185MPa squeeze pressure is not included, since the casting had a shrinkage hole, as is detailed in section 6.1.

The material was brittle and not all the 0.2%PS (or 0.1%PS) values could be calculated. Here, assessment is based on tensile strength and elongation.

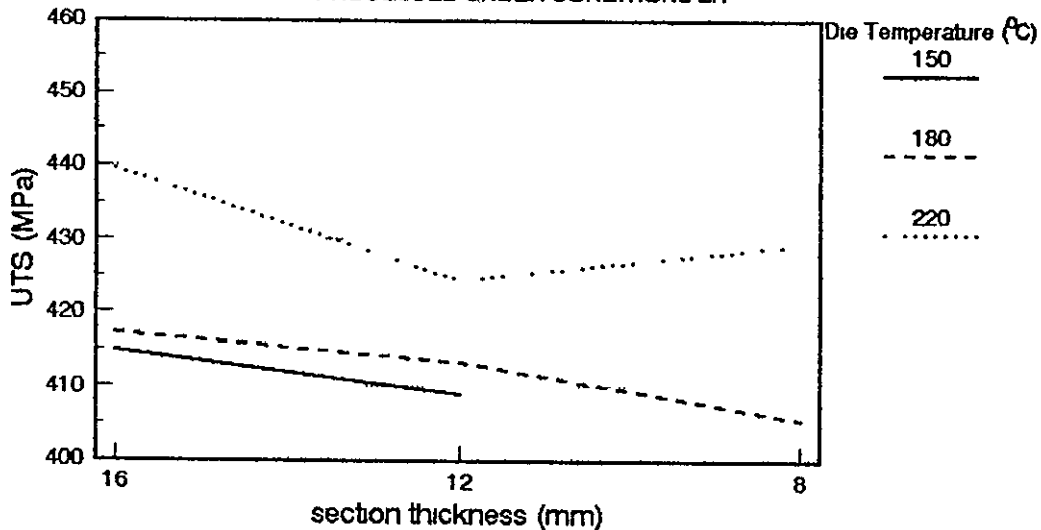
No effects of squeeze pressure or processing parameters, for example press speed and build-up, are apparent from the results. However, die temperature does have an effect on strength. Strengths are greatest at the lowest die temperature and weakest at the highest temperature, as shown in Figure 6.30. Elongation values in the range 2-4% are apparent for all die temperatures (Figure 6.31).

Figure 6.21 UTS OF SQUEEZE CAST ZA27  
IN THIN SECTIONS AT 595°C POURING TEMPERATURE  
PROCESSED UNDER CONDITIONS 2H



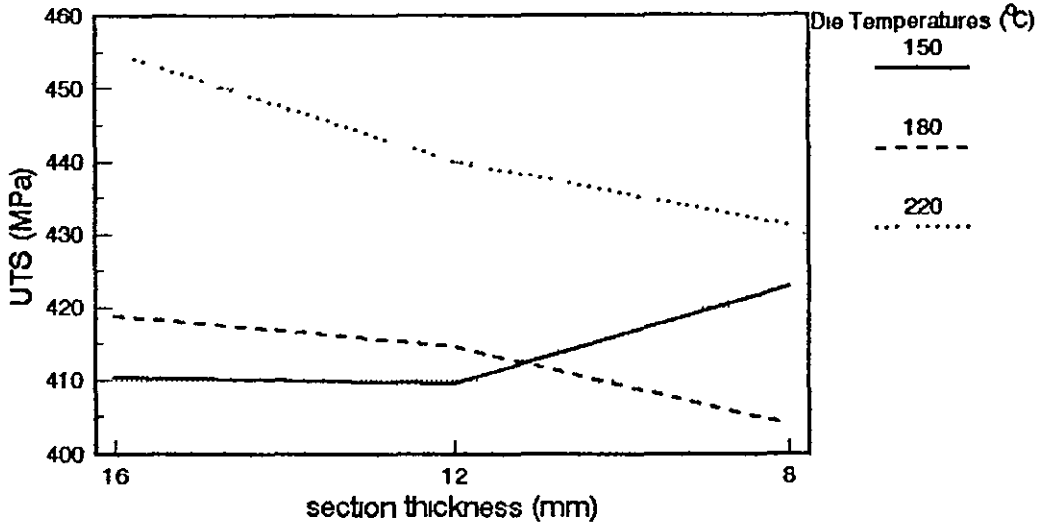
2H represents a delay of 8 seconds before the load is applied with a build-up of 8.3 tonnes per second.

Figure 6.22 UTS OF SQUEEZE CAST ZA27  
IN THIN SECTIONS AT 620°C POURING TEMPERATURE  
PROCESSED UNDER CONDITIONS 2H



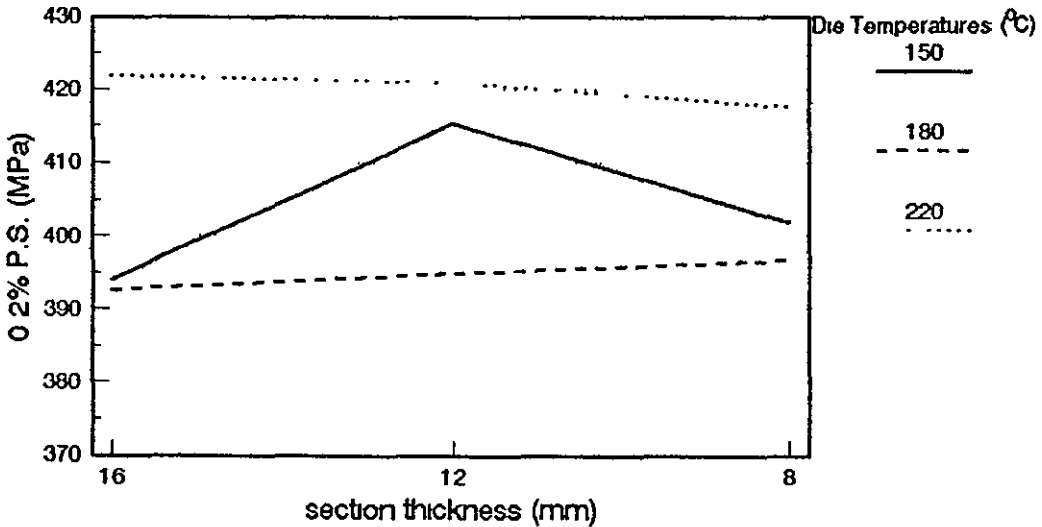
2H represents a delay of 8 seconds before the load is applied with a build-up of 8.3 tonnes per second.

**Figure 6.23 UTS OF SQUEEZE CAST ZA27  
IN THIN SECTIONS AT 650°C POURING TEMPERATURE  
PROCESSED UNDER CONDITIONS 2H**



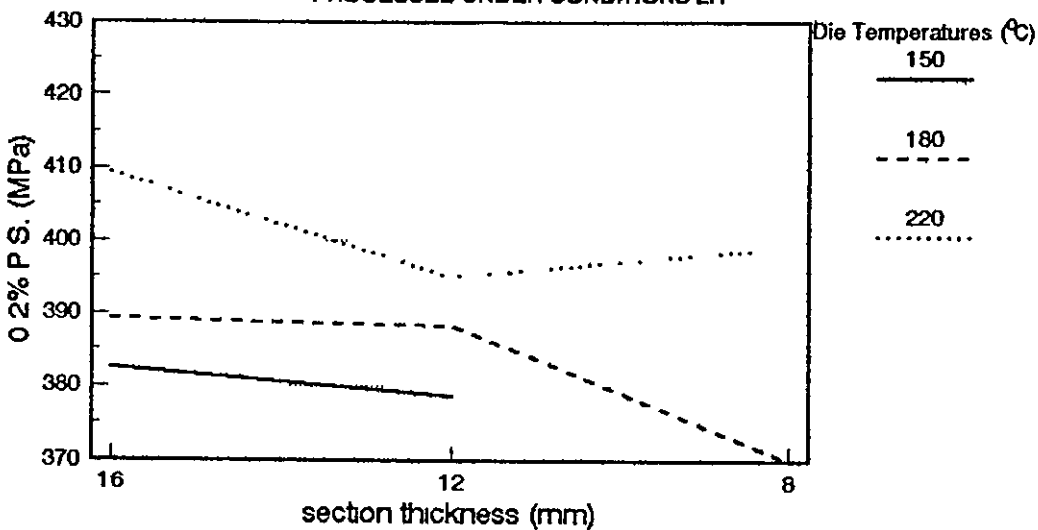
2H represents a delay of 8 seconds before the load is applied with a build-up of 8.3 tonnes per second.

**Figure 6.24 0.2% P.S. OF SQUEEZE CAST ZA27  
IN THIN SECTIONS AT 695°C POURING TEMPERATURE  
PROCESSED UNDER CONDITIONS 2H**



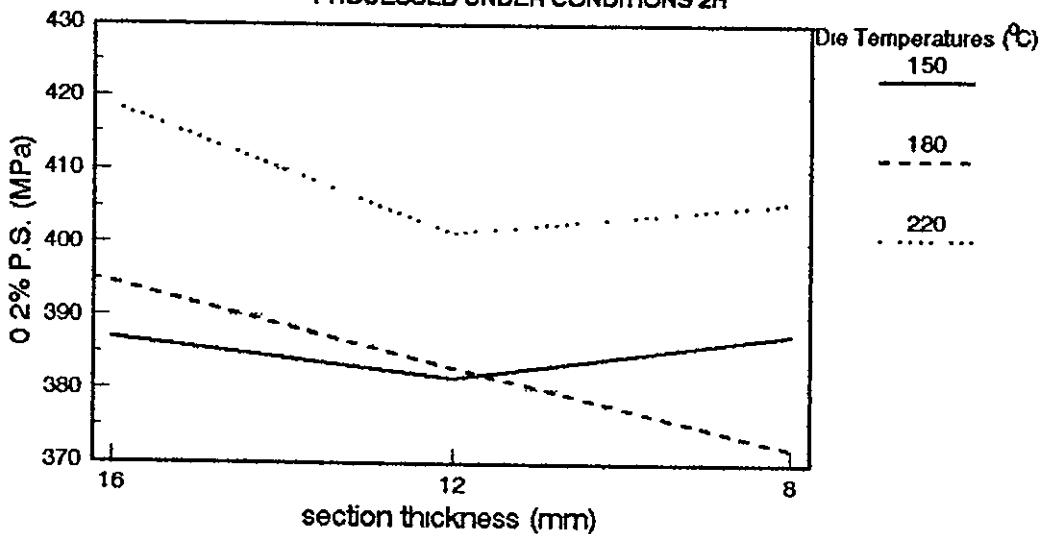
2H represents a delay of 8 seconds before the load is applied with a build-up of 8.3 tonnes per second.

Figure 6.25 0.2% P.S. OF SQUEEZE CAST ZA27  
IN THIN SECTIONS AT 620°C POURING TEMPERATURE  
PROCESSED UNDER CONDITIONS 2H



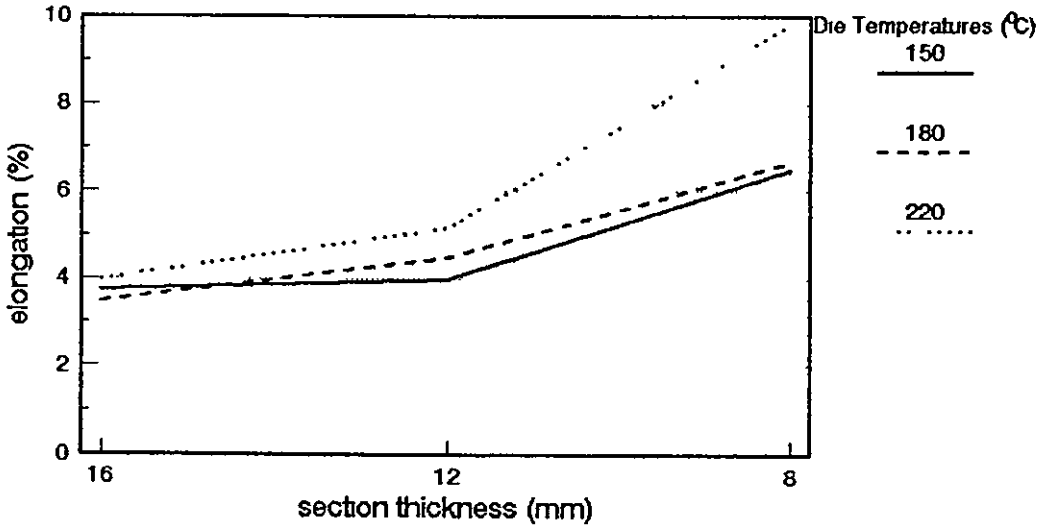
2H represents a delay of 8 seconds before the load is applied with a build-up of 8.3 tonnes per second.

Figure 6.26 0.2% P.S. OF SQUEEZE CAST ZA27  
IN THIN SECTIONS AT 650°C POURING TEMPERATURE  
PROCESSED UNDER CONDITIONS 2H



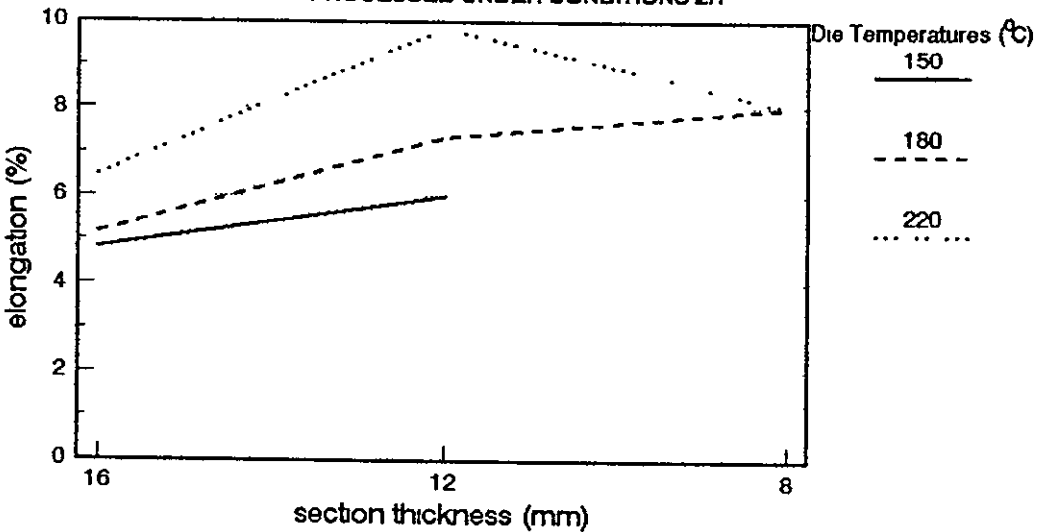
2H represents a delay of 8 seconds before the load is applied with a build-up of 8.3 tonnes per second.

Figure 6.27 % ELONGATION OF SQUEEZE CAST ZA27  
IN THIN SECTIONS AT 595°C POURING TEMPERATURE  
PROCESSED UNDER CONDITIONS 2H



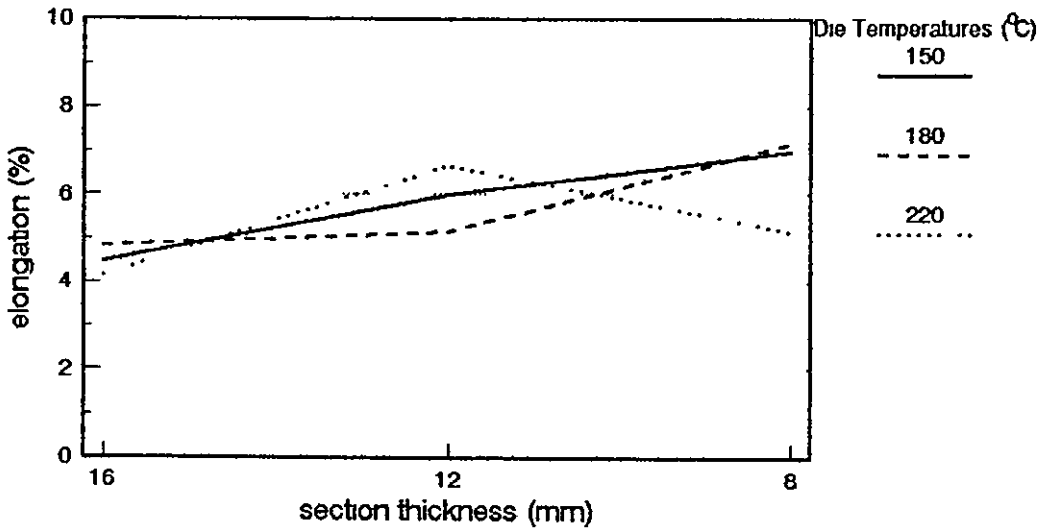
2H represents a delay of 8 seconds before the load is applied with a build-up of 8.3 tonnes per second.

Figure 6.28 % ELONGATION OF SQUEEZE CAST ZA27  
IN THIN SECTIONS AT 620°C POURING TEMPERATURE  
PROCESSED UNDER CONDITIONS 2H



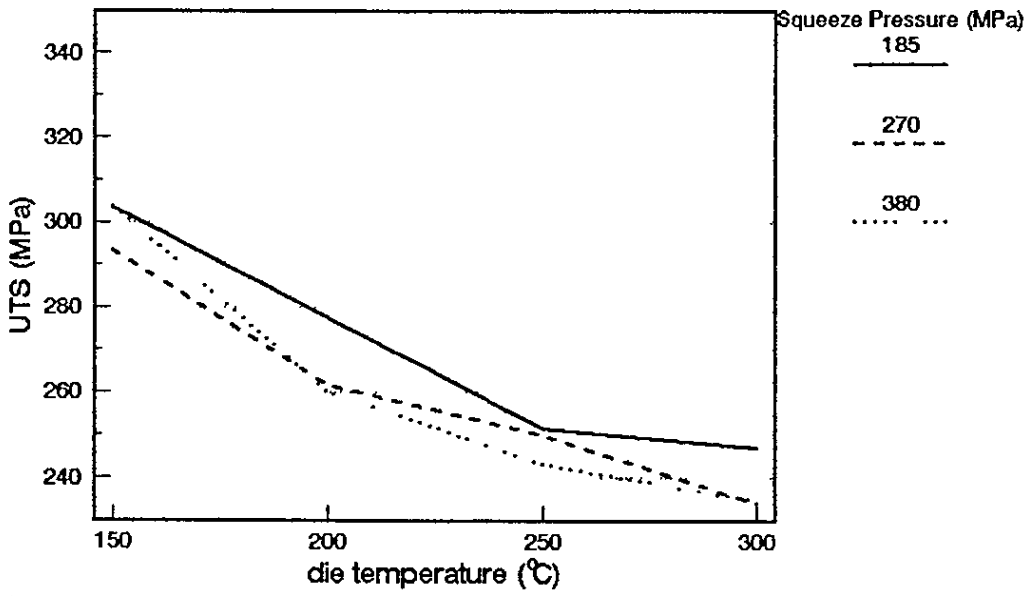
2H represents a delay of 8 seconds before the load is applied with a build-up of 8.3 tonnes per second.

Figure 6.29 % ELONGATION OF SQUEEZE CAST ZA27  
IN THIN SECTIONS AT 650°C POURING TEMPERATURE  
PROCESSED UNDER CONDITIONS 2H



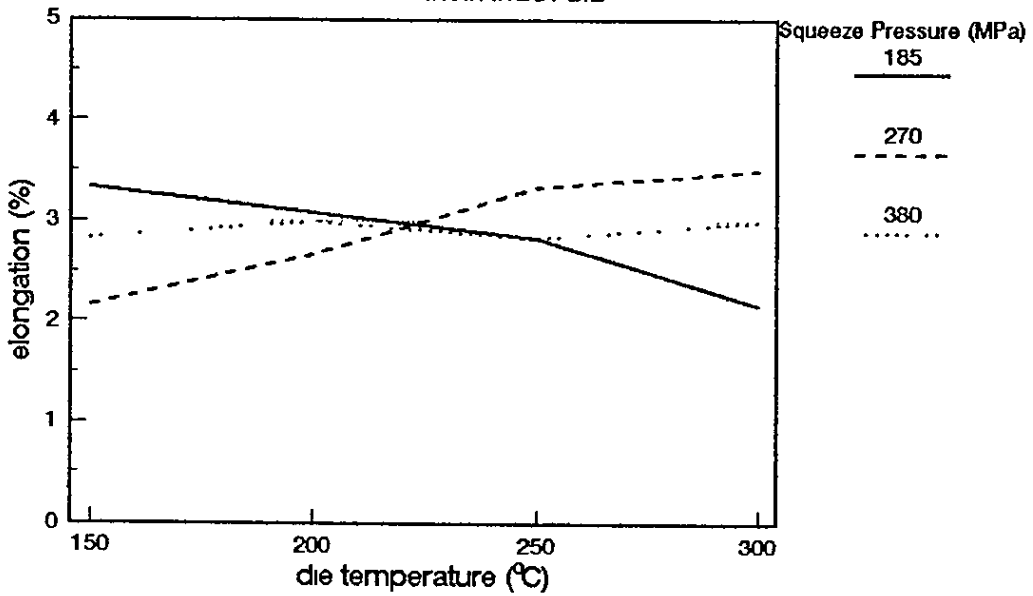
2H represents a delay of 8 seconds before the load is applied with a build-up of 8.3 tonnes per second.

Figure 6.30 UTS OF SQUEEZE-CAST ZA8  
IN AN INGOT DIE



For processing conditions see Table 5.2

Figure 6.31 % ELONGATION OF SQUEEZE-CAST ZA8  
IN AN INGOT DIE



For processing conditions see Table 5.2

Table J, in Appendix 1, shows the results of processing ZA8 by squeeze casting into thin sections. These results are shown in Figures 6.32 and 6.33. The same trend, demonstrated by the thicker sections, is noted here. Tensile strength decreases with increase in die temperature. The strengths at a given die temperature in thin sections are higher than those for the corresponding thick sections. Elongation values (Figure 6.33) are higher in the thinner sections than in the thick sections.

### 6.2.3 ZA12

Table K, in Appendix 1, shows the tensile results of thick section squeeze-cast ZA12. Three of the castings had a large shrinkage void, as described in section 6.1 and thus, no results were quoted (Figure 6.34). In most cases it was possible to determine 0.2% proof strength. A similar trend to that noted for ZA8 was apparent here, with strength reducing with increased die temperature. No noticeable effect of pressure or other processing parameters was evident. Elongation values lay within the 2-4% range (Figure 6.35).

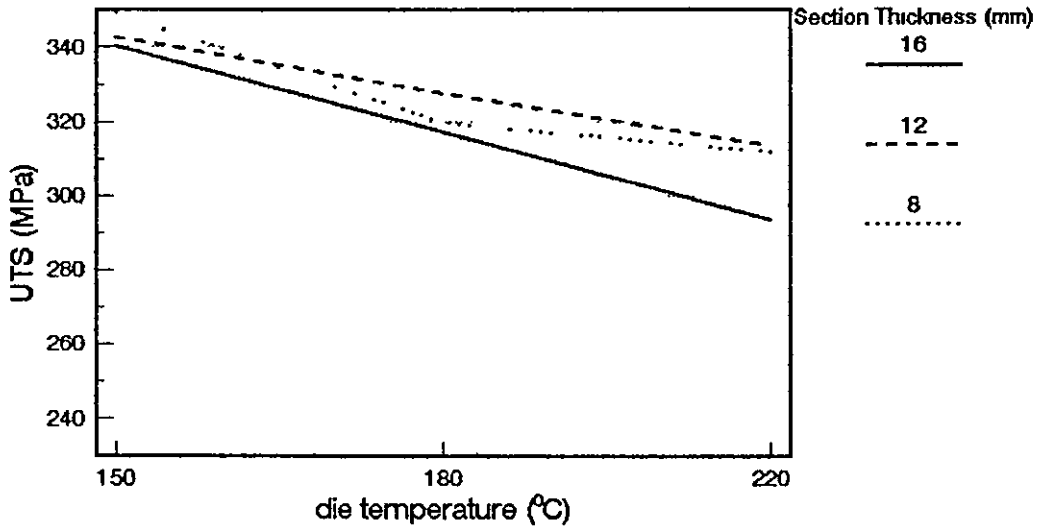
Thin section squeeze-cast ZA12 showed tensile strength variations in the range 349-375MPa, see Table L of appendix 1. The 0.2% proof strength is of the order 327-348MPa in the range considered and elongation values of up to 5% were also noted. All these results were improved, relative to the thick section results. The reduction in strength with increase in die temperature was not as marked with ZA12, compared to ZA8.

Figures 6.36 and 6.37 show the variations in strength and elongation of ZA12 with die temperature and section thickness.

### 6.2.4 Zn-37Al

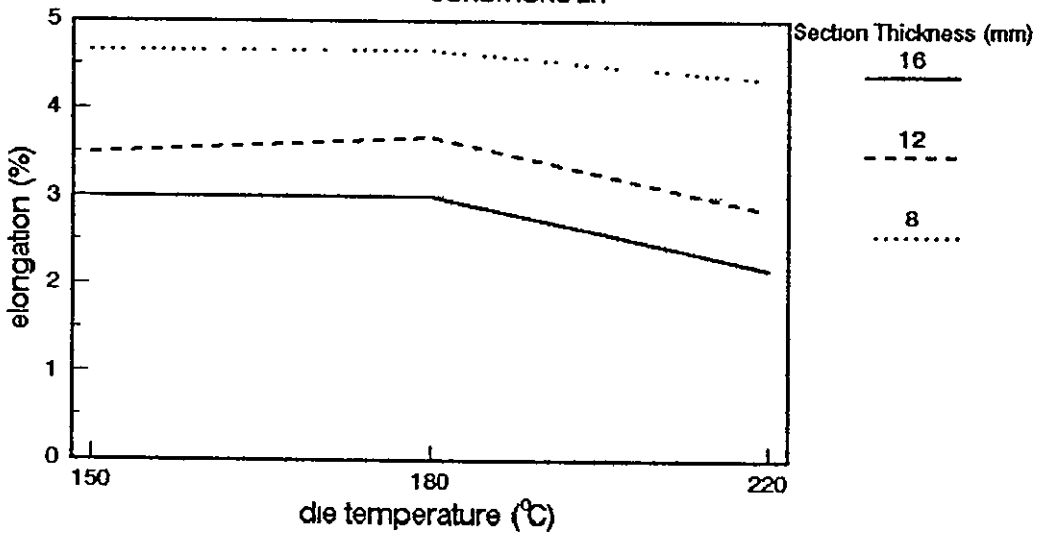
Table M of Appendix 1 shows the effect of squeeze casting parameters on the mechanical properties of thick section

Figure 6.32 UTS OF SQUEEZE-CAST ZA8  
IN A THIN SECTION DIE PROCESSED UNDER  
CONDITIONS 2H



2H represents a delay of 8 seconds before the load is applied with a build-up of 8.3 tonnes per second.

Figure 6.33 ELONGATION OF SQUEEZE-CAST ZA8  
IN A THIN SECTION DIE PROCESSED UNDER  
CONDITIONS 2H



2H represents a delay of 8 seconds before the load is applied with a build-up of 8.3 tonnes per second.

Figure 6.34 UTS OF SQUEEZE-CAST ZA12  
IN AN INGOT DIE

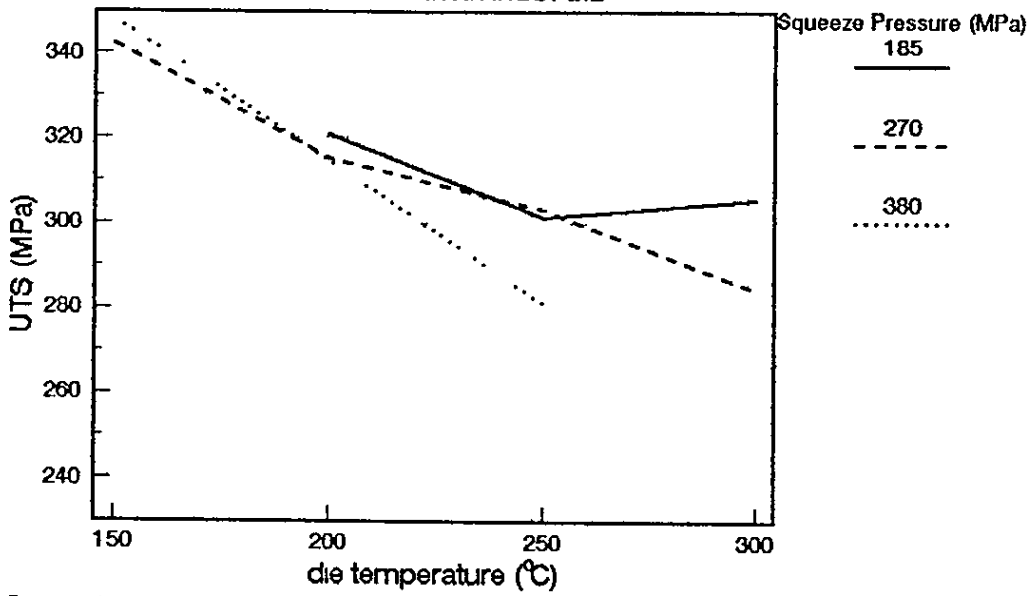


Figure 6.35 % ELONGATION OF SQUEEZE-CAST ZA12  
IN AN INGOT DIE

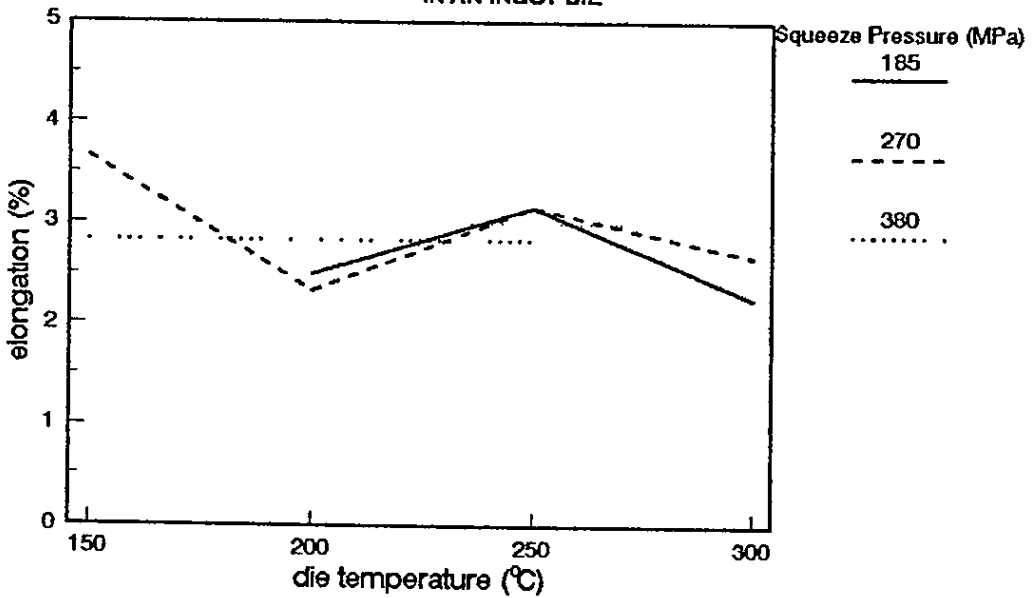
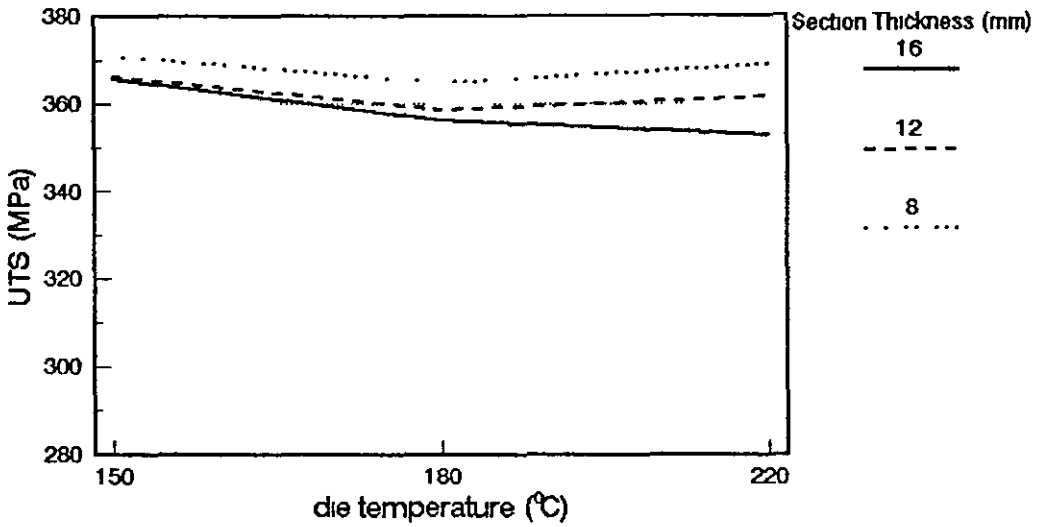
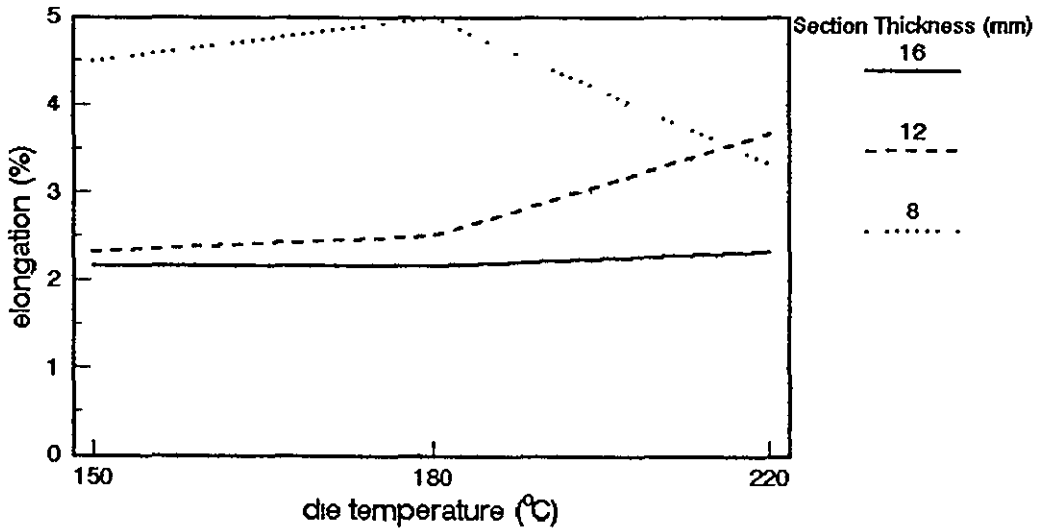


Figure 6.36 UTS OF SQUEEZE-CAST ZA12  
IN A THIN SECTION DIE PROCESSED UNDER  
CONDITIONS 2H



2H represents a delay of 8 seconds before the load is applied at a build-up of 8.3 tonnes per second.

Figure 6.37 ELONGATION OF SQUEEZE-CAST ZA12  
IN A THIN SECTION DIE PROCESSED UNDER  
CONDITIONS 2H



2H represents a delay of 8 seconds before the load is applied with a build-up of 8.3 tonnes per second.

Zn-37Al alloy. The variables studied were die temperature and pouring temperature, because it had become apparent that these were significant parameters affecting the properties of squeeze-cast ZA alloys. Here, highest strength values were obtained at 150°C, the lowest die temperature (Figures 6.38 and 6.39). Higher ductility values were always obtained at the lower pouring temperature, ie at 565°C, and they were highest at highest die temperature (Figures 6.40 and 6.41).

Thin section processing of Zn-37Al proved difficult so that results cannot be quoted.

### 6.3 Microstructures of Squeeze-Cast Alloys

Conventional light microscopy (LM) was attempted on all alloys but the results were unsatisfactory, especially with ZA8 and ZA12. The high cooling rate developed during squeeze casting gave rise to very fine microstructures, which could not be clearly resolved. Most of the figures presented here were prepared by SEM, using a sensitive back-scatter detector. Some measurements of microstructural features are also quoted. Their significance is discussed in Chapter 7.

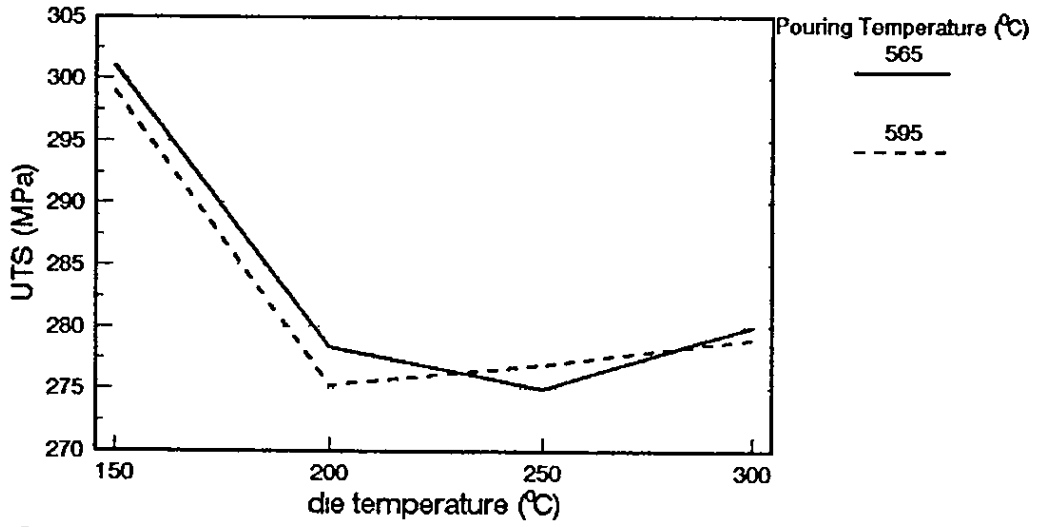
#### 6.3.1 ZA27

A light micrograph, showing a typical structure of squeeze-cast ZA27, produced in a thick (50mm) section is shown in Figure 6.42.

Microstructures of ZA alloys have been described by Murphy [83]. The light coloured central areas in Figure 6.42 are the prior, primary  $\alpha$  (or  $\alpha'$ ) phase, which has decomposed to  $\alpha+\eta$ . Surrounding the primary phase is prior  $\beta$ , which formed peritectically and has subsequently decomposed to  $\alpha+\eta$ . The eutectic is made up of a dark phase ( $\eta$ ), lighter prior eutectic  $\beta$  and white  $\text{CuZn}_4$  ( $\epsilon$ ) phase.

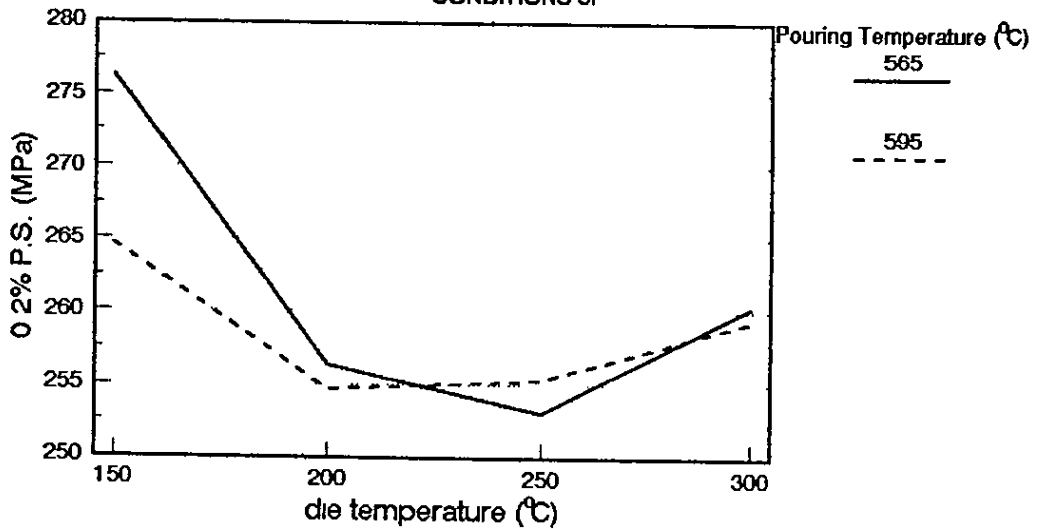
The structure is dendritic. Decomposition of the phases is not clearly resolved. More microstructural information can be obtained from the scanning electron microscope.

Figure 6.38 UTS OF SQUEEZE-CAST Zn-37Al  
IN AN INGOT DIE PROCESSED UNDER  
CONDITIONS 3F



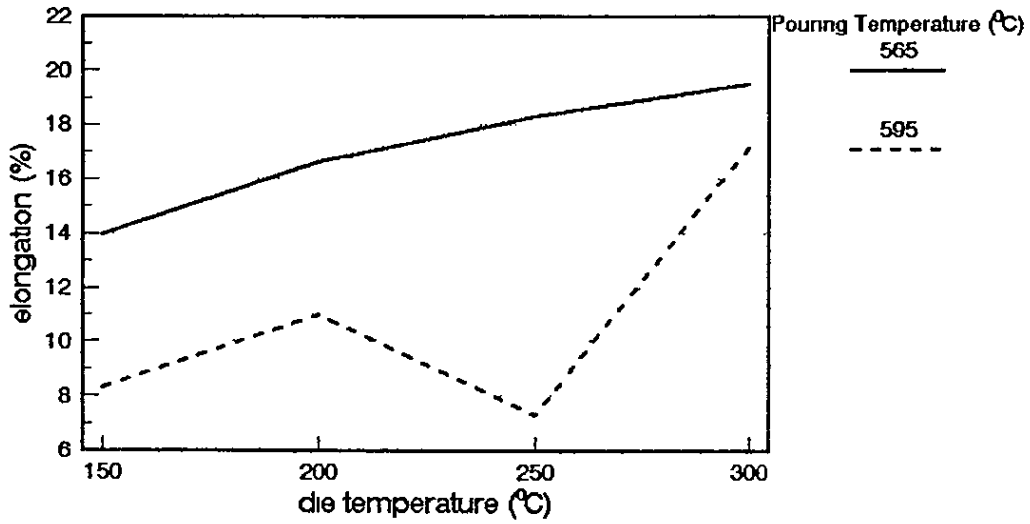
3F represents a delay of 4 seconds before the load is applied at a build-up of 11.5 tonnes per second.

Figure 6.39 0.2% P.S. OF SQUEEZE-CAST Zn-37Al  
IN AN INGOT DIE PROCESSED UNDER  
CONDITIONS 3F



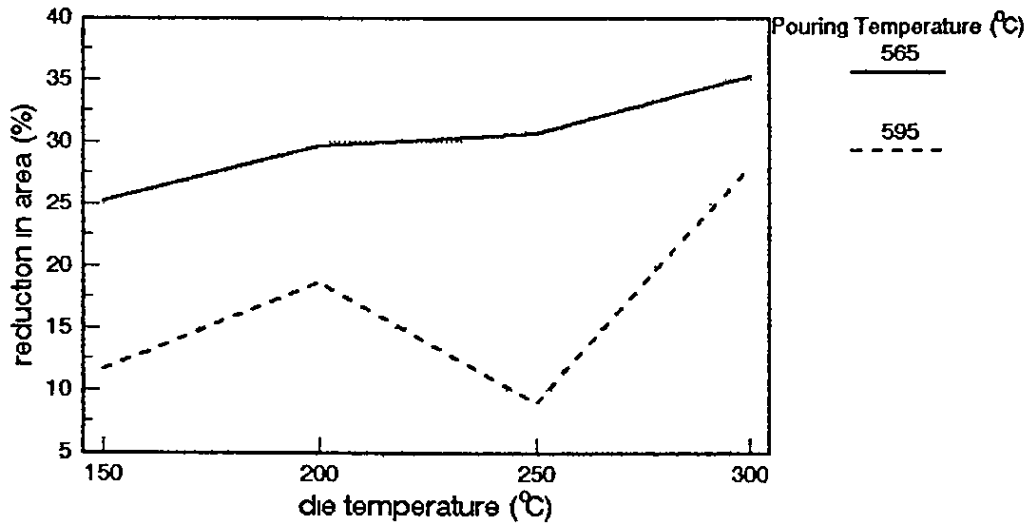
3F represents a delay of 4 seconds before the load is applied at a build-up of 11.5 tonnes per second.

Figure 6.40 ELONGATION OF SQUEEZE-CAST Zn-37Al  
IN AN INGOT DIE PROCESSED UNDER  
CONDITIONS 3F



3F represents a delay of 4 seconds before the load is applied at a build-up of 11.5 tonnes per second.

Figure 6.41 REDUCTION IN AREA OF SQUEEZE  
CAST Zn-37Al IN AN INGOT DIE PROCESSED UNDER  
CONDITIONS 3F



3F represents a delay of 4 seconds before the load is applied at a build-up of 11.5 tonnes per second.

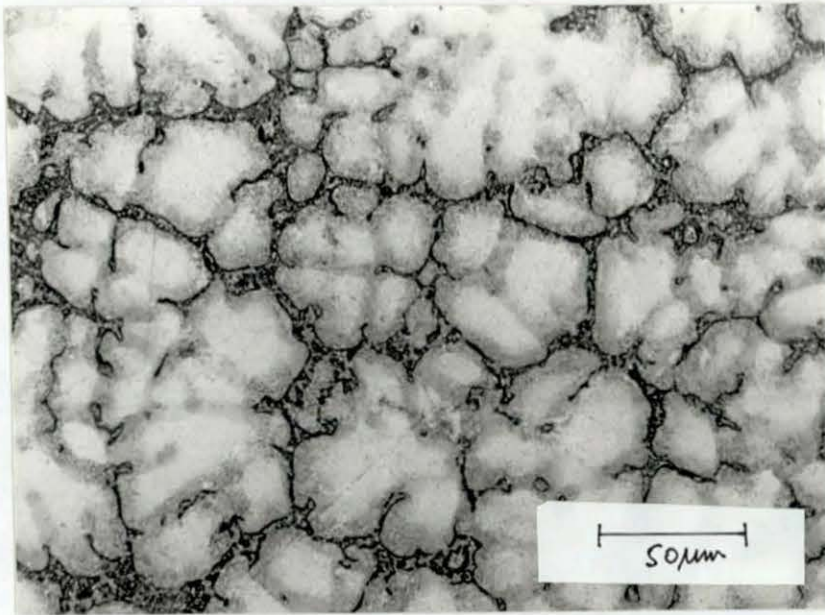


Figure 6.42 ZA27 (LM) 50mm Section  
Die Temp 180°C Pour Temp 555°C  
Squeeze Pressure 270 MPa

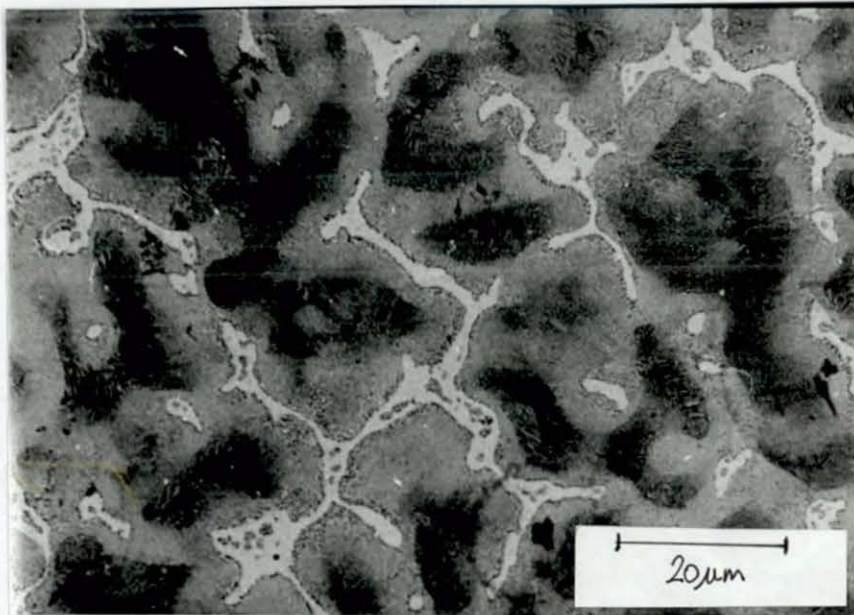


Figure 6.43 ZA27 (SEM) 50mm Section  
Die Temp 150°C Pour Temp 555°C  
Squeeze Pressure 270 MPa

Figures 6.43 to 6.51 show SEM micrographs of squeeze-cast ZA27. Atomic number contrast now shows the prior  $\alpha$  (or  $\alpha'$ ) as the darkest phase and eutectic as white. The prior  $\beta$  is grey. No difference is apparent between  $\epsilon$  and  $\eta$  in the eutectic. However, prior eutectic  $\beta$  is visible in castings produced at lowest die temperatures. The micrographs show a decrease in the amount of prior  $\alpha$  (or  $\alpha'$ ) with increasing die temperature and a decrease in the amount of eutectic. This is accompanied by an increase in the amount of prior  $\beta$ . Figures 6.45 and 6.46 show micrographs of the structures with the highest elongation values. A definite dendritic structure is apparent.

SEM micrographs of thin section ZA27 are shown in Figures 6.47 to 6.51. A finer structure, compared to the thicker sections, is obvious. Figures 6.47-6.48 show an increase in prior  $\beta$ , combined with a reduction in prior  $\alpha$  and eutectic with increased die temperature. The grain shape in Figure 6.47 gives a cellular appearance. Decomposition of the prior  $\alpha$  and  $\beta$  phases is clearly visible in Figures 6.49-6.51. The decomposition appears in accordance with that discussed in section 2.3.4.3.

Table 6.3 shows measurements of secondary dendrite arm spacing for ZA27, processed under different conditions.

### 6.3.2 ZA8

ZA8 solidifies as primary  $\beta$  in a  $\beta+\eta$  eutectic and then undergoes decomposition as described in section 2.3.4.3. Figures 6.52-6.55 show the effect of die temperature on the micro-structure of thick sectioned ZA8. The eutectic has a lamellar appearance at low die temperature and a more fibrous form at higher temperature. Decomposition of the prior  $\beta$  is clearly visible in Figures 6.53 and 6.55, showing a granular reaction at the edge and the auto-catalytic cellular reaction within the grain. A rim of zinc is noted around the decomposed  $\beta$ .

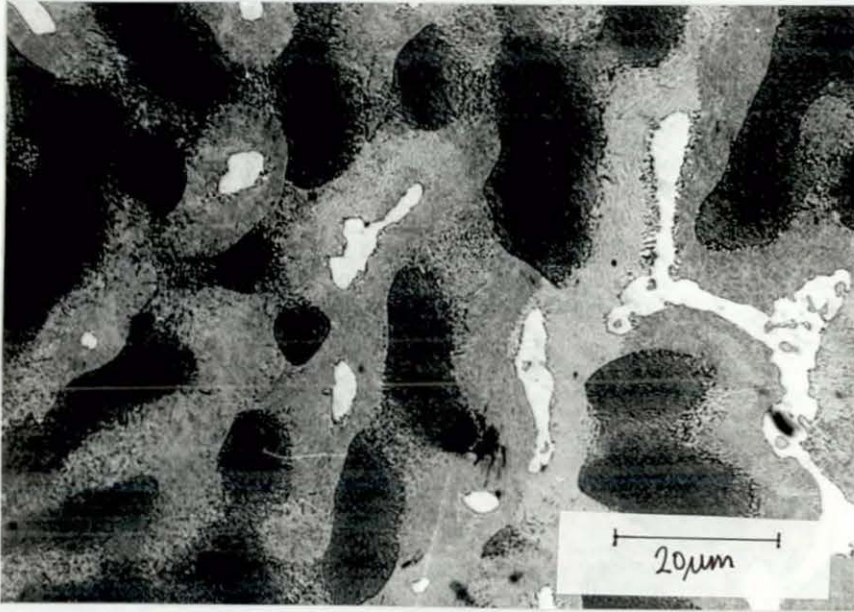


Figure 6.44 ZA27 (SEM) 50mm Section  
Die Temp 300°C Pour Temp 555°C  
Squeeze Pressure 270 MPa

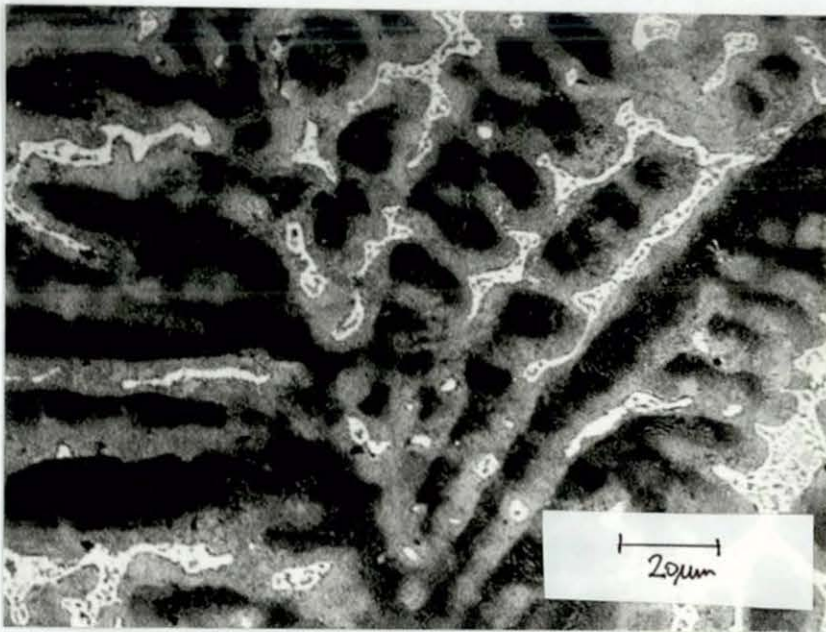


Figure 6.45 ZA27 (SEM) 50mm Section  
Die Temp 150°C Pour Temp 595°C  
Squeeze Pressure 185 MPa

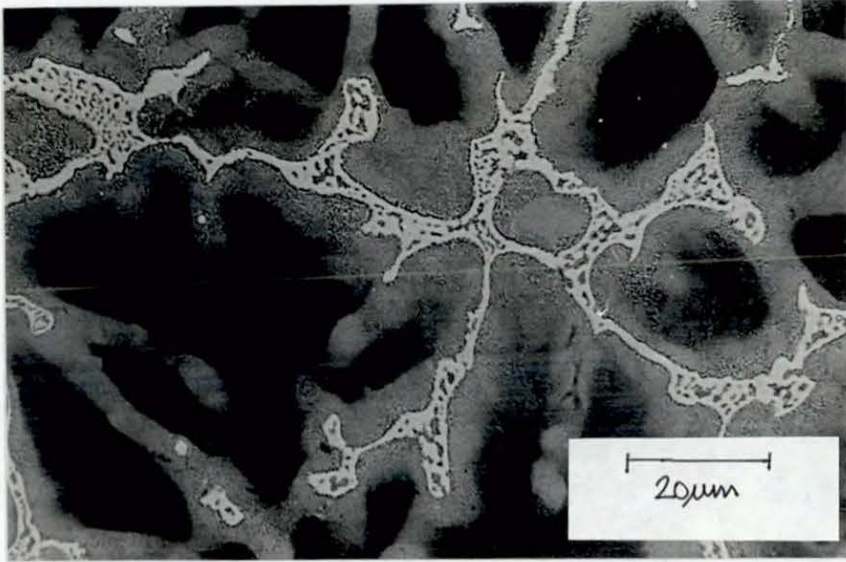


Figure 6.46 ZA27 (SEM) 50mm Section  
Die Temp 150°C Pour Temp 595°C  
Squeeze Pressure 185 MPa

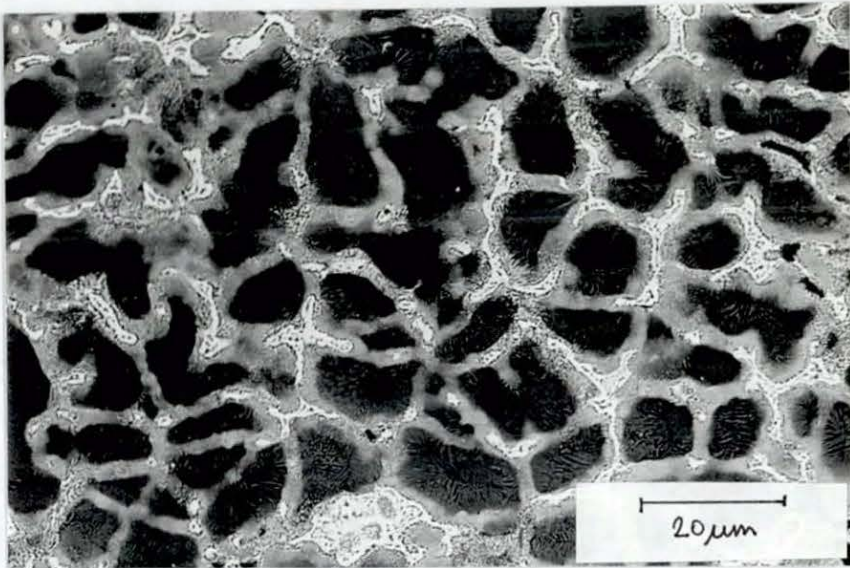


Figure 6.47 ZA27 (SEM) 12mm Section  
Die Temp 180°C Pour Temp 620°C  
Squeeze Pressure 68 MPa

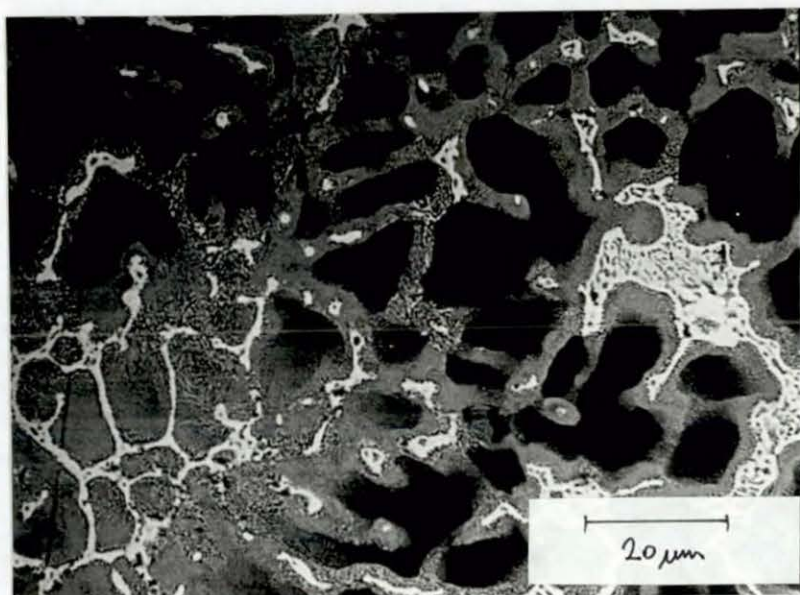


Figure 6.48 ZA27 (SEM) 12mm Section  
Die Temp 220°C Pour Temp 620°C  
Squeeze Pressure 68 MPa

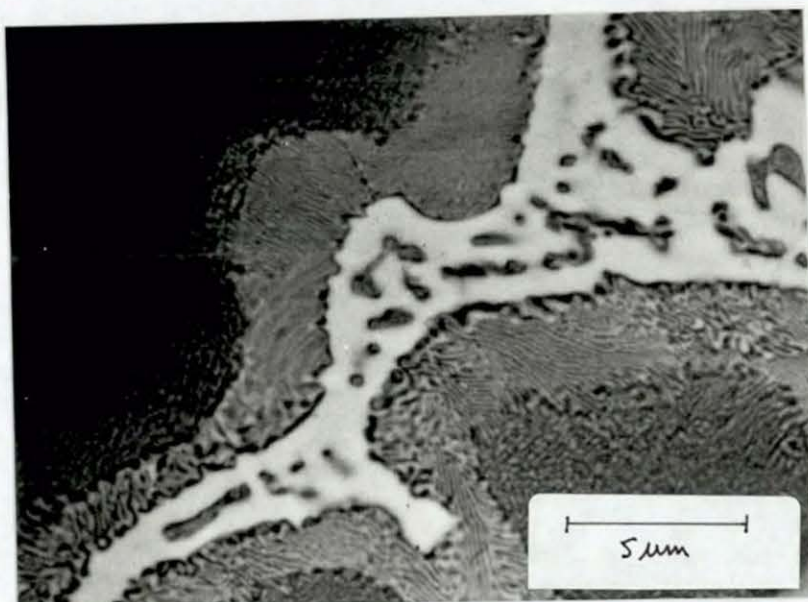


Figure 6.49 ZA27 (SEM) 12mm Section  
Die Temp 220°C Pour Temp 595°C  
Squeeze Pressure 68 MPa

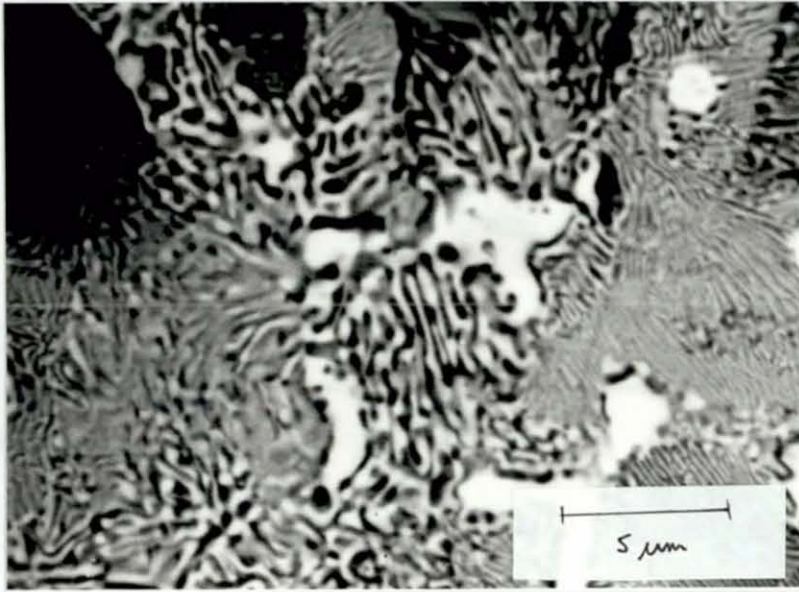


Figure 6.50 ZA27 (SEM) 12mm Section  
Die Temp 220°C Pour Temp 620°C  
Squeeze Pressure 68 MPa



Figure 6.51 ZA27 (SEM) 12mm Section  
Die Temp 220°C Pour Temp 650°C  
Squeeze Pressure 68 MPa

**Table 6.3 Secondary Dendrite Arm Spacings for ZA27**

Casting condition	Secondary D.A.S. ( $\mu\text{m}$ )
Gravity 50mm 150°C	15
Squeeze 50mm 150°C	8.6
Squeeze 12mm 150°C	6.8
Squeeze 50mm 300°C	12.7

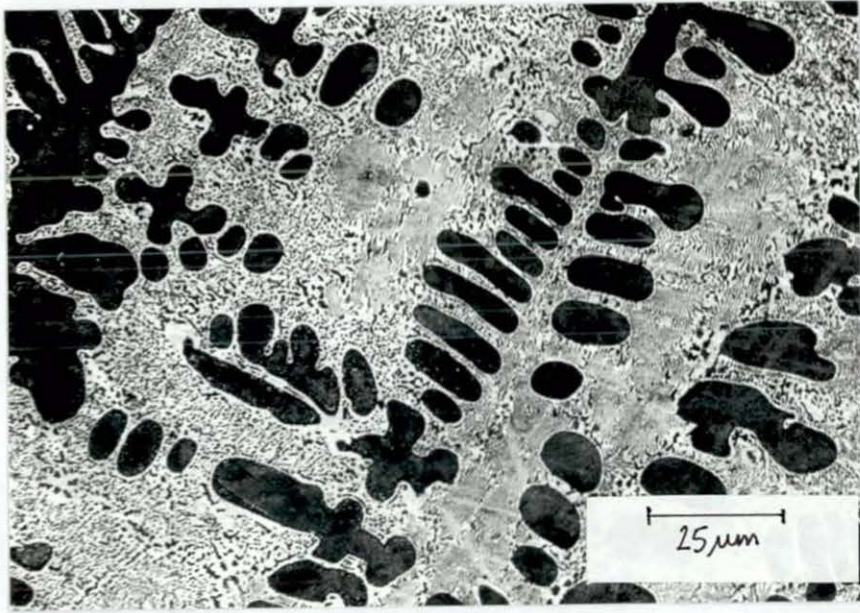


Figure 6.52 ZA8 (SEM) 50mm Section  
Die Temp 200°C Pour Temp 450°C  
Squeeze Pressure 270 MPa



Figure 6.53 ZA8 (SEM) 50mm Section  
Die Temp 200°C Pour Temp 450°C  
Squeeze Pressure 270 MPa

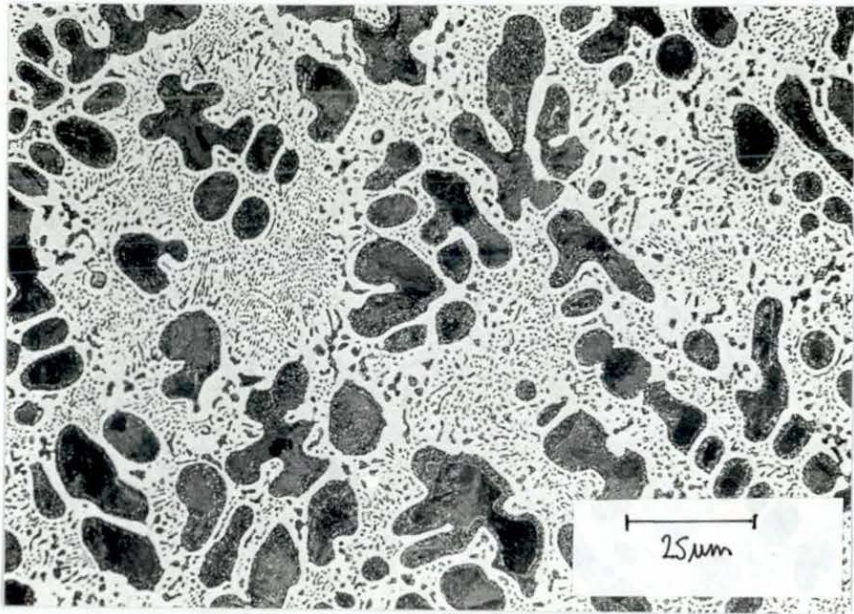


Figure 6.54 ZA8 (SEM) 50mm Section  
Die Temp 300°C Pour Temp 450°C  
Squeeze Pressure 270 MPa



Figure 6.55 ZA8 (SEM) 50mm Section  
Die Temp 300°C Pour Temp 450°C  
Squeeze Pressure 270 MPa

The scale of the structure in thin sections, Figures 6.56-6.61, is notably finer. Eutectic inter-lamellar spacing is reduced relative to the thicker sections. Decomposition of prior  $\beta$  is more evident at higher die temperature, where the eutectic tends to a more fibrous appearance (Figures 6.57, 6.59 and 6.61).

Tables 6.4 and 6.5 show measurements of inter-lamellar eutectic measurements and dendrite cell spacings in thick sectioned ZA8.

### 6.3.3 ZA12

The appearance of squeeze-cast ZA12 is generally similar to that of ZA8. However, the amount of primary phase is greater, with a corresponding decrease in the amount of eutectic.

Increasing the die temperature in thick sections changes the appearance of the eutectic from a mixture of fibrous and ribbon like, to fibrous, as shown in Figures 6.62-6.65. Decomposition of the primary phase is more noticeable in castings produced at higher die temperatures.

Thin section processing shows, in Figures 6.66-6.71, the development of a lamellar eutectic at all die temperatures. Decomposition of the prior  $\beta$  is visible by the two mechanisms previously discussed.

### 6.3.4 Zn-37Al

Figures 6.72-6.79 show the effect of increasing die temperature at fixed pouring temperature and squeeze pressure on the microstructure of Zn-37Al. In comparison to ZA27 very little eutectic is visible in these structures. The structures comprise a decomposed aluminium rich phase ( $\alpha$  or  $\alpha'$ ), surrounded by a decomposed  $\beta$  phase. The cooling rate is high enough at lower die temperatures to produce some eutectic  $\beta+\eta$ . Decomposition of  $\beta$  is clearly visible. The

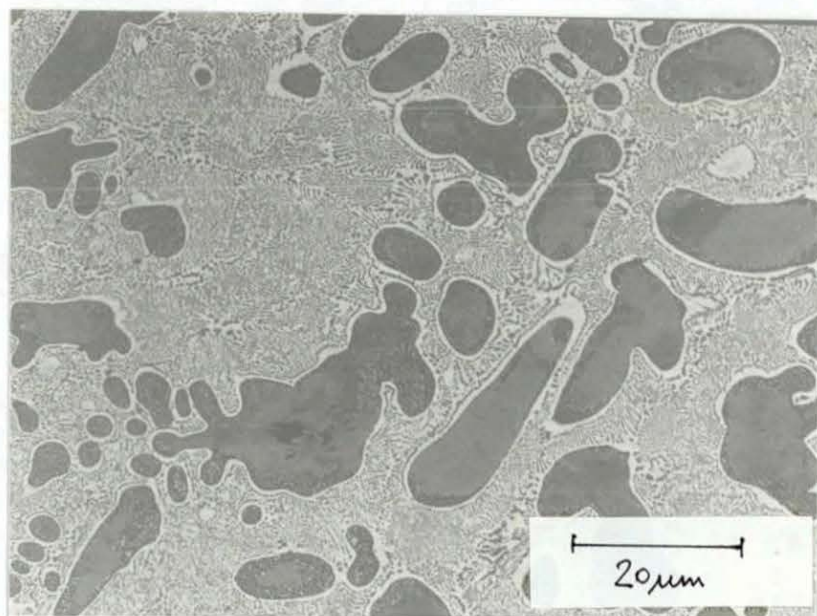


Figure 6.56 ZA8 (SEM) 12mm Section  
Die Temp 150°C Pour Temp 450°C  
Squeeze Pressure 68 MPa

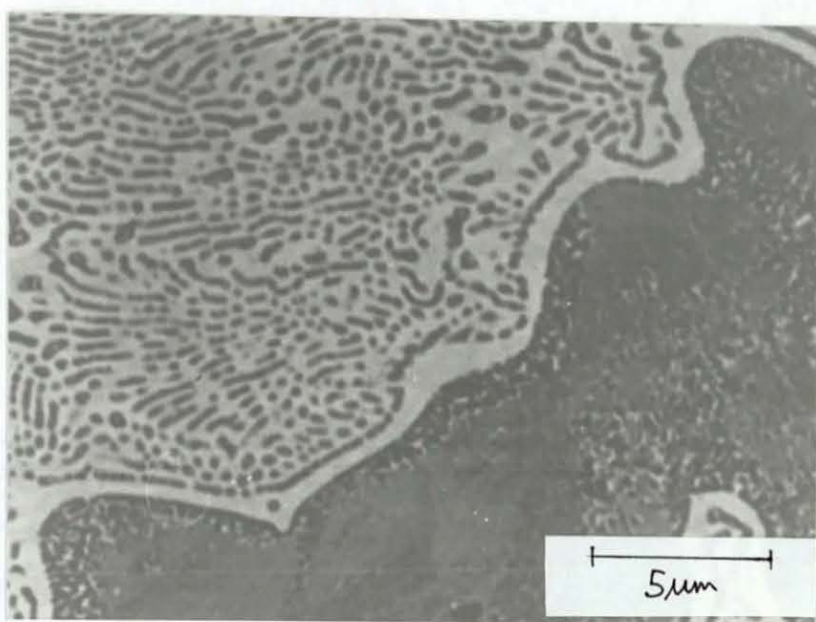


Figure 6.57 ZA8 (SEM) 12mm Section  
Die Temp 150°C Pour Temp 450°C  
Squeeze Pressure 68 MPa

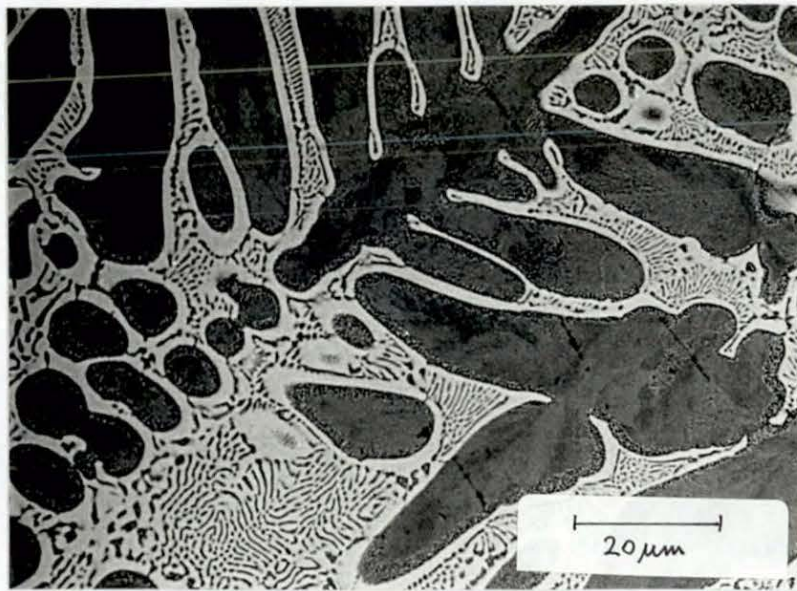


Figure 6.58 ZA8 (SEM) 12mm Section  
Die Temp 180°C Pour Temp 450°C  
Squeeze Pressure 68 MPa

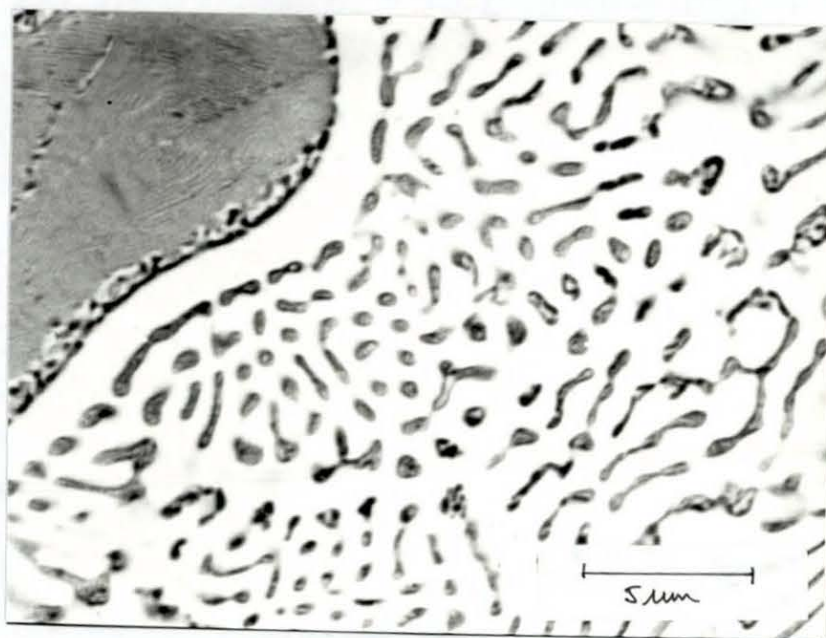


Figure 6.59 ZA8 (SEM) 12mm Section  
Die Temp 180°C Pour Temp 450°C  
Squeeze Pressure 68 MPa

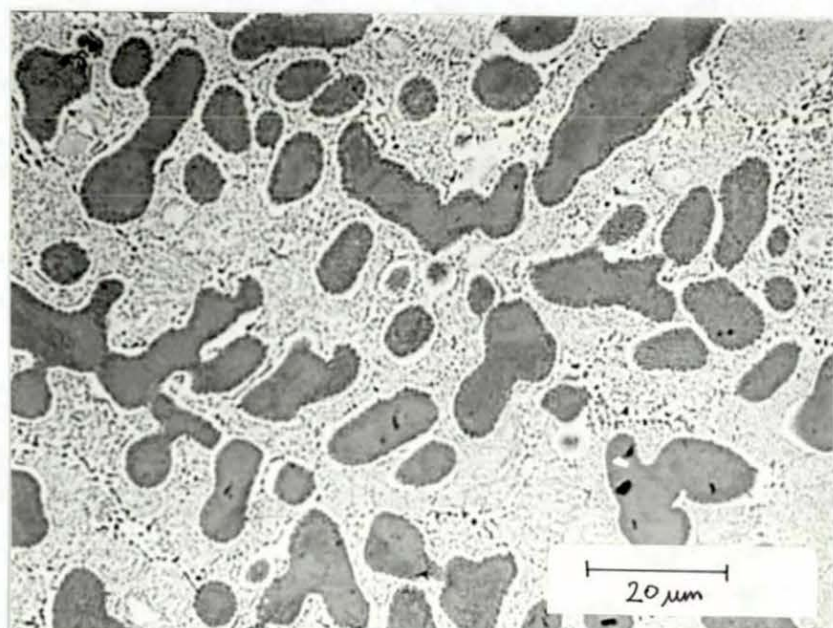


Figure 6.60 ZA8 (SEM) 12mm Section  
Die Temp 220°C Pour Temp 450°C  
Squeeze Pressure 68 MPa

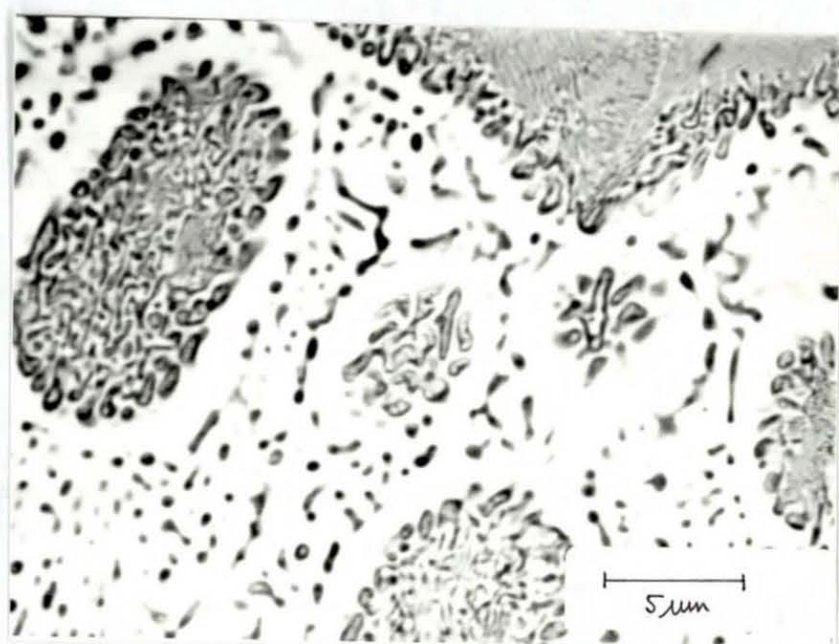


Figure 6.61 ZA8 (SEM) 12mm Section  
Die Temp 220°C Pour Temp 450°C  
Squeeze Pressure 68 MPa

**Table 6.4: Inter-Lamellar Eutectic Spacings in Squeeze-Cast ZA8**

Die Temperature (°C)	Spacing (μm)	R (μm/s)
150	0.42	570
200	0.55	330
250	0.65	240
300	0.72	190

**Table 6.5: Dendrite Cell Spacings in Squeeze-Cast ZA8**

Die Temperature (°C)	Average Dendrite Cell Spacing (DCS) (μm)
150	11.4
200	13.8
250	14.8
300	12.8

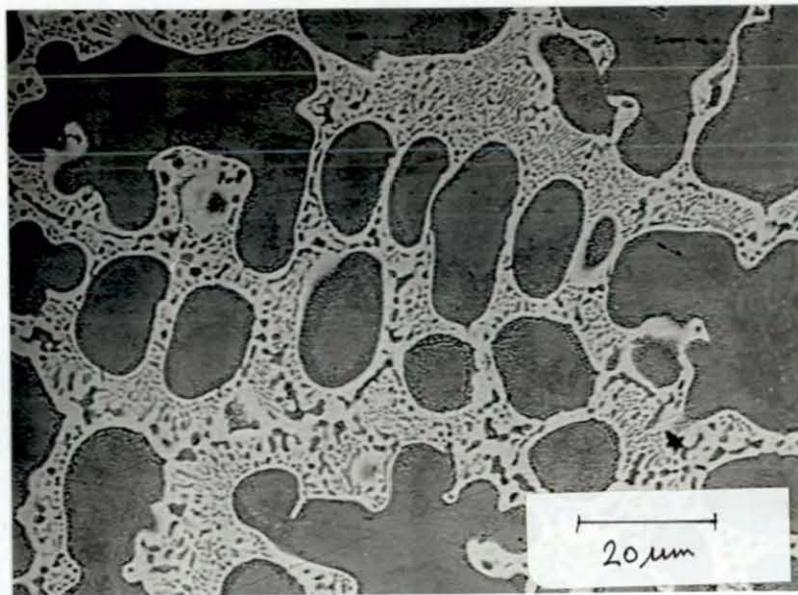


Figure 6.62 ZA12 (SEM) 50mm Section  
Die Temp 150°C Pour Temp 480°C  
Squeeze Pressure 270 MPa



Figure 6.63 ZA12 (SEM) 50mm Section  
Die Temp 150°C Pour Temp 480°C  
Squeeze Pressure 270 MPa

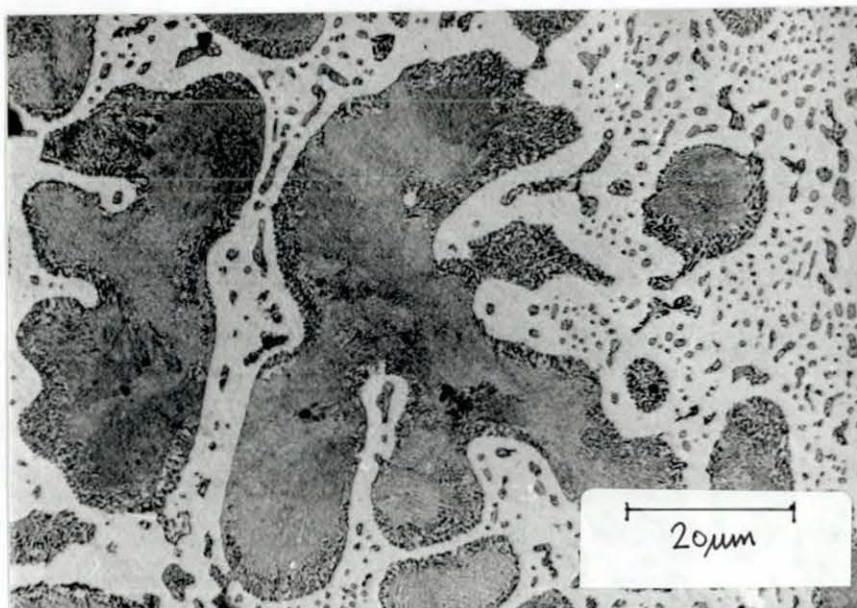


Figure 6.64 ZA12 (SEM) 50mm Section  
Die Temp 300°C Pour Temp 480°C  
Squeeze Pressure 270 MPa

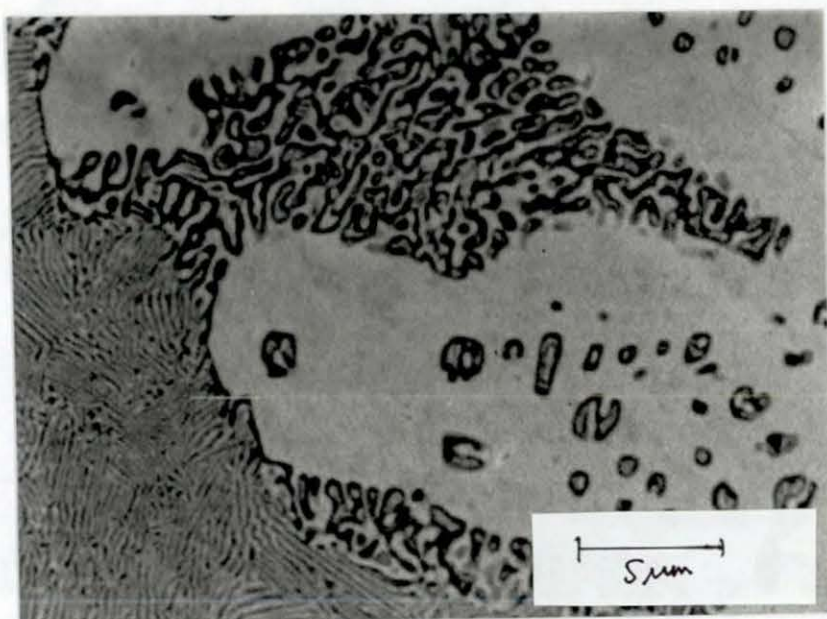


Figure 6.65 ZA12 (SEM) 50mm Section  
Die Temp 300°C Pour Temp 480°C  
Squeeze Pressure 270 MPa

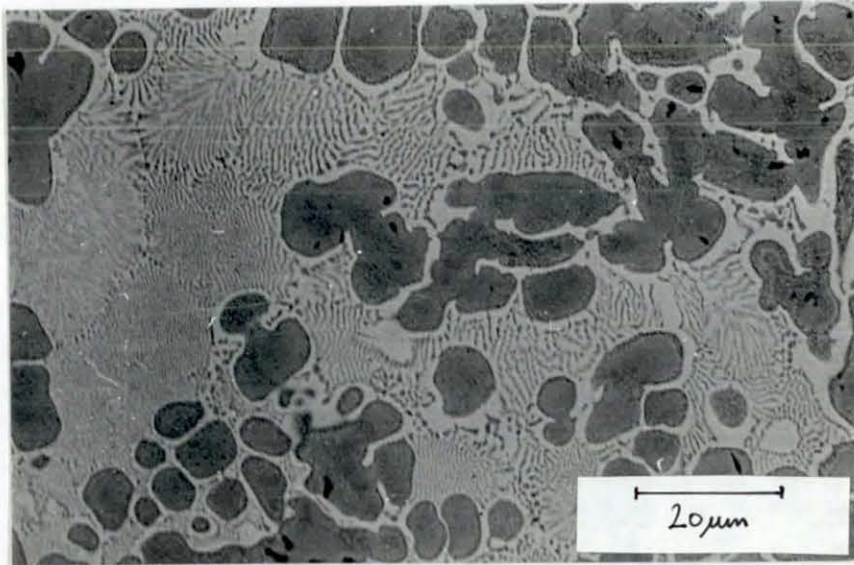


Figure 6.66 ZA12 (SEM) 12mm Section  
Die Temp 150°C Pour Temp 480°C  
Squeeze Pressure 68 MPa

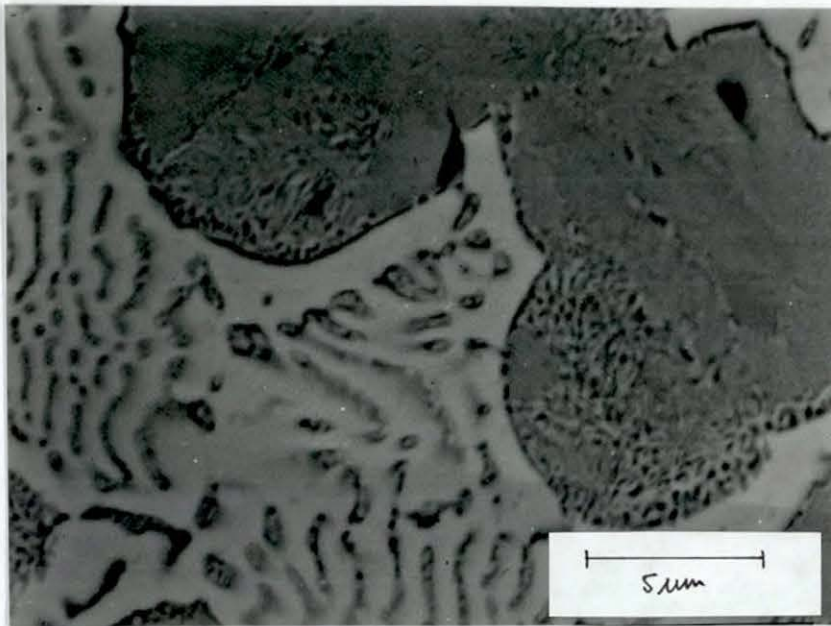


Figure 6.67 ZA12 (SEM) 12mm Section  
Die Temp 150°C Pour Temp 480°C  
Squeeze Pressure 68 MPa

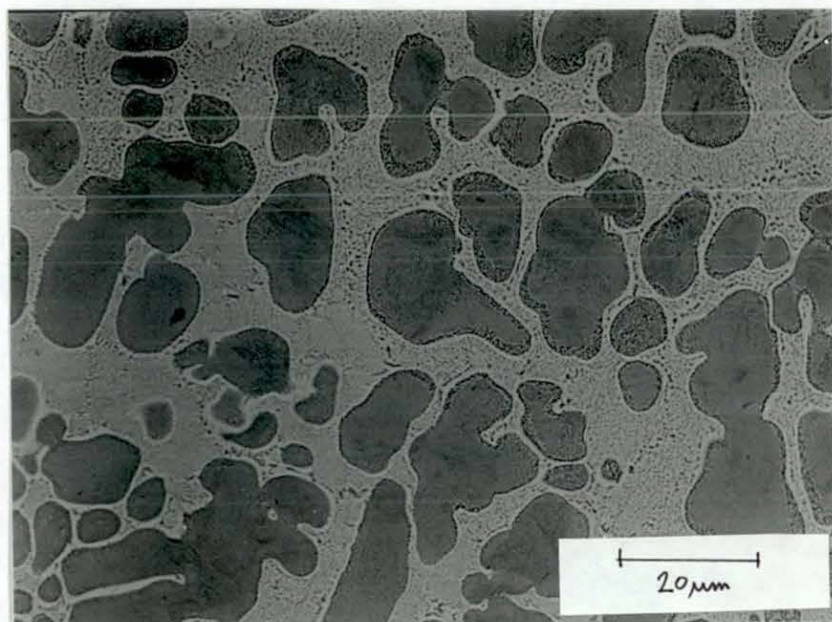


Figure 6.68 ZA12 (SEM) 12mm Section  
Die Temp 180°C Pour Temp 480°C  
Squeeze Pressure 68 MPa

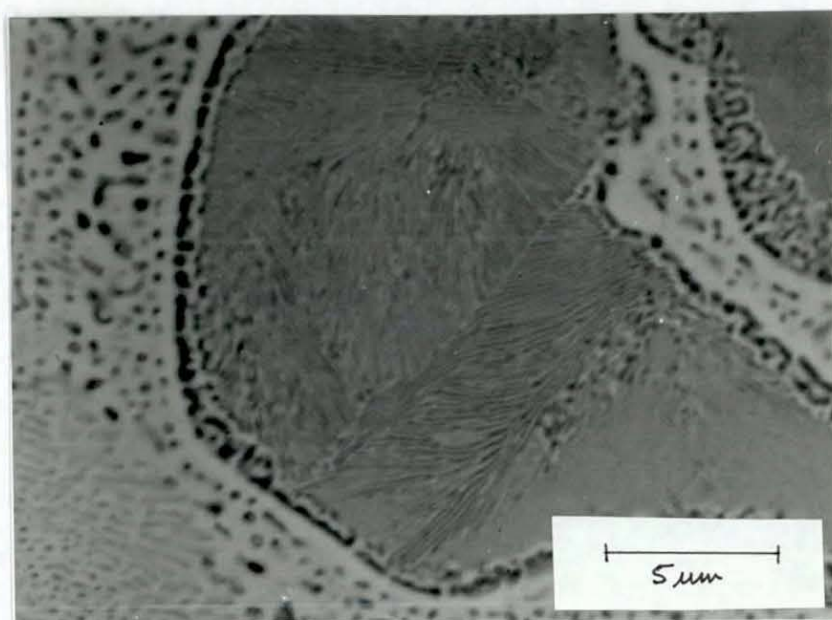


Figure 6.69 ZA12 (SEM) 12mm Section  
Die Temp 180°C Pour Temp 480°C  
Squeeze Pressure 68 MPa

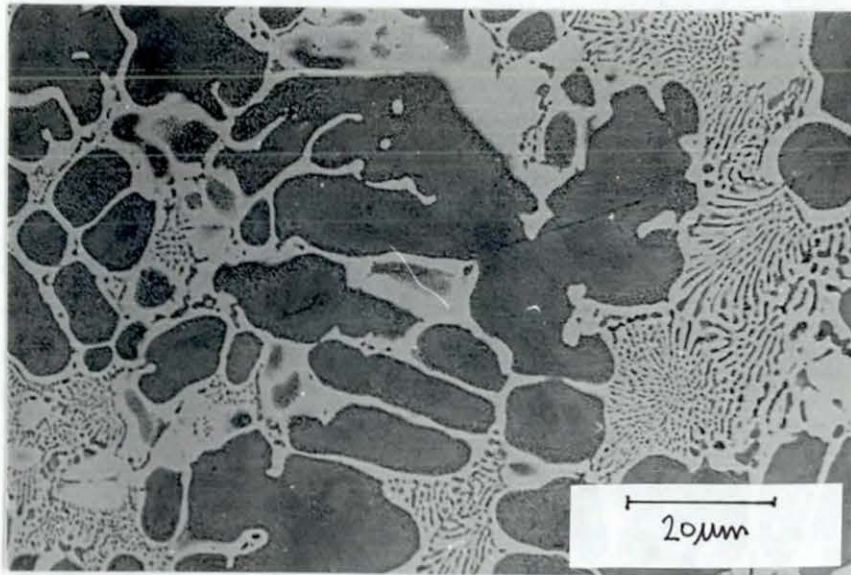


Figure 6.70 ZA12 (SEM) 12mm Section  
Die Temp 220°C Pour Temp 480°C  
Squeeze Pressure 68 MPa

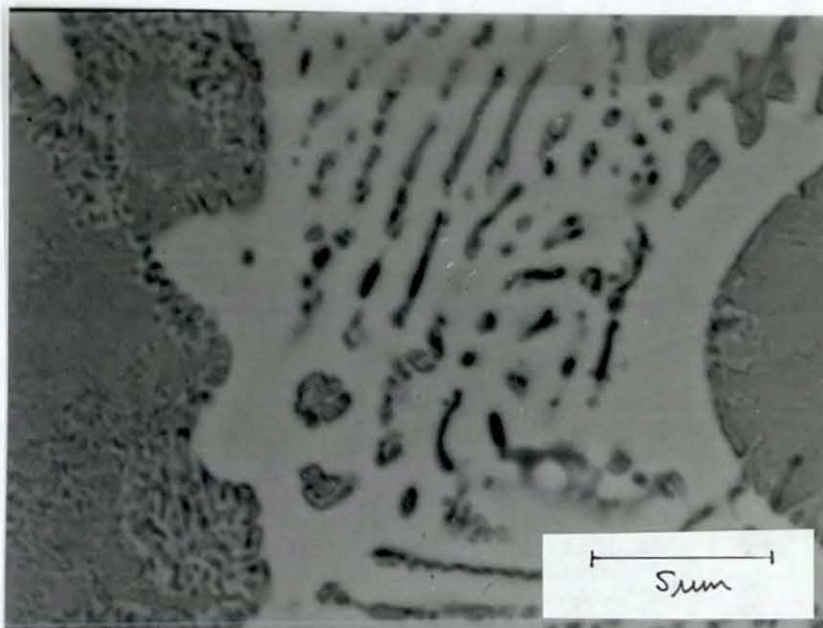


Figure 6.71 ZA12 (SEM) 12mm Section  
Die Temp 220°C Pour Temp 480°C  
Squeeze Pressure 68 MPa

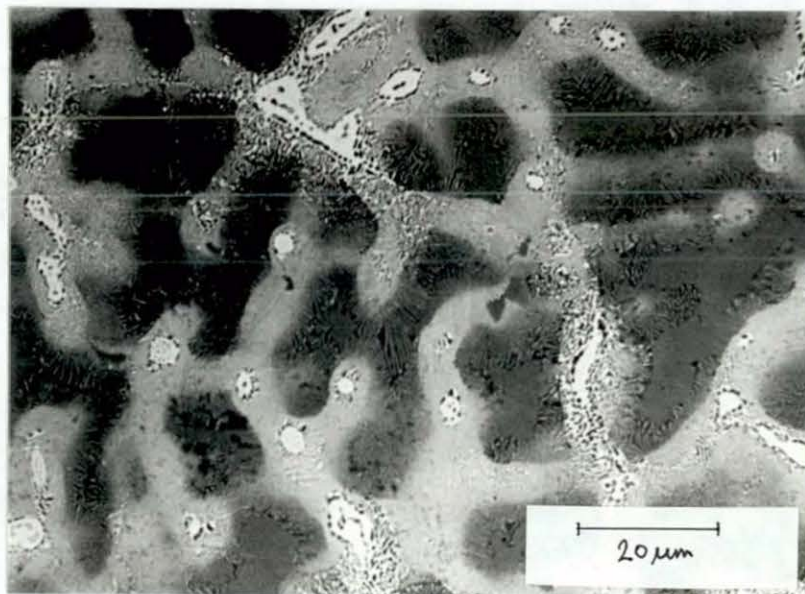


Figure 6.72 Zn-37Al (SEM) 50mm Section  
Die Temp 150°C Pour Temp 565°C  
Squeeze Pressure 185 MPa

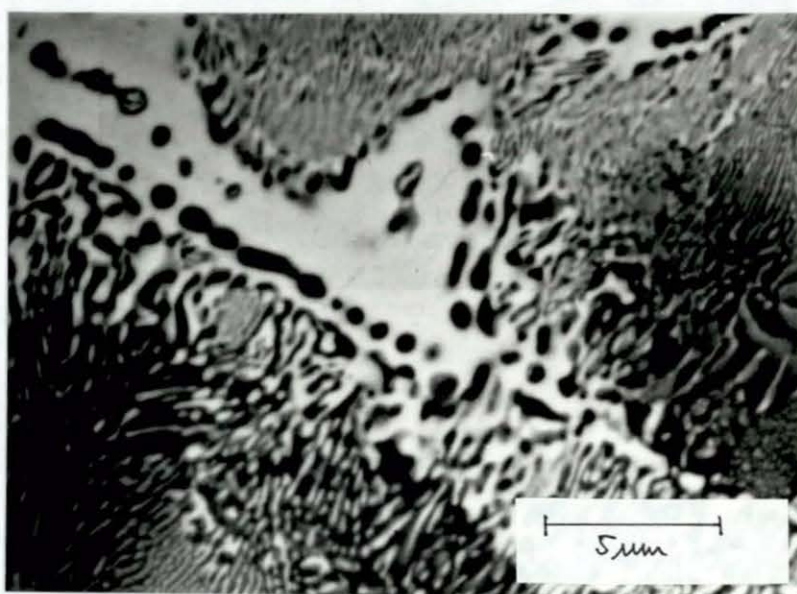


Figure 6.73 Zn-37Al (SEM) 50mm Section  
Die Temp 150°C Pour Temp 565°C  
Squeeze Pressure 185 MPa

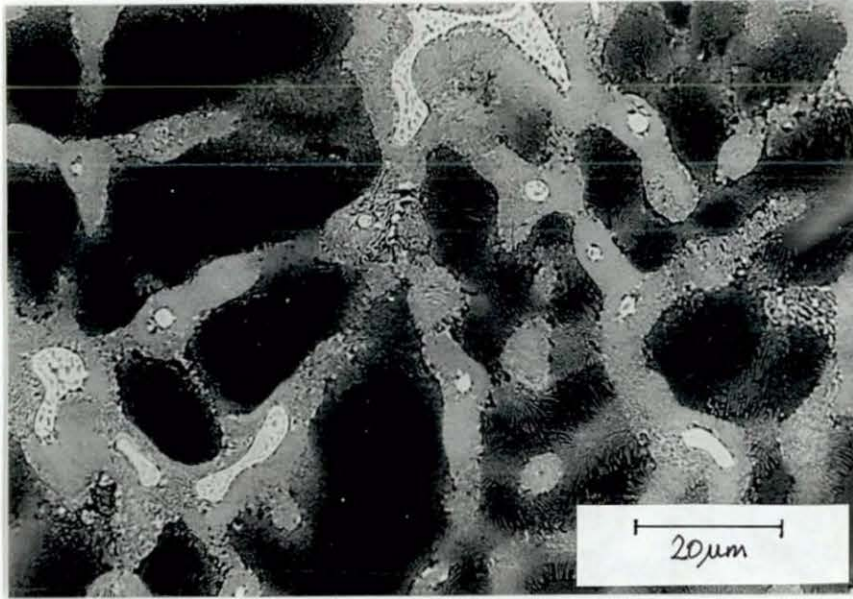


Figure 6.74 Zn-37Al (SEM) 50mm Section  
Die Temp 200°C Pour Temp 565°C  
Squeeze Pressure 185 MPa

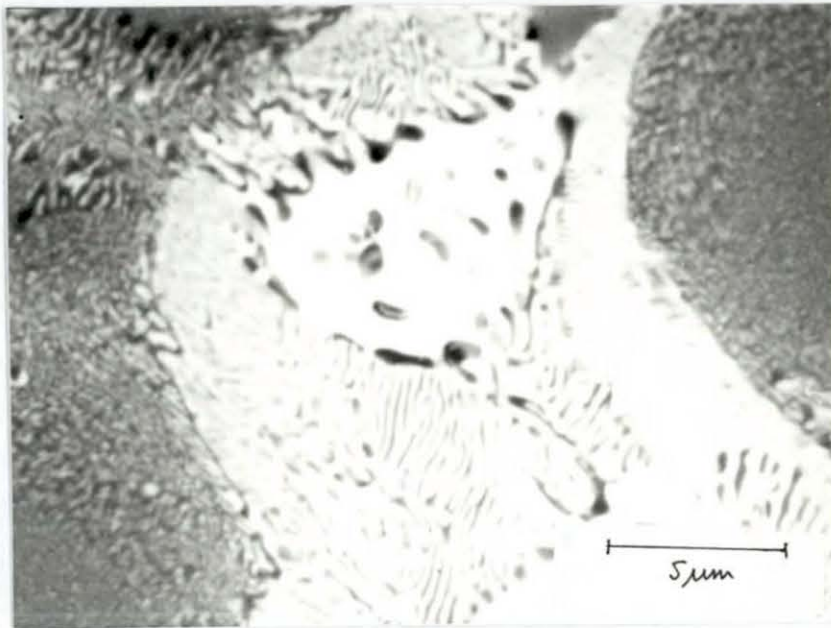


Figure 6.75 Zn-37Al (SEM) 50mm Section  
Die Temp 200°C Pour Temp 565°C  
Squeeze Pressure 185 MPa

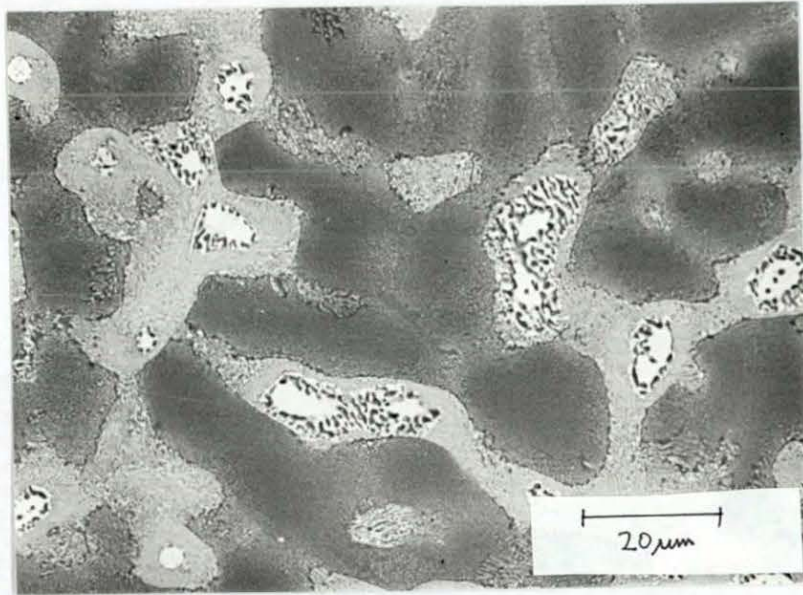


Figure 6.76 Zn-37Al (SEM) 50mm Section  
Die Temp 250°C Pour Temp 565°C  
Squeeze Pressure 185 MPa

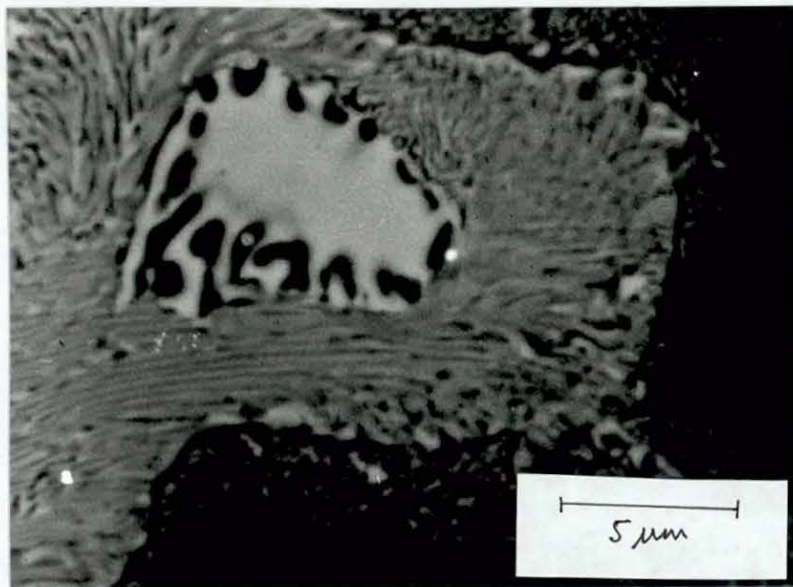


Figure 6.77 Zn-37Al (SEM) 50mm Section  
Die Temp 250°C Pour Temp 565°C  
Squeeze Pressure 185 MPa

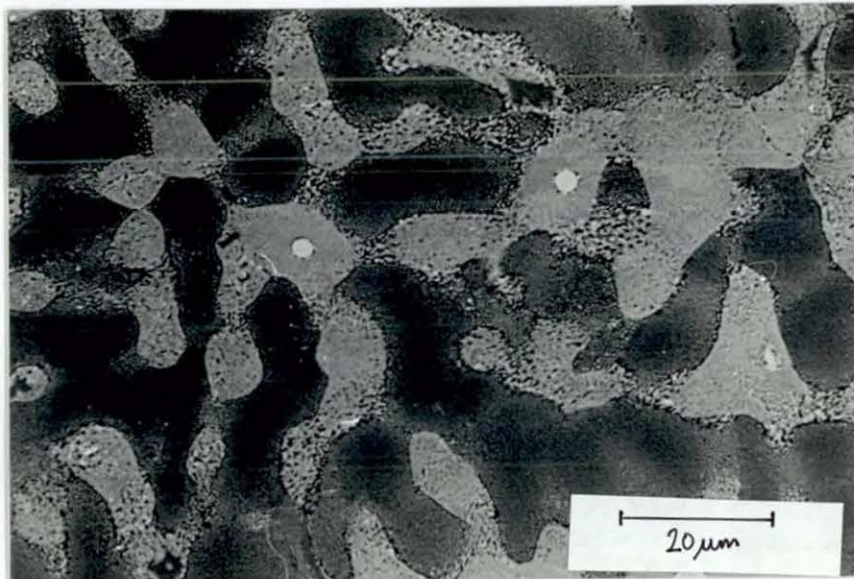


Figure 6.78 Zn-37Al (SEM) 50mm Section  
Die Temp 300°C Pour Temp 565°C  
Squeeze Pressure 185 MPa

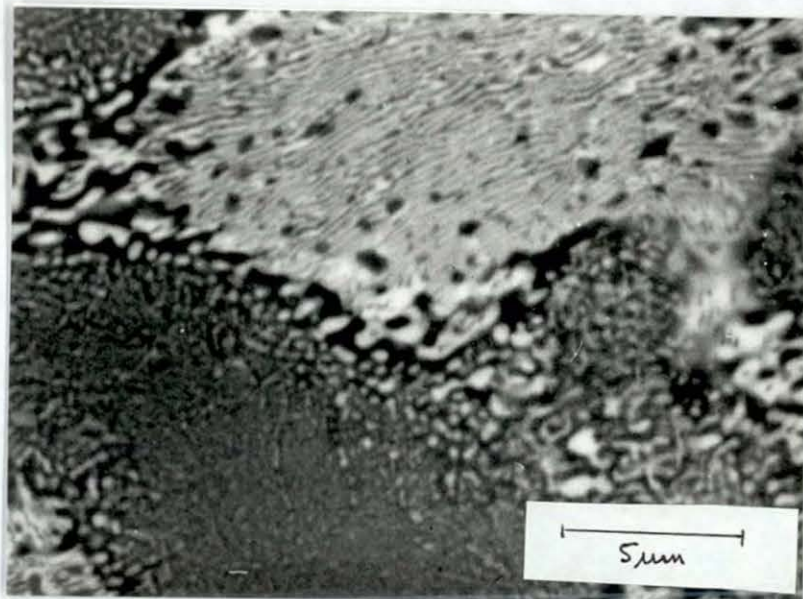


Figure 6.79 Zn-37Al (SEM) 50mm Section  
Die Temp 300°C Pour Temp 565°C  
Squeeze Pressure 185 MPa

amount of eutectic is seen to decrease with increased die temperature.

Figure 6.80 shows the appearance of thin section Zn-37Al. A fine structure with large areas of prior primary  $\alpha$ , very little prior  $\beta$  and a eutectic of  $\beta+\eta$  are noticeable features.

#### 6.4 Chemical Analysis

Table 6.6 shows results of EDS analysis on squeeze-cast thick section (50mm) ZA27 ingot sections. The results show that the composition of the prior  $\alpha$  ( $\alpha'$ ) phase stays relatively constant over the processing range. However, the tendency is for the eutectic to become progressively less rich in aluminium and the prior  $\beta$  richer in aluminium with increasing die temperature. As was the situation in mechanical property results, there was an anomaly at 200°C die temperature.

#### 6.5 Dilatometry

In order to investigate differences in mechanical behaviour of ZA27, processed under different conditions, dilatometry was carried out on selected samples of ZA27. Results are shown in Figure 6.81.

Significant growth occurred on heating at temperatures of about 290°C-310°C. Samples cast at die temperatures of 150°C and 200°C showed a reduction in growth after this range.

Also, to assess the long term stability of squeeze-cast ZA27, samples were held at 95°C for several weeks. Results are shown in Figure 6.82.

#### 6.6 Composites

Manufacture of the composites, containing 10, 15 and 20 v/o of  $\text{SiC}_p$  (F320 grit) in ZA27, was achieved by the vortex method. Large amounts of compaction contraction occurred for all mixtures, which was probably caused by entrapped gases, during stirring and pouring. Because of the constraints

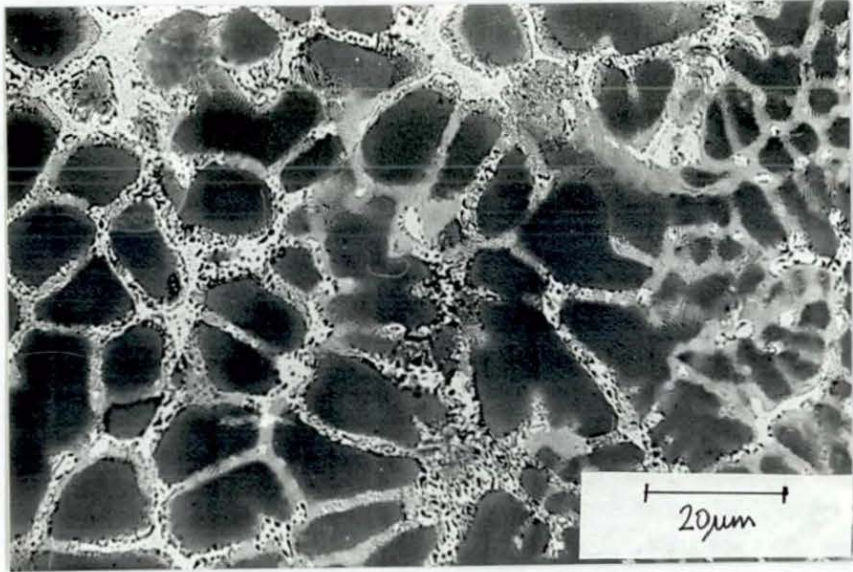
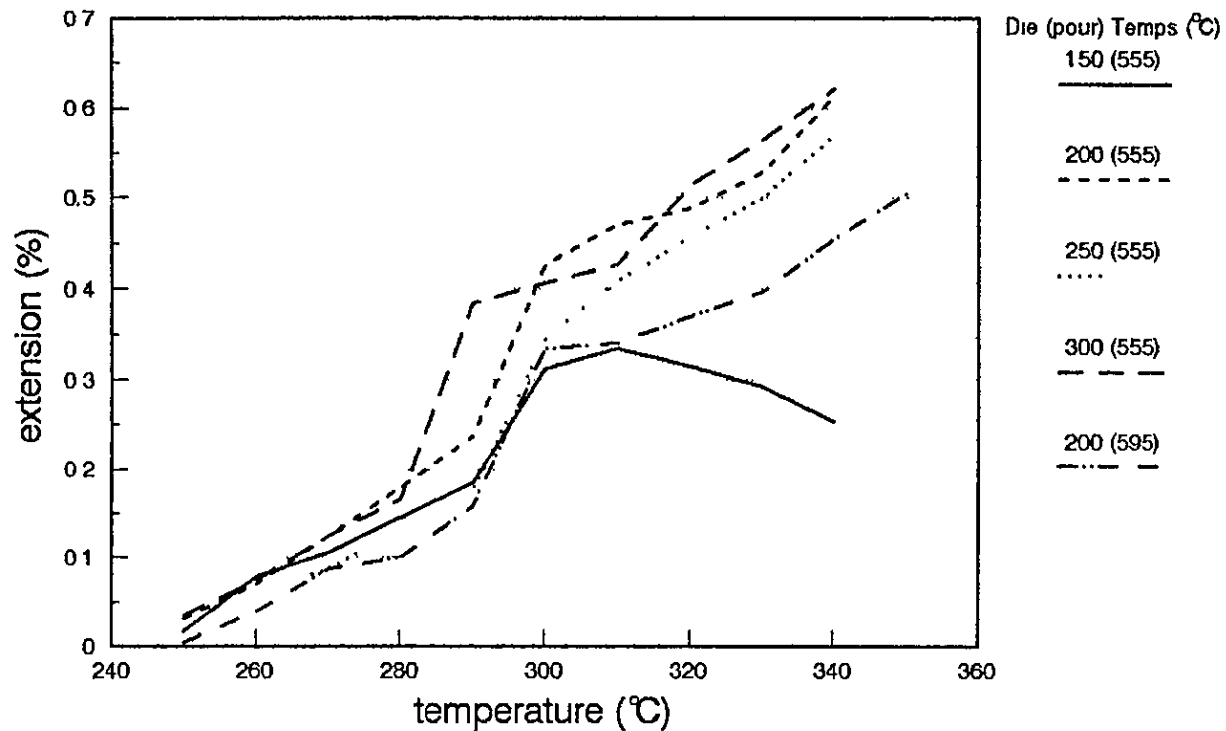


Figure 6.80 Zn-37Al (SEM) 16mm Section  
Die Temp 200°C Pour Temp 650°C  
Squeeze Pressure 68 MPa

**Table 6.6: EDS Analysis of Squeeze-Cast ZA27**

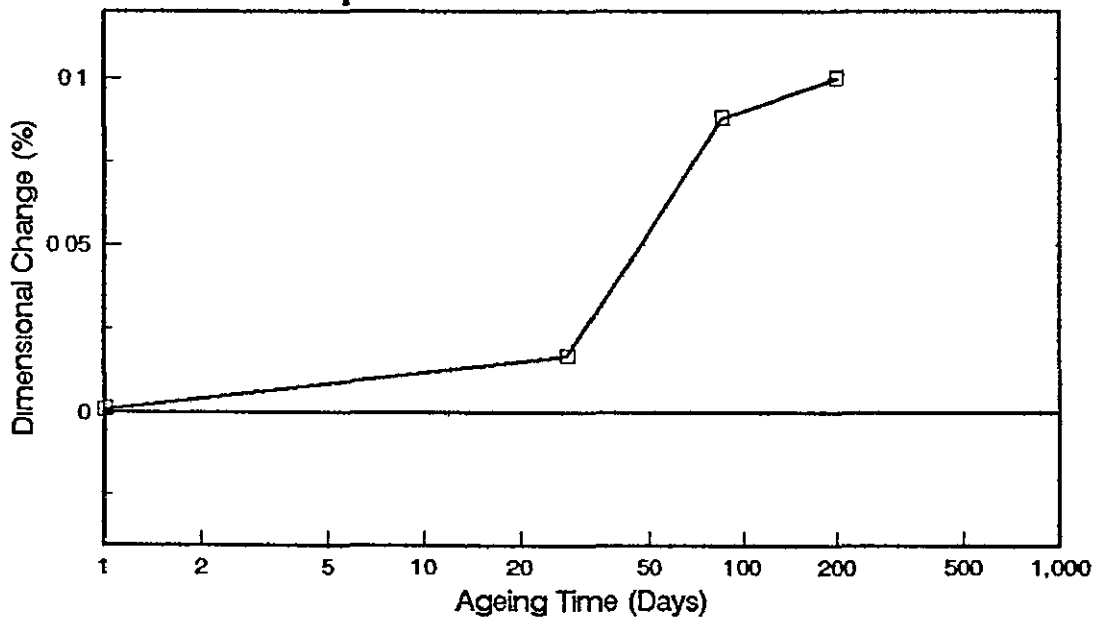
Die Temp (°C)	Area	weight %		
		Zn	Al	Cu
150	alpha	41.5	57.8	0.7
	beta	71.2	27.1	1.7
	eutectic	87.0	9.9	3.1
200	alpha	40.1	59.2	0.7
	beta	61.5	37.1	1.4
	eutectic	90.9	6.1	3.0
250	alpha	41.6	57.4	1.0
	beta	68.6	29.6	1.8
	eutectic	92.7	2.7	4.6
300	alpha	40.7	58.3	1.0
	beta	66.7	31.8	1.5
	eutectic	94.2	1.9	3.9

Figure 6.81 Dilatometry Results for ZA27



Sample heated to 250 °C initially

**Figure 6.82 Long Term Stability of Squeeze-Cast ZA27 at 95°C**



imposed by the design of the ingot die, the 15 and 20 volume% material were produced from remelted material, which was stirred gently prior to pouring.

All three dies were successfully filled with material and sound castings were produced. Only mechanical property results from the 50mm diameter ingots are reported.

## 6.7 Properties of Squeeze-Cast Composites

### 6.7.1 Room Temperature Tensile Tests

Table 6.7 shows a summary of the results from room temperature tensile testing of the composite material, compared to typical results from squeeze-cast ZA27. Young's Modulus is seen to increase with increased volume fraction of particulate. Strength results are lower than those of the unreinforced ZA27 at room temperature. However, the strength improves with increased volume fraction of material. Fracture occurs in a brittle manner before the yield point in the unreinforced material. Oxide films were present on the fracture surfaces of all composite samples.

### 6.7.2 High Temperature Tensile Tests

Attempts to measure the Young's Modulus in higher temperature tensile tests, at 60, 100 and 150°C, by strain gauges produced variable results. Only strength values are considered worthy of note and are shown in Table N (Appendix 2) and summarised in Table 6.8. Strength values are seen to decrease with increasing test temperature. It should be noted that composites apparently retain a high proportion of their room temperature strength at higher temperatures, when compared to the unreinforced alloy. At 150°C, the composite containing 20vol% SiC<sub>p</sub> is in fact stronger than the unreinforced alloy. Elongation values in the composites, even at higher temperatures, are low, being less than 1%. Figure 6.83 shows a plot of UTS for the composites vs temperature. Figure 6.84 shows the same results plotted against volume fraction of particulate.

**Table 6.7: Room Temperature Properties of ZA27 Composites**

Volume % of Particulate	Modulus (GPa)	Strength (MPa)	Elongation (%)
0	76	411	~10
10	80	228	<1
15	95	241	<1
20	110	279	<1

Results obtained from size 16 Hounsfield samples, machined from 50mm diameter ingots.

**Table 6.8: Higher Temperature Strength of ZA27 Composites**

Volume % of Particulate	Strength (MPa)		
	Temperature (°C)		
	60	100	150
0	359	299	205
10	203	173	176
15	243	190	171
20	261	260	220

(all elongation values <1%)

results obtained from size 16 Hounsfield samples, machined from 50mm diameter ingots

**Figure 6.83 UTS of Composites vs. Temperature**

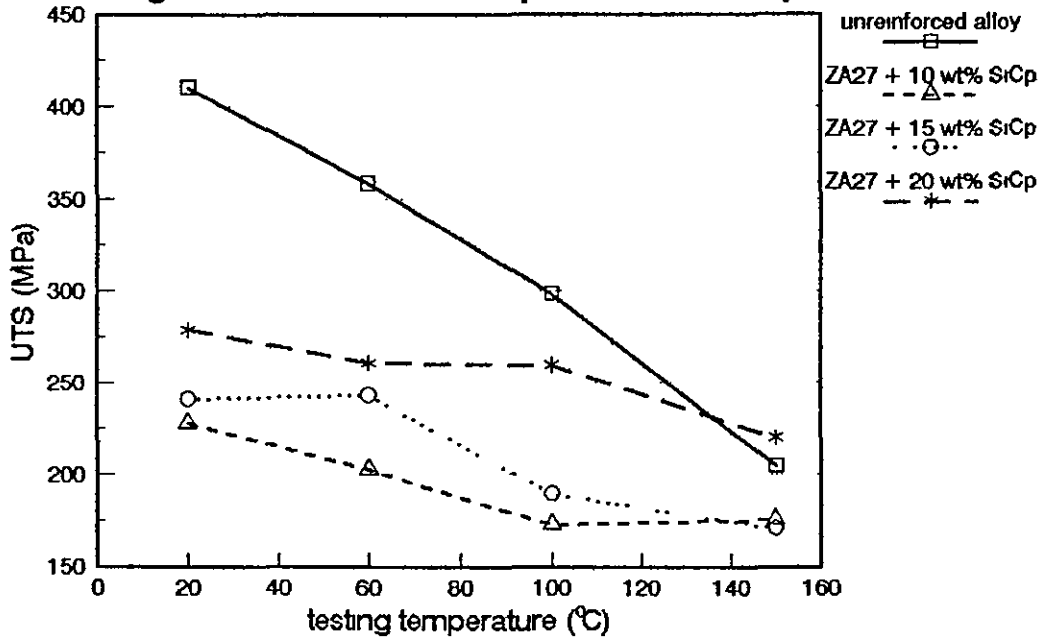
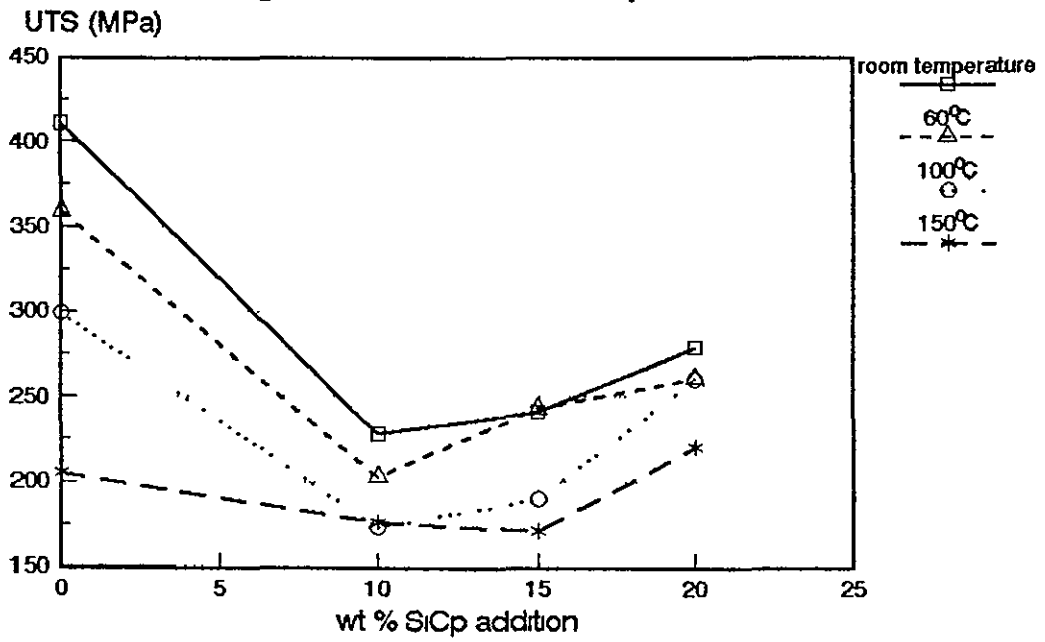


**Figure 6.84 UTS vs. SiCp Additions**



### 6.7.3 Compression Testing

Results of compression testing are shown in Table 6.9. Tests were carried out using cylindrical samples of length 13mm and diameter 9mm. Tests were performed using load control, at a rate of 7.5kN per minute, at both ambient temperature and 100°C.

The results show that the addition of SiC<sub>p</sub> to ZA27 gives a material with an improved 0.2% compressive proof stress. This increases with increased amount of particulate. Particulate strengthening is more significant at the higher temperature, when results are compared to the unreinforced alloy.

One interesting point to note is the comparison of the unreinforced alloy with the particulate reinforced materials after yield. The unreinforced alloy continues to work harden, however, the composites do not work harden as much. This is most apparent at 100°C, where load v. contraction curves cross over (Figure 6.85 and 6.86).

Values of stress at strains of 3.75% are also included for comparison in Table 6.9. The differences appear to be due to different performance after yielding.

Failure of the composites in compression was by brittle shearing at 45°, whereas the unreinforced ZA27 failed by barrelling.

### 6.7.4 Creep Testing

Results of creep testing, expressed in terms of inverse secondary creep rates in compression, are shown in Table 6.10. This compares the behaviour of squeeze-cast alloys with composite materials. As is common with creep testing, the results are variable. For instance, at 70MPa and 100°C, ZA8 is the best performer, whereas at 70MPa and 150°C the reinforced 20vol% composite is the best. At 140MPa the composite performs well. Clearly, creep behaviour will

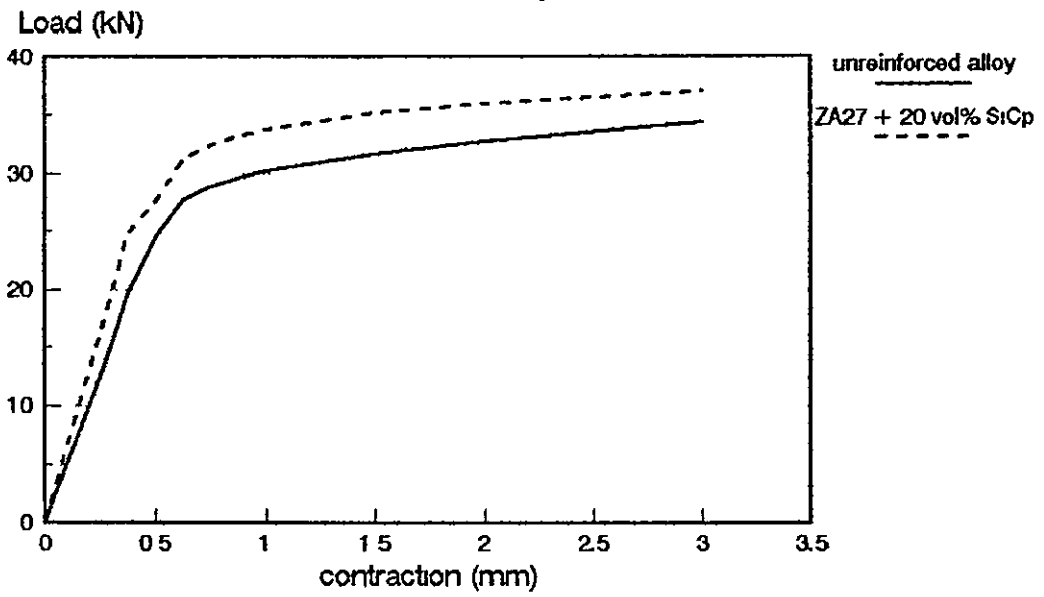
**Table 6.9: Compression Testing of Composites**

<b>Room Temperature</b>		
<b>Reinforcement (vol%)</b>	<b>0.2%PS</b>	<b>3.75% Engineering Strain</b>
0	353	487
10	369	468
15	412	419
20	432	526

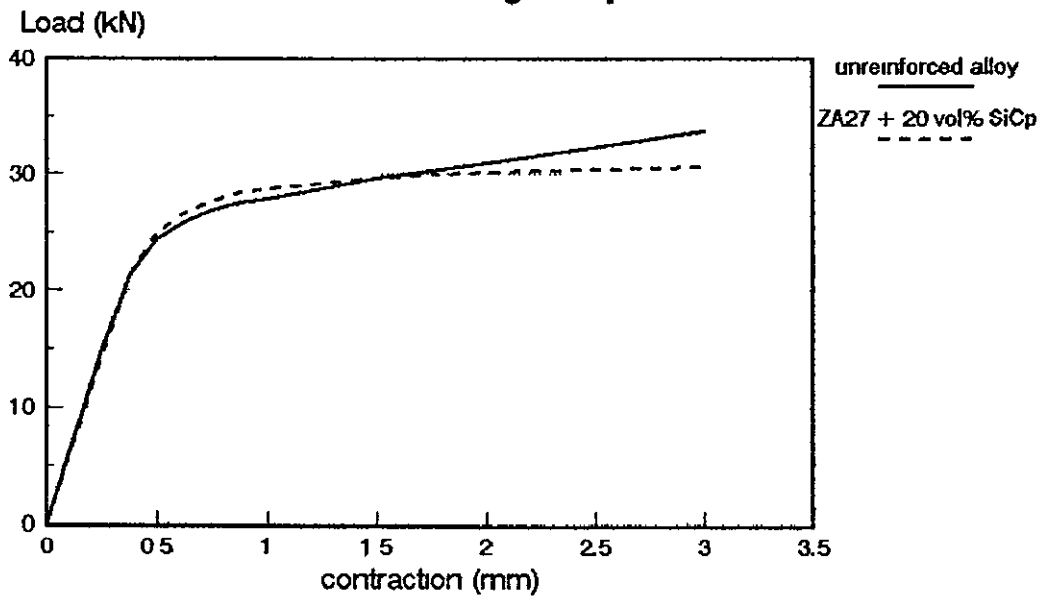
  

<b>100°C</b>		
<b>Reinforcement (vol%)</b>	<b>0.2%PS</b>	<b>3.75% Engineering Strain</b>
0	230	440
10	287	392
15	291	392
20	358	448

**Figure 6.85 Load - Contraction Curves  
Room Temperature**



**Figure 6.86 Load - Contraction Curves  
100°C Testing Temperature**

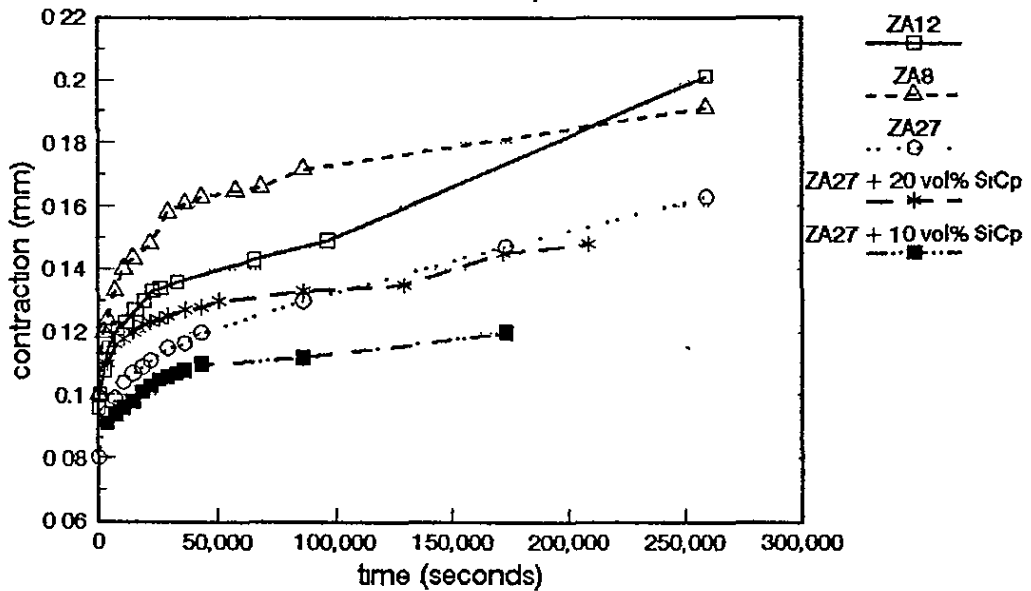


**Table 6.10: Inverse Secondary Creep Rates for ZA Alloys**

Material	Conditions			
	70MPa 100°C	70MPa 150°C	140MPa 100°C	140MPa 150°C
ZA8	14.57	0.06	0.036	-
ZA12	6.37	0.027	0.08	-
ZA27	7.08	-	0.68	-
ZA27 +10% SiCp	9.92	0.423	0.29	0.04
ZA27 +20% SiCp	7.18	0.58	1.93	0.16

(results are days per % contraction)

**Figure 6.87 Creep Data in Compression at 70MPa / 100°C**



depend on not just the alloy, but also its microstructure and the creep mechanisms operating at a particular load/temperature regime.

Contraction v. time curves for results at 70MPa and 100°C are shown in Figure 6.87. The effects of primary creep on the contraction are now also apparent.

### 6.8 Microstructures of Squeeze-Cast Composites

Light micrographs of unreinforced squeeze-cast ZA27 and reinforced squeeze-cast ZA27 are shown in Figures 6.88 and 6.89.

A reduction in the scale of the microstructure is evident in the reinforced samples. Particles clearly lie at grain boundary positions associated with the eutectic.

Lower magnification photographs in the unetched condition show the distribution of particles at volume fractions of 10, 15 and 20 v/o. Clumping is apparent in the 10 and 15 v/o samples but the 20 v/o sample is relatively homogeneous (Figures 6.90-6.92).

Fracture surfaces of composites tested at room temperature are included in Figures 6.93-6.95. These show particles embedded in the surfaces, well bonded to the matrix.

SEM back-scatter images (Figures 6.96-6.98) of sections through fracture surfaces produced in tests at 60, 100 and 150°C, show that the fracture changes from through matrix/particle interface to through matrix (via intergranular mechanism) with increased testing temperature.

Microstructures of samples which have undergone creep deformation are shown in Figures 6.99 - 6.102.

At 100°C and 70MPa, decomposition of the matrix microstructure appears greater in the composite materials

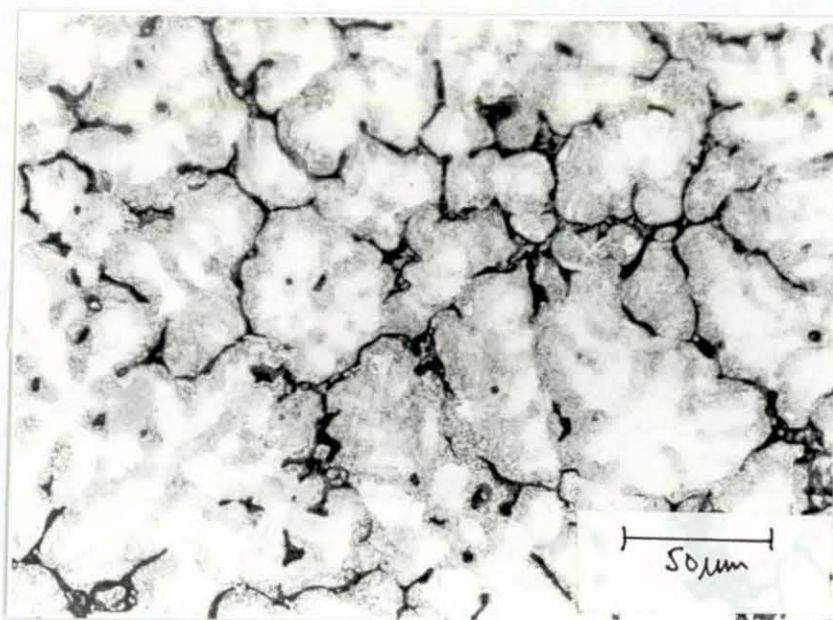


Figure 6.88 ZA27 (LM) 50mm Section  
Die Temp 180°C Pour Temp 595°C  
Squeeze Pressure 185 MPa

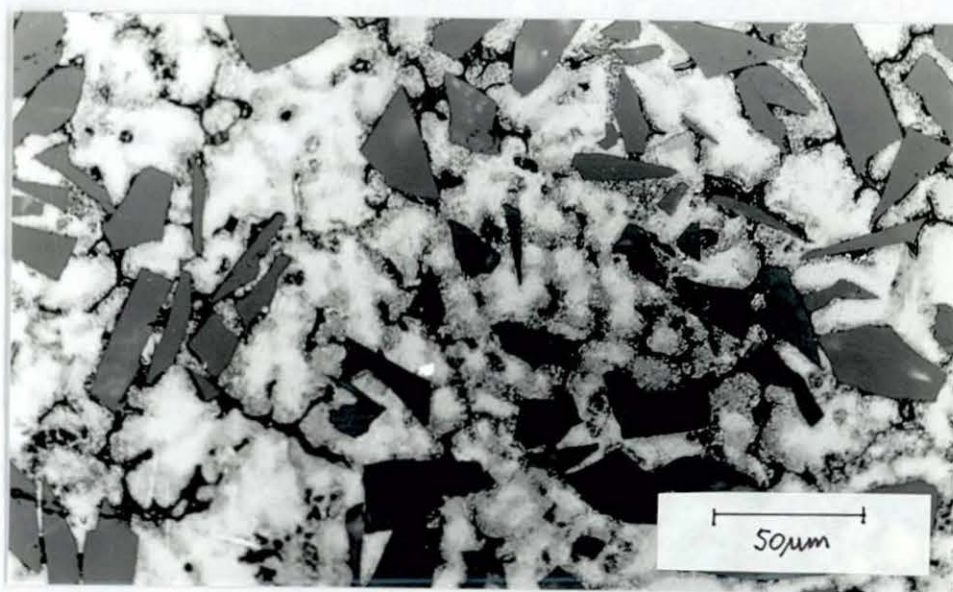


Figure 6.89 ZA27 + 20vol% SiCp (LM) 50mm Section  
Die Temp 180°C Pour Temp 595°C  
Squeeze Pressure 185 MPa

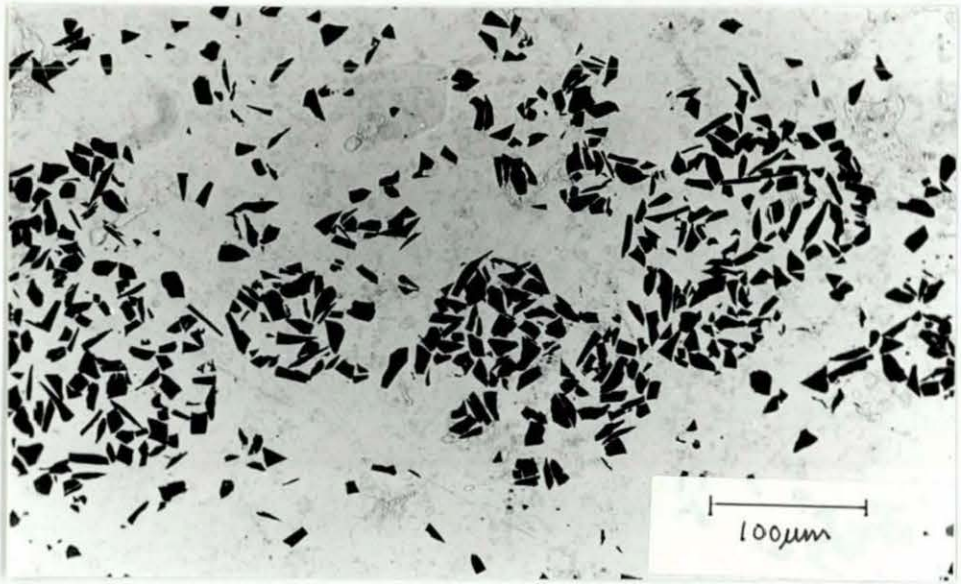


Figure 6.90 ZA27 + 10vol% SiCp (LM) 50mm Section  
Die Temp 180°C Pour Temp 595°C  
Squeeze Pressure 185 MPa

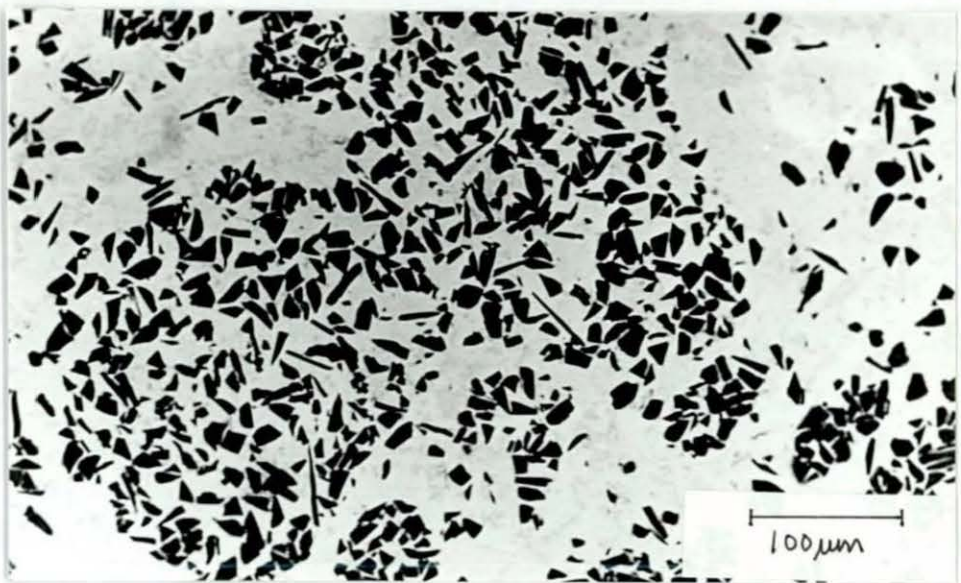


Figure 6.91 ZA27 + 15vol% SiCp (LM) 50mm Section  
Die Temp 180°C Pour Temp 595°C  
Squeeze Pressure 185 MPa

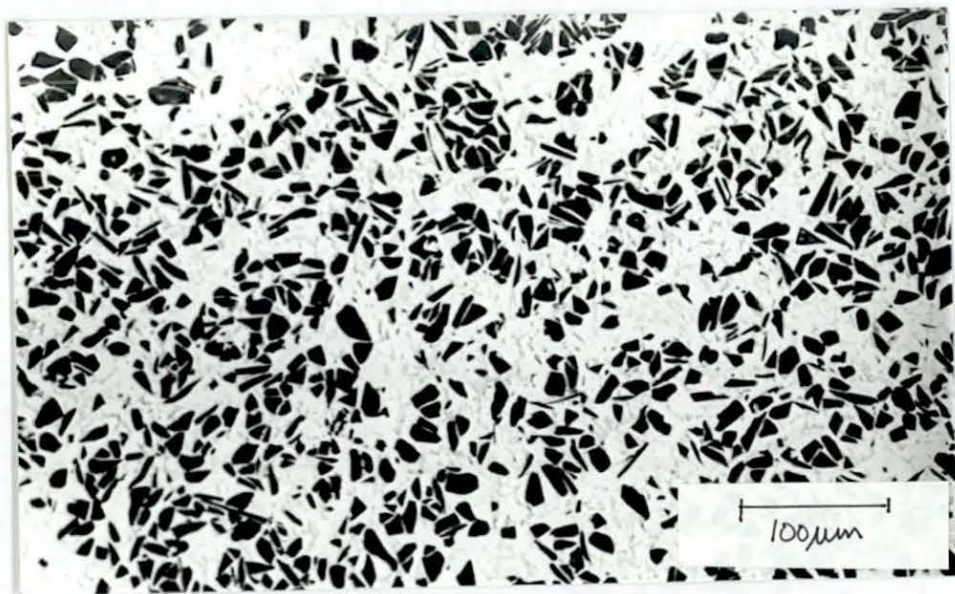


Figure 6.92 ZA27 + 20vol% SiCp (LM) 50mm Section  
Die Temp 180°C Pour Temp 595°C  
Squeeze Pressure 185 MPa

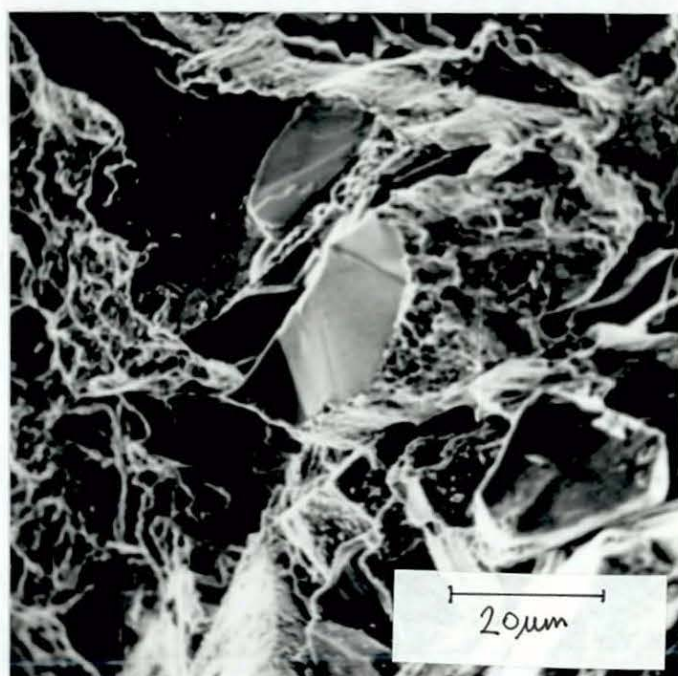


Figure 6.93 ZA27 + 10 vol% SiCp (SEM) 50mm Section  
Die Temp 180°C Pour Temp 595°C  
Squeeze Pressure 185 MPa  
Room temperature fracture

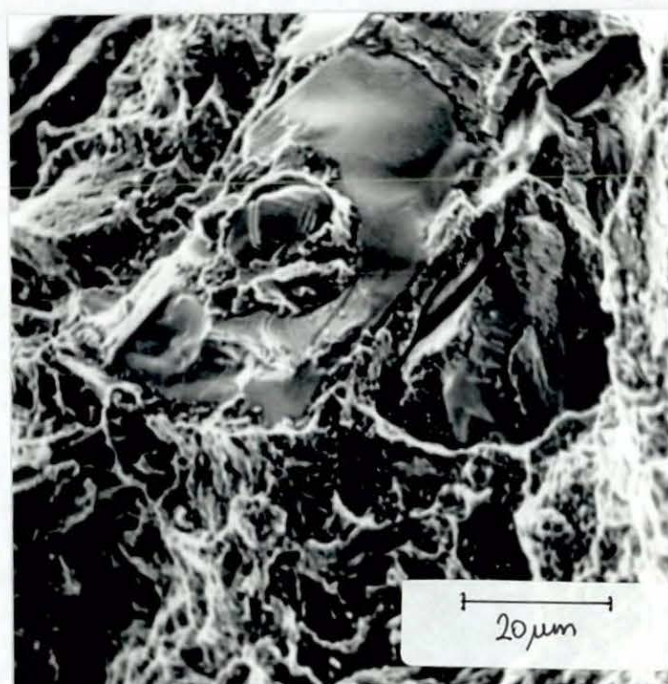


Figure 6.94 ZA27 + 15vol% SiCp (SEM) 50mm Section  
Die Temp 180°C Pour Temp 595°C  
Squeeze Pressure 185 MPa  
Room temperature fracture

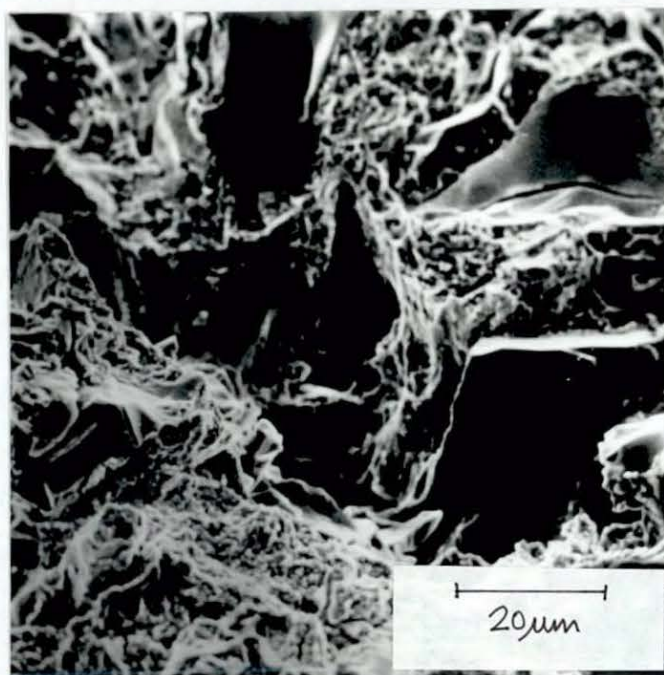


Figure 6.95 ZA27 + 20 vol% SiCp (SEM) 50mm Section  
Die Temp 180°C Pour Temp 595°C  
Squeeze Pressure 185 MPa  
Room temperature fracture

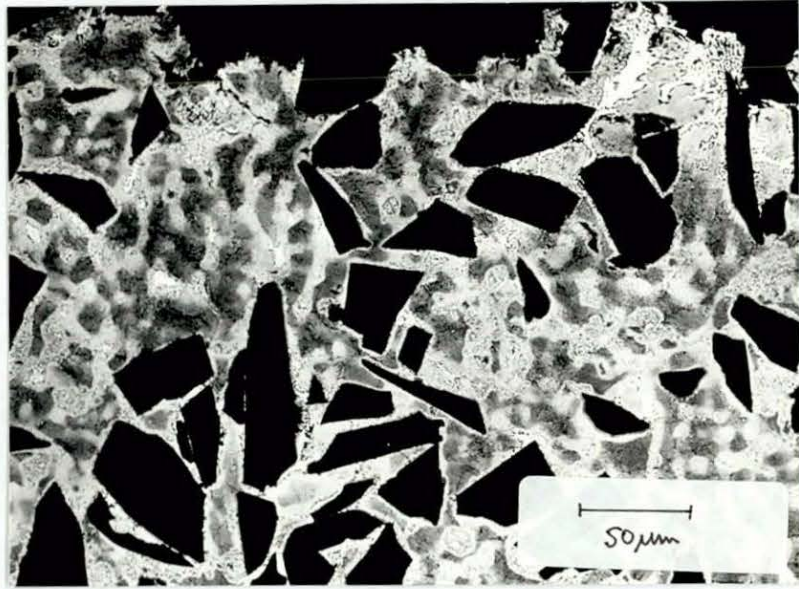


Figure 6.96 ZA27 + 20 vol% SiCp (SEM) 50mm Section  
Die Temp 180°C Pour Temp 595°C  
Squeeze Pressure 185 MPa  
60°C test fracture

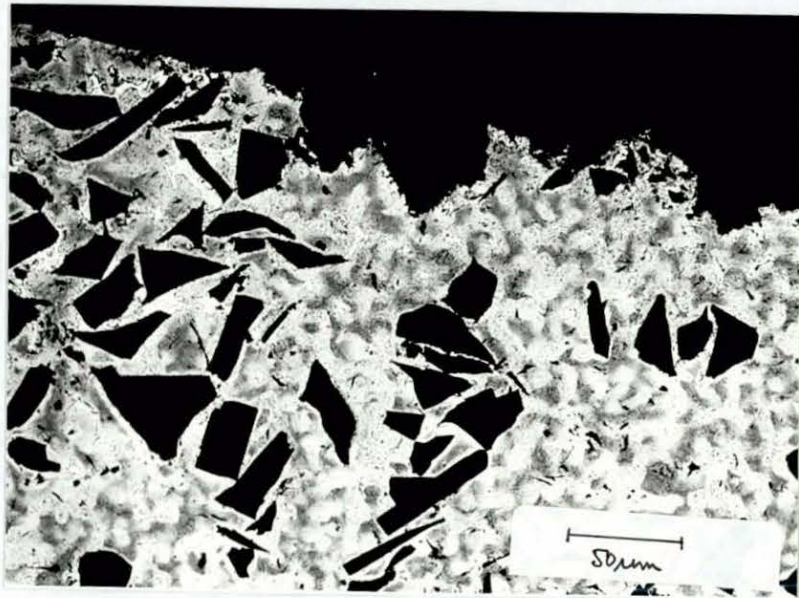


Figure 6.97 ZA27 + 20 vol% SiCp (SEM) 50mm Section  
Die Temp 180°C Pour Temp 595°C  
Squeeze Pressure 185 MPa  
100°C test fracture



Figure 6.98 ZA27 + 20 vol% SiCp (SEM) 50mm Section  
Die Temp 180°C Pour Temp 595°C  
Squeeze Pressure 185 MPa  
150°C test fracture

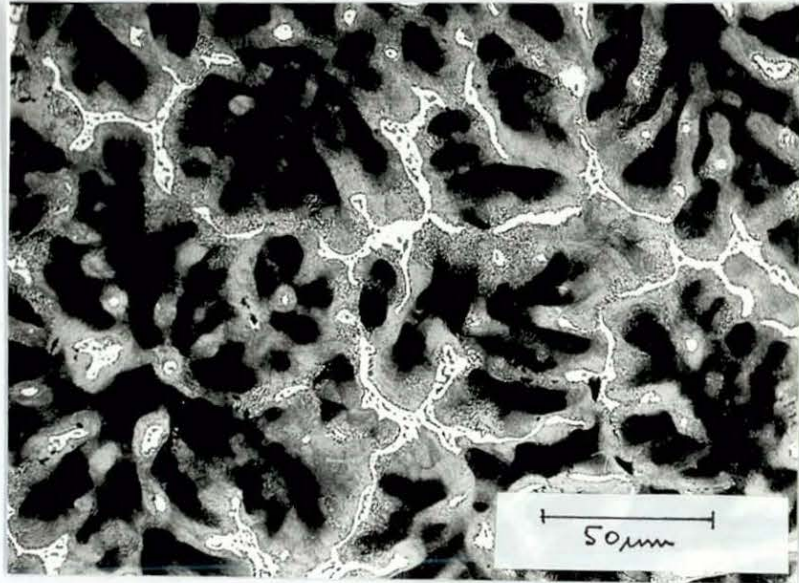


Figure 6.99 ZA27 (SEM) 50mm Section  
Die Temp 180°C Pour Temp 595°C  
Squeeze Pressure 185 MPa  
Creep at 100°C, 70MPa

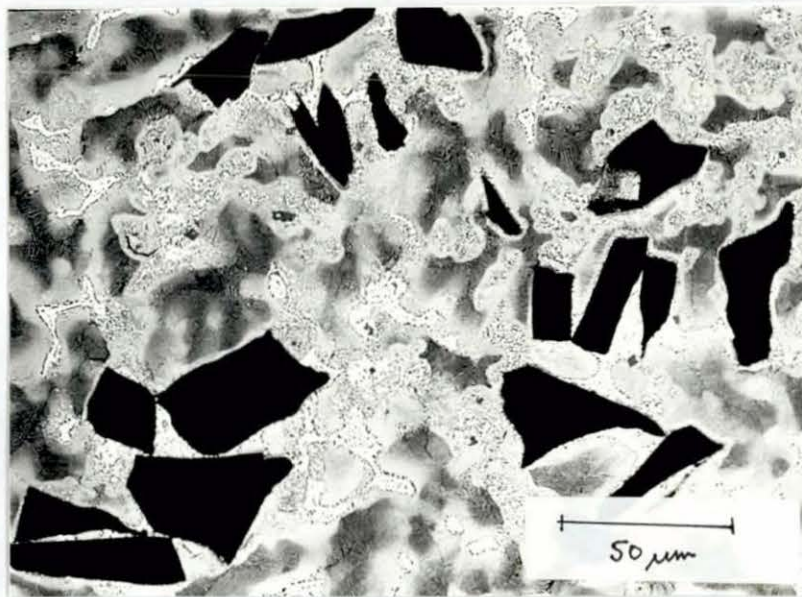


Figure 6.100 ZA27 + 10 vol% SiCp (SEM) 50mm Section  
Die Temp 180°C Pour Temp 595°C  
Squeeze Pressure 185 MPa  
Creep at 100°C, 70MPa

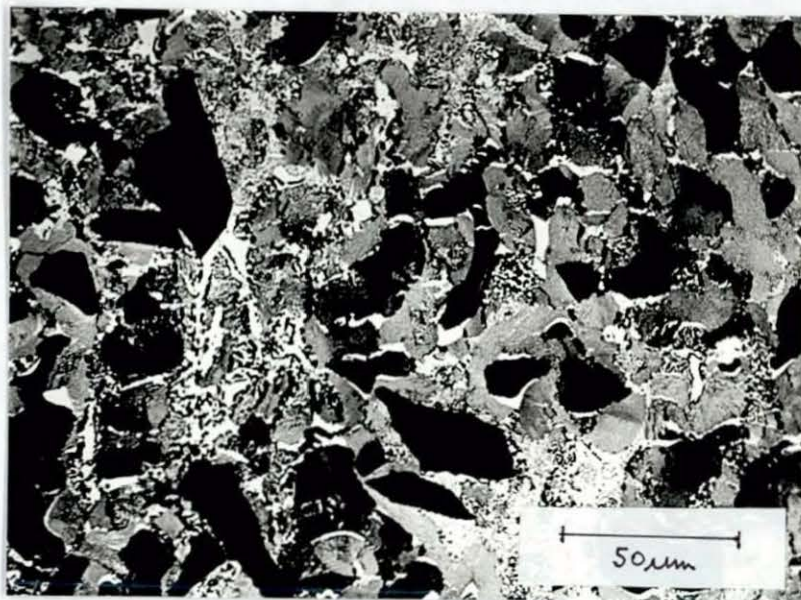


Figure 6.101 ZA27 + 20 vol% SiCp (SEM) 50mm Section  
Die Temp 180°C Pour Temp 595°C  
Squeeze Pressure 185 MPa  
Creep at 150°C, 70MPa

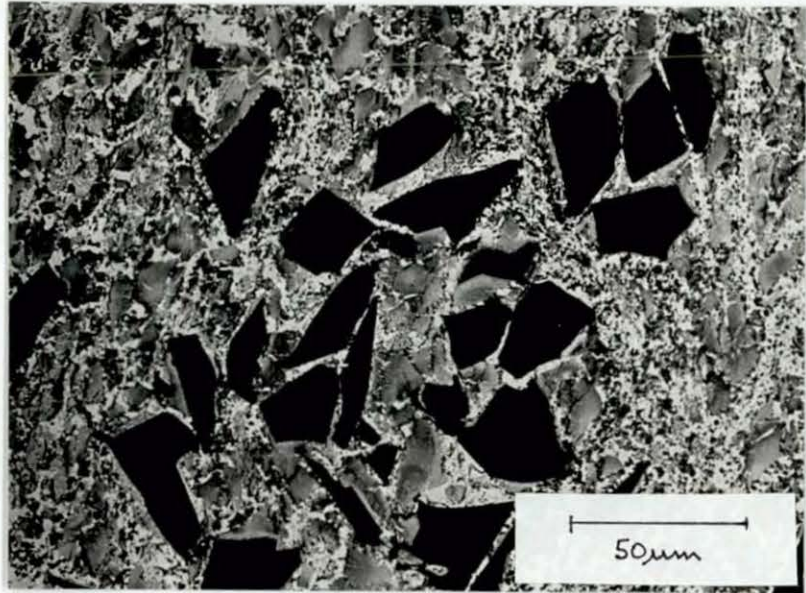


Figure 6.102 ZA27 + 10 vol% SiCp (SEM) 50mm Section  
Die Temp 180°C Pour Temp 595°C  
Squeeze Pressure 185 MPa  
Creep at 150°C, 139MPa

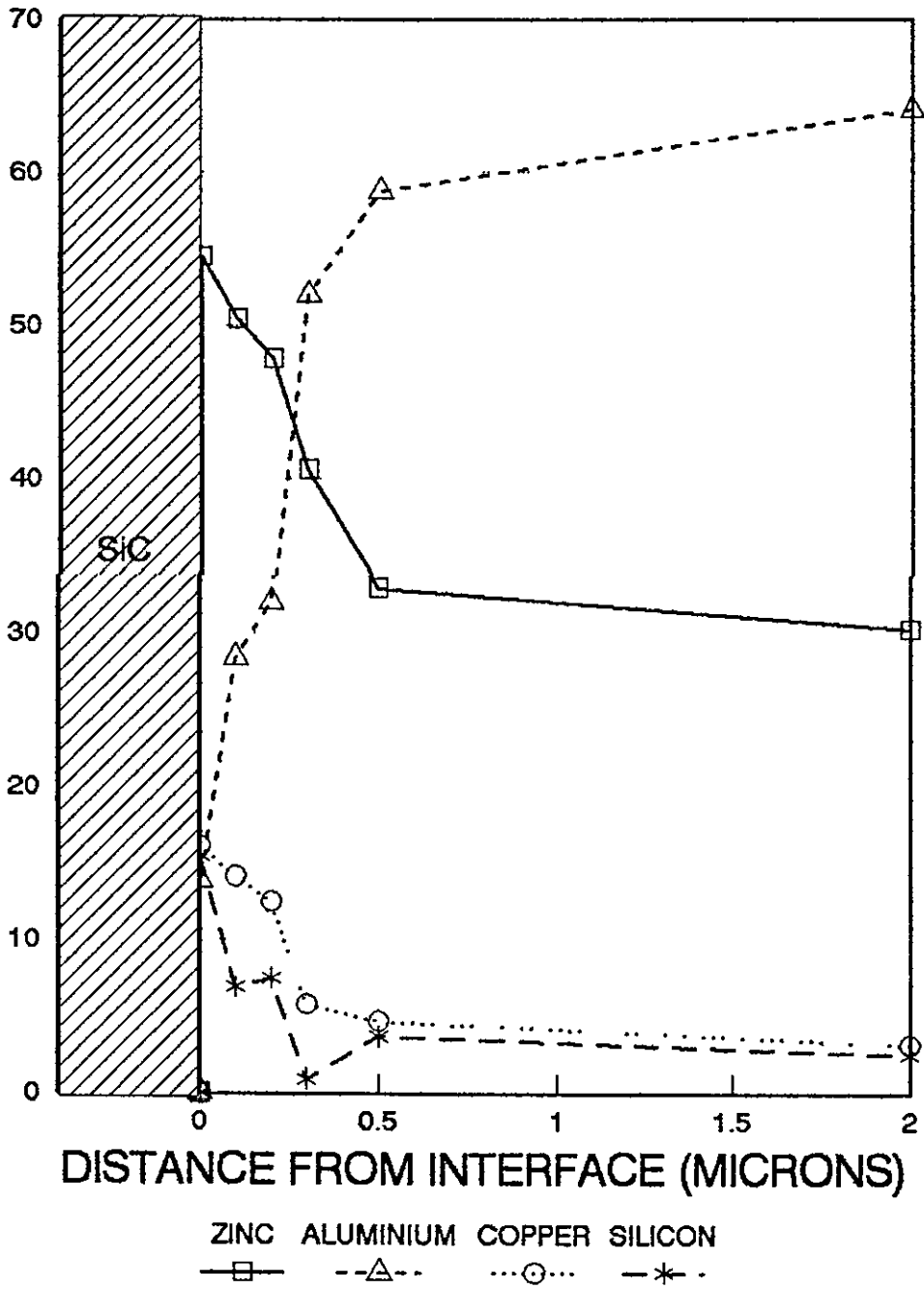
than in the unreinforced alloy (Figures 6.99-6.100). A feature of the high temperature creep microstructure is the appearance of an inter-connecting network of zinc rich phase, during deformation (Figures 6.101-6.102). These would be expected to be weak. The inclusion of large particulates may explain improved resistance to deformation at high temperature. Figure 6.102 shows that the matrix structure is largely decomposed.

#### 6.9 Chemical Analysis of Squeeze-Cast Composites

Figure 6.103 shows a plot of weight % of element vs. distance from a silicon carbide particle in ZA27 matrix alloy. There appears to be a build-up of zinc, copper (and silicon) concentrations near the interface relative to the matrix.

FIGURE 6.103 EDS ANALYSIS OF THINNED SPECIMEN  
OF ZA27 + SiCp (AS CAST)

WEIGHT % OF ELEMENT



## 7. Discussion of Results

### 7.1 Introduction

The results from this investigation are discussed in terms of the initial objectives. The basic aim of the first section was process optimisation, to enhance room temperature properties of a family of zinc base casting alloys. The second aim was to use the optimised processing conditions initially developed, to engineer an improved material system, based on ZA alloys, for operation at higher temperature.

The problem with the first aim is how to define process optimisation, so that it could be of significance to other workers in the field. That is, it may be possible to optimise a material property in a squeeze-cast component of 50mm section thickness, at a particular die temperature and pouring temperature. However, if the same processing conditions are used for a different shaped component, then they may give different properties. Similarly, different processes used to produce a component, may well yield products with considerable differences in mechanical properties. Reference to quoted properties, admittedly cast under different conditions, for ZA alloys produced by various processes (Tables 2.6 to 2.8) illustrates this. Thus, comparison of processes in terms of mechanical properties is qualitative rather than quantitative. A more precise yardstick is required. One possible solution is to consider cooling rate, in °C/second, through the solidification range.

Obviously, a thin sectioned pressure die casting would cool considerably faster than a thick sectioned casting in the same alloy cast into a sand mould. A different microstructure could thus be developed, with different properties. This is due to the amount of heat that has to be extracted, which will be greater in a thicker section, and the rate at which this heat can be extracted, which is dependent upon the mould and mould/metal interface characteristics.

Cooling rate data is available for some processes but it is difficult to collect for others, especially those involving rapid solidification. Collection of data for a range of section thicknesses is also time consuming. It is, however, useful to relate cooling rate during solidification, or time to pass from liquidus to solidus, to some form of microstructural feature. The particular feature to measure depends on the type of alloy system and the growth form. Solidification microstructures in single phase alloys can result from the following growth forms: planar, cellular, cellular dendritic or dendritic [84].

Commercial alloy structures generally comprise columnar or equiaxed grains of dendrites or eutectic, actual observed morphologies being determined by capillarity effects and diffusion of solute and/or heat [85]. Very rapid solidification may in fact produce an amorphous structure.

Metals have a low entropy of melting and grow in a non-faceted manner [86]. In substances with high entropies of melting the crystal behaviour is determined by growth defects. This is important in the growth of irregular eutectics, for example Al-Si alloys and cast iron. Dendritic growth is controlled by diffusion phenomena. Thermal diffusion gives rise to equiaxed dendritic growth in a pure substance, that is undercooling of the melt. Solute diffusion and constitutional supercooling leads to columnar growth in alloys. A combination of thermal and solutal diffusion gives equiaxed growth in alloys [87-89].

Eutectics can be regular or irregular, depending on the entropy of melting of one of the phases. Regular eutectics are generally of the metal/metal type, whereas irregular eutectics have one phase faceted [90]. The zinc-aluminium system gives a non-faceted/non-faceted type of growth, leading to regular eutectics. Regular eutectic morphologies are lamellar when the volume fraction of phases is approximately equal, or fibrous where the volume fraction of

one phase is below 0.25. Between these extremes a ribbon like morphology may be apparent. In eutectics coupled growth between two phases occurs in a way determined by:

- direction of heat flow
- inter-diffusion of components in the liquid
- crystallographic orientation.

In eutectic growth a planar interface usually occurs although a dendritic eutectic may be present in a rapidly solidified material [86].

The microstructural feature to relate to cooling rate must be independent of outside factors. Grain size is not a good indicator because it is affected by degree of undercooling and the presence of nucleating agents in the form of impurities or deliberate additions. Secondary dendrite arm spacing is usually taken as the best measure of solidification time in dendritic alloys. It is generally accepted that a reduced secondary dendrite arm spacing, in the absence of microporosity, will result in improved mechanical properties [91].

In simple solid solution + eutectic alloys, dendrite cell size is sometimes used as a measure of cooling rate [92]. Spacing between lamellae in the eutectic is usually used as a measure of solidification time in eutectic alloys [90].

If a microstructural feature can be related to a cooling rate then it should be possible to compare processes on the basis of microstructure. Other factors, such as grain size, may still affect mechanical properties through control of segregation etc. However, the secondary dendrite arm spacing will be independent of grain size.

Cooling rate, in  $^{\circ}\text{C}/\text{second}$ , can be broken down into the product of temperature gradient at the solid/liquid interface  $G$ , in  $^{\circ}\text{C}/\text{metre}$ , multiplied by the rate of movement of the

interface R, in m/s. It is possible that at a fixed cooling rate G and R could be different in different situations. The product G.R affects the scale of the structure, while the ratio G/R is important in determining grain shape through its relationship to the onset of constitutional super-cooling [88]. Optimum processing conditions for any alloy depend upon cooling rate and G/R respectively, to develop optimum scale and microstructural morphology. Squeeze casting promotes a high rate of solidification R, even in thick sections. This is due to good heat conduction from the casting, through the mould wall. Alloy suppliers sometimes quote conditions necessary to obtain a desired microstructure in terms of G and R. Comalco, for instance, in a patent application for 3HA alloy [93], quote that R should be between 150 and 1000 microns per second and G controlled so that a G/R ratio of  $500-8000^{\circ}\text{C.s/cm}^2$  is obtained. Not all processes, because of their inherently different processing conditions, will be able to achieve these conditions in a particular component. For example, sand casting will provide a relatively low R value but G could be altered by the use of chills, to give the optimum G/R value. At the other extreme, pressure die casting in thin sections offers a very high rate of solidification and consequently a different G/R ratio. Obtaining optimum G/R values depends upon the following factors:

- mould material
- section thickness
- mould temperature
- pouring temperature
- use of pressure.

Within a process, mould temperature, pouring temperature and section thickness are the factors with most influence on G and R. From the results in Chapter 6 it appears that mechanical properties of squeeze-cast ZA alloys were most influenced by these three factors through their influence on G and R.

According to the literature, different types of alloys are influenced by either G or R. In eutectic alloys R is the dominant influence on lamellar spacing in the eutectic [90]. The following discussion tries to relate microstructures and properties of squeeze-cast ZA alloys according to the criteria just discussed.

## 7.2 ZA27

### 7.2.1 Thick Section

All 56 ingots produced were sound, with equiaxed macrostructures across the whole section. Cooling rate data, which was obtained by inserting thermocouples into the centre of ingots, gave a typical cooling rate of  $78.26^{\circ}\text{C}$  per second when solidified under pressure. This compared to a cooling rate of  $1.67^{\circ}\text{C}$  per second when solidified under gravity. Squeeze casting therefore provided a cooling rate 46.86 times higher than gravity casting. It was not possible to generate data on the temperature gradients at the solidification interface (G) or the rate of movement of solidification front (R).

Mechanical property data, included in Tables A-E in Appendix 1, shows the effects of processing variables, ie die temperature, pouring temperature, time to apply pressure, time to build up pressure, and squeeze pressure on room temperature UTS, 0.2%PS, percentage elongation and reduction in area. Over the whole range of processing conditions the following variations were noted:

UTS	377-427 MPa
0.2% PS	345-402 MPa
elongation	4-21%
reduction in area	4-40%

Properties appeared to be most influenced by die temperatures and pouring temperatures. The range does indicate large

variations. More detailed investigation reveals the following:

• **Effect of Die Temperature**

Highest strengths (both UTS and 0.2% P.S.) were achieved at the highest die temperature (300°C). There were consistently low strengths at 200°C die temperature across the whole range of processing conditions. Elongation results did not appear to show a definite trend.

• **Effect of Pouring Temperature**

Highest 0.2% proof strength values occurred at 555°C and the lowest at 515°C. Highest ductility (both elongation and reduction in area) was obtained at the highest pouring temperature (595°C) combined with lowest die temperature (150°C), indicating the importance of temperature gradients on ductility.

• **Effect of Squeeze Pressure**

The results for all properties appeared variable. The only noticeable trend is when all the 0.2% P.S. results from Tables A-D, in Appendix 1, are averaged at specific die temperatures. The trend is one of increased 0.2%PS with an increase in pressure but the graph (Figure 7.1) ignores the effects of press speed and pressure build-up.

• **Effect of Press Speed**

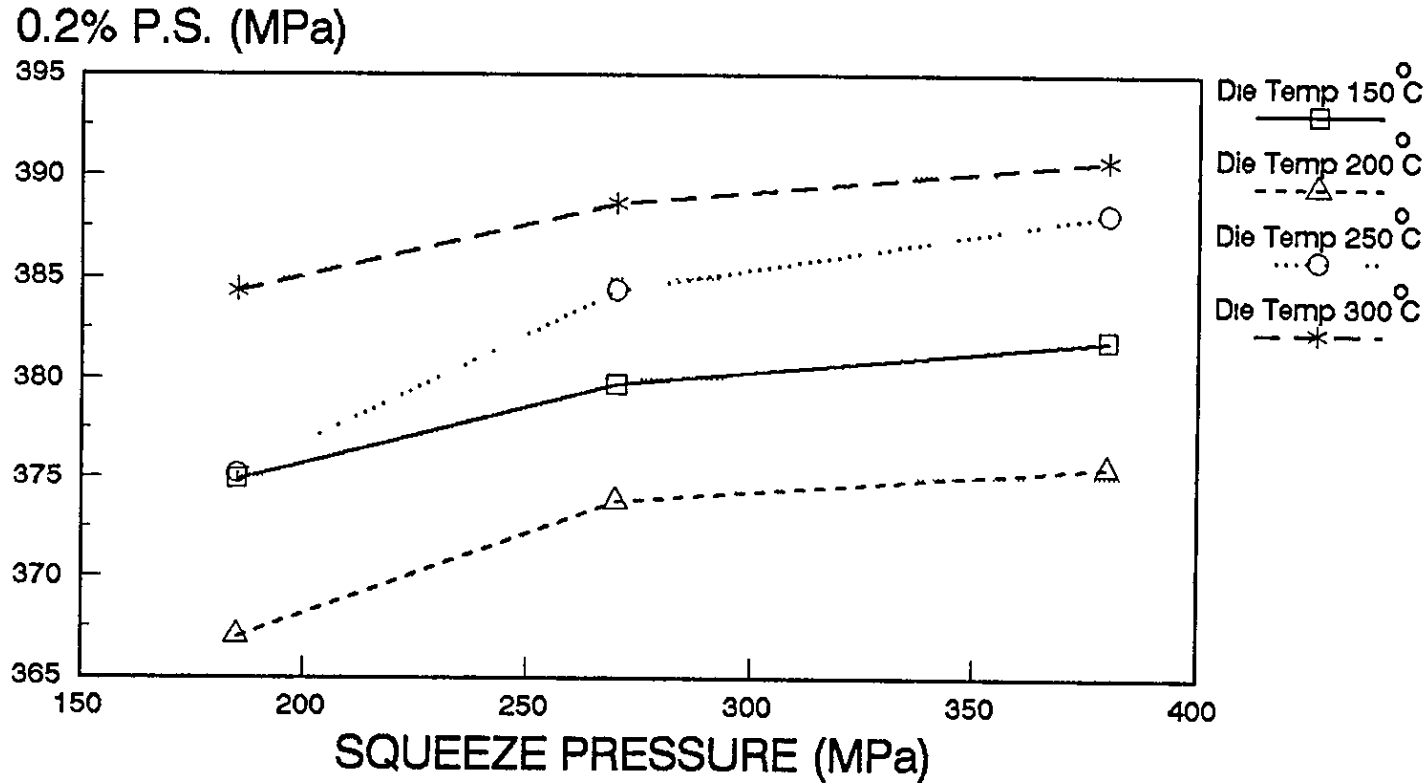
A higher press speed generally results in higher strength values. A higher press speed will result in the metal being pressurised at a higher temperature.

• **Effect of Pressure Build-up**

There are no apparent changes in strength or ductility within the range considered.

It is now necessary to explain these differences in terms of microstructure.

**Figure 7.1 Effect of Squeeze Pressure on the 0.2% P.S. OF Squeeze-Cast ZA27**



ZA27 is a long freezing range alloy, with a liquidus of 490°C and a solidus of 380°C. On solidification, it would be expected to form with a microstructure comprising an  $\alpha$  dendritic core, surrounded by a rim of  $\beta$ , created by a peritectic reaction. This occurs in a eutectic of  $\beta+\eta$ , which also contains some  $\epsilon$  phase ( $\text{CuZn}_4$ ). Solid phase transformations would alter the micro-morphology but the original areas could be distinguished. Measurement of the secondary dendrite arm spacing could be used to assess the time taken to solidify, whilst providing a comparison between processing conditions.

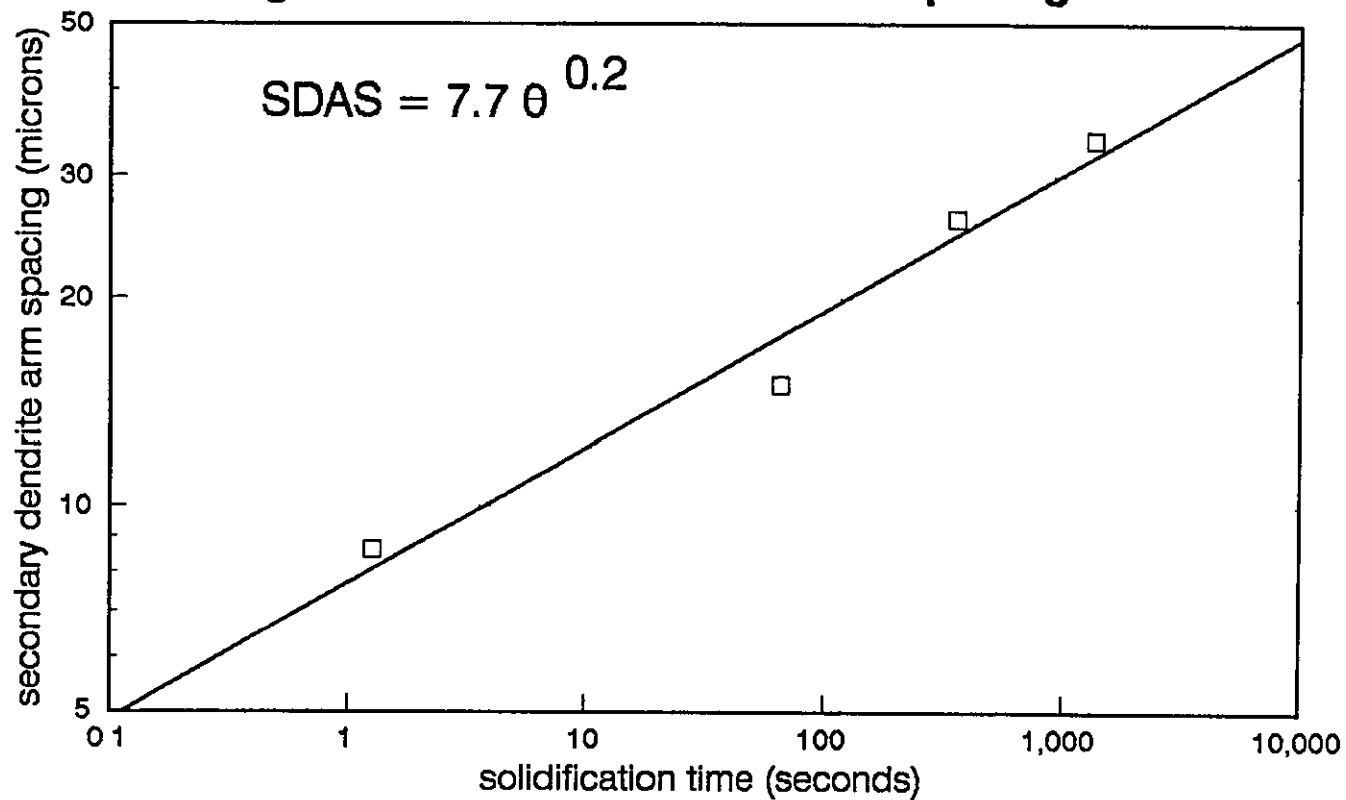
Data from this investigation, included in Table 6.3, combined with information from other sources [4,94] has been used to plot secondary dendrite arm spacing against solidification time (Figure 7.2). An equation relating the two is proposed, as follows:

$$\text{SDAS} = 7.7 \cdot \theta_t^{0.2} \quad (7.1)$$

where: SDAS = Secondary Dendrite Arm Spacing ( $\mu\text{m}$ )  
 $\theta_t$  = solidification time (s)

Thus, it is possible to estimate solidification time for a wide range of secondary dendrite arm spacing. The information from this investigation on squeeze casting appears to show that solidification time, or cooling rate, varies from 12 seconds (9.1°C/s) for a 50mm section cast into a die at 300°C, to 0.54 seconds (205°C/s) for a 12mm section casting produced in a die at 150°C. The structure of thin section castings appeared non-dendritic, especially in thinner sections. If secondary dendrite arm spacing was crucial in controlling mechanical properties, then one would expect the 0.2%PS to show a marked dependence on it. The trend is true to a certain extent but not in the predicted way. Normally, an increase in SDAS would result in a decrease of 0.2%PS. However, in this investigation the trend is not apparent. Low strengths at a die temperature of 200°C cannot be explained in terms of SDAS. The fact that

**Figure 7.2 ZA27 Dendrite Arm Spacings**



ZA27 solidifies peritectically may influence the SDAS vs. strength relationships. Clearly, there must be other factors controlling properties. References to the microstructures of ZA27 squeeze-cast at different die temperatures shows a number of interesting features on the larger microscopic scale, namely:

- a decrease in the amount of prior  $\alpha$  with increase in die temperature
- an increase in prior  $\beta$  with increase in die temperature
- decreasing amounts of eutectic with increasing die temperature

EDS analysis on samples produced at die temperatures of 150, 200, 250 and 300°C show, in Table 6.6, that the prior  $\alpha$  is, on average, 41.35% Zn, 57.8% Al and 0.85% Cu. The composition of the prior  $\beta$  varied more, especially around 200°C. A higher level of copper is noted in the prior  $\beta$ , compared to the prior  $\alpha$ . The general trend in prior  $\beta$  is a slight decrease in Zn and slight increase in Al, with increase in die temperature. At 200°C the prior  $\beta$  is considerably less rich in zinc and richer in aluminium than other cases.

The eutectic becomes progressively richer in zinc and less rich in aluminium with increasing die temperature. The copper content is higher in the prior  $\beta$  phase than in the prior  $\alpha$  phase and highest of all in the eutectic.

The appearance of these microstructural differences can be qualitatively explained as follows. At low die temperatures solidification is rapid. This causes the structure to be finer, due to more undercooling and higher solidification rate. The rapid solidification does not allow time for  $\beta$  to form to any large extent around the original  $\alpha$  resulting in a eutectic of  $\beta+\eta$ . At high die temperatures slower cooling allows more peritectic  $\beta$  to form, with a reduction in the amount of eutectic  $\beta$ , hence, giving higher eutectic zinc

concentrations. The copper contents in the eutectic are higher at high die temperatures because there is less saturation in the primary phases.

Closer examination of the microstructures at different die temperatures, but at the same pouring temperature (555°C), reveals the following:

- at 150°C

The SEM photograph, in Figure 6.43, shows the structure to comprise prior  $\alpha + \beta$  and a nearly continuous eutectic. Areas of the eutectic clearly contain  $\beta$ , but it is not possible to distinguish any  $\epsilon$  phase. This is due to its similarity in appearance to the white zinc-rich phase. An optical micrograph (Figure 6.42) shows a sample etched in 2% Nital, with white areas of  $\text{CuZn}_4(\epsilon)$  phase. Figure 6.43 shows a granular decomposition of prior  $\beta$  next to the eutectic, to form  $\alpha + \eta$ , accompanied by lamellar decomposition of the prior  $\beta$  and decomposition of the prior  $\alpha$  into  $\alpha + \eta$ .

(A comparison with a microstructure produced by a higher pouring temperature is provided in Figures 6.45 and 6.46. The significant feature of the high pouring temperature example is a more cellular dendritic nature indicating the importance of grain morphology on ductility.)

- at 300°C

At this die temperature (Figure 6.44) the eutectic is predominantly one distinguishable colour. Decomposition of the prior  $\beta$  and prior  $\alpha$  is still visible, although the granular decomposition of the prior  $\beta$  next to the eutectic appears not as marked. However, granular decomposition within the grains is clearly visible.

Trying to relate microstructures to properties is not straightforward. The general trend is a decrease in strength at 200°C die temperature. This is common to all sets of results in Tables A-E.

Strength appears to be provided by  $\beta$ , either in its peritectic or eutectic form. The  $\beta$  eutectic provides strength but lower ductility, while  $\beta$  in the grain provides strength and ductility.

At 150°C the eutectic  $\beta$  provides strength but a slightly low elongation value. The peritectic  $\beta$  at higher die temperatures provides higher strength.

High pouring temperatures provide maximum ductility. A high pouring temperature must increase the G/R ratio, thus changing the dendritic morphology to a more cellular-dendritic appearance.

Information from dilatometry shows that squeeze-cast ZA27 undergoes an expansion of 0.1% on prolonged artificial ageing at 95°C (Figure 6.82). On heating ZA27 in a dilatometer all samples showed an expansion corresponding to the transformation  $\alpha + \epsilon = T' + \eta$  (Figure 6.81). The contraction observed in the sample produced at 150°C is not readily explained but may be due to the high concentration of aluminium in the eutectic.

### 7.2.2 Thin Sections

This data was obtained for die temperatures over the range 150-220°C and at higher pouring temperatures, in the range 595-650°C. The effect of press speed and pressure build-up and indeed squeeze pressure were not studied. This is because the most significant parameters appeared to be pouring temperature and die temperature. Tables F-H in Appendix 1 show the effects of die temperature, pouring temperature and section thickness on room temperature tensile mechanical properties. Other parameters, viz. press speed and time to build-up pressure, were those necessary to fill the die cavities. Again, one of the problems is to try to put these results into context. The range of values found was:

UTS	404-456MPa
0.2%PS	363-422MPa
Elongation	4-10%

In these cases, thinner sections would result in high solidification rates and be accompanied by higher R values relative to the thick sections. Without measurements of G, which are very difficult to obtain it is not immediately apparent how temperature gradients are influenced overall by the combined effect of increased pouring temperature and thinner section. The appearance of the microstructure may give some clues.

It is possible to estimate the solidification time in some cases, by measurement of secondary dendrite arm spacings. However, in thinner sections the growth morphology appears to be non-dendritic. This is illustrated in Figures 6.47-6.51. The promotion of an apparent planar growth morphology suggests that the G/R ratio has in fact increased indicating that thinner sections result in very steep temperature gradients although the solidification rates also increase.

A high R value and increased undercooling must result in a high degree of nucleation in thin sections, and the steep temperature gradients allow the development of planar growth morphology. The eutectic in thin sections is predominantly inter-connecting. This observation would explain the relatively low elongation values in thin section ZA27 compared to that apparent in thicker sections.

#### • Effect of Die Temperature

The best strength properties were obtained at highest die temperatures while elongation values increased up to 620°C pouring temperature.

The obvious feature of a thinner section (higher R) are the finer scale of the microstructure and a change in appearance of the grain morphology from dendritic to petal-like. At low die temperatures in thin sections there is a continuous

eutectic. This petal-like appearance has been noted previously, in work with  $TiB_2$  modified ZA27 [95].

The same increase in peritectic  $\beta$  with increase in die temperature as was the case in 50mm sections is noted and the trend of highest strength at highest die temperature is again apparent.

### 7.2.3 Processing Map for ZA27.

The information from both thick and thin sections has been combined to produce a processing map for squeeze cast ZA27, Figure 7.3. Highest strength is apparent in thin sections due to a fine microstructure, but elongation values are comparatively low due to a nearly continuous eutectic. A high pouring temperature with a thick section at low die temperature gives a cellular dendritic structure and a high elongation. Between these extremes an equiaxed dendritic structure, with a well developed peritectic rim, gives the best combinations of strength and elongation

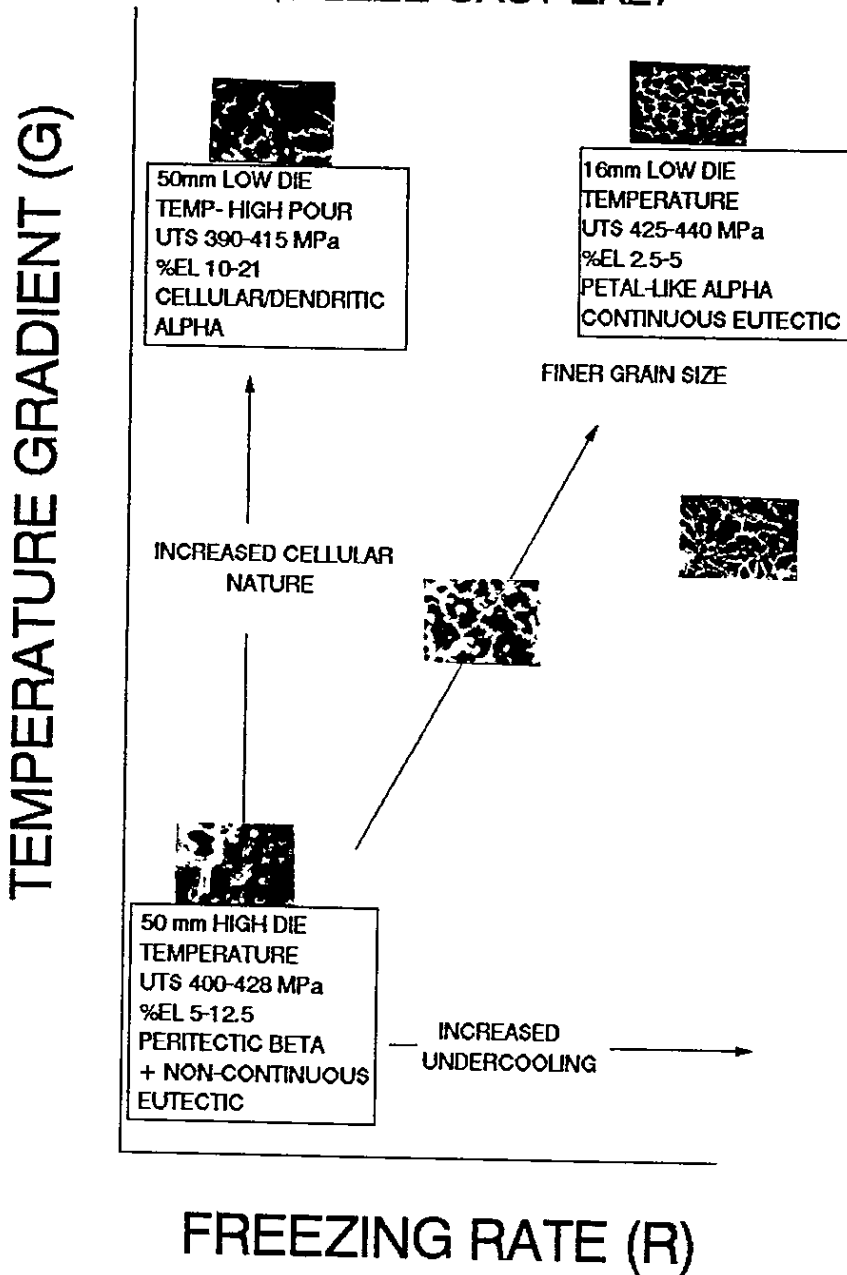
### 7.2.4 Comparison of Squeeze Casting with Other Processes

Figure 7.4 gives a comparison of tensile mechanical properties for different processing routes for ZA27, however this is probably best achieved by taking both strength and ductility into consideration.

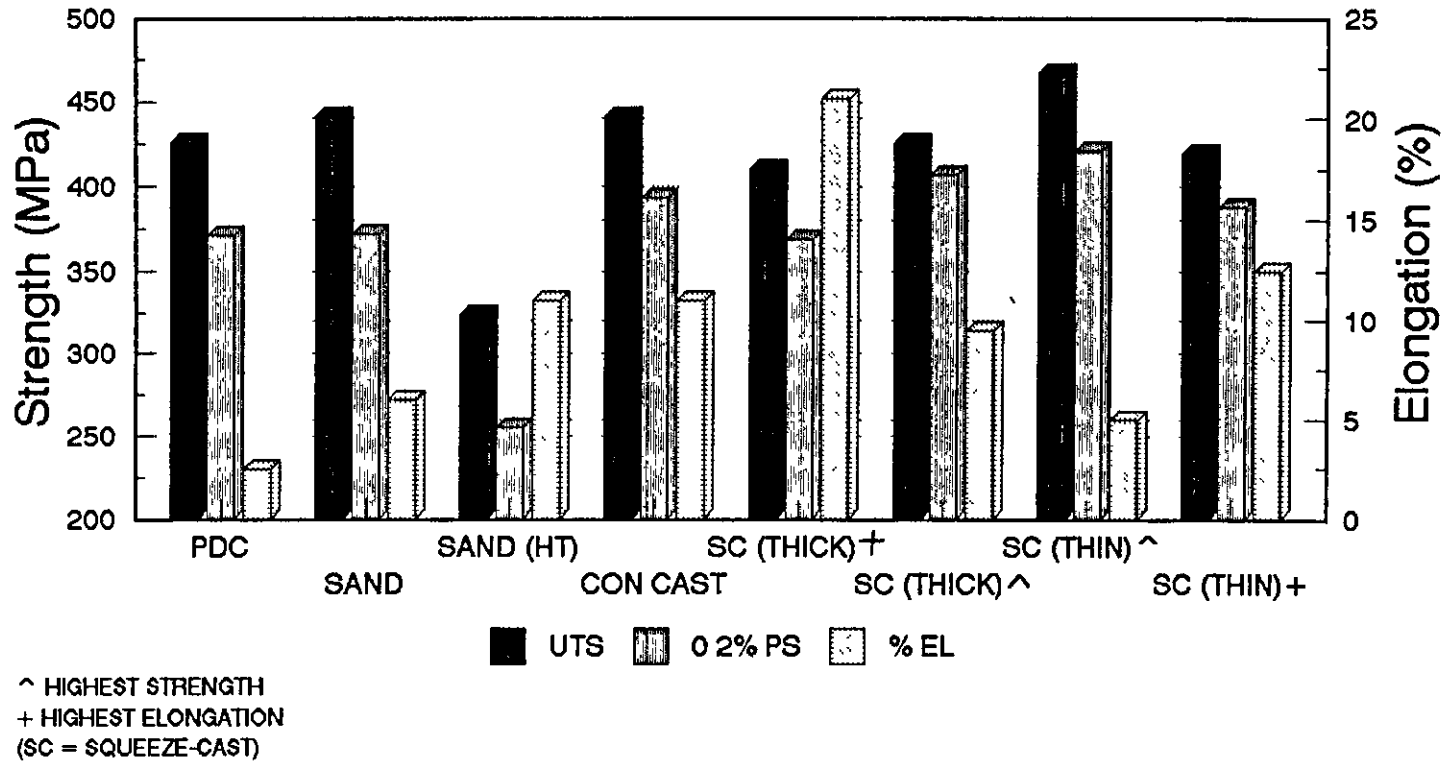
For example, sand-cast ZA27 can have a relatively high UTS of between 400 and 440MPa, combined with moderate elongation (3-6%), if judicious use of chills is practiced. To achieve higher elongation the material may be heat treated, however, an increase to between 8 and 11 % in elongation reduces the UTS by about 25%. Squeeze casting, however, can produce high elongation and high strength in the as-cast condition.

Similarly, pressure die cast ZA27 has a strength similar to that of sand cast ZA27 but elongation values are low, for example 2.5%. It would not be possible to heat treat the

FIGURE 7.3 PROCESSING MAP FOR SQUEEZE-CAST ZA27



**Figure 7.4 Comparison of Mechanical Properties  
of ZA27 Cast by Different Methods  
(Best Quoted Values)**



pressure die cast material because of the likelihood of blistering.

Combinations of strength and elongation have been compared via a Q value, or Quality Index [4]. Here, Q is defined as:

$$Q = UTS + 200\log_{10}(\%elongation) \quad (7.2)$$

Q values allow comparison of properties by combining the two parameters of strength and elongation together. Typical values of Q have been calculated for ZA27 in Table 7.1. Using this form of comparison it is clear that squeeze casting can produce a material with a higher Q value than other processes.

### 7.3 ZA8

According to the literature different types of alloys are more influenced by one or other of G or R. It is well known that eutectic alloys are influenced by a fast cooling rate, ie G.R with R being the most dominant factor [90]. In squeeze casting R is most influenced by section thickness and die temperature ( amount of heat to be extracted and conduction considerations). ZA8 is an alloy close to the eutectic composition. The results from this investigation, using ZA8, show that die temperature and section thickness influence the mechanical properties and microstructures of the alloy.

#### 7.3.1 Thick Sections

Highest strength was obtained at the lowest die temperature. Properties ranged from a UTS of 221MPa at 300°C die temperature to a UTS of 308MPa at 150°C die temperature. The relatively brittle nature of the squeeze-cast ZA8 did not allow calculation of proof strengths. Elongation values at the four die temperatures considered varied between 2.5 and 4% in all cases. Press speed and pressure build-up appeared to have no effect on properties.

**Table 7.1: Quality Indices for Cast ZA27**

**Definition:  $Q = UTS + 200 \cdot \log(\%Elongation)$**

<b>Processing Method</b>	<b>Q Value Formula</b>	<b>Q Value</b>
Sand Cast	$420 + 200 \cdot \log(4.5)$	550.6
Sand Cast, Heat Treated	$317.5 + 200 \cdot \log(9.5)$	513.0
Pressure Die Cast	$426 + 200 \cdot \log(1.25)$	445.4
Squeeze-Cast (Thick Section)	$402 + 200 \cdot \log(12.5)$	621.4
Squeeze-Cast (Thin Section)	$430 + 200 \cdot \log(6.75)$	595.9

Clearly, squeeze casting at one section thickness can provide a range of R values, depending upon die temperature.

The microstructure of ZA8 basically comprises a decomposed  $\beta$  (zinc rich) primary phase, surrounded by a eutectic of decomposed  $\beta$  and  $\eta$ . The eutectic at lower die temperature (Figure 6.52) has a lamellar appearance, but at higher die temperature (Figure 6.54) changes to a fibrous structure. Decomposition of the primary phase is more noticeable at higher die temperature.

### 7.3.2 Thin Sections

The strengths in thin sections of ZA8 are higher than those in thick sections, but there is the same trend of decreasing strength with increasing die temperature. Measured values of UTS ranged from 291MPa at 220°C die temperature to 355MPa at 150°C die temperature. Elongation values were similar to those in the thick section.

The faster rate of solidification (R) in the thin section results in a fine microstructure. Next to the primary phase in thin sections, the eutectic phase is lamellar but in thick sections definitely more fibrous. Increased strengths in thin section ZA8 can be explained because of a fine microstructure caused by increased undercooling and closer lamellar eutectic spacing caused by high R.

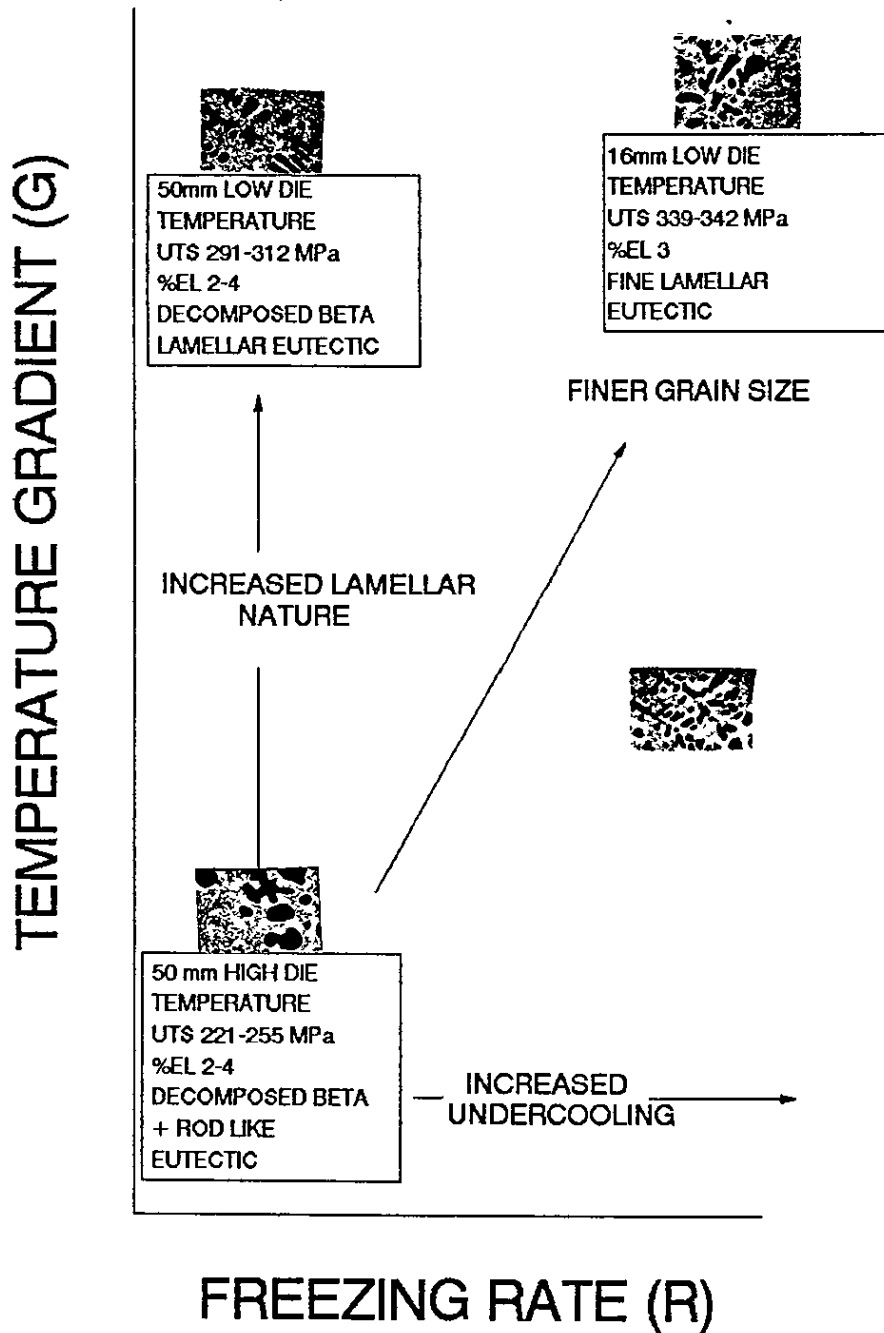
### 7.3.3 Processing Map for Squeeze-Cast ZA8

Figure 7.5 shows a processing map based on the results of this investigation. A higher temperature gradient, caused by reduced die temperature appears to promote a more lamellar microstructure. Increased freezing rate gives a finer lamellar spacing and a smaller grain size giving improved strength and elongation.

### 7.3.4 Comparison of Squeeze Casting With Other Processes

It has been shown in this investigation that the mechanical properties of ZA8 are highest at highest cooling rates, ie

FIGURE 7.5 PROCESSING MAP FOR  
SQUEEZE-CAST ZA8



low die temperatures and thin sections, which can be related to a fine grained structure with small inter-lamellar spacings in the eutectic.

Comparing strength and elongation values of squeeze-cast ZA8 with both sand casting and permanent mould casting processes (Figure 7.6) shows that the properties of squeeze-cast material are superior. This can be explained on the basis of a higher cooling rate.

The UTS values quoted for pressure die cast ZA8 are superior to those of the squeeze-cast material because of the higher cooling rate in thin section pressure die casting.

It is envisaged that squeeze casting could be used in situations where high strength in thicker sections is required.

## 7.4 ZA12

### 7.4.1 Thick Sections

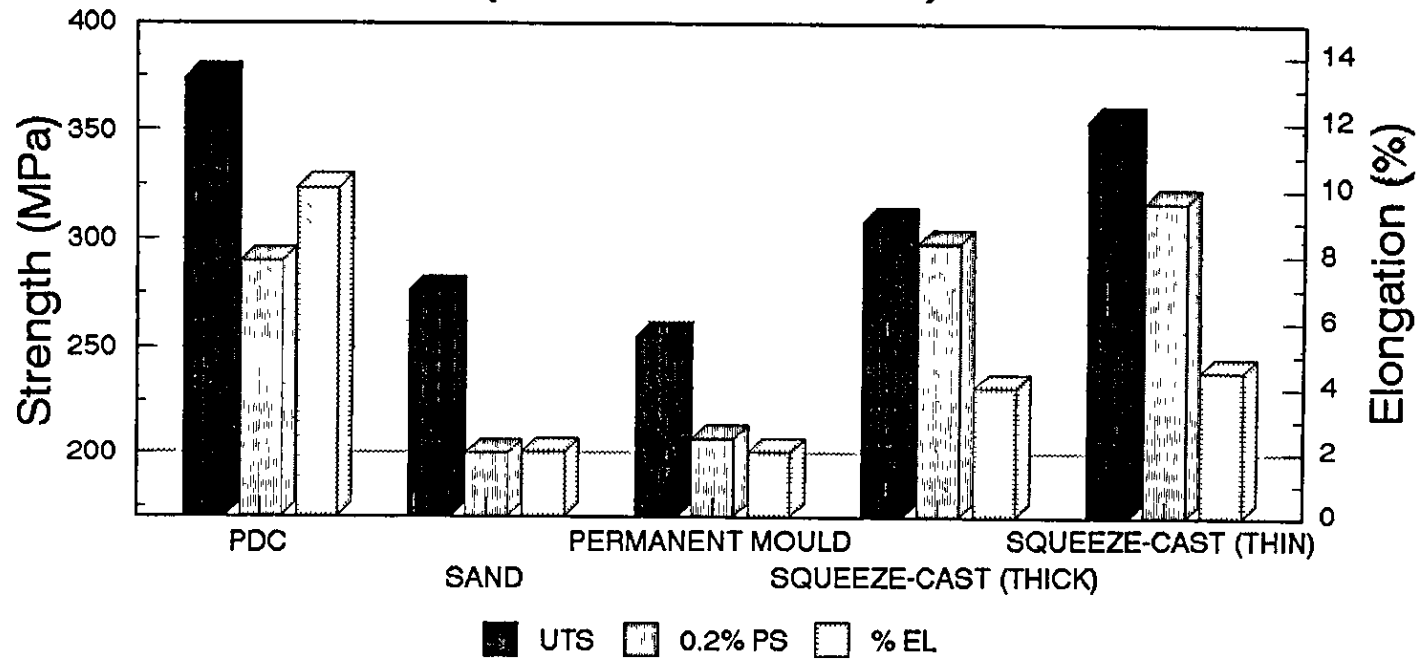
The mechanical properties of ZA12, as with ZA8, have a dependence on die temperature, with the properties improving at lower die temperature. Elongation values ranged from 2 to 4%.

The microstructure of ZA12 (Figures 6.62 - 6.65) contains more primary phase than does ZA8. The eutectic in ZA12 changes in appearance, from lamellar at low die temperatures to fibrous at higher die temperatures. Decomposition within the primary phase is more apparent at high die temperatures.

### 7.4.2 Thin Sections

The faster cooling rate which occurs in thin sections improves the mechanical properties of ZA12 relative to the 50mm section. UTS values vary from 349 to 371MPa. Grain size is finer than in the thicker sections (Figures 6.66 - 6.71).

**Figure 7.6 Comparison of Mechanical Properties  
of ZA8 Cast by Different Methods  
(Best Quoted Values)**



### 7.4.3 Processing Map for Squeeze-Cast ZA12

Figure 7.7 shows a processing map based on the results from this investigation. The same comments that applied to ZA8 are applicable in this case.

### 7.4.4 Comparison of Squeeze Casting with Other Processes

Like ZA8, the mechanical properties of ZA12 are higher for higher cooling rates. The strength and ductility of squeeze-cast ZA12 is superior to those for sand, permanent mould and graphite mould castings (Figure 7.8). The properties approach those attainable by thin section pressure die casting.

The 0.2% proof stress is higher for squeeze-cast ZA12, compared to pressure die-cast ZA12. This is due to the improved structural integrity.

## 7.5 Zn-37Al

It was decided to study a long freezing range alloy like Zn-37Al because it would normally be very difficult to cast the alloy sound. This is due to its relatively poor fluidity and its tendency to shrinkage porosity formation during solidification. The alloy could be processed by squeeze casting without problem, in a 50mm diameter die. However, filling thin sections by backward extrusion proved difficult. The alloy chosen was made up from commercially pure aluminium and electrolytic zinc. Neither of the strength enhancing elements, magnesium or copper, was added.

### 7.5.1 Thick Sections

The alloy was processed with fixed press speed and pressure build-up settings at two pouring temperatures and four die temperatures. Mechanical property results are shown in Table M (Appendix 1) and are presented graphically in Figures 6.38 - 6.41.

UTS and 0.2% proof strength are little affected by die temperature but elongation values are highest at lowest die

FIGURE 7.7 PROCESSING MAP FOR  
SQUEEZE-CAST ZA12

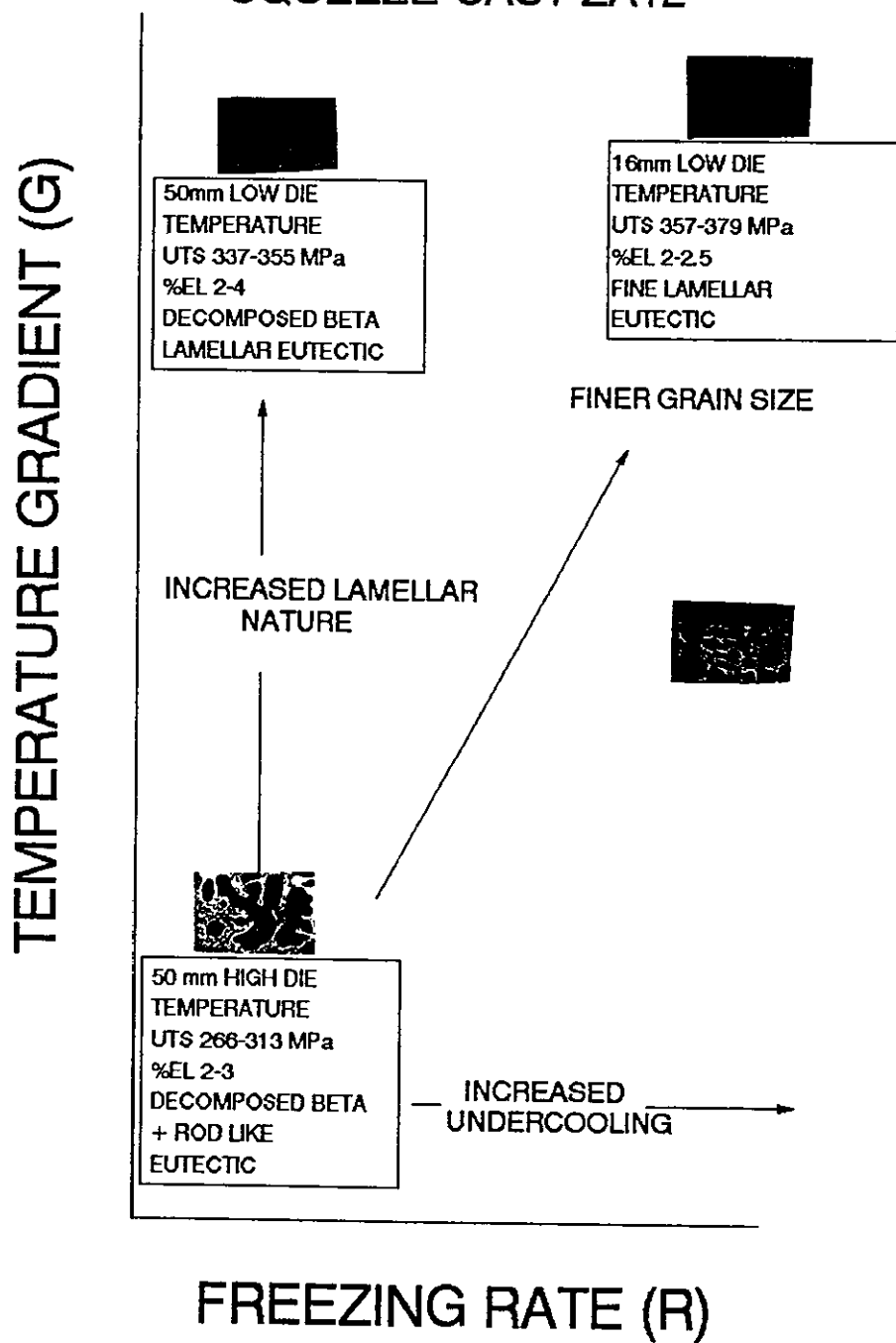
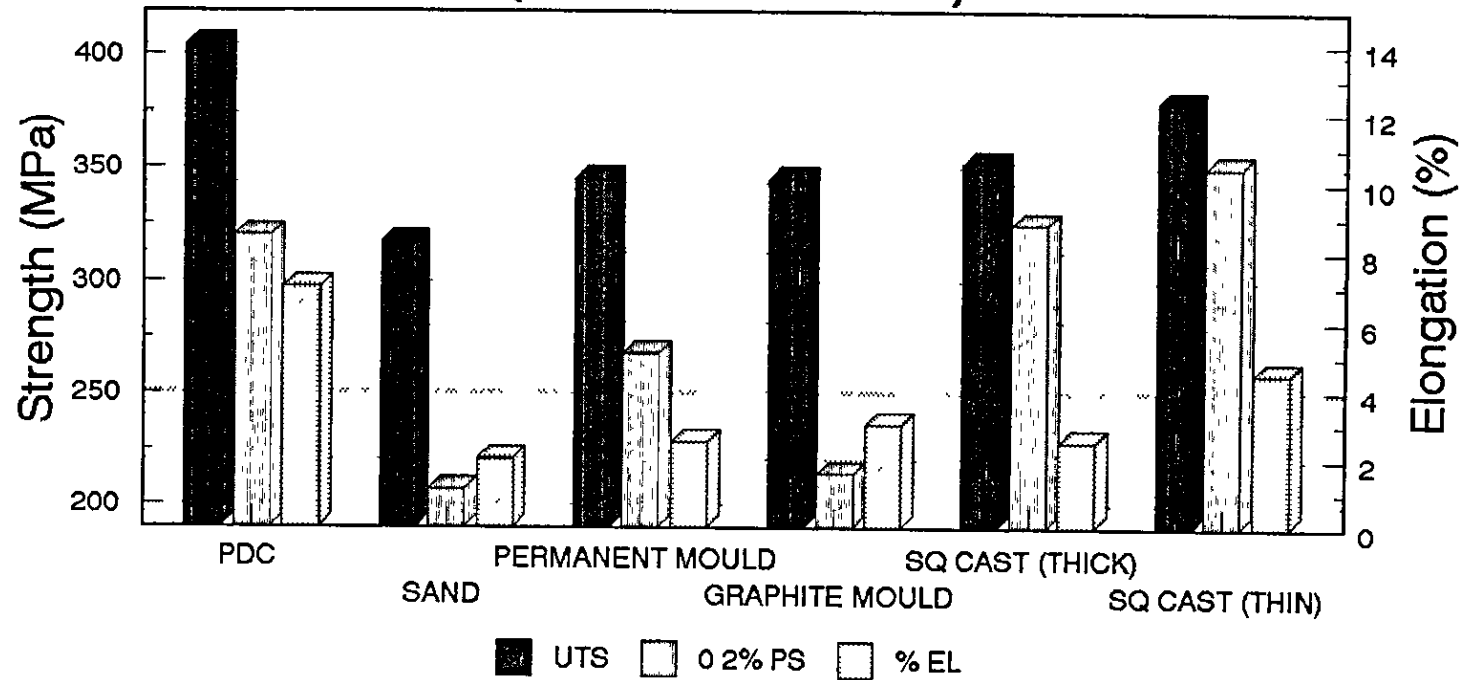


**Figure 7.8 Comparison of Mechanical Properties  
of ZA12 Cast by Different Methods  
(Best Quoted Values)**



temperature indicating again the importance of steep temperature gradients on ductility.

The microstructures from back scattered SEM photographs appear to comprise an  $\alpha$  core, surrounded by  $\beta$ . There are also small amounts of white zinc-rich  $\eta$  phase but the amount decreases with increased die temperature. A fine precipitate was present between the lamellae in the decomposed prior  $\beta$  in the sample produced at 300°C die temperature.

Higher strength in the samples produced at 150°C die temperature can be related to a finer grained structure. The increase in strength properties at 300°C die temperature compared to those at 250°C may be related to the appearance of fine precipitates in the decomposed  $\beta$  phase (Figure 6.79).

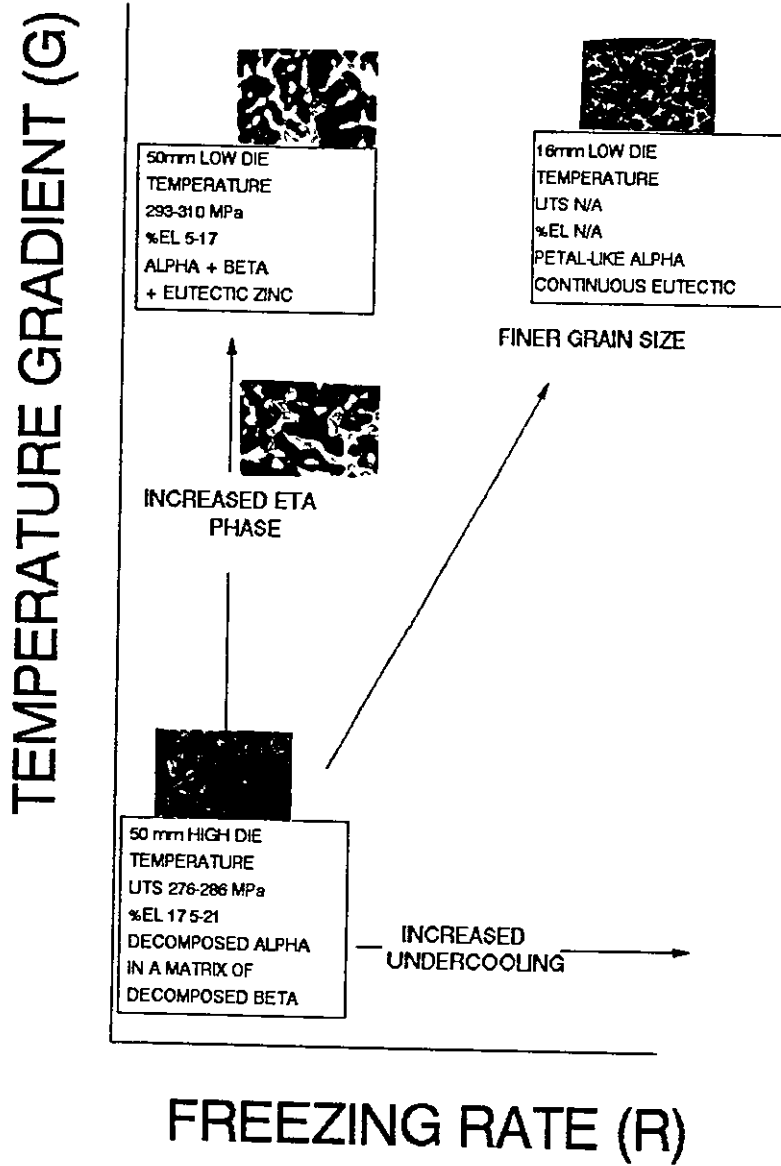
#### 7.5.2 Thin Sections

No mechanical property data is quoted because of the difficulty in obtaining formed components, however the microstructure (Figure 6.80) exhibits a large amount of petal-like  $\alpha$  phase surrounded by a small rim of  $\beta$  in a coarse eutectic. This is similar to the case of thin section ZA27 and is due to the high R value compared to that in a thick section.

#### 7.5.3 Processing Map for Squeeze-Cast Zn-37Al

Figure 7.9 shows a processing map based on the present investigation. The conclusions are different to the commercial alloys in that optimum elongations are achieved at the slowest cooling rates whereas highest strength is associated with fast cooling rates. In comparison with ZA27, which contains the strengthening elements copper and magnesium, Zn-37Al is weaker and it is also more difficult to process, especially in thin sections, because of its extended freezing range.

FIGURE 7.9 PROCESSING MAP FOR  
SQUEEZE-CAST Zn-37Al



## 7.6 Composite Materials

### 7.6.1 Composite Manufacture

Composite manufacturing by the vortex method, followed by squeeze casting was relatively straightforward. Particle addition to a melt required only simple stirring equipment. This can be as large as is necessary. The version used in this research was not successful in adding fine particles, ie those around  $10\mu\text{m}$ , and was slow, giving a production rate of 2 ingots per day. However, it is envisaged that with an alternative system, for example as is used by Duralcan, the method of stirring-in particles could be economically viable. The biggest drawback with the vortex system used appeared to be in the stirrer. Patented designs have a more elaborate system, rather than a simple propellor type stirrer. It was considered to be outside the scope of this investigation to concentrate on the method of introduction of particles to a melt. It was rather decided to prove they could be introduced and that the resulting mixture could be successfully squeeze-cast. However, it would have been most interesting to investigate the properties of squeeze-cast ZA27 with  $10\mu\text{m}$  particles of SiC.

The vortex method used in the research necessitated slow addition of particulate to the melt. At a faster rate, particle rejection was common, resulting in all the added particles being rejected. The process was labour intensive and only enough material for one ingot could be melted at one time.

Once the particulate had been added to the melt of ZA27, it was allowed to stir for at least  $\frac{1}{2}$  hour, until a homogeneous appearance was obtained. In general, the melt could be poured relatively easily. Difficulty of pouring increased with increased volume fraction of particles but the mixture which was most viscous (20vol%) could be processed in all three squeeze casting dies.

As the volume fraction of particulate increased, contraction during solidification also increased and it became increasingly difficult to produce sound ingots. Generally, the best solution was to remelt ingots, gently stir them and squeeze-cast them again.

Squeeze casting parameters chosen were those which gave optimum ductility in the plain alloy state. However it must be conceded that the particles, because of their characteristics, would act as heat centres and modify the solidification behaviour of the alloy.

### **7.6.2 Distribution**

Particles lay at grain boundaries associated with the eutectic phase. Micrographs showed that there was a tendency for particle clumping in 10 v/o composites, but that this reduced at higher v/o. Stefanescu et. al.[96] have written about the conditions necessary to obtain particle envelopment rather than particle pushing (leading to clumping) in solidification processing of MMC's. They state that envelopment is favoured by low temperature gradients, high rates of solidification and higher volume fraction of the reinforcing phase. Squeeze casting allows the production of castings at a high 'R' with 'G' being controlled by die and pouring temperatures.

Once a good melt had been achieved it was possible to cast it into both thick (50mm) and thinner (8-16mm) sections with good distribution.

### **7.6.3 Mechanical Properties**

#### **7.6.3.1 Tensile Testing**

With the exception of the increased Young's Modulus, testing the composites in uni-axial mode proved slightly disappointing. The composites always had strengths less than that of the plain alloy at room temperature. However, strength was seen to increase in the composite with increase in volume fraction. The best value of tensile strength in a

composite of 320MPa was accompanied by elongation of less than 1%. This compares unfavourably with the plain alloy, which typically would have a UTS of 411MPa and an elongation of at least 4, but up to 21%, depending upon the processing.

On the positive side, composites retained a higher proportion of their room temperature strength at elevated temperatures indicating that there was some contribution to reinforcement.

Failure during tensile testing always occurred below the expected yield point of the alloy, ie in a brittle manner. The presence of particles clearly results in an embrittling effect on the alloy. Clumping in the 10% composites is more apparent and a notch effect is the most likely cause of failure. An average value of UTS of 228MPa for the 10 v/o increased to 241MPa for the 15 v/o and 279MPa for the 20 v/o composite. Although the composite at 20 v/o is relatively homogeneous, the reduction in strength compared to the plain alloy still has to be explained. One reason may be related to the incidence of oxide films on the fracture surface. The vortex method creates turbulence in the melt and will draw air into the mixture as well as particles. The gas shield was not totally satisfactory in providing an inert gas shield. Another problem relates to the squeeze casting process itself. In squeeze casting the metal has to be clean as no provision for dross traps can be incorporated. In hindsight a better solution would have been to filter the composite melt before it entered the die. Residual stresses may also contribute to low tensile properties. The nature of these stresses is discussed in section 7.6.3.3.

#### **7.6.3.2 Composite Compression Testing**

Composites had higher yield strengths in compression at both room temperature and 100°C compared to the unreinforced alloy. The increased strength is due to composite reinforcement, but the behaviour of the material after yield is indicative of matrix/particle de-bonding. More de-bonding

will occur at higher volume fractions of particulate and this explains the behaviour in Figure 6.85.

### 7.6.3.3 Modelling Properties

The classical models to describe the behaviour of aligned continuous and discontinuous composite materials were developed by Cox, Eshelby and others [97]. They are based on a continuum mechanics approach, relying on load transfer by shear, between matrix and reinforcement. However, because particulate reinforcements have an aspect ratio effectively equal to unity, the theories cannot be used to model their behaviour in metals. In fact, until recently, no theory could apparently explain the increases in strength (both yield and UTS) observed in some particulate samples. Arsenault and his workers [97] are advocates of a theory which tries to explain strengthening due to increases in dislocation density brought about by differences in coefficients of thermal expansion between reinforcement and matrix phases and by smaller sub-grain sizes. This approach will be discussed later.

#### Elastic Modulus

Modulus modelling for particulate reinforced metals is usually considered to be between a lower bound:

$$E_{\text{lower}} \geq \frac{1}{V_m/E_m + V_p/E_p} \quad (\text{Ruess [98]}) \quad (7.2)$$

and an upper bound:

$$E_{\text{upper}} \leq V_m \cdot E_m + V_p \cdot E_p \quad (\text{Voigt [98]}) \quad (7.3)$$

where  $E_m$  = Young's Modulus of Matrix  
 $E_p$  = Young's Modulus of Particulate  
 $V_m$  = Volume fraction of Matrix  
 $V_p$  = Volume fraction of Particulate

Based on this statement, the modulus of a ZA27 base composite with  $\text{SiC}_p$  should be between the estimates listed in Table 7.2. The actual measured values fall between these two estimates, as is illustrated graphically in Figure 7.10.

### Strength

Some time ago, a listing of the components of composite strengthening mechanisms was proposed [97], as:

$$\Delta\sigma_{yc} = \Delta\sigma_{disl} + \Delta\sigma_{sg} \pm \Delta\sigma_{res} + \Delta\sigma_{tex} + \Delta\sigma_{comp} \quad (7.4)$$

where:

- $\Delta\sigma_{yc}$  = Change in yield strength of the composite
- $\Delta\sigma_{disl}$  = Increase in strengthening due to increase in dislocation density resulting from coefficient of expansion mismatch
- $\Delta\sigma_{sg}$  = Increase in strengthening due to reduced sub-grain size
- $\Delta\sigma_{res}$  = Difference in strengthening due to residual stresses
- $\Delta\sigma_{tex}$  = Strengthening due to differences in texture between 0 volume% and higher volume%
- $\Delta\sigma_{comp}$  = Classical composite strengthening by load transfer

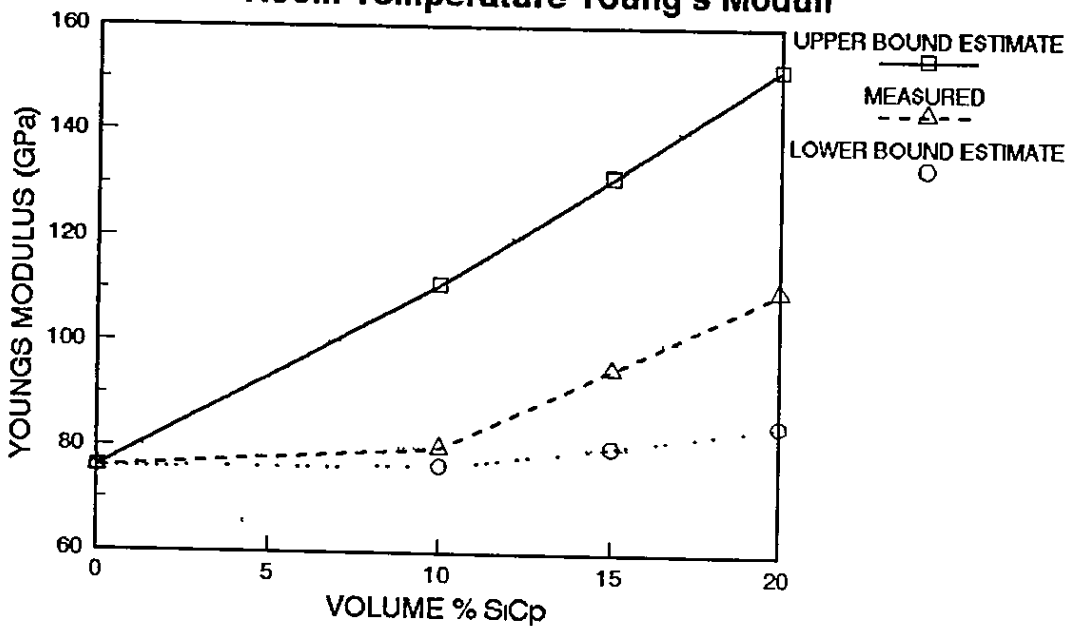
Harris [64] notes that yield appears to occur sooner (lower  $\sigma$  and  $\epsilon$ ) in composites probably due to:

- residual tensile stresses (because of coefficient of thermal expansion mismatches) generated during cooling from casting and heat treatment temperatures
- possible redistribution of precipitates, for example:
  - (1) segregation of elements to interface,
  - (ii) nucleation near reinforcement, due to enhanced dislocation density in the matrix,
  - (iii) removal of certain elements locally in the matrix.

**Table 7.2: Calculated Moduli of ZA27  
with SiCp Particulate Reinforcement**

Volume Percent of SiCp	Modulus Range (MPa)	
	Lower Value (Ruess)	Upper Value (Voigt)
10	76.5	111.0
15	80.2	131.5
20	84.4	152.0

**Figure 7.10 ZA27 - SiCp Composites  
Room Temperature Young's Moduli**



It is also probable that the formation of strong bonds allows less relaxation during cooling.

Nair et al [99] in their review of SiC reinforced aluminium alloys quote many examples of increases in strength with increasing volumes of reinforcement, compared to base alloy properties. However, the question that should be asked is whether it is prudent to compare the properties of the reinforced alloy with the base alloy. Nutt and Carpenter [100] discuss the effects of alloy depletion from the matrix. In an Al alloy-SiC system they state that Mg and Cu are depleted from the grain interiors, due to their roles in bond formation, and can no longer take place in the age hardening of the alloy. Papazian [101] also notes less GP zones and an increase in quench sensitivity in certain aluminium alloys with increased volume fractions of reinforcement. As strength is structure sensitive it may be incorrect to compare the strengths of composites with the base alloy.

Considering some of the above points in more detail. Residual tensile stresses can be approximately calculated from [102]:

$$\sigma_{\text{residual}} = \frac{(\alpha_m - \alpha_r) \cdot E_m \cdot E_r \cdot V_r \cdot \Delta T}{E_r \cdot (1 - V_r) + E_r \cdot V_r} \quad (7.5)$$

where  $\alpha_m$  = coefficient of thermal expansion  
of matrix

$\alpha_r$  = coefficient of thermal expansion  
of reinforcement

$\Delta T$  = difference between processing temperature  
and testing temperature

$E_m$  = Young's Modulus of matrix

$E_r$  = Young's Modulus of reinforcement

$V_m$  = volume fraction of matrix

$V_r$  = volume fraction of reinforcement

For a particular system the stresses are proportional to  $\Delta T$ .  
The equation takes no account of any stress relaxation by

creep and assumes that the parameters are constant over the temperature range.

Looking at typical figures for squeeze-cast ZA27 reinforced with SiC<sub>p</sub>:

$$E_{\text{SiC}_p} = 480\text{GPa} \quad E_{\text{ZA27}} = 76\text{GPa} \quad V_r = 0.2$$

$$\alpha_{\text{SiC}} = 4.7 \times 10^{-6} \text{K}^{-1} \quad \alpha_{\text{ZA27}} = 26.0 \times 10^{-6} \text{K}^{-1}$$

$$\Delta T = 180^\circ\text{C}$$

thus:

$$\sigma_{\text{residual}} = 158.5\text{MPa}$$

The calculated UTS of a composite based on 20 v/o SiC<sub>p</sub> in ZA27 is  $411 - 158.5 = 252.5\text{MPa}$ . This result is in line with practical observation of the strength of 20 v/o particulate reinforced ZA27, but other factors will contribute to the final value as is indicated in equation 7.4.

Arsenault and Wu [103] have calculated that the residual stresses would be largest for whisker particles and zero for round SiC particles. Particulate materials would lie somewhere in between.

Residual tensile stresses will tend to lessen tensile properties but improve compressive properties. Arsenault and Wu [103], looking at strength differential and Bauschinger effects in metal matrix composites, found the compressive yield strengths to be greater than the tensile yield strengths for SiC whisker and platelet reinforced materials. However, with spherical particles there was virtually no difference. In the former cases, the magnitude of both the strength differential effect and the Bauschinger effect increase with increasing volumes of reinforcements. It was noted in this work that the compressive yield strength of

SiC<sub>p</sub> reinforced ZA27 increased with increased volume fraction of reinforcement (Table 6.9), whereas in tension the material failed before yielding in a brittle manner.

Elevated temperature testing in this work up to 150°C showed that the composites retained a higher proportion of their room temperature strength compared to the base alloy. Composite strengthening and lower residual stress levels at elevated temperatures may account for this behaviour. Another observation is that the mode of fracture appears to change from through matrix/particles to through matrix with increased temperature of testing (Section 6.8). This suggests that the particle matrix bond is higher than the  $\beta$ /eutectic bond at elevated temperatures. Similar behaviour with Saffil reinforced Zn-32Al-2Cu has been observed in the work of Lo et al. [79].

At a high temperature/load regime it is probably possible to break the bonds between the matrix and the particle. Flom and Arsenault [104] report the SiC-aluminium alloy matrix bond breaking at elevated temperatures. This may have important consequences in heat treating of composites, their maximum temperature of use, and their behaviour under load. Bond breaking may account for the flat load-contraction curve noted in ZA27+20v/o SiC<sub>p</sub> compared to the plain alloy at 100°C (Figure 6.86).

Most of the quoted material properties for composites appear to have been obtained on samples that have been mechanically worked, following ingot processing. Presumably, this working affects the internal stress distributions and leads to improved properties.

#### 7.6.4 Creep of ZA Alloys and Composites

The results shown in Table 6.10 and Figure 6.87 are not consistent and appear to vary with both temperature and load.

This observation appears in line with other data on creep (e.g. in reference [1]).

Figure 6.87 shows the creep behaviour at 70MPa / 100°C (compression) for ZA8, ZA12, ZA27 and composites (ZA27 with 10 and 20 v/o SiC<sub>p</sub>). ZA8 exhibits the lowest secondary creep rate of the plain alloys but a larger amount of primary creep. The composite appears to give improved performance at higher temperatures and higher loads compared to the plain alloy. It seems likely that the mechanisms involved during creep vary both with temperature and load. At lower temperatures the particles may act as sources and sinks for vacancies, whereas at higher temperatures, the presence of particles may reduce the amount of grain boundary sliding or it may be that their presence alone as immovable obstacles is enough to give improved resistance.

Reference to the SEM microstructures (Figure 6.99-6.102) shows that the deformation mechanism in ZA27 at high temperatures (150°C) involves the formation of a zinc-rich network. The presence of SiC particles may disrupt this network and improve creep resistance.

### 7.7 Exploitation and Applications

ZA alloys are at an early stage in their product life-cycle and new applications are being developed via vigorous marketing. Engineers are being re-educated away from the ideas that zinc alloys are brittle and have limited structural applications. Squeeze casting too, as a commercial process, is in its infancy and designers are only now becoming aware of and beginning to use the technology. Designers would be more likely to use a new alloy with an existing process or a conventional alloy with a newer process. Having said that it is worthwhile investigating the advantages of squeeze-casting ZA alloys and composites and how the information in this work could be of industrial use.

Squeeze casting is marketed by GKN Squeezeform (for whom the author was employed as Senior Metallurgist on completion of his contract on the present project) as being a process able to produce castings with the strength of forgings using difficult to cast wrought aluminium alloys. Other users of the process (e.g. T & N) use conventional casting alloys but exploit the near-net shape capability and improved structural integrity achievable. Clearly, ZA alloys were developed for casting and would have to be exploited via the enhanced properties attainable by squeeze-casting. An as-cast strength of greater than 400 MPa combined with an elongation of greater than 10% is impressive for a non-ferrous material.

Is the information from the present investigation useful for commercial application? There was some doubt expressed about the validity of using a 50mm diameter ingot and its relevance to real castings. The author feels vindicated on this point as he has been involved in the manufacture of real components incorporating such thicknesses. It was shown in this investigation that both pouring temperature and die temperature were significant in controlling structure and properties in squeeze-cast ZA alloys and optimum conditions could be developed. In commercial practice it is the author's experience that processing conditions are chosen to form a sound component without the segregation which can be quite marked in long freezing range alloys. It is considered that the information in this work would provide a starting point from which optimum processing conditions for specific components could be developed. The information would also be of significance to workers in the process modelling field, especially those involved in the modelling of microstructures.

More information on the fatigue and fracture properties of squeeze-cast ZA alloys would have to be generated if they are to be used by designers working with finite element techniques. Also the wear properties of the squeeze-cast alloys would have to be determined. A big market for ZA

alloys relies on their excellent tribological properties. By controlling the solidification conditions in squeeze casting it may be possible to produce wear surfaces with optimum microstructures and properties.

Squeeze casting is probably the best way to produce sound as-cast metal matrix composites. This work demonstrated the feasibility of the manufacture of ZA27 + SiC<sub>p</sub> material. The properties measured were not spectacular but there is probably scope for further work on the tribological properties of the composites. If successful the incorporation of cast-in wear resistant inserts in squeeze-cast components may be one area of application.

It is considered that improved properties in composites could be obtained by using a finer particulate size and by filtering the melt before the metal is introduced into the die cavity.

## 8. Conclusions and Recommendations

### 8.1 Conclusions

1. Processing of ZA alloys by squeeze casting resulted in a high cooling rate, even in thick sections. A measured value of cooling rate was  $78.26^{\circ}\text{C}$  per second for ZA27 cast at  $555^{\circ}\text{C}$  into a 50mm diameter die at  $150^{\circ}\text{C}$ . Cooling rates of  $205^{\circ}\text{C}$  per second were deduced by secondary dendrite arm measurements in thinner sections.
2. The properties of squeeze-cast ZA alloys are influenced by cooling rates. Exact values of temperature gradients (G) and rate of movement of solidifying front (R) could not be measured but relative values led to the following deductions:
  - both ZA8 and ZA12 achieve maximum properties (tensile strength, 0.2% PS and elongation) when processed at highest cooling rates, which occur with, for example, thin sections and low die temperatures. Properties are better than in conventional gravity casting techniques and almost equal to those of pressure die casting.
  - the achievement of optimum strength and ductility in squeeze-cast ZA27 have different processing requirements. Highest elongation values were obtained at high G and relatively low R values. Optimum strength properties were achieved at a lower temperature gradient and faster rate of solidification in thin sections with 'cellular' microstructural appearances.
3. The properties of squeeze-cast ZA alloys can be related to their microstructures as follows:
  - increasing the cooling rate, and thus strength, results in a fine lamellar, eutectic structure within

both ZA8 and ZA12. ZA8 is most influenced because of its higher proportion of eutectic.

• the properties of ZA27 are influenced by the relative amounts and morphology of prior  $\alpha$  ( $\alpha'$ ),  $\beta$  and  $\eta$  in the microstructure. Strength in thick sections is conferred by  $\beta$ , which increases at lower cooling rates. Cooling rates are dependent upon R. Ductility is best with a higher volume of  $\alpha$  combined within a non-continuous eutectic.

4. Squeeze-cast thick section ZA27 showed a 0.1% growth, on ageing at 95°C.
5. Faster cooling rates and enhanced nucleation in thinner sections result in a cellular, rather than a dendritic primary phase. They also produce a stronger structure but the argument about the strengthening aspects of prior  $\beta$  at slower cooling rates still apply.
6. An alloy based on Zn-37Al could be squeeze-cast in thick sections, but was not fluid enough to be cast in sections <12mm. The alloy showed high elongation and may provide the basis for high strength alloy design specifically for squeeze casting.
7. Squeeze-cast ZA27 has the best ductility and thus should provide the most suitable matrix for metal matrix composites.
8. F320 grit SiC particulate material can be incorporated in ZA27 by the vortex method, without the use of wetting agents. The resulting mixture can then be successfully squeeze-cast.
9. The dispersion of SiC<sub>p</sub> is best in higher volume fractions (0.20) rather than lower (0.10). The latter

fraction appears 'clumped'. The particles lie in inter-granular positions for all volume percentages.

10. The addition of SiC particulate to ZA27 increases the room temperature Young's Modulus of the material, the modulus increasing with volume fraction. The values tend towards the lower end of the theoretical estimates.
11. Room temperature, uni-axial strengths of the composite were highest in the 0.20 volume fraction material. In all cases these are below the strength of the un-reinforced base alloy. Large oxide films on the fracture faces contribute to low strength in the material but it is considered that residual stresses caused by coefficient of thermal expansion mis-matches also are a factor.
12. Elongation values in uni-axial tensile testing of the composite at room temperature are low, 1% maximum. The composite fails below the yield point of the un-reinforced matrix material.
13. The composites retain a higher proportion of their room temperature strength, in uni-axial tensile tests at up to 150°C, compared to the base alloy.
14. A transformation from through particle/matrix to through eutectic/matrix fracture in composites was noted at testing temperatures between 100°C and 150°C.
15. Compression testing of composites at room temperature and 100°C showed highest yield strengths in the high volume fraction material. However, the composite material showed a tendency to flow more easily at constant stress, with higher volume fractions of particulate.

16. Creep testing was largely inconclusive, but indications were that composites performed better at higher temperatures and loads compared to the base alloys.

## 8.2 Recommendations

1. Further work on determining the engineering properties required by designers should be carried out on squeeze-cast ZA alloys. Of particular importance are push/pull fatigue properties and fracture toughness which are important for the latest design methodologies.
2. The determination of tribological properties of squeeze-cast ZA alloys under a variety of loading regimes may help in the penetration of ZA alloys into new markets.
3. It would be of great interest to study the properties of a squeeze-cast ZA27 / SiC<sub>p</sub> composite material made with a fine particle size (<10 $\mu$ m). The composite could be manufactured using improved stirring techniques and should be filtered before being poured into the die cavity to remove oxide films.
4. The development of alloys specifically for squeeze casting is an area ripe for investigation. Long freezing range alloys based on Zn-Al-Mg may provide suitable materials for the attainment of a light alloy with a yield strength of 500MPa and an elongation of 10%.

## References

- [1] Goodwin F E and Ponikvar A L (Editors)  
Engineering Properties of Zinc Alloys (3rd Ed)  
ILZRO (1989) New York
- [2] Gervais E  
Proc. 25th Conference Canadian Institute of  
Mining and Metallurgy (C.I.M.) (1986) 1
- [3] Gervais E, Levert H, and Bess M  
AFS Transactions. 88 (1980) 183
- [4] Barnhurst R J, Gervais E and Bayles F D  
AFS Transactions. 91 (1983) 569
- [5] Campbell J  
Cast Metals 4 (1991) 129
- [6] Lyon R  
Metals and Materials 1 (1985) 55
- [7] Chatterjee S and Das A A  
British Foundryman. 65 (1972) 420
- [8] Chatterjee S and Das A A  
ibid. 66 (1973) 118
- [9] Das A A and Chatterjee S  
The Metallurgist and Materials Technologist.  
13 (1981) 137
- [10] Zantout B  
PhD Thesis, Loughborough University of Technology.  
January (1986)
- [11] Arsenault R J and Fisher R M  
Scripta Metall. 17 (1983) 67
- [12] Anon  
Duralcan product information
- [13] Anon  
AVCO product information
- [14] Morgan S W K  
Zinc its alloys and compounds  
Ellis Horwood (1985) Chichester
- [15] Apelian D, Paliwal M and Herrschaft D  
Journal of Metals 33,11 (1981) 12
- [16] Meeus M, Kelchtermans H and Groothaert L  
Proc. 25th Conf. C.I.M. (1986) 171
- [17] Mykura N and Murphy S  
ibid. 45

- [18] Vijayalakshmi M, Seetharaman V and Raghunathan V S  
Materials Science and Engineering 52 (1982) 249
- [19] Lecomte-Beckers et al.  
Proc. 25th Conf. C.I.M. (1986) 35
- [20] Savaskan T and Murphy S  
Materials Science and Technology 6 (1990) 695
- [21] Zhu Y H, Yan B and Huang W  
Proc. 25th Conf. C.I.M. (1986) 23
- [22] Anon  
Information supplied from Noranda Handbook  
Courtesy Brock Metals
- [23] Dieter G E  
Mechanical Metallurgy (2nd Ed)  
McGraw Hill (1981) Kogakusha
- [24] Honeycombe R W K  
The Plastic Deformation Of Metals  
Edward Arnold (1977) London
- [25] Clegg A J  
Undergraduate Notes  
Loughborough University
- [26] Beeley P R  
Foundry Technology  
Butterworths (1972) London
- [27] Chadwick G A and Yue T M  
Metals and Materials 5 (1989) 6
- [28] Benedyk J C and Shaw W  
Light Metal Age 27 (1969) 5
- [29] Plyatskii V M  
Extrusion Casting  
Primary Sources (1965) New York
- [30] Anon  
UBE product information
- [31] Barlow J  
International Journal of Vehicle Design  
IAVD Conf. on vehicle design and components (1984)
- [32] Clegg A J  
Foundry Trade Journal International 9 (1986) 31
- [33] Epanchintsev O G  
Russian Castings Production (1972) 34
- [34] Lipchin T N and Bykov P A  
ibid. (1973) 109

- [35] Lipchin T N and Tomsinskaya M A  
Metalloved Term Obrab Met 10 (1980) 37
- [36] Aseada T, Yoshikawa M and Tuda H  
Bulletin of JSME 20 (1977) 489
- [37] Rajogopal S and Altergott W H  
AFS Transactions 93 (1985) 145
- [38] Rajogopal S  
Journal of Applied Metalworking 1 (1981) 3
- [39] Williams G  
Foundry Trade Journal 156 (1984) 66
- [40] Franklin J R and Das A A  
British Foundryman 77 (1984) 150
- [41] Benedyk J C  
6th SDCE Int Die casting congress Paper 86 (1970)  
Ohio
- [42] Williams G and Fisher K M  
Metals Technology 8 (1981) 263
- [43] Kaneko Y et al.  
Foundry Trade Journal 148 (1980) 397
- [44] Weinberg F  
Proc. Conf. Solidification Technology in the  
Foundry Casthouse  
Warwick Sept (1980) 131
- [45] Lynch R F, Olley R P and Gallagher P C J  
AFS Transactions 83 (1975) 561
- [46] Gervais E, Deep G and Kandiel A Y  
ILZRO Project ZD-287  
Progress Report No. 4 September (1981)
- [47] Yacoub M M  
PhD Thesis, Loughborough University of Technology  
(1987)
- [48] Parker D A  
Proc. Instn. Mech. Engrs. Vol 199 No. A3 (1985) 135
- [49] McGuire M F  
Diesel and Gas Turbine Progress 45 (1979) 59
- [50] Anon  
Alures Product Information
- [51] Kulkarni K M  
Proc. Conf. on Production Engineering  
Vol 2 (1977) viii 145

- [52] Wang C, Ying M and Tao J  
Proc 4th Int Conf on Composite Structures, Vol 2 98  
Elsevier Applied Science (1987) London
- [53] Dent P N and Murphy S  
Proc. 25th Conf. C.I.M. (1986) 127
- [54] Das A A et al  
ibid 213
- [55] Guerriero R, Parse J B and Tangerini I  
Ibid 229
- [56] Das A A et al.  
Cast Metals 1 (1988) 69
- [57] Gibson P R, Clegg A J and Das A A  
Foundry Trade Journal 152 (1982) 253
- [58] Chadwick G A  
Cast Metals 4 (1991) 165
- [59] Feest E A  
Metals and Materials 4 (1988) 273
- [60] Booth et al  
Metal Matrix Composite Developments in the USA  
BNF Metals Technology Centre UK (1987)
- [61] Feest E A et al.  
Metal Matrix Composite Developments in Japan  
Harwell Oxon UKAEA (1986)
- [62] Anon  
Course Notes on Duralcan Material  
Loughborough University (1989)
- [63] Chou T W, Kelly A and Okura A  
Composites 16 (1985) 187
- [64] Harris S J  
Materials Science and Technology 4 (1988) 231
- [65] Mortenson A, Cornie J A and Flemings M C  
Materials and Design 10 (1989) 68
- [66] Rohatgi R K, Asthana R, and Das S  
International Metal Reviews 31 (1986) 115
- [67] Fishman S G and Dhingra A K (Editors)  
Proc. Int. Symp. of advances in cast MMCs  
Chicago (1988)
- [68] Metcalfe A G  
Interfaces in Metal Matrix Composites  
Academic Press (1974) New York

- [69] Kelly A and Mileiko S T (Editors)  
Fabrication of Metal Matrix Composites, Chap 5  
Handbook of Composites Elsevier (1984)  
North Holland
- [70] Delannay F, Froyen L and Deruyttere A  
Journal of Materials Science 22 (1987) 1
- [71] Fletcher T R, Cornie J A and Russell K C  
Proc. Int. Symp. on advances in cast MMCs (1988)  
21
- [72] Naidich J V  
Progress in Surface and Membrane Science  
14 (1981) 353
- [73] Gaskell D R  
Introduction to Metallurgical Thermodynamics  
McGraw-Hill (1973) Washington DC
- [74] Warren R and Andersson C H  
Composites 15 (1984) 101
- [75] Dunn J  
The Engineer Vol 266 No.6899 (1988) 42
- [76] Champion A R et al.  
Proc. 2nd Int. Conf. on Composite Materials  
ICCM II (editors Norton B et al.)  
New York AME (1978) 882
- [77] Skibo M D and Schuster D M  
International Patent PCT/US87/00940
- [78] Cornie S et al.  
Proc. Int. Symp. of advances in cast MMCs (1988)  
155
- [79] Lo J S H et al.  
Proc. 28th Conf. CIM (1989) 412
- [80] Dignard-Bailey L, Dionne S and Lo S H  
Conf. Proc. Fundamental Relationships between  
microstructures and mech props of MMCs  
USA (1989) 23.
- [81] Franklin J R  
Internal Communication  
Loughborough University
- [82] Badia F A and Rohatgi P K  
AFS Transactions 77 (1969) 347
- [83] Murphy S and Savaskan T  
Practical Metallography 24 (1987) 204.

- [84] **Trivedi R and Kurz W**  
Solidification of Single-Phase Alloys  
Metals Handbook Volume 15 (1988)  
ASM International Metals Park Ohio
- [85] **Kurz W and Fisher D J**  
Fundamentals of Solidification  
Trans. Tech. Publications (1984) Aedermannsdorf
- [86] **Chadwick G A**  
Metallography of Phase Transformations  
Butterworths (1972) London
- [87] **Minkoff I**  
Solidification and Cast Structure  
John Wiley and Sons Inc. (1986) Chichester
- [88] **Chalmers B**  
Principles of Solidification  
John Wiley and Sons Inc. (1964) New York
- [89] **Winegard W C**  
An Introduction to the Solidification of Metals  
Monograph and Report Series 29  
Institute of Metals (1964) London
- [90] **Magnin P and Kurz W**  
Solidification of Eutectics  
Metals Handbook Volume 15 (1988)  
ASM International Metals Park Ohio
- [91] **Campbell J**  
Castings  
Butterworths Heinman (1991) Oxford
- [92] **Granger D A and Elliott R**  
Solidification of Eutectic Alloys  
Aluminium-Silicon Alloys  
Metals Handbook Volume 15 (1988)  
ASM International Metals Park Ohio
- [93] **Smith D M**  
UK Patent GB 2085920 B (1981)
- [94] **Barnhurst R J and Gervais E**  
AFS Transactions 93 (1985) 591
- [95] **Walmag G, Lamberigts M, and Coutsouradis D**  
Proc. 25th Conference C.I.M. (1986) 5
- [96] **Stefanescu D M et.al.**  
Metallurgical Transactions A 19A (1988) 2847
- [97] **Arsenault R J**  
Composite Structures 4 Vol 2  
Edited by Marshall I H (1987) 70

- [98] Piggott M R  
Load Bearing Fibre Composites  
Pergammon (1980) New York
- [99] Nair S V, Tien J K and Bates R C  
International Metal Reviews 30 (1985) 275
- [100] Nutt S R and Carpenter R W  
Materials Science and Engineering 75 (1985) 169
- [101] Papizan J M  
Metallurgical Transactions A 19A (1985) 2945
- [102] Milliere C and Suery M  
Materials Science and Technology 4 (1988) 41
- [103] Arsenault R J and Wu S B  
Materials Science and Engineering 96 (1987) 77
- [104] Flom Y and Arsenault R J  
Materials Science and Engineering 75 (1985) 151

## Appendix 1:

### Mechanical Properties of Squeeze-Cast Zinc-Base Alloys

Table	Alloy	Section Thickness	Processing Parameters
A	ZA27	50mm	2F, 555°C Pour
B	ZA27	50mm	2H, 555°C Pour
C	ZA27	50mm	3F, 555°C Pour
D	ZA27	50mm	3H, 555°C Pour
E	ZA27	50mm	3F, 185MPa
F	ZA27	Thin	2H, 68MPa, 595°C Pour
G	ZA27	Thin	2H, 68MPa, 620°C Pour
H	ZA27	Thin	2H, 68MPa, 650°C Pour
I	ZA8	50mm	450°C Pour
J	ZA8	Thin	2H, 68MPa, 450°C Pour
K	ZA12	50mm	480°C Pour
L	ZA12	Thin	2H, 68MPa, 480°C Pour
M	Zn-37Al	50mm	3F, 185MPa

Key.

- F Full Power Pressure (pressure build up of 11.5 tonnes/s)
- H Half Power Pressure (pressure build up of 8.3 tonnes/s)
- 2 Slower Press Speed - 6s delay with 50mm die, 8s with thin section die.
- 3 Higher Press Speed - 4s delay with 50mm die.

**Table A: Squeeze-Cast ZA27 - 50mm Section**  
 Processing Parameters 2F, 555°C Pour

Die Temperature (°C)	Squeeze Pressure (MPa)	UTS (MPa)	0.2% Proof Stress (MPa)	Elongation (%)	Reduction in Area (%)	
150	185	406	353	4.5	4	
		393	366	3.5	7	
		n/a	n/a	n/a	n/a	
	270	270	404	392	5	8
			409	373	6	10
			411	367	10	15
	380	380	414	373	6	10
			416	373	8	10
			417	369	5.5	7
200	185	406	372	4	7	
		399	353	6.5	12	
		403	349	8	10	
	270	270	398	357	11	18
			402	360	10	15
			389	382	6	10
	380	380	399	352	8	15
			402	363	14	17.5
			400	360	8	12
250	185	410	372	4.5	10	
		409	368	5.5	12	
		414	381	9.5	16	
	270	270	409	381	6.5	14
			409	372	10	18
			405	376	6	10
	380	380	408	375	8	10
			407	378	10	17
			n/a	n/a	n/a	n/a
300	185	414	385	10	15	
		411	372	10	17	
		409	377	7.5	14	
	270	270	414	387	10	17
			411	382	5	9
			411	382	5.5	9
	380	380	404	377	10	17
			402	377	4.5	8
			401	376	4	9

**Table B: Squeeze-Cast ZA27 - 50mm Section**  
 Processing Parameters 2H, 555°C Pour

Die Temperature (°C)	Squeeze Pressure (MPa)	UTS (MPa)	0.2% Proof Stress (MPa)	Elongation (%)	Reduction in Area (%)	
150	185	412	372	5	7	
		413	369	5.5	11	
		411	363	4.5	7	
	270	270	412	373	5	12
			411	371	10	15
			412	368	5.5	11
	380	380	413	376	8	11
			413	373	7.5	10
			417	380	7	10
200	185	399	371	5	10	
		355	330	7	17	
		n/a	n/a	n/a	n/a	
	270	270	399	364	11	16
			396	367	4	6
			407	367	6	12
	380	380	402	375	11.5	19
			403	363	6.5	13
			397	375	7.5	12
250	185	409	380	8	16	
		407	374	6	11.5	
		404	372	7	13.5	
	270	270	414	386	6	10
			407	400	7.5	15
			407	365	5.5	10
	380	380	411	384	5.5	10
			408	382	4	9
			415	384	5	6
300	185	417	385	10	17.5	
		414	386	5	12.5	
		420	380	6.5	12	
	270	270	413	381	8.5	16.5
			414	387	7	12.5
			416	375	5	7.5
	380	380	410	383	10	13
			n/a	n/a	n/a	n/a
			414	383	5	15

**Table C: Squeeze-Cast ZA27 - 50mm Section**  
 Processing Parameters 3F, 555°C Pour

Die Temperature (°C)	Squeeze Pressure (MPa)	UTS (MPa)	0.2% Proof Stress (MPa)	Elongation (%)	Reduction in Area (%)	
150	185	425	387	6	7.5	
		424	387	6	9	
		423	387	6	7	
	270	270	411	390	4.5	5
			410	381	4	8
			411	384	4.5	6
	380	380	423	396	10	12
			419	393	6	10
			421	394	9.5	13
200	185	399	379	14.5	26	
		399	379	8	15	
		399	372	7.5	12	
	270	270	407	388	6	11
			407	388	5.5	10
			407	382	9.5	17
	380	380	405	390	8	13
			402	383	4.5	10
			406	381	9.5	15
250	185	414	377	5	12	
		408	380	5	5	
		411	372	8	20	
	270	270	415	388	12	25
			414	382	10.5	16
			415	383	9.5	16
	380	380	421	396	10	16
			420	393	7	12
			420	395	4.5	9
300	185	419	392	6	8	
		419	385	6	7	
		418	385	8	14	
	270	270	425	404	10	15
			427	400	5.5	11
			427	400	5.5	9
	380	380	426	407	9.5	19
			428	400	7.5	12
			427	400	7.5	15

**Table D: Squeeze-Cast ZA27 - 50mm Section**

Processing Parameters 3H, 555°C Pour

Die Temperature (°C)	Squeeze Pressure (MPa)	UTS (MPa)	0.2% Proof Stress (MPa)	Elongation (%)	Reduction in Area (%)	
150	185	n/a	n/a	n/a	n/a	
		413	387	10	16	
		411	378	4	8	
	270	270	408	392	9	15
			405	385	10	16
			405	380	7	10
	380	380	425	394	6.5	10
			428	383	5.5	9
			426	379	12	20
200	185	404	386	12.5	20	
		401	379	10.5	10	
		400	367	10	14	
	270	270	400	377	5	10
			402	379	9	12
			401	375	9	13
	380	380	413	392	5.5	10
			412	391	8.5	9
			409	381	10	10
250	185	405	374	6	10	
		407	379	10	15	
		403	373	8.5	15	
	270	270	419	399	15	35
			419	391	15	30
			417	390	16	36
	380	380	427	397	6.5	11
			426	395	7.5	11
			423	391	7.5	10
300	185	429	398	10	25	
		418	383	6	11	
		420	384	5	10	
	270	270	414	392	10	20
			417	386	7	15
			415	387	12.5	26
	380	380	422	397	10	16
			422	401	10	15
			425	397	8	16

**Table E: Squeeze-Cast ZA27 - 50mm Section**

Processing Parameters 3F, 185 MPa

Die Temperature (°C)	Pouring Temperature (°C)	UTS (MPa)	0.2% Proof Stress (MPa)	Elongation (%)	Reduction in Area (%)
150	515	405	361	9.5	15
		401	366	5	10
		401	361	5	8
	595	415	361	20	40
		411	369	21	36
		n/a	n/a	n/a	n/a
200	515	391	345	7.5	10
		393	343	7.5	12
		390	348	6	10
	595	392	350	19.5	40
		391	350	17	35
		390	338	10	10
250	515	391	359	8	11
		388	356	4.5	6
		388	363	8	16
	595	421	383	8	10
		401	367	6	10
		418	372	6	10
300	515	382	360	5	n/a
		n/a	n/a	n/a	n/a
		382	370	5	n/a
	595	415	385	12.5	25
		417	377	10	15
		411	366	9.5	10

**Table F: Squeeze-Cast ZA27 - Thin Sections**  
 Processing Parameters 2H, 68MPa, 595°C Pour

Die Temperature (°C)	Section Thickness (mm)	UTS (MPa)	0.2% Proof Stress (MPa)	Elongation (%)
150	16	n/a	n/a	n/a
		425	383	3.5
		440	405	4
	12	447	422	5
		437	406	4.5
		437	418	2.5
	8	434	404	7
		437	405	5
		431	397	7.5
180	16	415	384	2.5
		417	394	3
		429	400	5
	12	423	390	6
		427	402	2.5
		419	393	5
	8	421	397	5
		416	391	5
		427	402	10
220	16	450	420	4.5
		459	425	5
		459	421	2.5
	12	450	423	5.5
		449	423	5
		448	417	5
	8	445	415	8.5
		443	418	10
		447	420	11

**Table G: Squeeze-Cast ZA27 - Thin Sections**

Processing Parameters 2H, 68MPa, 620°C Pour

Die Temperature (°C)	Section Thickness (mm)	UTS (MPa)	0.2% PS (MPa)	Elongation (%)
150	16	418	389	5
		421	388	4.5
		406	371	5
	12	396	362	5.5
		416	382	5.5
		415	392	7
	8	n/a	n/a	n/a
		n/a	n/a	n/a
		n/a	n/a	n/a
180	16	422	398	5
		411	381	5.5
		419	389	5
	12	410	387	7.5
		415	388	8
		415	390	6.5
	8	401	374	4
		410	366	12
		n/a	n/a	n/a
220	16	434	407	7
		443	414	5.5
		442	407	7
	12	425	401	9.5
		420	388	12.5
		428	396	7.5
	8	438	410	7
		433	401	7.5
		417	387	9.5

**Table H: Squeeze-Cast ZA27 - Thin Sections**  
 Processing Parameters 2H, 68MPa, 650°C Pour

Die Temperature (°C)	Section Thickness (mm)	UTS (MPa)	0.2% Proof Stress (MPa)	Elongation (%)
150	16	n/a	n/a	n/a
		403	384	4.5
		418	390	4.5
	12	411	388	5.5
		407	377	7.5
		411	380	5
	8	437	403	6.5
		411	372	7.5
		n/a	n/a	n/a
180	16	419	398	4.5
		416	383	5
		422	403	5
	12	422	389	5.5
		408	381	4.5
		414	379	5.5
	8	399	363	5
		409	379	6.5
		404	374	10
220	16	457	422	5
		467	421	5
		441	413	2.5
	12	431	397	6
		438	399	9
		451	408	5
	8	434	406	5.5
		427	403	5.5
		433	408	4.5

**Table I: Squeeze-Cast ZA8 - 50mm Sections**

Pouring Temperature 450°C

Die Temperature (°C)	Squeeze Pressure (MPa)	Processing Parameters	UTS (MPa)	0.2% PS (MPa)	Elongation (%)
150	185	2F	308	298	4
			291		2.5
			312		3.5
	270	3F	294	292	2
			290		2.5
			297		2
	380	2H	303	302	2.5
			306		4
			303		2
200	270	2H	258	268	3.5
			272		2
			255		2.5
	380	3F	265		3
			258		4
			258		2
250	185	2H	255	255	3
			252		3.5
			248		2
	270	2F	252		3
			245		4
			253		3
	380	3H	245		4
			241		2
			244		2.5
300	185	3F	246	255	2
			240		2
			255		2.5
	270	3H	242	242	4
			221		4
			239		2.5
	380	2F	235		3
			237		2.5
			232		3.5

**Table J: Squeeze-Cast ZA8 - Thin Sections**

Processing Parameters 2H, 68MPa, 450°C Pour

Die Temperature (°C)	Section Thickness (mm)	UTS (MPa)	0.2% PS (MPa)	Elongation (%)
150	16	342	325	3
		339	315	3
		341	314	3
	12	344	286	4
		344	302	4
		341	308	2.5
	8	344	316	4.5
		355	317	4.5
		349	310	5
180	16	329	304	3.5
		325	310	3.5
		298	298	2
	12	315	300	4
		336	302	2.5
		332	299	4.5
	8	327	305	5
		334	303	5
		298	283	4
220	16	292		2.5
		291		1.5
		298	298	2.5
	12	318	297	4
		316	302	2.5
		307	307	2
	8	307	287	4.5
		312	292	4.5
		317	299	4

**Table K: Squeeze-Cast ZA12 - 50mm Sections**

Pouring Temperature 480°C

Die Temperature (°C)	Squeeze Pressure (MPa)	Processing Parameters	UTS (MPa)	0.2% PS (MPa)	Elongation (%)
150	270	3F	347	319	3
			339	317	4
			341	313	4
	380	2H	352	325	2.5
			337	320	4
			355	319	2
200	185	3H	321	296	3
			325	305	2
			317	302	2.5
	270	2H	306	293	2.5
			324	300	2
			316	295	2.5
250	185	2H	295	284	4
			303	291	3
			306	292	2.5
	270	2F	299	286	3.5
			304	291	3
			306	293	3
	380	3H	280		2
			273		4
			290	285	2.5
300	185	3F	n/a	n/a	n/a
			298	289	2
			313	295	2.5
	270	3H	289	288	2.5
			266		2.5
			298	292	3

**Table L: Squeeze-Cast ZA12 - Thin Sections**

Processing Parameters 2H, 68MPa, 480°C Pour

Die Temperature (°C)	Section Thickness (mm)	UTS (MPa)	0.2% Proof Stress (MPa)	Elongation (%)
150	16	368	348	2
		368	344	2.5
		361	341	2
	12	357	328	1
		371	343	3
		371	343	3
	8	379	350	4.5
		360	329	4.5
		374	344	4.5
180	16	358	337	2
		356	337	2
		355	336	2.5
	12	358	327	2.5
		362	331	2.5
		356	331	2.5
	8	366	340	5
		372	325	5
		357	327	5
220	16	349	345	2.5
		350	342	2.5
		360	344	2
	12	363	333	4
		358	333	4
		364	332	3
	8	371	337	2.5
		371	337	4
		365	339	3.5

**Table M: Squeeze-Cast Zn-37Al - 50mm Section**

Processing Parameters 3F, 185 MPa

Die Temperature (°C)	Pouring Temperature (°C)	UTS (MPa)	0.2% Proof Stress (MPa)	Elongation (%)	Reduction in Area (%)
150	565	310	291	10	19
		300	269	15	24
		293	269	17	33
	595	300	259	5	5
		297	267	10	15
		300	268	10	15
200	565	277	251	18	34
		273	254	18	30
		285	264	14	25
	595	272	255	12.5	21
		274	249	14.5	20
		280	260	6	15
250	565	271	247	19.5	25
		272	251	16.5	31
		282	261	19	36
	595	275	253	10	10
		274	249	6	7
		282	264	6	10
300	565	278	263	21	38
		276	254	20	38
		286	264	17.5	30
	595	283	267	17.5	32
		276	258	14	20
		278	253	20	32

## Appendix 2:

### Mechanical Properties of Squeeze-Cast Zinc-Base Alloy Composites

Table	Alloy	Section Thickness	Processing Parameters
N	ZA27 + SiCp	50mm	3F, 595°C Pour

**Key:**

F Full Power Pressure (pressure build up of 11.5 tonnes/s)

3 Higher Press Speed - 4s delay with 50mm die.

**Table N: Squeeze-Cast ZA27/SiCp Composites - 50mm Section**  
 Processing Parameters 3F, 595°C Pour  
 Die Temperature 180°C

Volume % SiCp	Sample	Testing Temperature			
		Ambient	60°C	100°C	150°C
0	1	411	359	299	205
10	1	177	192	208	189
	2	240	181	160	175
	3	253	236	150	165
15	1	184	252	150	180
	2	228	235	230	n/a
	3	253	n/a	198	161
20	1	252	269	238	228
	2	306	253	281	211
	3	n/a	205	170	220

